Real Time Imaging of Fluid Flow In Porous and Absorbent Materials

Rebecca Jane Yerworth

PhD

University College London

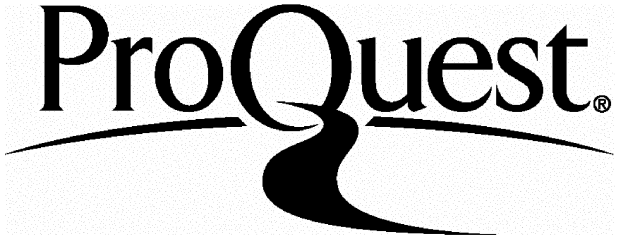

Abstract

This thesis demonstrates the design, commissioning and use of systems for the imaging of absorbent incontinence products in real time. The primary aim was to create tools with which to study the interaction of fluids with incontinence pads as an aid to the development of more effective products. Three imaging systems were developed that together form a flexible toolbox of complementary techniques that have been validated using clinical data.

Most of the work concentrated on an optical imaging system for laboratory and clinical use. The development of this system is described from the initial concept, through the design stage, to the commissioning and use of this technique. The system uses an array of sensors that, for laboratory work, can be embedded in a simple flat holder or a curved holder representing the lower portion of the human torso. For clinical work the sensors have been incorporated into a ribbon cable.

Data can be displayed in various formats depending on the information required. These data presentation techniques range from image sequences of the fluid spread, wet area versus time curves or single characterising numbers.

The two other techniques can provide complementary information. X-ray imaging, reveals finer details of structures within the materials, but cannot be used clinically, while resistive imaging is used for clinical validation of laboratory results but is time consuming to use and only yields binary (dry or wet) information from each sensor.

In order to control fluid application a specialised fluid delivery system was designed and built during this project. This device is temperature controlled and capable of replicating a wide range of physiologically realistic flow-rate/time profiles.

Data from laboratory studies using the optical imaging device show clearly identifiable differences in performance between products. The effect of using different postures and flow-rate/time profiles has also been demonstrated.

Contents

Table of illustrations

Chapter 1

Chapter 2

Chapter 3

Chapter 4

Chapter 5

Chapter 6

Chapter 7

Chapter 8

Chapter 9

Appendices

Table of Tables

Chapter 1

Chapter 2

Chapter 3

Chapter 4

Chapter 5

Chapter 6

Chapter 7

Chapter 8

Chapter 9

1: General introduction

1.1 Introduction

There are many fields where the interaction between fluid and porous/absorbent materials is important: for example, hydrogeology applications such as studying the percolation of rainwater through soil and rock to determine the catchment area of a spring-water aquifer and its rate of refilling, or, when fibrous mats are used to contain an oil spill. In the latter case, the interaction of both oil and water with the material must be considered if the mat is to be used at sea and only the oil removed. An example of a medical application would be the design of a wound dressing which may be required to absorb exudate without sticking to the wound. The particular area of application in this thesis is that of urine absorption in incontinence pads. How fluid interacts with absorbent materials is not fully understood. Some of the microscopic and fundamental properties have been studied (Gillespie, 1959) (e.g. fluid rising, in the material via capillary action), more recently Grow and Osczevski (1998), for example, have studied the relative effects of water content and fabric type on the drying time of materials and sometimes quantitative information about the macroscopic situation can be seen (e.g. the product will hold 500 ml of water). Where there is an information and knowledge gap, however, is in relating these two extremes and providing information on how the overall clinical performance of a product is determined by the interaction between urine and the materials and design features incorporated in the product. This work seeks to bridge the gap, devising techniques that can be used to study materials in both clinical usage and in the laboratory.

1.2 Incontinence - a Background

Norton (1996) provides an excellent introduction to the subject of incontinence, covering the various aspects in more detail than is appropriate here and has been a valuable text in preparing this summary.

Urinary incontinence is defined by the International Continence Society (1998) as the involuntary loss of urine that is perceived as a hygienic or social problem and is objectively demonstrable. Incontinence is not a disease but a symptom of a wide range of conditions, both physical and neurological, some of which are understood and others that are not. Faecal incontinence is also possible, but is not considered here due to its lower prevalence, ~0.5% of the adult population (Norton 1996), and the fact that it normally involves (semi-) solid matter rather than fluid and must be contained, rather than absorbed, by the product.

Urinary incontinence is a surprisingly common condition: 10-15% of the adult population in the western world experience significant symptoms (at least two incidents per month) at any one time, according to one survey (Thomas et al. 1980). However, Defever et al. (1997) provide a summary of all relevant studies, indicating that figure 22-30% of the population have some form of urinary incontinence,

with about 20% of these (6% of the total population) experiencing daily incontinence. The reason that these estimates vary widely relates to the interpretation of the above definition, and the methodology used for data collection. Some studies consider leaks of a few millilitres, less than twice a month as incontinence while others considers a leak as incontinence only when it becomes a problem. The definition of 'a problem' will vary from individual to individual, and is subjective, as well as depending on toilet facilities (e.g. is there a toilet near by if they have an urgent need – a long distance lorry driver would have more problems than a home worker), their standards of personal hygiene, and many other factors. This prevalence of incontinence in the population is not evenly distributed with respect to age but is far more common in old age, particularly for men (Fig.1.1). This is demonstrated by the fact that 40-70% of elderly people living in nursing homes or hospitals are incontinent (Royal College of Physicians of London, 1995).

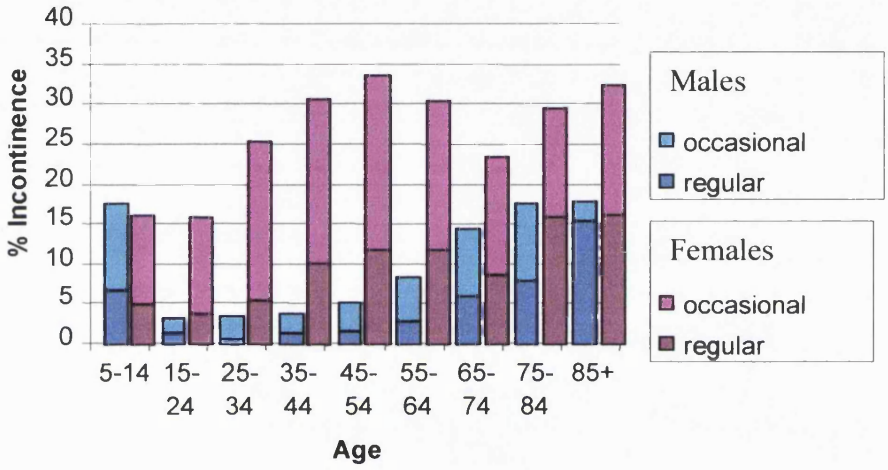

Fig.1.1 Prevalence of urinary incontinence as a function of age and gender (Thomas et.al. 1980)

Nor is all incontinence of the same severity; rather, it ranges from an occasional few millilitres, to the sudden emptying of a full bladder several times a day. As with prevalence, severity is not evenly distributed across the age spectrum, but is heavily skewed towards old age. Incontinence is also far more common in women than in men (Fig.1.1). This is for a number of reasons including the shortness of the urethra, providing little resistance to fluid flow. Also, during childbirth a woman may sustain damage to her pelvic floor. These, combined, may result in stress incontinence, where urine leaks when the abdomen is stressed (e.g. by coughing.) This is the most common cause of incontinence in this middle age range. The most common form of incontinence among men under 30 is nocturnal enuresis, i.e. bed-wetting. Although in some cases this may be triggered by emotional stress, in other cases there may be no known cause. It is hypothesised that there is a neurological cause, due to a fault in the pathway by which the need for the toilet would normally cause one to wake up. In older people the most common form of incontinence is urge incontinence although this is supplemented, in men, by incontinence due to prostate problems. Urge incontinence is the inability to reach the toilet in time due to a reduction in the amount of time between perceiving the need and leaking. This may be exacerbated by reduced mobility. The other main reason for reduced continence in old age is mental deterioration, i.e. dementia, confusion or memory loss. This can be compounded by a change of surroundings (e.g. upon moving from one's

own home of many years to residential care), resulting in disorientation. Another issue is distortion of the definition of 'appropriate', for example, for someone with a confused mind, sitting quietly in a corner on a pad, without other underwear, this may feel more like a toilet than a bathroom with nurses present removing privacy.

Other causes of urinary incontinence include spinal injuries and localised nerve damage. Congenital defects (e.g. miss-positioning of the urethra) and disease may also result in incontinence.

Being incontinent has many associated problems. Some of these are physical, relating to skin health and the need to carry supplies of an appropriate incontinence product, as well as disposing of or washing used products and other soiled items. For other people the social stigma or the fear of social stigma associated with this condition can be a severe handicap, even if their incontinence is minimal. A contributing factor to this latter, particularly in western cultures where body odours are taboo, is smell, or again, the fear of smelling of stale urine. These factors can lead to an altering or curtailing of a persons social life and to changes in their style of dress, particularly if the condition is unacknowledged, and therefore, not treated or managed. Another problem that may arise from incontinence is financial, with the burden of extra laundry and care costs as well as incontinence aids/pads themselves. Carers also have a difficult task, as they have to adjust to an increased workload and the mutual embarrassment that can arise from helping someone with their toilet.

Incontinence is not an untreatable condition and there is much that the medical profession can do to alleviate the severity or to provide a cure. This can be achieved through drug therapy, physiotherapy, surgical intervention, behavioural methods (e.g. bladder training where a person may be encouraged to gradually increase the time interval between lavatory visits) or a change of diet, depending on the underlying cause. For example, pelvic muscle exercises, to strengthen the muscles that keep the bladder closed, and vaginal cones, which apply pressure to the bladder neck to keep it closed, are used in the treatment of stress incontinence. Surgery may correct congenital defects or cure prostate related incontinence. However, despite major advances in this work there will always be a proportion of incontinence that can not be cured. This is indicated in a summary of treatment results compiled in the Leuven report (Defever at al. 1997). This indicates that, for example, pelvic muscle exercises have a good record at improving stress incontinence (75-90%) but a low cure rate (12-23%). Surgical options have a higher cure rate, accompanied by a significant frequency of complications (e.g. urethral sling cure rate 62-97%, complications 22-30%). For this reason many devices have been developed over the years for containing excreted urine and preventing leakage. These may be used, with personalised toileting plans, to gain what is termed 'social continence', that is, a state in which the incontinence, although still present, is no longer a social of hygienic problem. The products that are available will be discussed later but it is worth noting at this point some factors that a user or care provider will need to consider when choosing a product:

- The severity, frequency and nature of the incontinence
- The level of independence of the incontinent person and their lifestyle, for example, whether they live an active life, care for themselves or are in a nursing home.

- Ease of putting on/taking off the product, the requirements for this will depend on the manual dexterity and mobility of the users and/or their carer.
- How well the product stays in place during the normal activities of the user. This will be a more demanding criterion for a keep fit teacher who is always on the move than for a wheelchair bound person.
- How discreet and normal is the person's appearance when the product is in use, again this will partially depend on the tastes of the user. If they like tight fitting clothing the product would be harder to hide than under loose clothing. Any noise or smell associated with the product should also be considered.
- Ideally the product would be completely free from leakage but this is not true in practice. The level of leakage a person will tolerate will depend on the actual/perceived consequences of a leak (for example humiliation and extra laundry) and the importance they place on other factors such as appearance.
- How comfortable the product is for the user
- Whether the product adversely affects skin health, for example by keeping the skin moist and prone to soreness.
- The product should meet current safety legislation
- The environmental impact of using the product should be considered both in terms of the manufacture of the product and its disposal or laundering.
- The total daily cost of using the product again in terms of purchase and disposal/laundry should be considered bearing in mind that it may be a false economy to use a cheaper per piece product which needs changing more often.

This list is drawn from an ISO/DIS guidance document (ISO/DIS 15621:1997 (E)). It is easy to see that many of these factors are compromises, whose balance point varies between purchasers, for example a thicker pad may leak less but be less discreet. For example, someone buying in bulk for a hospital may consider cost and ease of putting on/taking off most important, whereas someone living independently in the community may consider discreteness of the product the overriding factor – especially if they prefer a close fitting style of clothing.

It is worth adding that the disposal or washing requirements of the product should also be taken in to account, both in terms of time and cost.

The factor of cost is an increasingly important one, especially in light of an ageing population. By combining prevalence data from Thomas' study (1980) with projected population trends (Office of Population Censuses & Surveys 1991), as seen in Fig.1.2, it can be seen that, although the total population in the UK is only expected to increase by 4% over the next twenty years, the number of people over 65 is set to increase by 29%, from nine million to twelve million. This will mean that the number of incontinent people will increase by 9%, more than twice the increase seen in the total

population and will cause an estimated rise in the prevalence of incontinence of 0.75%, to 16.4%. Since a greater proportion of incontinence in elderly people is severe, compared with younger sufferers, these figures do not show the full impact of this population trend. Market forces within the health service are also likely to focus attention on care costs. Both Britain and the USA currently spend about 2% of their annual health care budget (Norton, 1996) on incontinence, in 1991 this amounted to £56m (Norton, 1996) on products in Britain alone of which about two-thirds (Cottenden, 1999) is on absorbent products. It is estimated that the total cost of treating and managing incontinence will rise to at least £2b by the year 2020 (Royal College of Nursing, 1997).

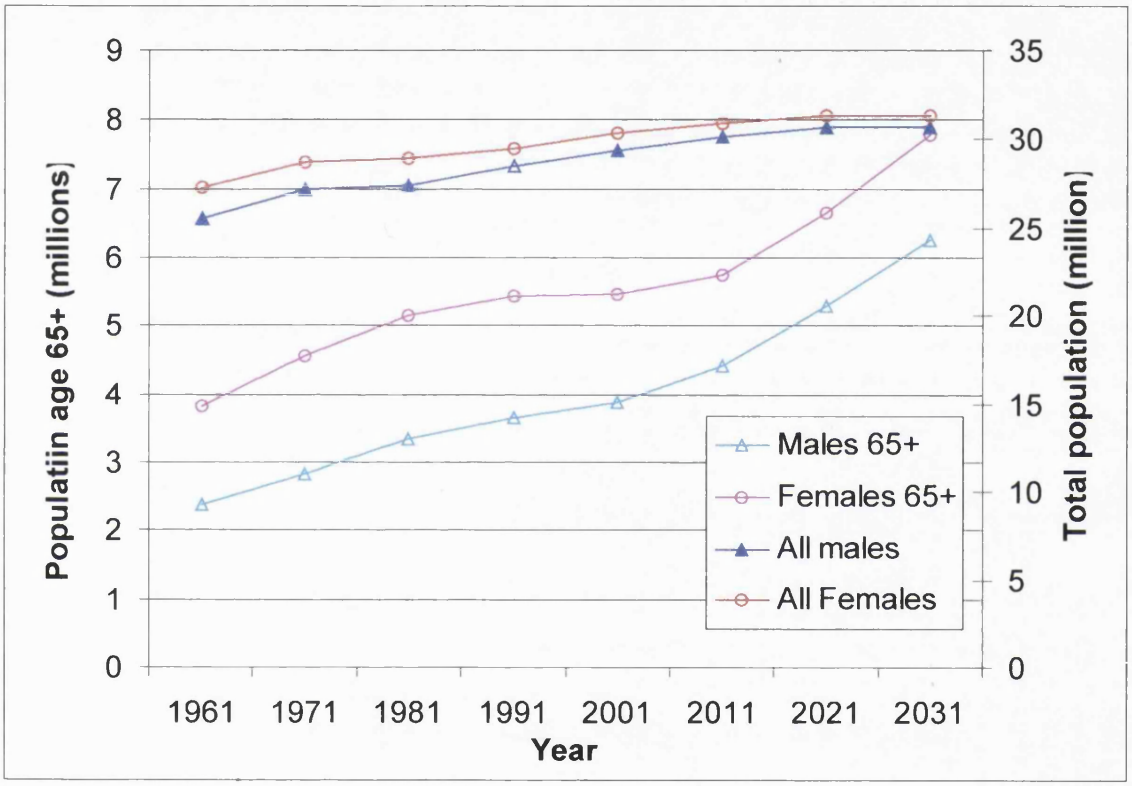

Fig.1.2 UK population trends 1961-2031

1.3 Incontinence Products

1.3.1 Types of incontinence products

Many devices have been developed over the years for containing excreted urine, in addition to others for preventing or controlling the leak in the first place. Apart from design improvements over the years, one reason for having so many different products on the market is the different physical needs of users, both in terms of the severity of their incontinence and their manual dexterity. Other factors such as aesthetics are also important. Other reasons for this variety include cost and product differentiation to obtain market share but, while the patent literature in this area is rich, the number of fundamentally different designs is limited. This huge range of devices, as catalogued in the Incontinence Products

Directory (1998), can be sub-divided in many ways, one of the most obvious being 'absorbent' and 'non-absorbent'. Norton (1996) provides a good over view of the range of aids available and their suitability for various conditions.

Non-absorbent products are sometimes more discrete and/or leak less than absorbent products but usually require greater manual dexterity to use. More non-absorbent devices are available for men than women because of anatomical differences. If a suitable non-absorbent product can be found this is probably preferable, although, the above reasons mean that absorbent products are the only choice for many sufferers, particularly among the elderly.

Non-absorbent devices include catheters and penile sheaths, which convey urine from the bladder into a collecting bag. Other examples include constrictive, occlusive devices, and stimulators. The aim of these is to retain the urine in the bladder until appropriate. These devices are not included in this study as they exploit completely different technologies to those used in absorbent products.

An example of the quantities of fluid that an incontinence product may have to manage was illustrated during a study of disposable body-worn pads for heavy incontinence (Cottenden 1993). In this study heavy incontinence was arbitrarily defined as at least 120g of urine voided into each of at least 50% of pads used over a two-day period. As can be seen from Fig.1.3, a wide range of urine weights were recorded, with some users frequently producing in excess of 300g although, the mean weight was much less at about 150g. The negative pad weights are an artefact due to the subtraction of an average dry pad weight from the wet weight.

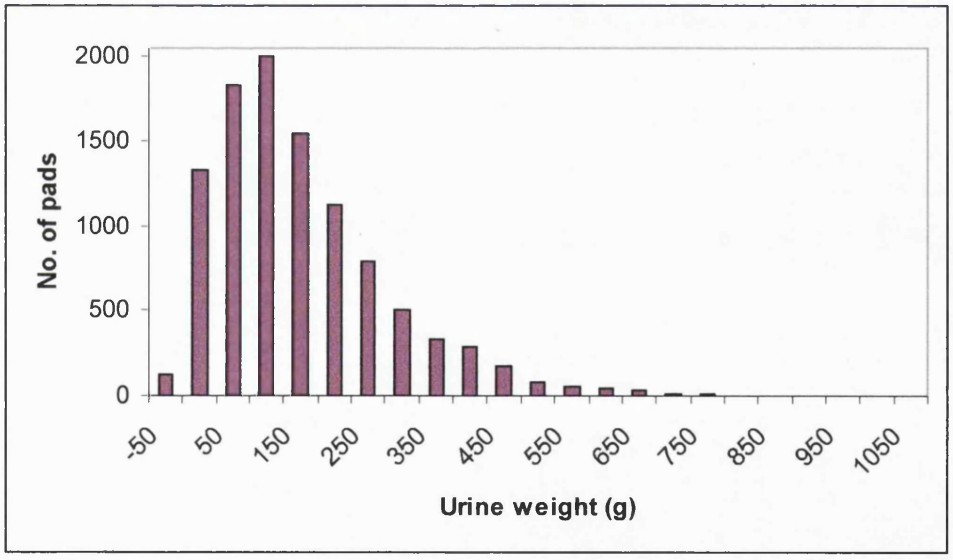

Fig.1.3 Frequency distribution of Urine weights in pads used by heavily incontinent adults

Flow rate, as well as total fluid volume, is an important factor when considering pad design. Although there have been many studies recording the flowrates produced during deliberate micturition, and this is routinely measured during clinical diagnosis, there is little information on incontinence events. However, one study (James and Niblett, 1988) sought to address this by measuring the number and volume of individual incontinence events that occurred during a program of activity including running,

jumping and coughing. The study found and characterised differences between two types of incontinence (stress and detrusor instability) in terms of volume of fluid loss per event and total fluid loss during program of activity. Both of these were higher for incontinence due to detrusor instability. Although they could not directly measure flow-rates their results suggest that these are also dependent on the incontinence type, flow-rates of 30ml/s or more being possible with detrusor instability,

1.3.2 Absorbent Incontinence Products

The absorbent section of the incontinence product market is the largest, accounting for about two thirds of all expenditure on incontinence products in the U.K. (Cottenden 1999) and can be further subdivided. A product can be *reusable* (made of materials that can be laundered and used again), or *disposable* (for single use). The other main criterion for distinguishing products is the way in which they are used. Products are either bodyworn, or a bed (or chair) pad placed underneath the person. It is worth mentioning the variety or bodyworn pads that are available. Disposable products can either be 'one-piece' (like a baby's nappy) or 'two-piece'. The two-piece products consist of a disposable absorbent pad and a reusable (normally) pant. This pant can be either a stretch pant or a product with a pouch to contain the pad. Reusable products may follow the same form as a disposable pad or be incorporated into an otherwise normal pant. The fact that there are currently nearly eighty products on the UK market (including the different sizes available) which can be categorised as large, two piece, disposable body worn pads (Fader et al. 1998), indicates the complexity of the task of comparison.

A selection of absorbent products, chosen to illustrate the main types of products described above, is shown in Fig.1.4.

Fig.1.4 A selection of absorbent incontinence products

a, Reusable bed pad ('Kylie Standard', Smiths Industries Medical Systems)

b, Disposable bed pad (International Disposables Corporation (UK) Ltd.)

c, Disposable two-piece body-worn pad for heavy incontinence ('Moliform Normal', Paul Hartmann AG)

d, Stretch net pants for use with two-piece pads ('Security Stretch Briefs', Müller elastics GmbH & Co.)

e, Disposable diaper-style pad for heavy incontinence (Attends medium, Procter and Gamble Ltd.)

f, Reusable pant for light incontinence ('Kylie style', Smith Industry Medical Systems)

Although there are many varieties, most disposable absorbent incontinence products have the following three components:

Coverstock - This is the top layer of the pad, usually made from a non-woven material and, ideally, having the following properties:

- It should help maintain the integrity of the pad, i.e. help to keep the product in one piece, preventing it disintegrating /breaking up.
- Allow fluid quickly into the pad but prevent fluid leaving the pad

- Provide a comfortable, skin-friendly surface in both wet and dry states. A skin-friendly surface will help to prevent the formation of sores and other forms of skin deterioration, a soft texture and ability to keep urine away from the skin will be useful in this respect.

Absorbent core - Perhaps the most important part of a pad. This is the component where most variation occurs. A typical disposable pad will contain some or all of the following materials:

- Fluffed wood pulp fibres of various grades
- Super absorbent polymers that swell up in urine, holding many times their own weight in fluid.
- Tissue paper

The functions of the absorbent core include:

- Absorbing fluid as rapidly as it arrives
- Holding on to fluid tenaciously, despite changes in pressure
- Remaining comfortable for the user (if the core breaks up it could form hard uncomfortable ridges)
- Being capable of receiving repeated fluid doses ('insults')
- and, if reusable, surrendering the fluid easily during washing and drying

To facilitate this multi-functionality, pads are increasing in complexity. Current trends are towards multi-layered structures with each layer concentrating on one aspect. For example one material may be good at receiving fluid quickly allowing a second material, with good water holding properties but slower reaction time, to slowly drain the first which would be left ready for a second 'insult' – as each application of fluid is called. The better the fluid management the less surplus absorbency is required. Such a reduction in the maximum absorbency would have a positive impact on the costs of manufacturing, laundering and disposal of products.

Plastic backing - acts as an additional barrier to escaping fluid whilst aiding pad integrity.

Other components that may be present in pads include:

- Shaping elastics, particularly in the crutch area, this is designed to reduce leakage in this area by making the crutch cup shaped.
- Cuffs, of similar material to the coverstock, protruding from the coverstock, mainly used to contain faeces
- Fastening or fixing devices e.g. sticky tapes to hold the pad in place
- Wetness indicator strips to aid the carer when deciding if a pad needs changing

Reusable incontinence pads will contain heavier duty, washable versions of these components with the absorbent core usually being made from non-woven felts.

Fig.1.5 and Fig.1.6 show the disposable absorbent pad from a typical two-piece body-worn product and cross-sectional diagram of a product with three absorbent layers.

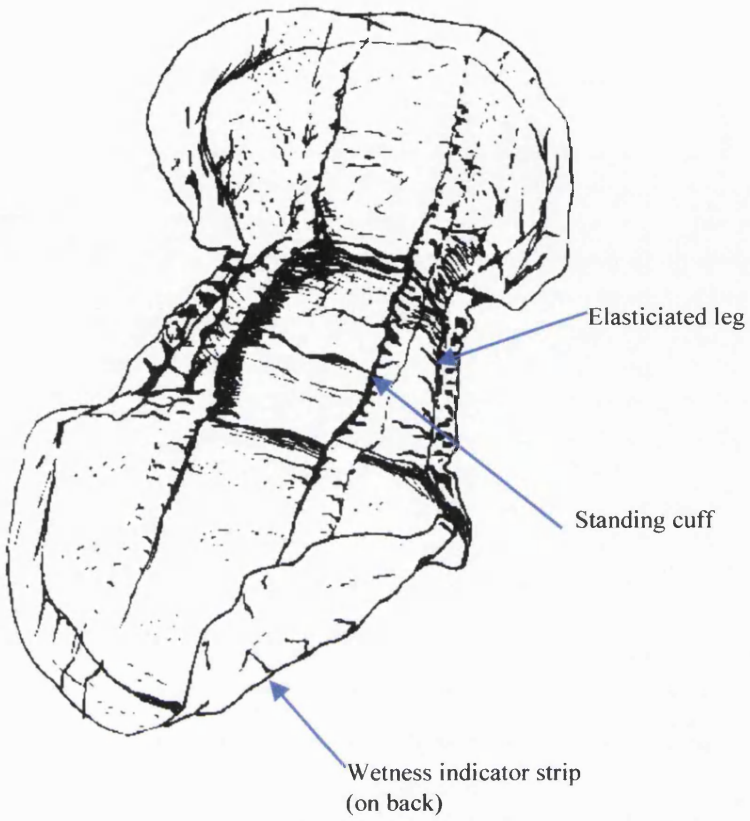

Fig.1.5 A typical disposable pad from two piece product

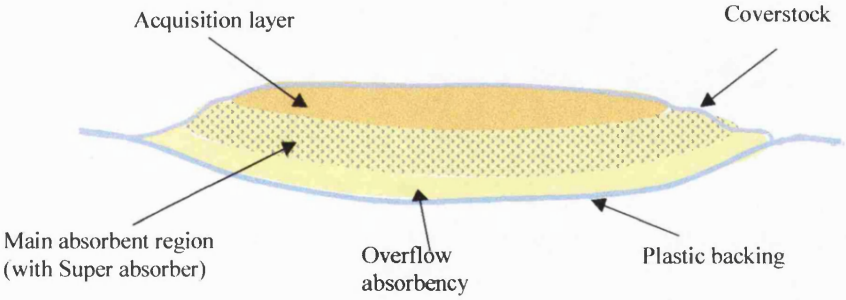

Fig.1.6 Cross-section through a typical multi-layer disposable product

There are advantages and disadvantages with both reusable and disposable pads. Reusable pads do not require as much storage space as disposable ones, only space for as many as are needed until the next batch are returned from the laundry. Cost-wise the initial outlay is much greater for reusables than for disposable pads, unless they are hired from a laundry, like sheets often are. Day to day costs may be lower for reusables as only the laundering costs need to be considered. For disposable pads the cost of disposal, as well as purchase, should be taken into account. Hygiene is another issue relating to reusable products, raising the question of cross-contamination due to inadequately laundered pads. However a

study by Cottenden et. at. (1999) demonstrated that the risk is minimal if the standard foul wash procedure specified by the NHS executive is followed.

The laundering versus disposal question raises environmental issues in addition to the cost issues and may be helping fuel the current trend which is shifting from disposable products towards reusable ones, particularly in the area of bed pads. The change is driven by the perceived cost and environmental savings involved. It is not as yet clear which of these two (reusable or disposable) is best. Defever et al. (1997) reviews the four studies in this area and finds their conclusions contradictory. The outcome of a study by Williams et al. who found that a specific reusable pad (Kylie) was significantly superior (40%) to disposable products, is in contrast to a studies by Brown (1994), McMurdo et al. (1992) and Sowell et al. (1987) The results of these three indicated that good quality disposable products were 16%, 1.5% and 70%, respectively, cheaper to use than reusables. Results regarding skin health were also inconclusive, following the same pattern as the cost results.

However, despite the wide range of products available, the performances of current pads are far less than desirable. One study of two-piece disposable pads (Fader et al.1998) recruited 228 subjects who each used between four and eight pad ranges. The users/carers were asked to fill in a questionnaire, on each product, after using it for a week. This study found that only 25% of products were considered good or acceptable by at least 90% of the carers. Another study run on similar lines, this time looking at bed pads, found their leakage rates to be unacceptable more than 50% of the time (Cottenden 1998).

There is much scope for product improvement. The reasons for this are that no device suits everybody and many of the devices do not behave ideally. As new materials and manufacturing techniques become available these are incorporated into the products and may improve the situation. Some improvement to design can be achieved rationally but a lot of product innovation is a 'black art' based on educated guesses by those in the industry. This is particularly true of absorbent products where interaction with the wearer is dynamic and complex. Although many laboratory quality assurance tests (see section 2.3) are carried out by manufactures and others, there is very little information on how these relate to the clinical setting. The little work that has been done in seeking to bridge this gap is mainly statistical, seeking significant correlations between leakage rates and laboratory quality assurance tests (Cottenden & Ledger 1983), not seeking to understand the mechanism behind the relationship.

It is this knowledge gap that the work described in this thesis seeks to bridge, by providing quantitative information and real time images of fluid distribution in incontinence pads

2: Literature review

2.1 Introduction

The perfect incontinence pad would:

- Never leak or smell
- Be visually discrete and not rustle
- Be economic to buy and dispose of or wash
- Be comfortable and promote skin health

Two main groups of people are interested in how products match up to these criteria:

- Those making purchasing decisions
- Product developers

People in the first group fall into three subgroups: those purchasing products for themselves, carers looking for products for a specific person, and budget holders, purchasing in bulk. Each of these is seeking to differentiate between many, subtly different, constantly evolving, products. Each will have different priorities in their decision making.

Although there is currently a lot of product testing that is done, this mainly (but not exclusively) consists of quality assurance type tests (see section 2.3). This thesis aims to take the work further than this into product imaging. For this reason this literature review briefly covers user evaluations and standard laboratory evaluations, areas which impinge on, but are not directly relevant to this research. The limited amount of work in the imaging and event logging fields is then reviewed followed by relevant information from other disciplines that form the basis for techniques proposed in this thesis.

2.2 Clinical evaluations of Incontinence pads

A clinical evaluation tests pads in a realistic situation and tests all factors (e.g. leakage, fit, smell) simultaneously. Many studies have been performed over the years (e.g. Cottenden et al. 1993, Fader et al. 1987) and an ISO protocol has been written (International Standards Organisation, 1996). This protocol sets out to address the limitations of many of the early studies, which either involved small numbers of products or methodologies that were not rigorous. However, studies that follow this protocol are time consuming and costly to perform. The authors of one such study (Fader et al. 1998) observed that probably 50% of the products had changed before the study was published. This was considered usual, although it was noted that some of these changes may have been in response to weaknesses highlighted by the study - a positive by-product of the study.

The data gathered in such studies is mainly qualitative, requiring subjective opinions such as to whether the pad leaked 'a lot', ' a little' or 'not at all'. Quantitative data in the form of pad weights can

also be gathered, for example to estimate the leakage performance at different urine weights, but this requires very many pads due to the statistical noise present is such data

2.3 Laboratory evaluations (non-imaging) of incontinence pads

There are many tests that can be performed on absorbent products within the laboratory setting and a variety of motives behind them. These tests can study the whole product, a composite section cut from the product, or the individual materials before they are assembled into a pad.

The simplest tests are usually quality assurance tests, designed to check, quickly and cheaply, that a sample (of anything from the raw materials to the finished product) meets the specifications.

Such tests are usually based around the following themes:

Absorption Capacity Tests, measure the volume of fluid a pad or sample will hold under little or no pressure.

Retention Capacity Tests, measure the ability of the pad or sample to hold water when under pressure.

Leakage Performance Tests, measure the volume of a specific fluid dose which is not absorbed.

Acquisition Time tests, measure the time taken for a specific volume of fluid to be absorbed under controlled conditions.

Wetback Tests, measure the amount of fluid that escapes from a pad/sample under pressure. This is usually measured by wetting a sample in a controlled manner and allowing it to soak for a predetermined time. Filter paper is then placed on the sample with a weight on top. After a set time the filter paper is removed and weighed. The difference between the dry and wet filter paper weights equals the mass of escaped fluid.

Wicking tests, these measure the ability of fabric to draw water out of a reservoir, usually against gravity. The result can either be expressed as the mass of water absorbed in a given time, or the height that the fluid has reached.

All of these tests measure parameters that one would expect to relate to clinical performance; for example the wetback tests may give an indication of how dry a subject's skin will keep, a factor which may have an effect on skin health. For this reason tests similar to the above are often used when designing or comparing products.

The third area into which laboratory tests may fall is whole product testing, again trying to predict clinical performance but with very little published validation of the results by comparison with clinical data. This approach often uses anatomically accurate mannequins for leakage performance and absorption capacity tests. These mannequins come in a wide range of sizes and postures, with some having moving legs to imitate the effect of walking. Most incorporate fluid delivery systems for applying variable flow-rate/time profiles. Most mannequin work, however, is a 'black box' approach, assessing the probability of the product leaking. Apart from possibly locating the sight of leakage no insight is

given into the leakage mechanism. Also little work on the clinical validation of mannequins has been carried out and what has been done suggests poor correlation between clinical and mannequin data (Cottenden, 1993).

Despite this intuitive link there is very little published information on how these factors affect clinical performance. The ability of these tests to predict the performance of pads in clinical use is poor. Cottenden et.al. describe two series of experiments designed to assess the ability of such techniques to predict the clinical leakage performance of large disposable, body-worn pads (Cottenden et. al, 1993) and small body-worn disposable incontinence pads (Cottenden et. al, 1997). In each case a small number of products (six or nine) were chosen, representative of all common designs. These were tested clinically by subjects who normally used a similar product. Each subject used each product for one week, saving each used pad for subsequent weighing and noting whether the pad had leaked a lot, a little, or not at all. At the end of the week the subject (or their carer) were asked to rank the leakage performance of the pad on a five-point scale. The leakage data obtained was then analysed using a linear logistic regression model to determine the leakage performance of each pad as a function of urine weight.

Technical test centres were recruited from a range of countries and asked to run whatever tests they thought would produce a correlation with the clinical data. In each case more than 30 tests were run resulting in over a hundred test variables.

The correlation between each of these technical test parameters and the pad leakage rates at representative urine weights were calculated.

In the second trial, of the 153 test variables only two yielded at least one correlation which reached significance at $p=0.01$ level. A similar proportion of test variables performed well in the first study. This indicates that a lot of work needs to be done in bridging this gap between the laboratory and the ward.

As a result of the above studies two ISO standards have been written (International Standards Organisation 1996 & 1997). The first of these is a simple absorption capacity measurement for the comparison of large incontinence products, with the proviso that these capacities are an overstatement of clinical performance. The second standard relates to products for light incontinence and cites a wetback test as the appropriate leakage performance measure.

Tests from any of the above categories could be used to study interactions of fluid with absorbent products, looking more at absorption mechanisms than how well the sample performs. For example, comparing the results from an absorption capacity test with those from a vertical wicking test would give an indication of how much the fluid flows freely through the pores of the material and to what extent the wicking properties of the fibres move the fluid from its point of entry. The more the fluid that is absorbed during vertical wicking compared to the absorption capacity test the greater the effect of wicking is likely to be in moving the fluid about the material. Such results would be used for further product development.

A number of companies run test houses which specialise in testing these and similar products. A selection of such companies are mentioned below.

Courtray Consulting Labservice, in France, have a range of equipment, from acquisition and wet-back tests to mannequin tests and an imaging system that will be mentioned separately

Datasorb is an UK based company, one of their latest products is called the 'PROTESTER' and can automatically test pad samples.

ATS, in France, offers a range of tests, including the use of mannequins and a consumer test service. These are mainly designed for the baby diaper and sanitary product markets.

Hy-Tec produce, among other products, the 'Ekotester' which incorporates a grid of 9 resistive sensors for measuring wicked height during vertical wicking. The kit can also look at fluid absorption and retention under pressure.

2.4 Devices for studying incontinence pads – imaging and event-logging

Some attempts have been made to image whole pads both in the clinical setting and the laboratory. In addition attempts have been made at providing clinical enuresis alarms to recognise incontinence events. These are detailed in this section. Apart from these techniques, and a limited use of dyes and visual inspection during technical testing, no imaging of the fluid spread in absorbent incontinence products has been tried.

Imaging and event logging have been grouped together because, between them, they cover the area of this work, namely imaging of products as worn by subjects. Very few current devices meet both sides of this criterion, the ability to image and to be used clinically, but current techniques that may be extended to do so are considered here.

2.4.1 Resistive imaging (Cottenden 1987)

This work relates the use of electrode pairs invasively placed within a pad. Each electrode pair consists of a twisted pair of lacquered wires, bared at the tip and held approximately 2mm apart. These are inserted, in a suitable array, through the back of the pad where they are used to monitor the resistance of the material between the tips of the pair of wires. The resistance of a dry pad is very high, essentially that of air, when the pad becomes wet this resistance falls to virtually zero because urine is a conducting solution. This means that a sudden drop in the electrical resistance between each pair can be detected that signals the arrival of a fluid front. A system has been constructed which monitors the resistance between each pair every 0.1s and detects the time at which this resistance drop occurs. The times of these changes are logged and then used, with knowledge of the positions of each electrode pair, to draw time contours indicating the progress of the fluid front.

This system was designed so that the sensors were electrically isolated from the mains power supply, so as to meet the appropriate legislation applying to clinical instruments. It has been used to monitor fluid spread in a pad that was being worn. The images produced are real-time, two-dimensional images in the plane of the pad although some information in the third, through thickness, dimension of the pad may be gained if sensors could be placed within different layers of a multi-layer pad. The

geometry of the pad did not cause limitations as the electrodes could be used in any known position. Although this system provides accurate, easily understood information it has a number of major limitations. The system is not suitable for routine studies, due to the care and time needed in manually positioning the electrodes within each pad, and the fact that the structure of the product is inevitably altered a little by the presence of the sensors and the process of positioning them. Another disadvantage with this system is that, due to the limited number of imaging sensors used, the data set produced is sparse. Wetting times are known at the locations of the sensors surrounded by areas for which no information is available. The other problem with this data set is the uncertainty of electrode positions, which may have shifted over time, due to patient movement or pad disintegration, or upon removal of the pad. This introduces a degree of uncertainty into the results.

2.4.2 Resistive mapping using pin electrodes (Shishoo 1987)

This independently developed technique is very similar to that in the previous section. Again the fluid flow imaging is achieved through observation of changes in electrical resistance. In this second case pin electrodes were formed into a 'bed of nails' onto which a pad could be pressed, overcoming the need for a skilled, time-consuming set-up for each experiment. Although the use of pin electrodes makes the rig suitable for the routine testing of products it prevents the system from being adapted for experiments on pads as they are worn by patients. The pin nature of the electrodes used, which were attached to a curved frame and designed to pierce the plastic backing of the pad, would be likely to penetrate sufficiently far, in the stressed condition of pad usage, for patient comfort and safety to be in jeopardy.

In comparing these two techniques it can be seen that whilst these techniques produce accurate images, with three spatial and one temporal dimensions, there is a trade off between having a robust, easy to use system, and one suitable for use on pads worn by patients.

2.4.3 The Urilos nappy (James et al 1971)

James et al developed a device for use in urodynamics investigations that became known as the Urilos nappy. Like the above techniques this nappy utilised the change in electrical resistance caused by the presence of urine. The measurement sensor consisted of a pair of elongate, interleaved electrodes embedded in a reusable nappy or bed pad. The electrodes could be any reasonable configuration, e.g. interleaved spirals, to cover the area of pad likely to get wet.

'When incontinence occurs in a patient wearing the nappy, a zone of the area covered by the electrode becomes moist' and this results in a change in electrical conductivity whose magnitude depends on the size of the wet zone. Due to variations in the electrical properties of urine, even in a given patient, the nappy had to be preloaded with an even distribution of an electrolyte before electrical conductivity could be consistently related to urine volume.

The device fulfilled the design aim of quantifying urine leakage as a function of time and had a repeatability of 20% over a range of 1-100ml. However, this is not an imaging device, giving no

indication of the fluid distribution. Also because the electrodes were built into the nappy they could not be applied to other products without severely disrupting the pad structure.

2.4.4 X-ray Profiles (LIXI 1996)

A system has been built which enables X-rays to be used to produce two-dimensional projections of the three-dimensional fluid distribution within wet pads. This system provides excellent 2D resolution but no information in the third dimension. The system would be suitable for routine lab use, but would not be suitable for clinical use due to the inherent danger of ionising radiation to biological tissue. In addition this system has been used to study the sodium content of super-absorbent polymers, an area which is not relevant to this study.

2.4.5 Thermistor and impedance warning detectors (Tamura 1995)

Two other techniques, which do not involve imaging, have been used to detect/log incontinent events. One uses temperature changes, while the other utilises the conductive properties of urine to complete an electrical circuit. The aim of these devices was the detection of fluid arriving anywhere in the pad so as to save care time and help maintain hygiene, by changing pads on wetting rather than at pre-set times when the pad may either still be dry or have been wet for hours. Both of these systems functioned well but had no need to determine spatial resolution.

The fundamental principles utilised for the impedance detector are the same as those used in the resistive methods and add no new insights. The Thermistor device, which was slightly less reliable (detecting 13 out 17 events as opposed to 32 out of 35 for the impedance device) is unsuitable for transfer to imaging. Complications arise due to the small volumes of fluid involved and the fact that the fluid would cool, which would hinder calibration of the sensors.

2.4.6 An overview of possible techniques (Yerworth 1996)

Two of the techniques mentioned above were used in a Masters degree project, along with a number of other approaches, which had not previously been used for studying incontinence. In all, seven methods were assessed for potential further development. Three of these (capacitance imaging, electrical impedance tomography (EIT) and electrical capacitance tomography (ECT)) were concluded to be impractical or less effective than other techniques studied in terms of their sensitivity to fluid presence and their spatial resolution. The remaining four - resistive mapping, optical imaging, X-ray imaging and MRI (Magnetic Resonance Imaging) were recommended for further study. It was anticipated that MRI was more likely to be suited to the study of fundamental fluid interactions between product components, rather than whole product studies. This is because of the tradeoffs between field of view, spatial resolution and temporal resolution meant that high resolution could not be obtained in real-time. This was made worse by the fact that the region of interest in a pad does not occupy a single plane but would necessitate multiple image slices being gathered.

2.4.7 Panda (Courtray Consulting, Lab service 1999)

This is a commercially available imaging technique, which is offered along with a range of other services. The device, known as the 'Panda' captures video images of fluid spread at the patient surface of a product from inside a transparent mannequin. Although this is a useful visualisation tool, quantitative analysis of such images would be difficult because of the complex geometry involved and the acute angles with which some areas of the product are viewed by the single camera.

2.5 Optical sensing systems for other uses

This section looks at a number of other situations to which optical imaging (other than photo graphic) has been put. The examples given were chosen for their possible relevance to this work.

Hill (1998) describes a system for the rapid non-destructive testing of carbon fibre reinforced plastics. This system utilises reflected light to determine the orientation of carbon fibres in each layer of a carbon fibre reinforced plastic component. A probe is lowered into an existing hole in the material under test. Laser light is shone at each point on the surface in turn building up an image of the reflected intensities. The intensity of the reflected light is greatest for fibres orientated perpendicular to the laser and is least when they are parallel to the beam. The smallest probe size fits in a 4mm hole. Although reflections from fibres are of interest here, the carbon fibres are embedded neither in air nor in water. Also this is a static situation, not dynamic. There are many other differences between this situation and that of fluid flow in an absorbent product, such as constraints of sensor size and volume scanned. This test also has the major disadvantage of requiring a hole in the sample.

Elwell (1995) has written a guide to medical uses of near Infrared spectroscopy. This is representative of most clinical uses of light for diagnostic purposes and describes the use of near infrared radiation for determining the various characteristics of blood, e.g. flow, volume and oxygen saturation. All of these parameters are measured by comparing the absorption of two or more wavelengths of light due to the presence of haemoglobin compounds within the tissue. No such strong absorbers are consistently present within urine and thus relative absorption of light can not be used in the current study.

Graham (1998) and Michie et.al. (1995) both describe fibre-optic sensors which "can detect and locate water at any point along the length of a fibre-optic cable, which can be many kilometres in length". Each device consists of a hydrogel coated, inert fibre core to which an optical fibre is bound. In the presence of water (or other trigger which the hydrogel has been designed to respond to) the hydrogel will swell, bending the optical fibre and causing light attenuation and backscatter. This fibre is coupled to an optical domain reflectometer, which uses the delay in receiving the backscattered light to calculate the location of the trigger. The authors anticipate that such a system could be used to detect the concentrations and positions of specified bio-molecules. This could be done medically by incorporating the such optical fibres in to skin sensors, and catheters for internal investigations.

This technique was assessed by Michie to be able to detect water ingress regions 50cm long within a 100m sensor, incorporated into a bridge. It was also found that the induced bend in fibre, due to

the swelling hydrogel, was of the order of 5μm. Such a scale and stiffness are incompatible with the requirements of this project, where the resolution required is 20mm over a 50cm length or smaller and sensor bending due to subject movement is likely to be far in excess of 5μm. It is probable that at this scaling the timing necessary would only be possible using pulsed lasers and a streak camera, which would be impractical and uneconomical.

Another disadvantage of such a technique is that the sensors would have to be placed inside the pad, which would disrupt the structure.

It is worth noting here that Proctor and Gamble (1999) have proposed a patent for using a fibre optic cable to detect wet in diapers. This, however, is not seeking to identify the position of the fluid.

In conclusion, the above novel applications of light to imaging are unlikely to contribute significantly to the area of interest, although the same fundamental properties of scattering and absorption of light could be utilised.

2.6 Relevant X-ray literature

The possibility of using X-ray stereography was raised in previous work (Yerworth, 1996). X-ray stereography uses a pair of images of an object, obtained from different imaging angles. For viewing, one image is presented to each eye, normally with the aid of a special viewing device, which allows each eye to view only one image. This approach relies on the brain's ability to reconstruct a three dimensional image of the world from the information supplied by the two eyes.

The attraction of X-ray stereography is the excellent resolution that can, theoretically, be obtained in time and three-dimensional space. Also there is great flexibility in what detection system is used. X-ray film is cheap, with high resolution, but requires a delay between images to change the film. CCD and Image Intensifiers can work in real time but have their own disadvantages: with CCD this is the small size of the detector; and with image intensifiers, it is their availability. Large area solid-state detectors are another option.

The major problem with X-ray stereography is the necessity, if one is to produce real time sequences, for either two X-ray heads (Tobe et al. 1966) or a mechanism for moving a single head accurately in a negligible time (Takahashi et al. 1976 and Mutsumasa and Yasashi, 1980). The latter requirement is difficult considering the weight of the X-ray head. This problem is in addition to the problem associated with all X-ray work, that X-rays are ionising radiation and so could not be used for on-patient studies.

X-ray stereography was developed in the early decades of this century (Middleditch, 1918) for medical use but it is now rarely used except in some dental situations, having been superseded by CT (Computerised Tomography). CT provides images of slices through an object. Although this provides a superior diagnostic tool for clinicians the information obtained is of much lower spatial resolution than X-ray stereoscopy and images can not be obtained in real time.

From the above it is noted that finding a working, real-time stereography system is not straightforward. Dental applications are unlikely to need a real time system.

The viewing of image pairs is a separate topic and developments in this area are not restricted to X-ray stereography, but are also relevant to optical photogrammetry and other areas. The viewing system is independent of the method by which the images were created. Aerial photography, surveying and microscopy all make use of stereoscopic effects and have developed stereoviewers. These viewers range from simple mirror arrays to computer controlled devices that enable 3-D co-ordinates to be calculated. Any of these could be used, if available, to view X-ray images.

It can be seen from the above that the limitations likely to be encountered if this technique is used centre on the practical availability of measurement systems, not on what is theoretically achievable.

2.7 Resistive sensors for other uses

The resistive sensors discussed above provide only binary information (Cottenden, 1987 and Shishoo 1987); that is, they give a dry or wet reading. In soil science, however, a resistive sensor has been developed which yields the degree of saturation (Colman, 1949). This poses similar problems to the aforementioned techniques with the addition of two other significant disadvantages. Firstly, the sensor is not a real-time instrument. It takes several minutes for water to diffuse into the device and reach the same situation level as the surrounding soil. Secondly the sensor is relatively large at a few cm square. This would affect the spatial resolution achievable. These problems are likely to make this design unsuitable for transfer to the study of incontinence products.

3: Aims and Objectives

The aim of this project is to facilitate the design of improved incontinence pads by the development of instruments/techniques capable of plotting the distribution of urine in absorbent materials, in real time, in both the clinical and laboratory setting. Such a system would complement existing pad analysis techniques and offer some significant advantages, including the ability to combine quantitative data collection with clinical reality.

The motive behind this project is to improve the performance of current absorbent incontinence products and hence reduce physical and mental discomfort experienced by users. Other benefits could potentially be to ease the burden on carers and to improve the efficiency of products whilst reducing their cost. Thus the objective of the research is to provide a toolbox of imaging techniques for pad designers. The information gained from these techniques will directly enable design problems to be more specifically identified and addressed than at present. This should lead to more rational design strategies. These techniques should also provide a means of testing how clinically realistic the results from quality assurance tests are. This would indicate the significance of the results provided by these tests.

A further potential advantage is the apparatus would yield data whose relationship to the clinical performance of products is established and understood. This would reduce the need for costly, time consuming, and noisy (in terms of data repeatability) clinical trials of prototype products. This should speed up the design process.

All these effects would combine to enable the development of improved and better understood products. Ideally such a toolbox needs to contain techniques that either singly or together:

- Image 3D fluid flow in opaque absorbent products in real time.
- Are suitable for use with a patient worn pad and in the laboratory.

Furthermore:

- The system(s) should not disrupt the structure of the pad.
- It/they must be robust, economic and usable by ward/nursing home staff.
- It must be possible to display the information it/they yield in clear, logical format.

A multi-pronged approach is taken to the design of this toolbox, utilising the complementary techniques of resistive imaging, optical imaging and X-ray imaging. This strategy is based on the

findings of previous research (Yerworth 1996), which indicated that no one technique would be able to fulfil all the above criteria.

Resistive Imaging is the most basic technique, capable of forming binary images of the fluid distribution in patient worn pads and developed over ten years ago (Cottenden, 1987). Optical imaging has the potential to fulfil most of the criteria and is the main technique developed within this project. X-ray imaging, in various formats, is the only technique identified, which is suitable for 3D images but is also useful for high-resolution, two dimensional, studies. Apart from the work by LIXI (1996) neither of these last two techniques had been applied to the study of incontinence pads previous to a very brief assessment of their potential in a precursor to this study (Yerworth 1996)

Thus, before the main area of optical imaging is addressed, the supporting techniques (resistive and X-ray imaging) will be described, and their further development specific to this research detailed (Chapter 4). Also included in Chapter 4, is a description of a fluid delivery system, necessary for the realistic replication of fluid insults in the laboratory, which was designed and built for this work.

These various strands are brought together in the final chapters where they are used to support and validate each other, adding to an overall picture of pad performance.

4: Supporting techniques

4.1 Resistive imaging

4.1.1 The theory

The electrical resistance between the ends of a pair of wires is dependent on the material that separates them. Air has a high electrical resistance relative to urine, an ionic solution

Therefore if the resistance between two wires placed within a porous non-conducting material is measured it can be ascertained whether the material is wet (low resistance) or dry (high resistance) at that point. If measurements are taken at a series of discrete points an image of the wet area can be built up and by monitoring all these points over a period of time a sequence of images can be produced.

4.1.2 The 'Pee plotter'

Throughout this work an existing measurement instrument has been used (Cottenden 1987). A simplified description of this instrument is given below:

Each sensor consists of a twisted pair of lacquered copper wires that have the lacquer stripped off for a few millimetres at one end. These ends are held approximately 2 mm apart with non-conducting adhesive, as shown in Fig.4.1. These sensors must be placed within the absorbent material to enable measurements to be made, piercing any plastic backing.

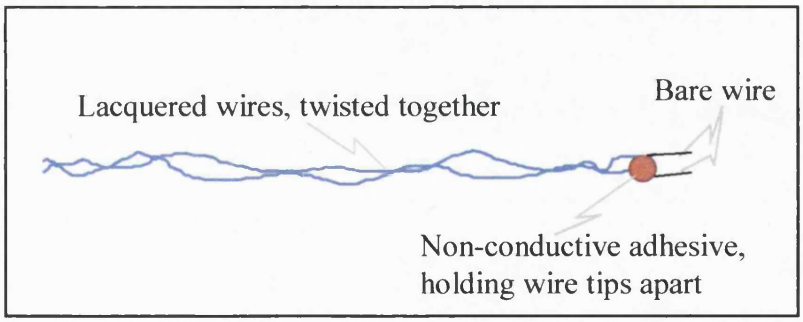

Fig.4.1 Schematic diagram of a resistive sensor

The current equipment is designed to use up to 128 of these sensors, which can be held in any appropriate configuration. For simplicity, the sensor pattern was usually based on a rectangular grid marked on the back of the product to be studied, as it lay flat. Instrumenting a pad in this way did not affect its ability to conform to the shape of the wearer during use.

The array of measuring sensors was scanned every 0.1 seconds by a control unit. This unit generated a periodic test voltage that was applied to one wire of an electrode pair. The resulting current, flowing in the other wire was sensed and compared to a threshold value. This is shown schematically in

Fig.4.2. The time at which the pad current first exceeded the test threshold, due to a drop in the resistance between the wire tips, was sent to the host computer along with the sensor number. This time corresponded to the time at which water arrived at the location of the sensor. The system was designed so that once this threshold had been crossed no further monitoring of the sensor was performed for the duration of the experiment.

A false wetting time could arise if the wire tips become bent so that they touched. This, combined with the single voltage threshold present mean that further wetting of that sensor, or reversal of a short-circuit between the wire tips due to pressure changes, could not be observed.

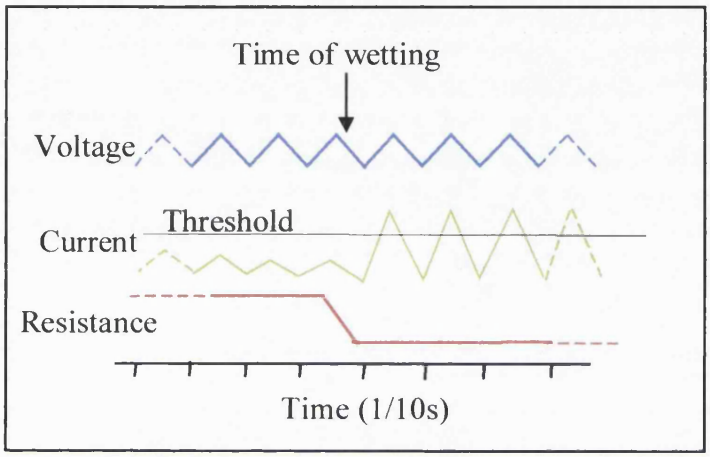

Fig.4.2 Comparison of test voltage with pad voltage

Fig.4.3 shows the complete system as used in clinical experiments. The sensor tips were embedded in the pad in an appropriate grid pattern then the rest of the wire was gathered into one of four bundles which was plugged into the connection box when data collection was ready to start. A stand for holding the connecting box next to the subject is not shown in this picture. The connecting box was linked by 2m long leads to the control unit. This enabled the rest of the apparatus to be placed a discrete distance from the subject. The control box was in turn controlled using a dedicated programme on a computer.

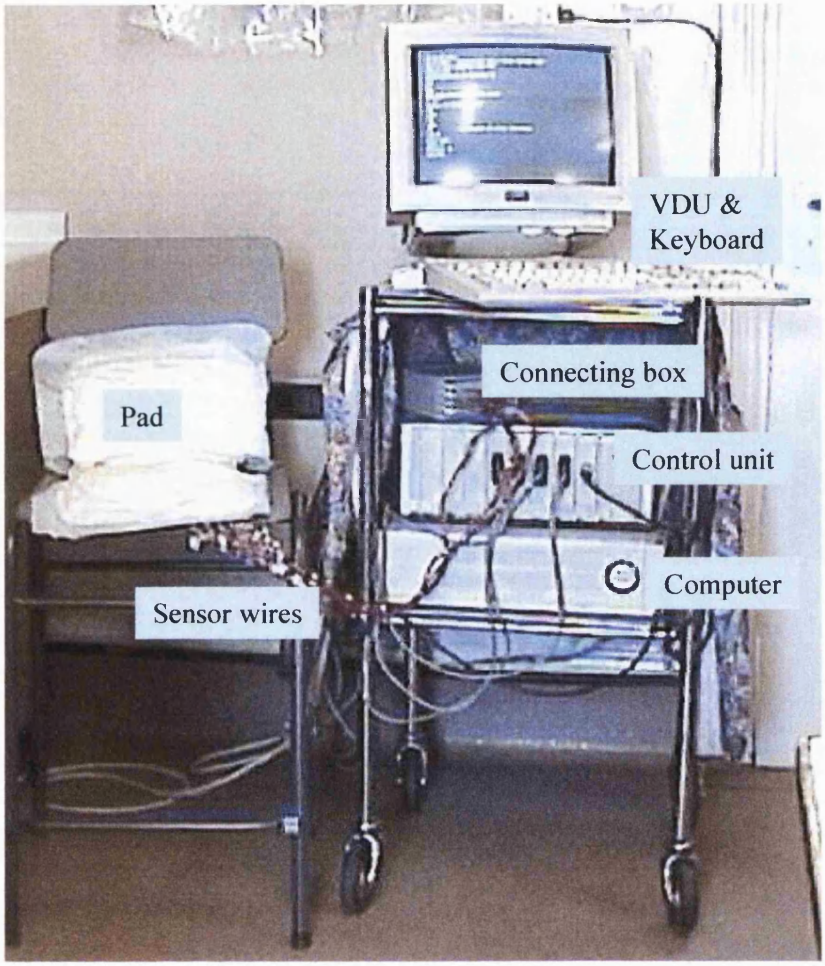

Fig.4.3 The resistive imaging device ready for a clinical experiment

The wetting time and electrode number pairs, generated in this way, were used with the aid of an interpolation routine, to draw a contour map of wetting times which indicated the progress of the fluid. However, with more complicated patterns of fluid spread a better method of data presentation is shown in Fig.4.4 and Fig.4.5. These diagrams indicate both sensor position and status. Each pixel in the image represents one sensor position, within a rectangular array. Due to the limited number of sensors, and shaping within the crutch region of many absorbent pads, not all these positions were occupied by a sensor. Those pixels that did not contain a sensor are coloured black. These two diagrams represent temporal information in different ways. The data used in these figures was obtained from a clinical experiment using a Molyform extra pad (see Table 8.2 for details). The subject was sitting for the duration of the experiment and the final weight of fluid in the pad was 150g. Fig.4.4 shows a series of images, reconstructed from the data with the pixels corresponding to all currently wet sensors coloured white. The number above each image is the time, in seconds, since the estimated time at which fluid application occurred. Fig.4.5 shows a single image frame but with the pixels colour coded according to the time interval in which the sensor registered wet. Again 0s is the time of fluid onset, not the start of data collection. With both these figures a non-linear time scale is used so as to show immediate and long-term effects of fluid application within the same figure. In both these images it can be seen that some

sensors, distant from the fluid entry point (marked in Fig.4.5), registered wet, some doing so from the outset of the experiment. It is likely that these sensors were short-circuited, in the process of insertion, or by transiently high pressures as the pad was put on.

Although the figures imply that each sensor covers the whole area of the pixel, whereas they actually provide a point measurement at the centre of the pixel, these figures are less prone to spurious artefacts than contour maps of interpolated data. One reason for this is that the information is not continuous, with some areas not containing sensors. Another reason is that contour maps highlight those sensors that failed or were slow to register as wet due to incorrect positioning of the sensor or failure of one of the wire tips to pierce the plastic. Two such sensors are marked on Fig.4.5 and are present in the same locations in Fig.4.4.

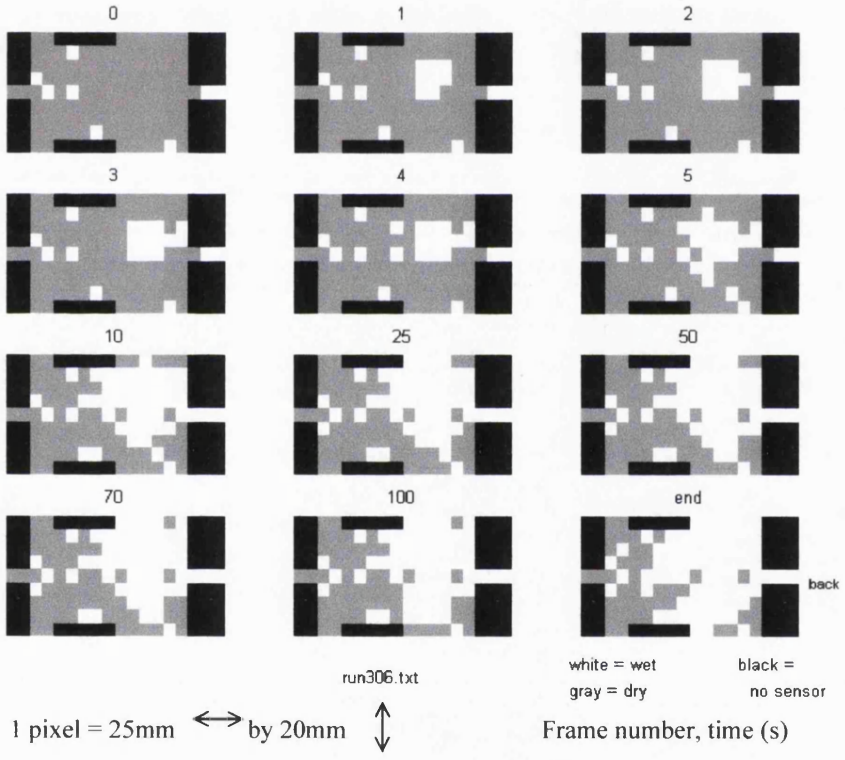

Fig.4.4 An image sequence, time normalised to start of fluid insult.

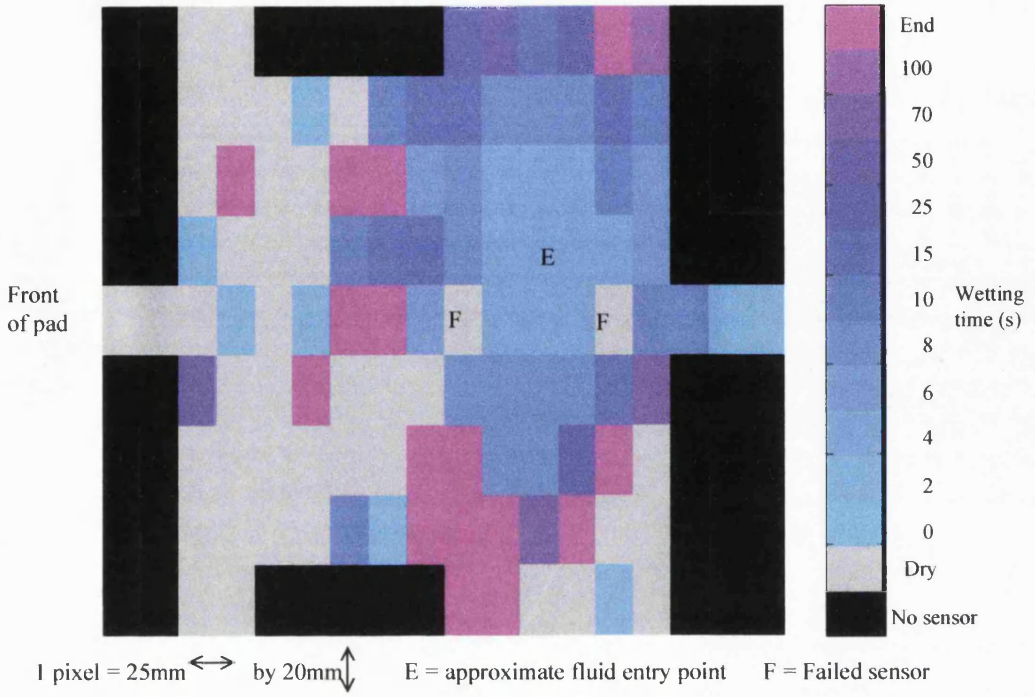

Fig.4.5 Typical image, time normalised to start of fluid insult

The information contained within an image sequence such as Fig.4.4 can be converted into a contour map of sensor status at a single time. This should not be confused with the contour maps of wetting time mentioned above. Contour maps of sensor status (see Fig.4.6) use two contour levels: one defining the area containing sensors and the other containing all the wet sensors. This method of display enables information obtained using the resistive sensors to be overlaid over data from another source.

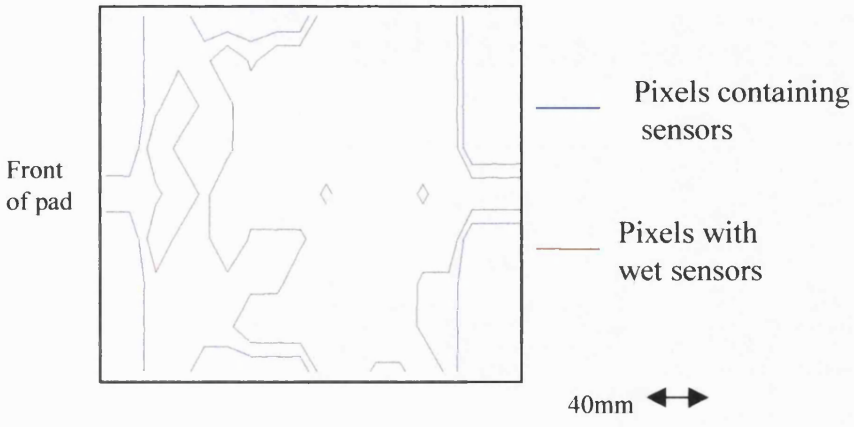

Fig.4.6 A contour plot of sensor status

4.1.3 Clinical experiments

Clinical imaging of incontinence pads was carried out using resistive sensors. Initially only 64 sensors were available and were arranged in a pad (Molyform extra, see Table 8.2 for details) as shown in

Fig.4.7. This was used in a clinical experiment with the subject in a sitting position. The final weight of fluid in the pad was 138g. Although this image shows the fluid spreading out, a lot of information is missing because of the sparse spacing of the sensors. Also the wet area extends beyond the region covered by sensors. In view of this, more sensors were made so that the number of sensors was increased to 112. Typical results gained using these sensors, with more even coverage of the pad, have already been seen in Fig.4.4 and Fig.4.5. These clearly show that the fluid entered the pad behind (right of picture) and slightly to the right (top of picture) of the pad centre. In this particular case (Fig.4.5) the wet area again extended beyond the region covered by sensors. The resolution of these images is dependent on the spacing of the sensors which was varied from 20mm by 20mm per sensor to 25mm by 20mm depending of the size of pad and volume of fluid expected. Other resolutions are possible, depending on the size of area to be studied.

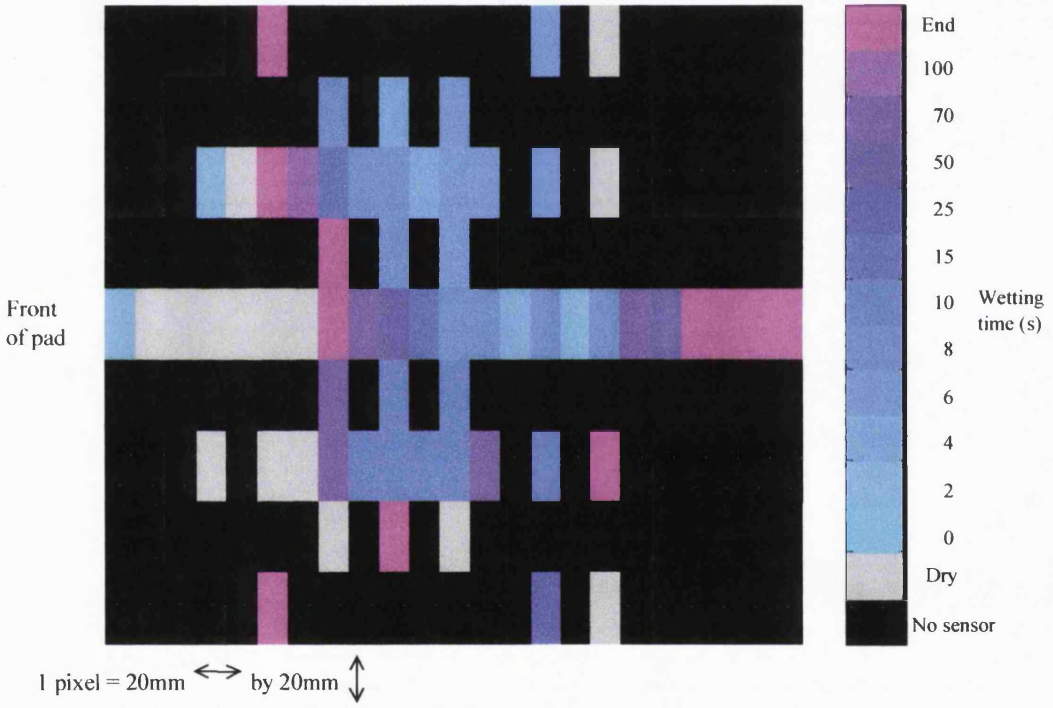

Fig.4.7 An image using 64 resistive sensors.

4.1.4 Limitations of the system

This equipment enables unambiguous data to be gathered on the wet/dry status of different pad locations, revealing the dynamic fluid distribution in pads. Importantly, the system is safe for clinical use enabling products to be studied under the same conditions as they are normally used.

However, a number of problems exist with the current system. Only binary information is obtained about the wet/dry status of a sensor and this cannot easily be changed. This means that the degree of fluid saturation at a given point cannot be determined. In addition the system is unable to detect the re-wetting of sensors that occurs during repeated insults. This means that secondary insults can only

be identified if they cause the fluid spread to increase. The arrival time of these insults is only estimated approximately as an unknown time lapse is required for the fluid to spread from the point of entry to beyond the original wet area. Also, although specified as checking all sensors every 0.1s, the current set-up (which was developed in 1987) only allows one sensor change to be recorded per 0.1s period. Thus if several sensors trigger simultaneously, timing information becomes inaccurate. This could be resolved with updated electronics.

A fundamental limitation with resistive imaging is that the sensors have to be inserted inside the pad backing in order to make electrical contact with the fluid, thus slightly disrupting the pad structure. Although sensors for use in the laboratory can be made ridged enough to pierce the plastic of a pad pressed on to them, such sensors would pose a hazard to the subject in a clinical trial. Therefore soft wire was used for the sensors necessitating a time-consuming set up period for each experiment as a slit had to be made in the plastic for every sensor, which was then slipped inside and fixed with sticky tape.

Although it is possible to place individual sensors in different pad layers the accuracy with which their positions could be maintained when the pad is deformed during use dictate that this device is essentially only capable of monitoring fluid spread in a single plane, albeit curved.

4.1.5 Conclusion

Despite these limitations this device was already available and approved for use with human subjects by the start of this project. This meant that a number of data sets could be obtained from the clinical setting of a long-stay ward for the elderly. This data was used for comparison with laboratory data from other techniques, in order to assess their faithfulness in imitating the real situation. This work is described in section 7.3.2.

4.2 X-ray imaging

4.2.1 The Theory

A conventional planar X-ray image is produced by passing a divergent beam of X-rays, originating from a focal spot, through a substrate and detecting the resultant intensity pattern using any of a range of detectors. The most common of these detectors is radiographic film, which is very similar to photographic film in that it is darkened where an X-ray hits. This produces very high-resolution images (down to a few tens of microns) and can be digitised using an ordinary scanner or specialised digitiser, depending on the quality required. The efficiency of the film is very low (<1%) and can be increased through the use of intensifying 'screens'. These are plates that enable a much higher percentage of the X-rays to be captured: a 45-fold increase in efficiency is typical (Farr et.al, 1997). These screens usually contain compounds of rare earth metals that readily capture X-rays. The energy from the X-ray is then re-emitted as visible light that can be detected by the X-ray film. This improved efficiency is at the slight expense of resolution because of spreading of light from the point where the X-ray was absorbed in the

intensifying screen. There is a wide range of screens available with different efficiencies – or speeds - depending on the use.

Other detectors enable continuous real-time monitoring to be achieved. However, these are usually less efficient or have lower spatial resolution than film/screen combinations and are less readily available. Examples of these detectors are image intensifiers, CCD chips and solid state detectors.

Stereographic X-ray imaging, as mentioned in the literature review, uses any of the above detectors to produce two views of the object. A known angle or distance separates these views. Stereography does not produce a true 3-dimensional representation of the object but relies on the fact that the human brain can 'reconstruct' a model of the world from the two views presented to it, one view to the left eye and one to the right.

Therefore, all that is needed for image reconstruction is to present two views of an object, one to each eye, and the brain will automatically do all the processing, combining them into one 3-dimensional image. A viewing system is normally needed, so that each eye sees only the image assigned to it. This viewer may consist of an arrangement of mirrors and eyepieces, as shown in Fig.4.8, or a pair of 'glasses' with colour (usually red/green) or polarisation filters. For the latter case the images must be suitably encoded, e.g. one image tinted red, the other green when using coloured filters. The images can be presented in hard copy or electronically. Another method, only suitable for electronic images, is to alternately flash the images on a monitor screen and view them with special liquid crystal glasses, acting as shutters, which are synchronised with the screen, so that alternate images are viewed by alternate eyes.

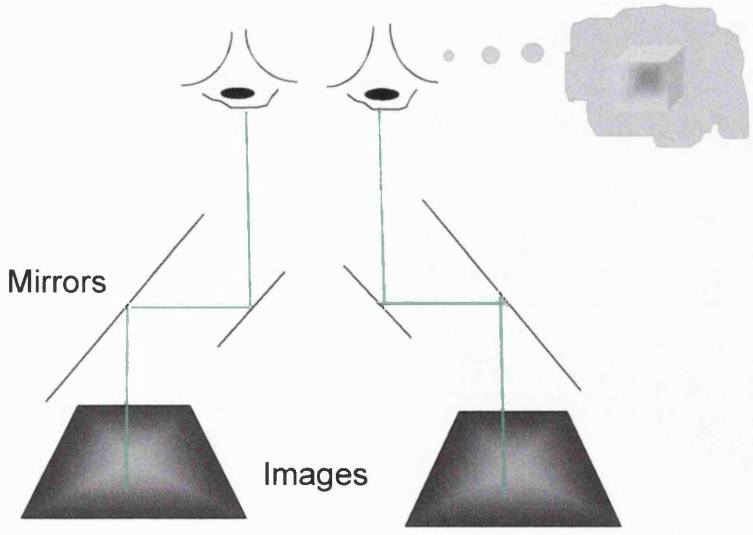

Fig.4.8 Reconstruction of a stereoscopic pair of X-ray images

The theory of stereography does not limit the resolution achievable, either in space or in time. These are dependent on the detection method and, when only one X-ray tube is available, the mechanism for moving it between the two imaging angles, during image capture. Only detection speed is relevant if

two X-ray tubes are used. There are two ways in which temporal resolution can be measured. These are the time to capture one image pair and the time between subsequent image pairs. The more important of these is the time taken to capture an image pair, particularly if the images are taken sequentially, with a time delay whilst the angle is changed. Fluid redistribution could occur during this period, introducing artefacts into the images.

X-rays, unlike visible light are not significantly scattered by the components of an incontinence pad when either wet or dry. Neither are they significantly absorbed by any component at the X-ray energies normally used clinically (50kVp – 140kVp). This, however, is not a problem as a radio-opaque dye can be added to the laboratory test fluid. Such iodine-based dyes, if chosen appropriately, do not follow a path significantly different from that which water or saline would have followed (as demonstrated in previous work (Yerworth 1996)). The other approach is to use lower X-ray energies (e.g. 28kVp) as used in mammography. At these energies water can be detected without the addition of a contrast medium.

4.2.2 Stereoscopic experiments

The aim of the preliminary experiments was to build on previous work (Yerworth, 1996), where a planar X-ray image of a pad was captured on film. The objective here was to obtain a pair of stereoscopic images.

The radio-opaque dye used in these experiments was 'Omnipaque' from Nycomed. This was diluted with water as appropriate for each experiment, dependent on factors such as the material thickness. For example a solution of 1:3 Omnipaque contained one part 'Omnipaque' to three parts water by volume.

Several iterations were required to achieve images that were suitable for viewing stereoscopically: consideration was given to the angle of separation between the images, the contrast and brightness of the images and temporal resolution. For these experiments the central portion from a disposable pad (Molyform Extra, see Table 8.2 for more details) was wetted with 20ml of 1:3 Omnipaque solution and left for 10 minutes to reach equilibrium before imaging. The edges of the pad were marked with paperclips, applied to different layers of the product. These acted as reference points when the images were viewed. Although a static fluid distribution was sought the time between images was such that there was uncertainty in distinguishing temporal and space effects. This time was reduced by the use of two film cassettes but this introduced the complication that different exposure times had to be used for each cassette in order to compensate for differences between the efficiencies of the screens that they contained. This latter problem was easily remedied when identical film cassettes became available.

The contrast in the image is important, and dependent on several independently variable factors:

- The concentration of iodine in the test fluid
- The energy and exposure time of the X-ray beam
- The separation distances between the X-ray source, the sample and the film

These all need to be adjusted so that the resultant image covers as wide a range of grey scale values as possible, whilst avoiding pure black and white. No 'ideal test values' can be stated because they are also dependent on the thickness of the test sample and the characteristics of the film cassette or other detection medium. However, an example of the values that may be used, is given in Table.4.1.

Distance from focal spot	800mm
Angle between images	16°
X-ray energy	40kVp, 150mA
Exposure time	0.15s
Omnipaque concentration	1:3 (Omnipaque : water)

Table.4.1 Example parameters used to capture a stereoscopic pair of X-ray images

Once a suitable image pair had been obtained, containing wire markers as reference points, the most appropriate method of viewing was sought. The main options available were to use a simple mirror viewer, as in Fig.4.8, or to scan the images into a computer and view them electronically using liquid crystal goggles synchronised to the computer display. With both methods of viewing, interpretation of information in the third dimension was very subjective: a trained eye can see more than an untrained eye. This is particularly true for wet areas of pad where there are no well-defined edges or objects but only fuzzy boundaries to wet regions. It was found, however, that the greater the amount of information, in terms of spatial and colour resolution, presented to the viewer, the more able s/he was to fuse/reconstruct the images. Since computer monitors have a lower spatial and colour resolution than film, viewing the films through a mechanical viewer was superior to scanning them into a computer and viewing them electronically. These images are not included in this document because the stereoscopic effect would be lost.

Mathematical reconstruction of the images was not possible due to the semitransparent nature of the image and the indistinctiveness of the edges.

An image pair was also successfully captured on a single film, using two X-ray tubes simultaneously. The experimental set-up for this is shown in Fig.4.9. The use of two tubes in this way removed all possibility of temporal artefacts, thus this technique could be used to obtain snap shots of dynamic fluid flow. The disadvantage with this system was that it was not possible to image samples in a

horizontal plane because there was no means of supporting the X-ray sources and lead shielding in the correct positions.

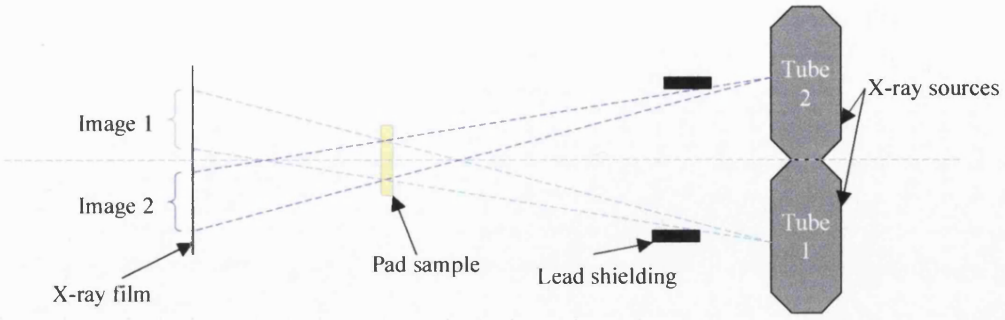

Fig.4.9 Set up for obtaining a stereoscopic pair of images simultaneously.

4.2.3 High resolution studies

X-ray imaging was also used for high-resolution studies. The high resolution of X-ray, coupled with direct correspondence between image intensity and the amount of water or iodine (and hence fluid) at that point meant that the intensity profile across a sample could be accurately measured. It was also possible to look at the effect, on the fluid distribution of structures smaller than the resolution of the optical viewing system. These structures included quilting patterns, which are often present in reusable products.

Initial experiments were conducted using the same equipment as for the stereoscopic studies, with the images being captured on film and then digitised with a high resolution scanner.

Samples from some reusable bedpads were imaged in this way. Each material sample was laid on a Perspex tray and 250ml of warm (~37°C, to aid absorption) 1:19 Omnipaque solution applied to the centre of the sample. An exposure time of 0.4s and X-ray energy of 40kVp were used.

Fig.4.10 shows part of the image of one of these bedpads (Ganmill, Standard 221). Fluid shows up brightly in this image, with the right side of the material wettest. The arch shapes are where the fabric was quilted. These are dark on the quilt lines because the material at this point was too thin to contain much fluid. However, to the right side of the image the arches are highlighted by brighter bands either side of the stitching. This is due to the quilting lines of this material acting as wicking channels along which fluid flowed preferentially, wetting the adjacent felt.

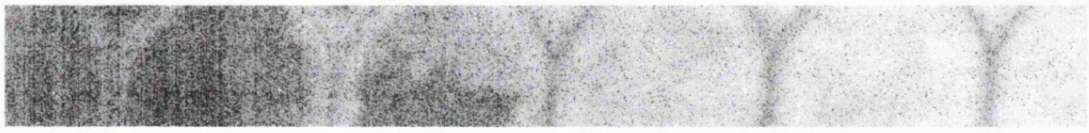

Fig.4.10 X-ray image of water spread in a quilted needlefelt fabric

Such images can be collected using normal X-ray film, or a solid state detector.

Access became available to an amorphous silicon imaging device. This was used in conjunction with an X-ray mammography unit. A comparison of this system and the other system, which was used with film cassettes, is given below.

The mammography unit X-ray source produced X-rays of much lower energy than the other system. (28kVp compared with 40kVp). This meant that water could be used without an iodine contrast medium whilst maintaining the same contrast in the image. The other main advantage of the mammography unit was that it had built-in platforms/ holders for maintaining the sample and detector at the required distances from the X-ray source. The mammography unit could also be used with the sample horizontal or vertical.

The amorphous silicon device had various advantages and disadvantages compared with the use of film. The spatial resolution and area coverage of both was excellent. The silicon device had a resolution of 127μm per pixel, and potentially a total area of 40cm by 30cm. This was easily matched by X-ray film. However they had different imaging capabilities with regard to temporal resolution. Film recorded the image instantly, but a minute or two was required between frames to change the film cassettes. This increased considerably if cassettes needed to be reused during the experiment. The silicon device could have an exposure of 0.2s and images could be comfortably spaced at 45s intervals, allowing time for the data to be saved and the equipment reset. The other advantage of the silicon device was that it produced images in digital format. This enabled line profiles across the image to be obtained easily and image contrast to be varied post-capture without the additional step of image digitisation.

This mammography unit and amorphous silicon detector were used to image a number of materials. This experimental set up was found to be particularly helpful for monitoring the fluid distribution over time within composite reusable materials. An image processing routine was written for extracting and plotting multiple line profiles from series of these images.

Fig.4.11 shows a series of images and Fig.4.12 shows line profiles from a heavily embossed, thermally bonded, nylon material (Cambrelle). This is a very thin material (~1mm). The sample was placed on a Perspex tray and imaged 30s after 0.5ml of water had been applied using a syringe. The sample was imaged again after a further 5 minutes. Another 0.5ml of water was then applied to the same location and the sequence repeated. The regular pattern of embossing can be seen in the image sequence and it was this that caused the closely spaced spikes seen in the intensity profiles, particularly along the short axis. A paperclip was used to mark the right hand corner of the fabric, to aid in the alignment of the data from each image.

The equivalent fluid depth or saturation variation is calibrated in millimetres of water by comparison with the results gained from imaging a wedge of water formed with a sloping dish. The slope of the line profile through this wedge-shaped water sample was compared with the geometry of the wedge in order to calculate the correct greyscale to millimetres of water conversion factor. The fluid depth is (initially) greater than the material thickness due to puddling of the fluid.

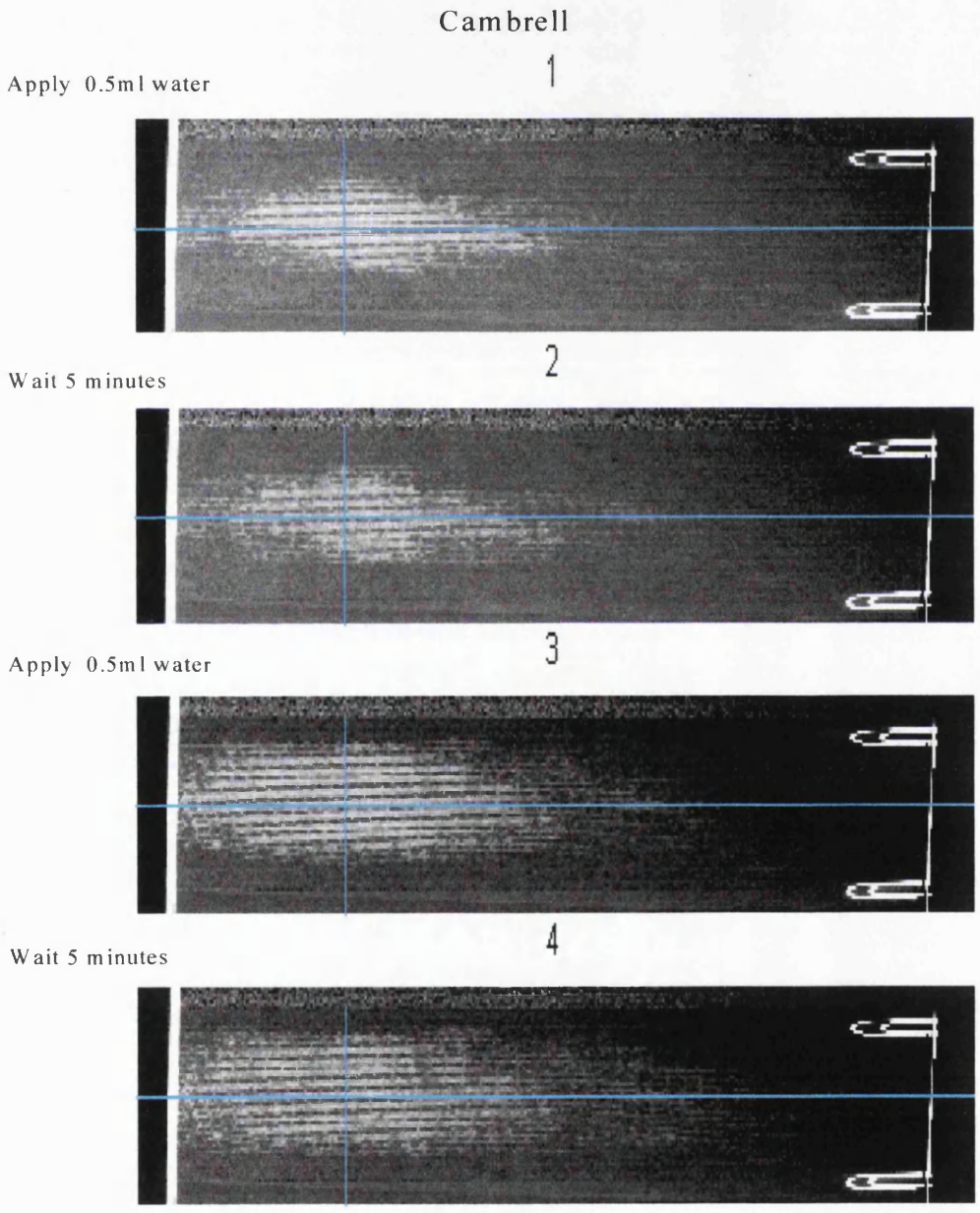

Fig.4.11 Sample and X-ray image sequence of water in a heavily embossed fabric, blue lines indicate the positions of the line profiles shown in Fig.4.12

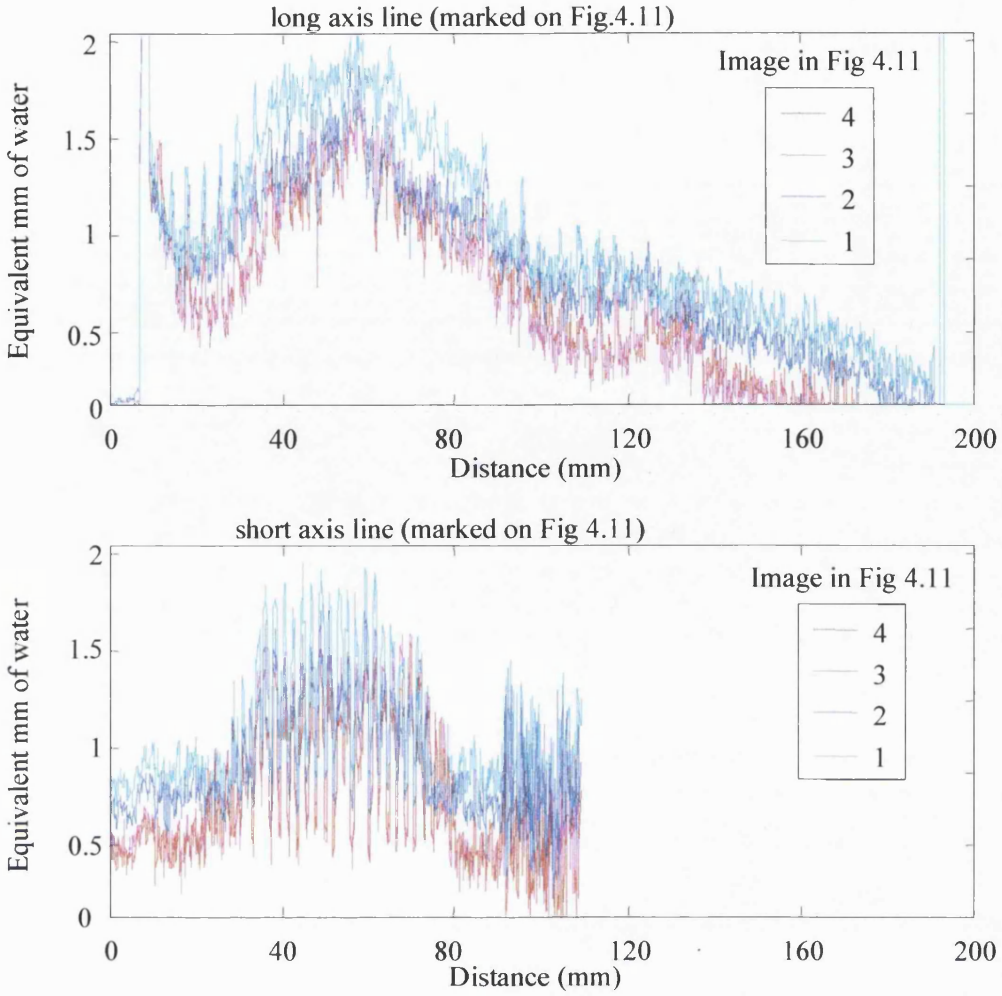

Fig.4.12 Line profiles through X-ray images shown in Fig.4.11

The system was also used to image disposable body worn pads. Fig.4.13 and Fig.4.14 show images of the central region of a Tena Plus pad (see Table.8.2 and Fig.8.5 for details) to which 100ml of water had been applied through the tube which can be seen in the lower portion of the image. The first image (Fig.4.13) was taken 45s after fluid application; the second (Fig.4.14), 135s after the fluid was applied. The horizontal red and green lines mark the position of the line profiles seen in Fig.4.15.

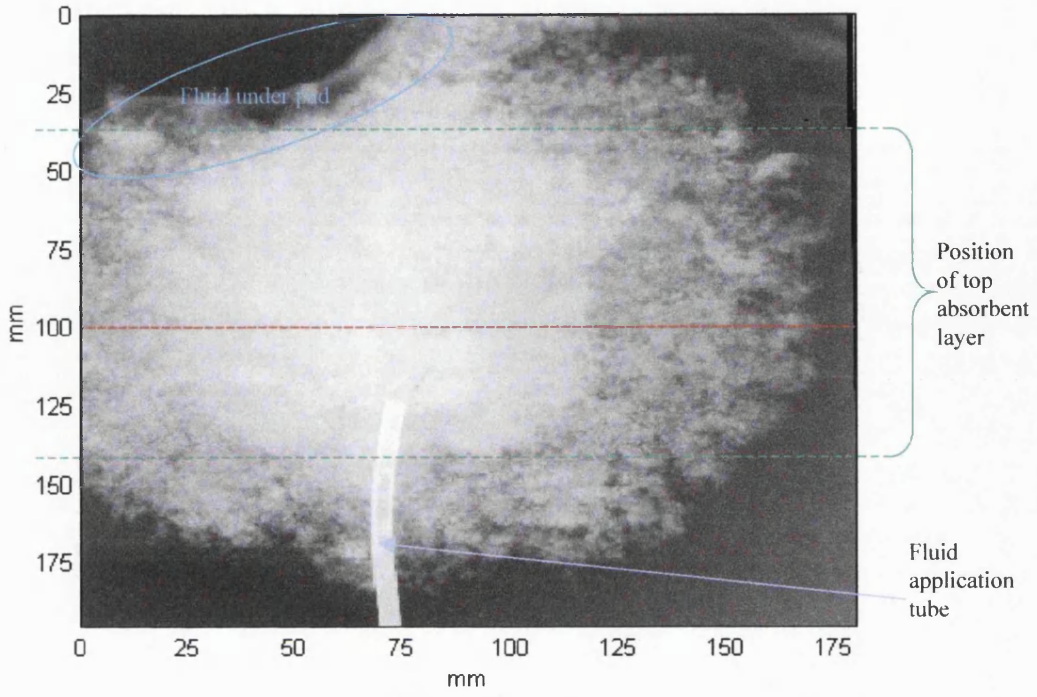

Fig.4.13 X-ray image of water in a disposable pad captured using an amorphous silicon device and mammography unit, 45s after fluid application, red line indicates position of line profile in Fig.4.15

Three distinct regions can be seen in Fig.4.13. The central region contains the highest concentration of fluid. The second region surrounds this, contains a lower concentration of fluid and is less uniform than the first. The third region of fluid can be seen in the top, left hand corner of the image. This region has a much smoother texture than the other two and is probably free water, which flowed under the pad during fluid application. Tena pads have two absorbent layers, both of which contain superabsorbent powder. The top layer is designed as an acquisition layer and is much narrower than the second layer. The width of this top layer corresponds to the width of the innermost region on the image. Although the acquisition layer extended the whole length of the pad section used, the bright, central region of the image does not. This indicates that the second layer is better at spreading the fluid via wicking than the top, acquisition layer. This is consistent with the design aims of an acquisition layer, which is to receive fluid quickly, acting as a buffer zone for those regions of the pad which are designed to spread and hold the fluid.

The second of this pair of images is shown in Fig.4.14. The same regions can be seen in this image as the first and they are very similar in shape, although the outer region has spread a little and the boundary between the two main regions is less distinct. The texture of the images, however, is much more granular in the second image. This is probably due to the superabsorbent powder, whose granules swell, over a period of a few minutes, draining fluid from the surrounding fluff pulp and increase to 70 or 80 times the original size, with a final size of 1-2mm.

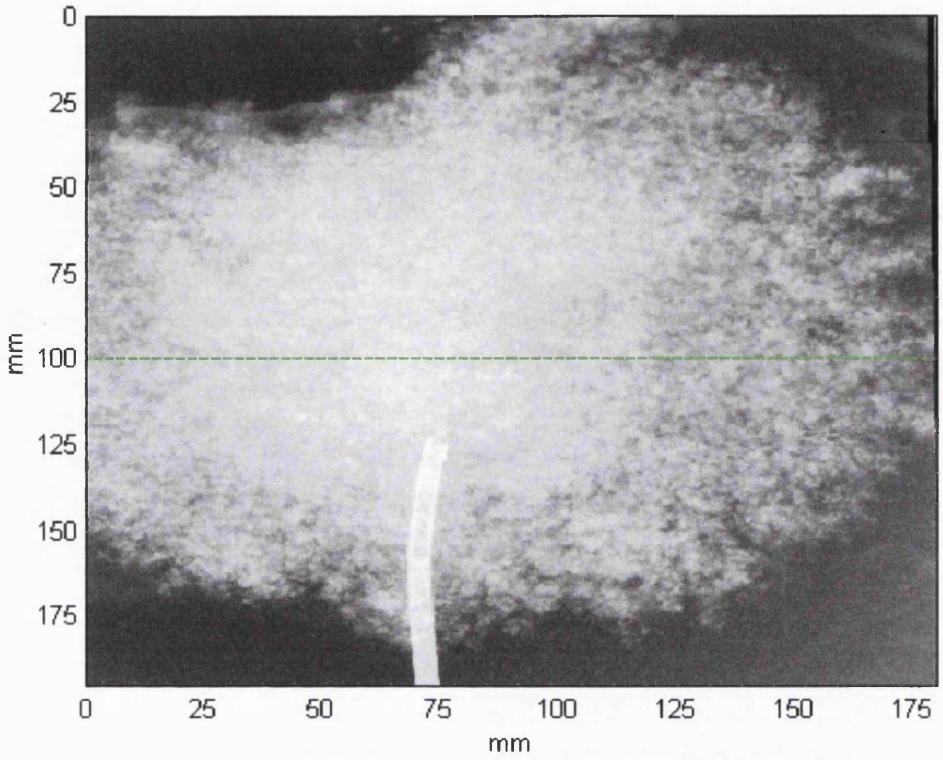

Fig.4.14 X-ray image of water in a disposable pad captured using an amorphous silicone device and mammography unit, 135s after fluid application, green line indicates position of line profile in Fig.4.15

Fig.4.15 shows a line profile across the two images and shows that at 45s the central region contains approximately twice as much fluid, per unit area, as the outer region. By 135s (Fig.4.14) this difference has slightly decreased as the fluid redistributes within the pad. This redistribution is probably due to the wicking properties of the fluff pulp. However, this is counterbalanced by the fluid retention properties of the swelling superabsorber. It is because of this latter, combined with the variations in pad thickness across the image – the edges were thinner than the centre - that only a slight evening of the fluid distribution is observed.

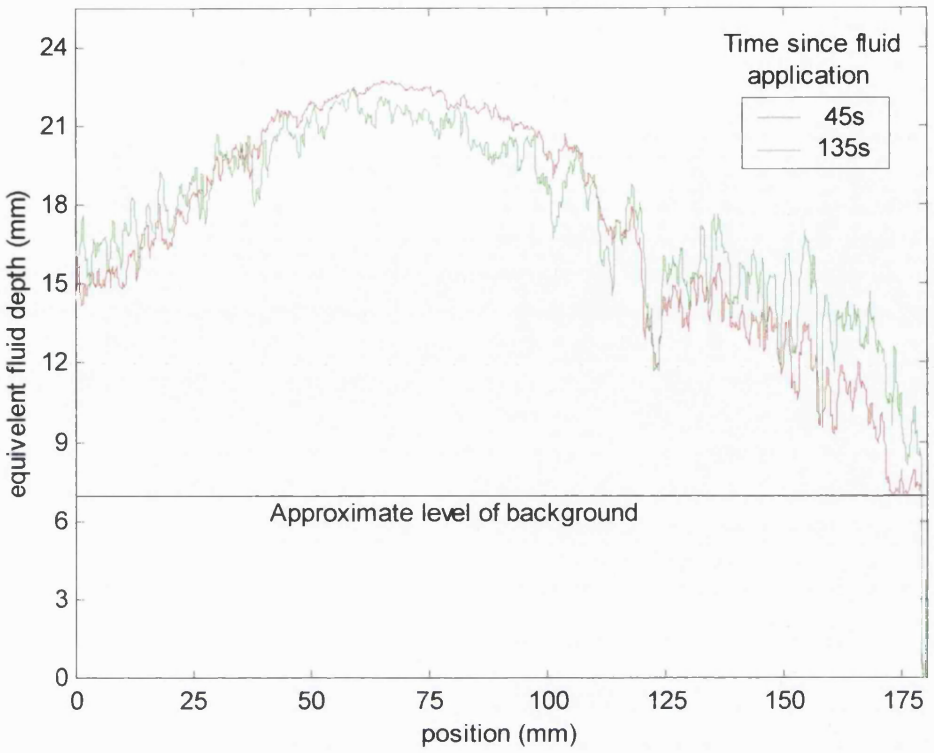

Fig.4.15 Line profile of fluid content across the pad shown in Fig.4.13 and Fig.4.14, at two different times

4.2.4 Conclusions from preliminary experiments

Three-dimensional imaging of fluid in pad samples is possible, both for still and dynamic cases, although the time between frames is currently at least 2 minutes for a film-based detection system. This enables the properties of different layers within a product to be studied, at high resolution, as they interact during fluid application.

Planar images can be captured with minimum time intervals of 30s using an amorphous silicon detector. This has the advantage of producing high contrast, high resolution, digital images. Since this detector is used in conjunction with an X-ray mammography unit no contrast medium is required for fluid distribution to be detected, removing the possibility of the contrast medium modifying the behaviour of the fluid.

X-ray imaging can be used to measure the relative amount of water at each point in a planer image directly, regardless of whether the fluid is evenly distributed throughout the depth of the sample, or concentrated in one layer, for example in the bottom half of the pad. This enables X-ray imaging to be used to calibrate the optical imaging system. At these energies the X-ray beam is also slightly attenuated by the other materials in the field of view so an image of the initial, dry, sample would need to be subtracted before calculating the absolute fluid content per unit area. This facility would allow the results from equivalent experiments, using the optical imaging device and X-ray imaging, to be compared and

would enable the relationship between optical intensity change and fluid content to be determined more accurately.

4.3 'The Mechanical Bladder'

A controllable fluid delivery system that mimics the range of flow-rates and volumes presented by the human bladder is necessary for laboratory study of pads. This is necessary if the various types and levels of incontinence are to be mimicked. For example, it has been found (James and Niblett 1987) that stress incontinence is likely to consist of small volumes at low flow-rates, whereas unstable bladders produce larger volumes with flow-rates of up to 30ml/s. It was also noted in this paper that the volume voided by incontinent people varies considerably, even within the same subject. This fact is confirmed by pad weighing data, (see Fig.1.6), which shows that some pads have to cope with 4 or 5 times the modal volume of fluid.

In order to achieve this aim the chosen pump system should at least meet the following specification:

- Produce a flow rate range of 2-30ml/s, variable in steps of 1ml/s
- have non-pulsatile flow
- Be able to produce complex, pre-programmed flow-rate/time profiles. In order to achieve this control the flow-rate should be independent of the pressure drop across the pump head
- Have a capacity of 1000ml

Also, although not affecting the pump technology, the pump should be made from materials that:

- Allow for body temperature fluid to be delivered
- Are resistive to the corrosive properties of saline

4.3.1 Choice of pump

Although a wide range of pump technologies were investigated it was found that commercially available devices did not meet the specification given above. Descriptions of these pump types, their characteristics and limitations are described below.

Peristaltic pumps can deliver precise volumes at precise flow-rates, which can be varied easily by varying the supply voltage. However, flows are highly pulsatile. Pumps can produce flow-rates and deliver volumes to match the highest outputs of incontinent people, and the flow rate produced is virtually insensitive to the pressure drop across the pump-head. The pulsatility could be substantially reduced with the insertion of an air-filled damping chamber but a result of this would be to introduce a non-linearity so that the flow-rate would no longer be proportional to applied voltage.

Bellows pumps have a pumping chamber that periodically contracts delivering precisely controlled volumes and mean flow-rates, which are independent of the pressure drop across the pump-head. However, the flow is very pulsatile, unless the stroke volume is greater than the output volume required. Within a stroke the flow-rate could be precisely controlled, however, commercially available pumps do not have the required stroke volume.

Syringe pumps precisely deliver a pre-set volume at a precise, predetermined, flow-rate. The flow is non-pulsitile and not affected by the pressure drop across the pump-head. Available devices are, however, designed for processes requiring small volumes (<60 ml) at very low flow-rates.

Centrifugal pumps are very sensitive to pressure head changes, such as those caused by the fluid reservoir emptying and changes in resistance to flow, e.g. due to a pad swelling and partially blocking the outlet. Also these pumps do not have a linear response of flow-rate to drive current making accurate control of these pumps impractical.

Diaphragm pumps are similar in principle to a high frequency bellows pump with a tiny stroke volume. They are not made for the required flow-rate range and cannot be controlled so as to deliver precise volumes.

Gear and impeller pumps move water using the principles of a water wheel. In general they do not produce the higher flow-rates required or use motors that are designed for intermittent use only, e.g. as windscreen washer pumps and so are unable to produce the required volumes. These pumps would also be sensitive to the pressure drop across the pump-head.

Thus it was concluded that the required specification fell in a 'dead space' between small laboratory pumps and large industrial pumps. The only pumps that seem to be in this range are pulsatile or are made for applications such as caravaning, where accuracy is not an issue.

In response to this it was decided to design a purpose built device based on syringe pump technology (Fig.4.16). This technology was chosen because of the simplicity of this design with regards to producing target flow-rate/time profiles. Unlike any of the other systems, except single stroke-bellows pumps, fluid does not enter the pumping chamber during the fluid delivery period, hence the fluid reservoir has no effect on the fluid output. Also, with a cylindrical pumping chamber, fluid output is directly proportional to the number of revolutions of the drive motor. If the changing shape of the bellows could be accounted for, a single stroke bellows pump would be functionally equivalent to a syringe pump, but without the risk of leakage presented by a moving piston seal. However, a bellows pump would be more prone to wear as well as more difficult to make.

The device as built consists of an acrylic cylinder, sealed at the lower end except for an outlet port. Housed at the bottom of the cylinder are a small heater and a temperature probe so that the fluid can be heated to, and maintained at, body temperature (37°C) or some other value. The upper end of this chamber is a sealed piston that is driven by a computer-controlled stepping linear actuator via a dedicated control board. Guide rods keep the piston perpendicular to the cylinder axis, preventing it from twisting and jamming. The rest of the device is a supporting frame. Also incorporated in the piston is a filling

tube and air bleed (not shown). Top filling reduces the load on the linear actuator, which is important because of the limited power of suitable devices and also makes bleeding easy.

Stepping linear actuators are made in two size ranges, the smaller range containing relatively inexpensive devices used for applications such as moving the print head within a printer. Larger stepping linear actuators are proportionately much more expensive, and so were considered inappropriate for this application. The largest 'small' linear actuator available produced a starting force of 125N, had a step size of 0.025mm and a maximum travel distance of 170mm. The piston diameter had to be chosen so that the maximum volume required the piston to travel through less than the maximum travel distance of the motor whilst having as small a diameter as possible in order to reduce the power required of the motor.

The work required of the motor was also kept as low as possible by use of a relatively large outlet tube.

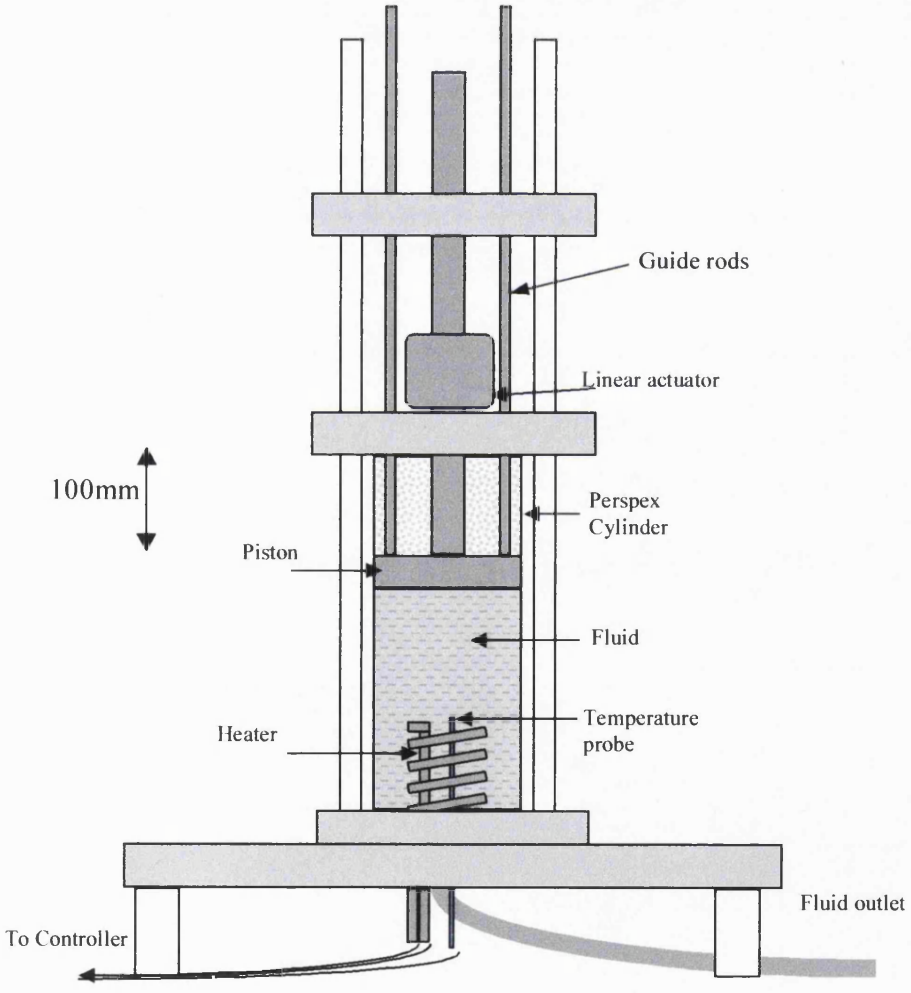

Fig.4.16 Schematic diagram of the Mechanical Bladder

The capabilities of the system, as built, are summarised in Table.4.2 and a photograph of it is shown in Fig.4.17. A listing of the computer program is given in Appendix 1 and the technical drawings of the device in Appendix 2. The maximum volume is far in excess of normal bladder volume but is in

the same range as extreme volumes recorded during pad weighing exercises (see Fig.1.5) and allows for multiple insults to be delivered without refilling. The accuracy can be set much more accurately than 1ml in the stepper motor control program, but factors, such as how much fluid was removed from the outlet tube when the apparatus is wiped between experiments, mean that working accuracy is approximately 2% of the delivered volume.

The flow-rate range is designed to cover normal clinical flow-rates, but is limited at the lower end, to approximately 2ml/s minimum, by the stall speed of the motor. The resolution is dependent on the control programme.

The temperature range covered is in excess of that required for this work due to the use of standard components. The accuracy is determined by the characteristics of the thermostat.

All these accuracy levels are much better than the expected variation in experimental results due to random differences between pads (see ch7 – Commissioning the system).

	Range	Step size	Accuracy
Delivered volume	0-1000ml	1ml	+/- 2%
Flow-rate	2-30ml/s variable with time	0.2 or1ml/s	+/- 0.2ml/s
Temperature	Room -> 100 °C	2°C	2°C

Table.4.2 Specifications of Mechanical Bladder

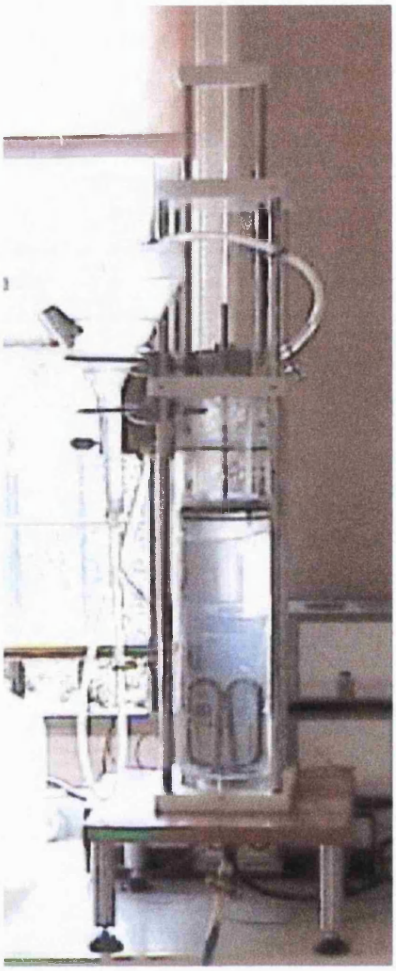

Fig.4.17 Photograph of the Mechanical Bladder

4.3.2 Flow-rate time profile generation

A train of clocking pulses received from the controlling computer determines the flow-rate/time profile delivered by the mechanical bladder. A QBasic program was written which generates these pulses from input text files. This profile can be repeated after pre-determined time intervals to replicate multiple insults.

The text files describe flow-rate/time profiles by specifying the flow-rate (ml/s) every 0.05s. This time interval was chosen as a suitable balance between flow accuracy and the size of the input file that describes the flow profile. This provides great flexibility in the design of flow-rate/time profiles, which can range from a constant flow-rate to the highly varying flow-rates that occur clinically. As spontaneous event are harder to trigger, than deliberate voids, whilst flow-rate measuring equipment is set up, there is very little data for the type of incontinence for which large pads are used – the main area of interest in this study. For this reason the flow-rate/time profile of a normal void is shown in Fig.4.18 and used as the basis for estimating the shape of incontinence events. For every 0.05s time interval the

computer program reads the flow-rate from the input file and calculates the number of steps of the linear actuator needed in this time interval. A pulse train is then generated which evenly spaces these steps across the 0.05s time period. Setting one of the serial port control lines alternately high and low sends this pulse train to the linear actuator. This signal is filtered on leaving the computer to remove the negative component of the signal, converting it into the format required by the stepper motor control board. It is important that the control steps should be evenly distributed throughout the time period to prevent stalling of the motor.

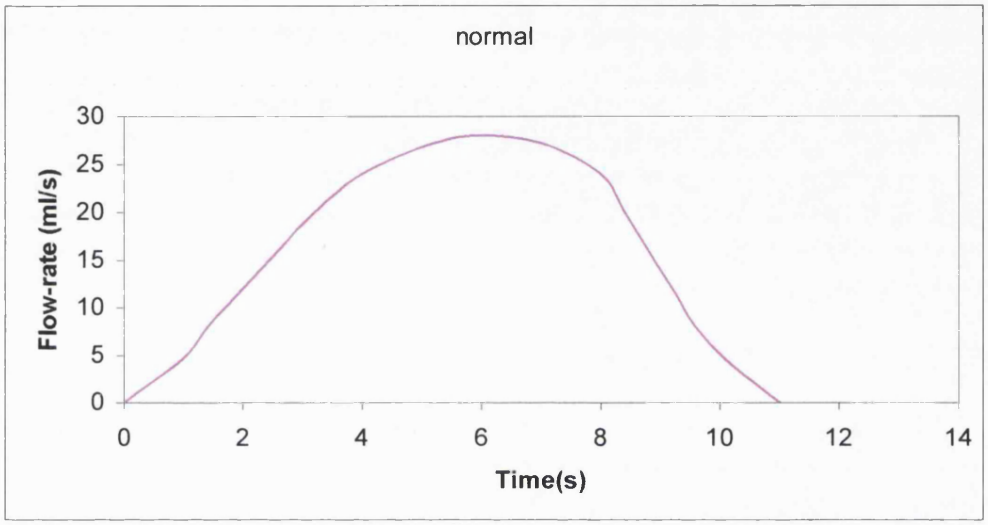

Fig.4.18 Typical flow profiles from a normal human bladder (Norton 1996)

Because all clinical urine flow-rate/time profiles are different, an arbitrary curve equation was chosen which matched the general shape of profiles (Equation 4.1). This base shape is modified systematically, by the use of two scaling factors, to generate the range of profiles seen in this study.

$$f = y(-3.5*10^{-7}*(xt)^4+2*10^{-4}(xt)^3-3.7*10^{-2}(xt)^2+2xt+40) \qquad \textit{- 4.1}$$

Where f = flow-rate (ml/s)

t = time (s)

x & y are duration and peak flow-rate scaling factors, respectively.

Fig.4.19 shows a selection of the flow-rate/time profiles used in subsequent experiments. The code for all these profiles is in the form of f_*volume*_*rate* where *volume* is the total volume (ml) of fluid delivered and *rate* is the peak flow-rate (ml/s) at which the fluid is delivered. For example the file f_100_10 delivered a total volume of 100ml, with peak flow-rate of 10ml/s.

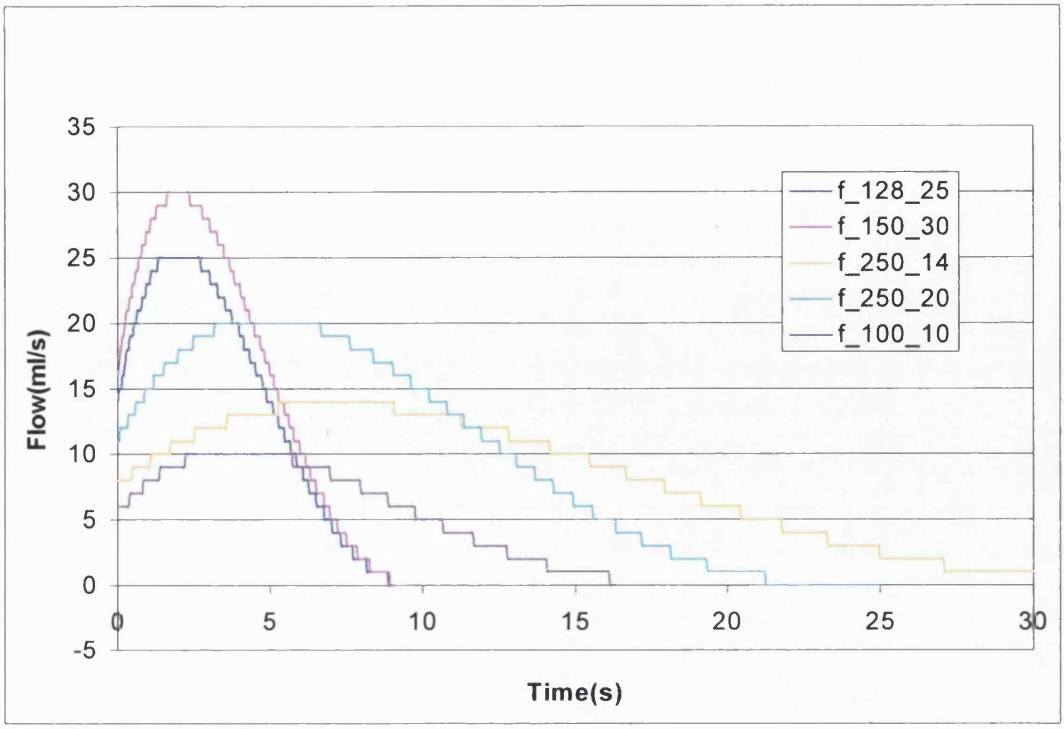

Fig.4.19 Some typical flow-rate time profiles produced by the Mechanical Bladder

4.3.3 Commissioning the system

The most problematic part of the mechanical bladder was the piston seal. This caused a number of problems as it had to be made watertight without generating excessive friction. The seal used consisted of a pair of annular rubber flaps sandwiched between the layers from which the piston was made and projecting from the sides. Grooves in the piston allowed the seals to lie flat against the cylinder and produce a tight seal (Fig.4.20). Initially the flaps protruded to far and extending beyond the groves on the piston. This caused the seal to snag and more rubber to be pulled out from the piston. This exacerbated the problem and caused the piston to become almost immovable, requiring a force far in excess of that which the linear actuator could generate. Trimming the seals removed the excessive friction but made the seal prone to leakage. A layer of silicone grease between the piston seals prevented leakage and further reduced fiction. The two seals were arranged to point towards each other in order to trap the silicone grease in the correct location.

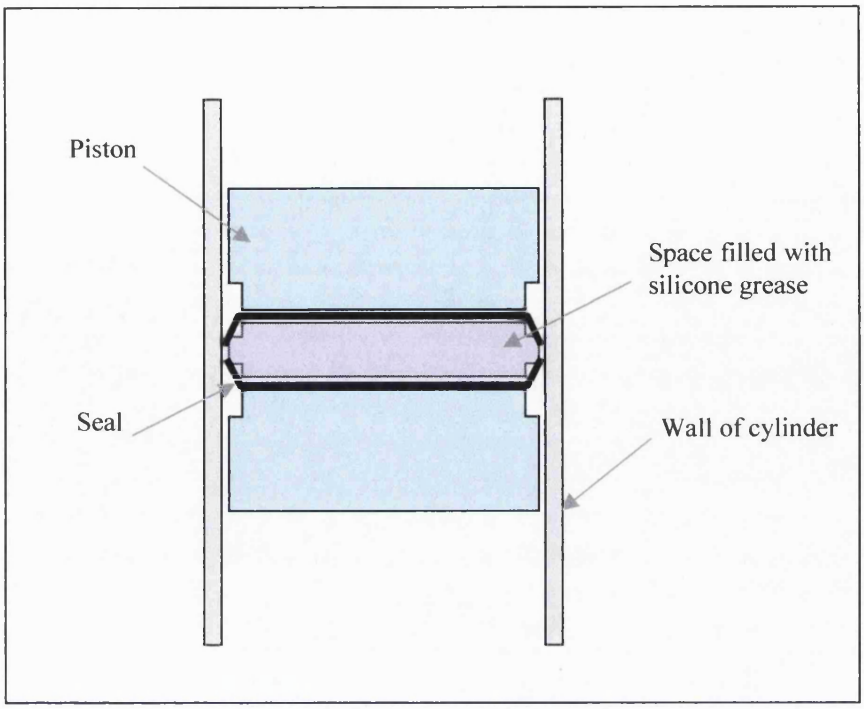

Fig.4.20 Cross-section of Mechanical Bladder piston showing seal arrangement

The accuracy of this equipment, with regards to flow reproducibility, volume and temperature, was assessed in conjunction with the optical imaging system. Details of their combined performance can be found in section 7.2.

5: Optical imaging – Background theory and preliminary experiments

5.1 The theory

Different materials interact differently with light, reflecting, scattering and refracting it to different degrees. Wet and dry materials often look different because of their differing interactions with light. These differences can be used to map fluid distribution in partially wetted materials, the resolution primarily depending on the detector system used.

The well-known optical principles used in this technique are described below (for additional information see Appendix 3).

Refraction. The speed of light varies according to the material it is travelling in. This speed (v) is usually expressed relative to the speed of light in a vacuum (c) and is called the refractive index of the material (n):

$$n = c/v \qquad \textit{-5.1}$$

Thus when a beam of light encounters the boundary between two different materials it will change speed. If the incident light beam meets the boundary at an angle other than 90° to the beam it will alter direction according to the following equation:

$$n_1/n_2 = \sin\theta_1/\sin\theta_2 \qquad \textit{- 5.2}$$

where n_1 and n_2 are the refractive indices of the two materials and θ_1 and θ_2 are the angles by which the light deviates from the normal on either side of the boundary.

This direction change may be such that the light runs along the boundary, in this case the incident angle is at the 'critical angle'. In addition, total internal reflection occurs when the critical angle is exceeded, preventing the light from leaving that material. All these effects are shown schematically in Fig.5.1.

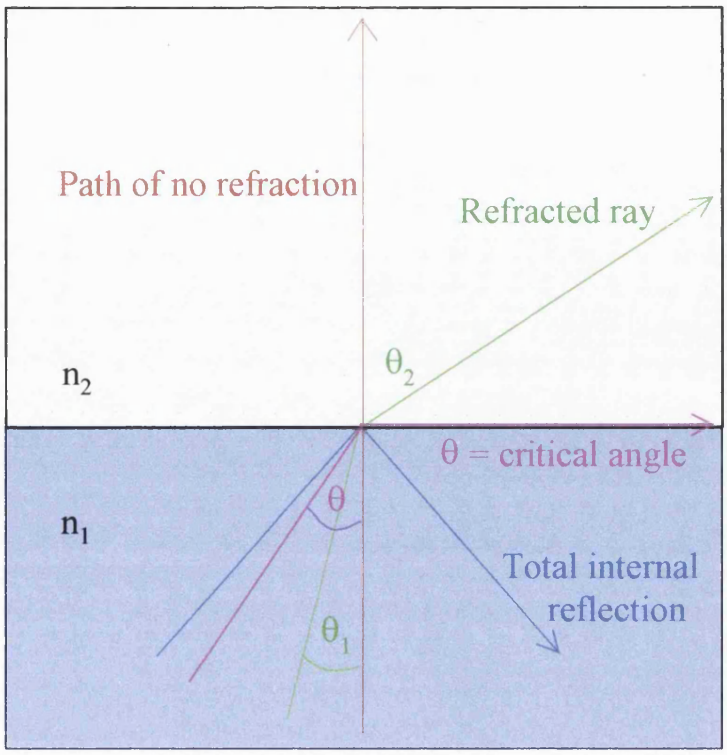

Fig.5.1 Refraction of light at the interface between two media ($n_1 > n_2$)

Absorption. The energy of a light photon can be transferred to an atom or molecule: this is known as absorption. Every substance has a characteristic absorption spectrum, absorbing different wavelengths to different degrees. In a clear solution containing absorbing but not scattering molecules, the light intensity falls exponentially with distance according to Beer's Law:

$$I = I_0 e^{-\mu_a . d} \qquad - 5.3$$

Where I_0 is the input light intensity, I is the intensity at a distance d through the absorber and μ_a is the absorption coefficient of the material.

An example of absorption can be seen in inks. Red ink is clear, and objects viewed through it are not obscured; rather everything looks red. This is because the dye molecules within the ink absorb the other wavelengths of light, leaving only red light. The same is true for blue ink but in this case it is the blue wavelengths that are least absorbed by the dye.

Scattering. Light photons travelling through an ideal non-absorbing material would still eventually be removed from their original path. This is due to scattering. Photons are electromagnetic waves and may interact with the molecules and atoms of the material by recoiling from the electric field that surrounds every atom. This causes a reduction in the intensity of light in the direction of the original beam. This reduction can be calculated from an equation analogous to Beer's Law:

$$I = I_0 e^{-\mu_s . d} \qquad -5.4$$

Where μs is the scattering coefficient of the material.

Light can be scattered many times within a highly scattering medium such that, after short distances, a significant amount of light can be re-emitted from the original entry site of the light. Any light which leaves the material at an angle greater than 90° to its original path is known as backscattered light. An example of backscatter is observed when driving in fog. Light from car headlamps is highly scattered by the water droplets in the air and a large proportion can be backscattered, dazzling the driver. Even dry air scatters light a little; it is this effect that enables a laser beam to be seen crossing a room: otherwise its path would be invisible until it reached a scattering object, like a wall.

The combined effect of absorption and scattering can be found by the addition of their coefficients. This enables equations 5.3 and 5.4 to be combined:

$$I = I_0 e^{-(\mu_a + \mu_s).d} \qquad -5.5$$

This theory uses simple equations but absorbent incontinence products present many, randomly orientated boundary layers to light, one every time a fibre or other structure is encountered. Thus the complexity of the system to which they are applied means that an empirical study is far more appropriate than a theoretical prediction.

The absorbent material of an incontinence pad scatters visible light to a high degree. This is due to the structure of the material, which principally comprises fibres separated by air gaps. When the air is replaced by liquid the refractive index difference between the fibres and the gaps is greatly reduced. This results in less scattering of the light at each boundary, with the effect that light travels further in the material and less is backscattered to the original entry site.

At visible wavelengths very little absorption of light occurs in either the material of a dry pad or in water, as can be seen by visual inspection: most products appear white when dry and semi-transparent when wet, apart from their plastic backing.

Optical measurement is becoming more common in medicine, with the introduction of pulse oximeters and other oxygen saturation monitors, all of which compare the absorption of light at a small number of wavelengths (Elwell, 1995). However, in general, these techniques do not help with this work as they are concerned with observing the human body, which, it will be seen, is subtly different in its optical properties from those found in absorbent materials.

Although, superficially, human bodies and wet incontinence pads are optically similar - both are highly scattering and have a large proportion of water in their structure - closer inspection reveals significant differences in their measurable properties. Most optically-based clinical studies concentrate on the relative concentrations of trace absorbers; for example, blood oxygen saturation measurement

utilises the differing absorbencies of various states of haemoglobin. Other systems have been designed to image structures deep within soft tissue. This requires the removal of scattered light to leave only transmitted light and again utilises differential absorption to distinguish tissue types. As mentioned, incontinence pads do not absorb light strongly and so this form of contrast is not available.

Thus in this case, unlike medical studies, it is the degree of water, from zero to saturation, which is being assessed and not trace substances. This is the major difference between this study and clinical uses of light for imaging.

5.2 Preliminary experiments

The series of experiments described below were conducted to establish the possibilities and constraints of using light to study the dynamic fluid distribution in incontinence pads, as well as seeking to identify a practical approach to building such an imaging system.

Throughout this section two materials were used as test samples. A reusable needlefelt made from a blend of viscose and polyester fibres (VB180MF from BUSM) was used as a 'model' system because this had a uniform specification across large areas and was much more homogeneous than the pads of interest. This felt was used singly or in multiple layers, depending on the thickness required.

In addition, disposable pads (Molyform Extra, supplied by Paul Hartmann AG) were used as a representative pad. These pads had a variable cross section, being thicker in the centre, where they also contained the most superabsorber. Samples were cut from the centre of the pad to contain superabsorber, or from the ends of a pad, where the core was of more uniform composition but contained much less superabsorber.

5.2.1 Comparison of reflection and transmission

When the source and detector are placed on opposite sides of a sample the light TRANSMITTED through the sample is measured. This is therefore known as *transmission* mode, as shown in Fig.5.2. When the source and detector are on the same side of the pad baskcattered light is measured. This is effectively light REFLECTING from multiple depths within the pad structure and is therefore known as *reflection* mode.

In previous work (Yerworth, 1996) it was observed that when light from a bright source was passed through a pad sample with a fluff pulp core containing superabsorber there was a change in the intensity of light emitted from the other side as the pad sample became wet. There were two major problems with this approach. The first involved the arrangement of the input and measuring sensors. For convenient imaging of incontinence pads, whilst they are being worn by a subject, the input and sensing elements need to be situated on the same side of the pad – the back – to minimise discomfort and avoid obstructing fluid entry. Secondly, the light source and sensor connections used were bulky, covering an area of approximately $1cm^2$. This size would probably limit spatial resolution and would be inappropriate

for clinical studies as the depth of the sensors was correspondingly large. The following experiment sought to address both of these problems.

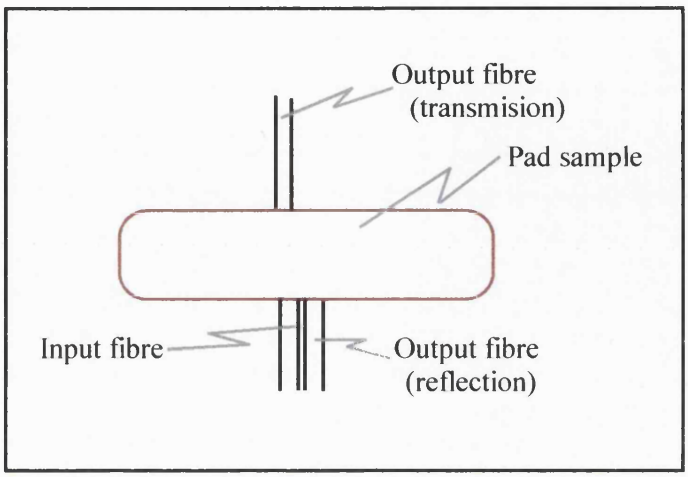

Fig.5.2 Arrangement of optical fibres for transmission and reflection mode detection of fluid in absorbent materials

The aim of the experiment described below was to discover if a significantly smaller size light source provided sufficient illumination for the results of the work mentioned above, to be replicated. The potential for placing source and detector on the same side of the pad (reflection mode) was also assessed.

The light source used in these experiments was a red, 3mW laser Diode. A photodiode with integral amplifier was used as a detector. This detector was a light to voltage converter, dark corresponding to 0V and light to a negative voltage proportional to the intensity of the light. This voltage was measured using a voltmeter. The laser was directly coupled to the cut end of a 1mm diameter plastic optical fibre that carried light to a sample of disposable pad (Fig.5.2). Another length of the optical fibre (approximately 0.5m) carried light from the pad surface to the detector where it was held against the surface of the detector. Plastic optical fibre was chosen because this is more flexible than glass fibre. A diameter of 1mm was used as this was readily available.

Experiments were performed using both reflection and transmission modes. As shown in Fig.5.2 one input fibre from the light source and one output fibre to the detector, known collectively as an optode, were held against the pad surface. Samples cut from the middle of disposable pads, were used in their dry state and when saturated with water. Each experiment was repeated three times.

Fig.5.3 shows the mean light intensity for dry and wet pad samples. Also shown is the mean change in intensity between wet and dry conditions. Each is shown for the two optical fibre arrangements, transmission and reflection. Error bars corresponding to one standard deviation are shown.

In percentage terms all the error bars are of the same order of magnitude, although those for transmission mode are too small to show. The large size of the error bars is due to alignment problems

between the photodiode and the optical fibre. This was constant for the duration of an experiment but varied between repeats due to movement of the optical fibre relative to the diode. It was subsequently stabilised by clamping the fibre and detector into a more permanent holder. Despite this a clear difference can be seen between the performance of the transmission and reflection modes. In transmission mode light intensity increased upon wetting of the pad sample where as in reflection mode the intensity decreased. However, the size of this change was much larger for reflection mode, the change for transmission being only just detectable. This indicated that reflection mode was the better option for studying fluid distribution in pads.

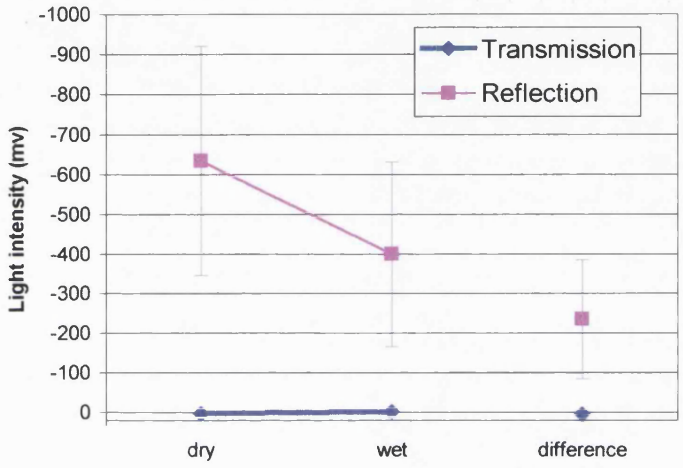

Fig.5.3 Relative light intensity changes for transmission and reflection mode detection of fluid in absorbent materials

5.2.2 Effect of fluid application rate

Previous work (Yerworth 1996) indicated that the detected light intensity change that occurred between wet and dry states was not instantaneous.

The aim of this experiment was to explore this effect in order to assess the potential of the optical technique for yielding information relating to the degree of water saturation of a product. This is important if subtle differences in product performance are to be detected. Therefore this experiment sought to qualitatively demonstrate the ability of the optical technique to differentiate between levels of fluid saturation within a pad sample.

With an optode held in reflection mode, a 30mm by 30mm dry disposable pad sample was damped with 10 ml of water via a fluid reservoir containing an exit hole, as shown in Fig.5.4. Two different hole sizes were used, which resulted in two different flow-rates: approximately 2.7ml/s and 0.7ml/s. The same light source and detector were used as for the experiment in section 5.2.1. The addition of an analogue to digital converter allowed the voltage output to be continuously recorded on a computer.

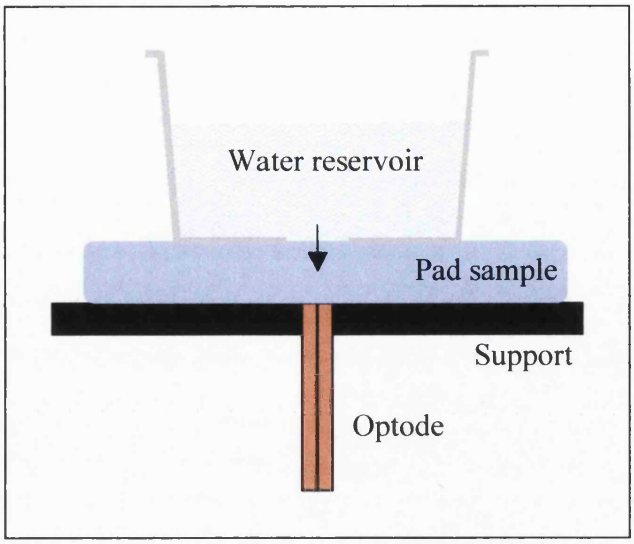

Fig.5.4 Fluid application method for preliminary experiments

In each case data collection was started approximately 10 seconds before the fluid was applied. At these small volumes it can be assumed that water saturation is in some way related to the volume of water applied to a pad up to a given time, the fluid barely spreading beyond the illuminated area of the pad. Therefore it can be assumed that the effective water saturation of the pad was increasing during this experiment in a way related to the fluid flow rate.

Fig.5.5 shows that the lower flow-rate delivery produced a slower increase in intensity than the higher fluid flow-rate. However, the lower flow rate was present for a longer duration so as to apply the same volume of fluid and the final intensities were similar for the two flow rates. This indicates that some information on the degree of water saturation is available. If only binary (wet/dry) information could be achieved, both flow rates would have exhibited a sudden change in intensity at the same threshold value, although the different flow rates may have required slightly different times for such a switching threshold to have been reached.

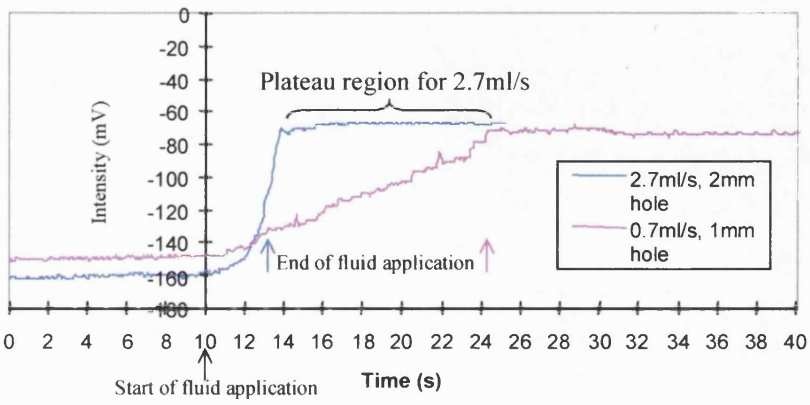

Fig.5.5 Effect of fluid application rate on light intensity reflected from an absorbent material

5.2.3 *Correlation between fluid volume and reflected intensity from a wet pad*

Leading on from the experiment described in section 5.2.2, this experiment sought to identify if there was a simple mathematical relationship between the degree of wetness of a sample and the intensity of light reflected from it.

Samples of reusable felt (30 mm by 30 mm) were damped in a controlled manner by applying the fluid through a reservoir as shown in Fig.5.4. A range of volumes of water were used form 0 to 32ml. Each sample was used once only and the reusable felt was used so that all samples were as identical as possible. The intensity traces followed a similar from to those in Fig.5.5: the reflected light intensity reached a plateau region after wetting had finished. The intensity of this plateau was taken to be the wet intensity of that sample and was plotted against the applied fluid volume as shown in Fig.5.6. The different point styles represent three batches of tests performed on different days.

Equations of various formats (linear, exponential, logarithmic, polynomial, power) were applied to this data and it was found that the best fit line according to the least squares rule was achieved with an exponential curve. The resultant curve is plotted on Fig.5.6 and fits the equation:

$$Y = 132.1e^{-0.0428X} \qquad \textbf{- 5.5}$$

It had a goodness of fit value of $\kappa^2 = 0.83$ ($\kappa^2 = 1$ is a perfect fit) which means that this curve is a reasonable fit to the data.

This indicates that there is an exponential relationship between the volume of water applied to the sample and the output voltage of the photodiode. Therefore, there is a relationship between water saturation and the intensity of backscattered light. However, since the absolute saturation of the sample was not known, only the volume of water added, the precise relationship could not be determined.

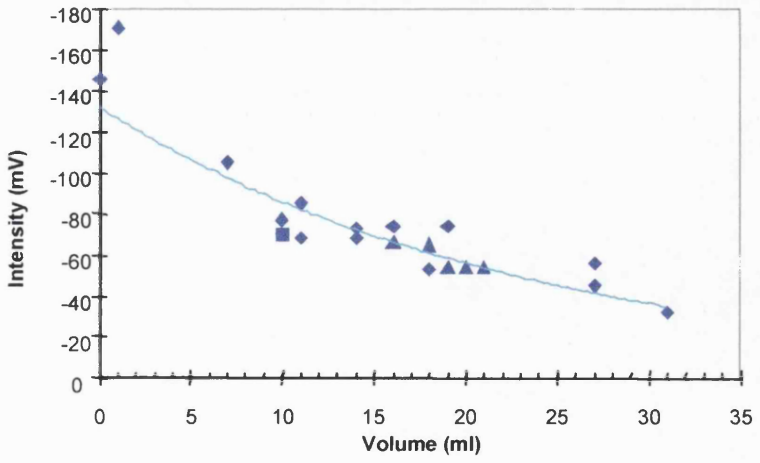

Fig.5.6 Correlation between fluid volume applied and light intensity reflected from an absorbent material

5.2.4 *The effect of varying the wavelength of light*

An experiment was performed in previous work (Yerworth, 1996) to generate the optical transmission spectra for both wet and dry pads for a range of wavelengths of light. This indicated that red light was of a suitable wavelength for use with these materials. Red light was chosen because wet and dry pad states can be determined at these wavelengths and many light sources are available in this range. This measurement, however, was made in transmission mode, so this experiment had to be repeated in reflection mode to check whether the spectral response was the same.

Light from a stabilised tungsten halogen light source was transmitted to the back of a disposable pad sample through a glass fibre bundle of diameter 3.3mm, as shown in Fig.5.7. Reflected light was collected with a second bundle placed adjacent to the first. This reflected light was focused onto the slits of a 0.32m spectrograph equipped with a 601/mm grating blazed at 750nm. Spectra between 600-1050nm were collected on a front illuminated, nitrogen cooled, CCD camera. The pixel bandwidth was 1.1μm and the input slit was set to give a spectral resolution of, typically, 5nm. At the light intensities used, system noise was minimal, dominated by shot noise (random fluctuations in dark current). Measurements were taken with the sample dry and when water had wicked above the height of the sensors. The log ratio of the dry and wet intensities is used for comparison of the performance of the different wavelengths because the measured intensities cover a range of several orders of magnitude. A log ratio of one indicates that light reflected from a dry and wet pad is of identical amplitude. If the ratio is less than one the light intensity is increased by wetting of the material, and if it is greater than one the light intensity is reduced. The log ratio for each wavelength of the spectra was found according to equation 5.6:

$$I_r = \frac{\ln(I_o)}{\ln(I_w * S)} \qquad \textit{-5.6}$$

where I_o and I_w are the intensities reflected from the dry and wet pad respectively and I_r is the log ratio. S is a scaling factor that is necessary because a shorter measurement time had to be used for the wet pad than the dry pad to prevent the results being clipped due to saturation of the detector.

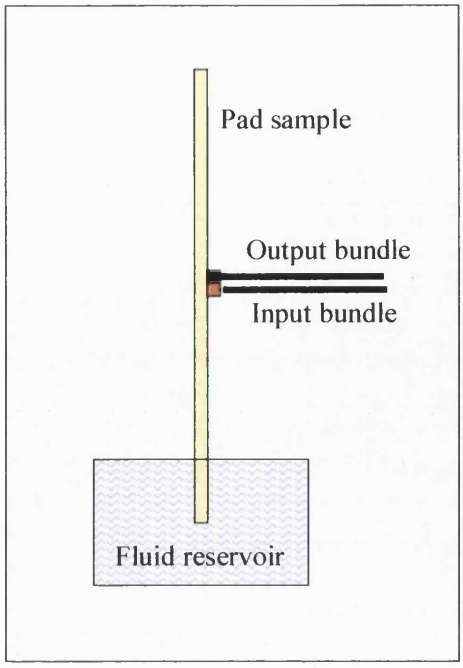

Fig.5.7 Experimental arrangement for measuring the effect of varying the wavelength of light

Fig.5.8 shows the resultant spectrum for reflection mode together with the original spectrum obtained in transmission mode. Although neither graph has used the correct S value (because that for the transmission data was unavailable) and hence the traces are vertically shifted, it can be seen that these spectra have the same general shape. This indicates that red light (660nm) is appropriate for reflection mode as well as transmission mode measurements. An increase in light intensity is seen, upon wetting in both cases, although a decrease was expected for reflection mode. The explanation for this is revealed in section 5.2.5. The size of the optodes used in this experiment mean that the results are due mainly to the crosstalk effect rather than reflection. However, since the light is still back scattered, as opposed to the forward scattered light measured in transmission mode, the conclusions drawn are not invalidated

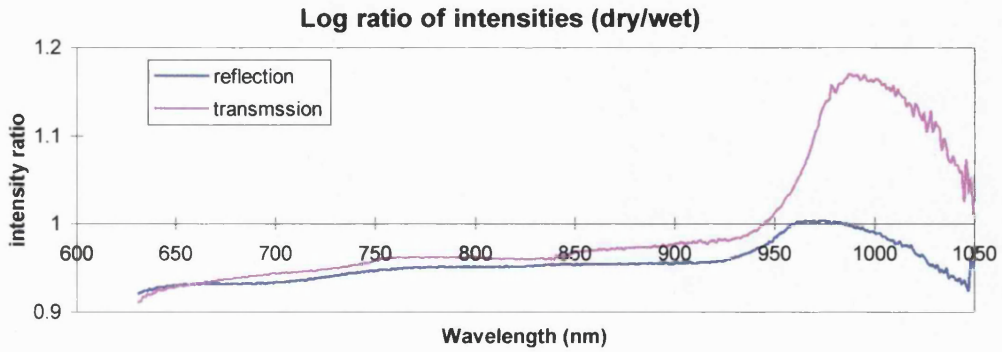

Fig.5.8 Log ratio of light intensities from dry and wet absorbent materials at a range of wavelengths

Fig.5.8 shows that a distinguishable difference in intensity, between the wet and dry states, is seen at most wavelengths, both in transmission and reflection mode. A water absorption peak is

present in the near infrared (wavelengths >950nm). The actual intensities recorded by the CCD are shown in Fig.5.9, The shape of this graph is dominated by the spectral response of the CCD device - a shape shared by many light detectors – although, in this case, the peak response was shifted towards the infrared by cooling the device.

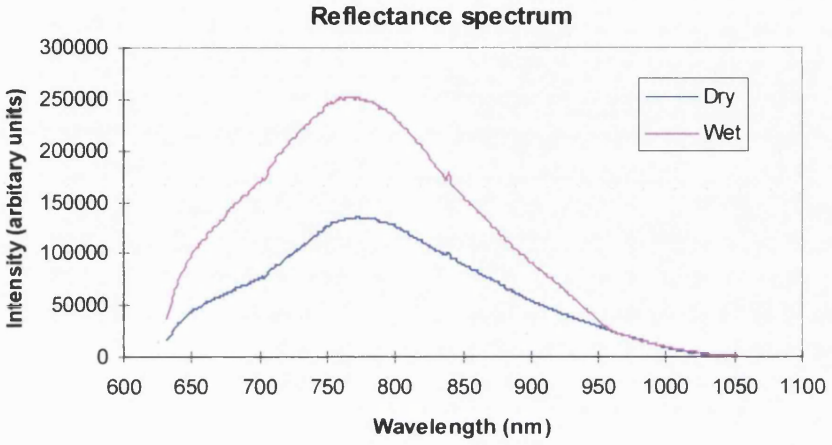

Fig.5.9 Intensity of light reflected from dry and wet absorbent materials at a range of wavelength

When interpreting the results, account was taken of the fact that most sensing devices have a spectral response similar to that of a CCD. This response has a peak in the visible region (~750nm) and falls off rapidly in the infrared, above about 950nm. Thus, it is more appropriate to use a wavelength at the peak of the detector response curve than to work in the water absorption peak between 950 and 1050nm.

5.2.5 Upgrade of equipment to 24 sensors

At this stage, the number of optodes in use was increased from two to 24 to enable localised imaging to be achieved. In addition the photodiodes used for light detection were changed to smaller devices which were easier to mount and showed a greater intensity change upon pad wetting than the original photodiodes. This is shown in Fig.5.10, where the (modulus of the) intensities for one of each type of photodiode are shown as they simultaneously monitored fluid spread in a disposable pad sample. The illuminating fibres continued to be illuminated by a single red 3mW laser. The beam was expanded with a series of lenses in order to illuminate all 24 fibres.

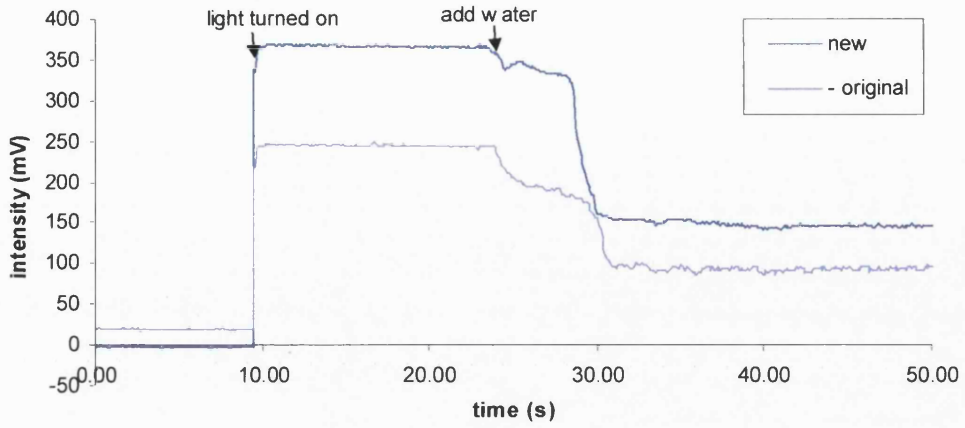

Fig.5.10 Performance of original and new photodiodes

5.2.6 *Crosstalk*

The object of this experiment, and subsequent model, was to determine the optimum spacing between optode pairs to yield maximum spatial resolution without an unacceptable level of light leakage between optodes; that is, the distance at which the light from an input fibre should not significantly influence the response of the neighbouring output fibres.

Output optodes were arranged in a cross shape with an inter-optode distance of 5 mm, as shown in Fig.5.11. A single input optode was placed adjacent to the central output optode. A section cut from the centre of a disposable pad, containing superabsorber, was used as the sample. Intensities were recorded from the dry pad for each optode and while fluid was applied to the centre of the pad until the whole pad was saturated. The cross-shaped arrangement effectively yielded four measurements at each distance from the input optode, as shown in Fig.5.11 where each point at the same distance is given the same colour.

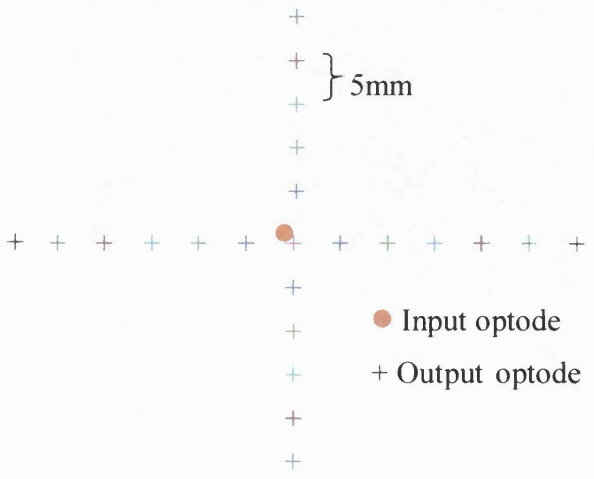

Fig.5.11 Optode arrangement for crosstalk measurements

Fig.5.12 shows a plot of light intensity against time for seven individual sensors, each line representing the worst case for that separation distance. The worst case is the fibre at a given distance that detects the most light. For the first few readings the input light was on, it was then turned off to show the effect of background light. With the input light turned on again, and without moving the pad sample, the pad was wetted and data recorded until a plateau of constant light intensity was reached for all sensors. Note that the output from the sensor adjacent to the input (pink line) is plotted against the right hand axis, as it is ten times more intense than the others are. Upon wetting, an intensity decrease is seen at the central (0mm) optode while the other optodes showed an increase in intensity as light travels further in the pad before being backscatttered.

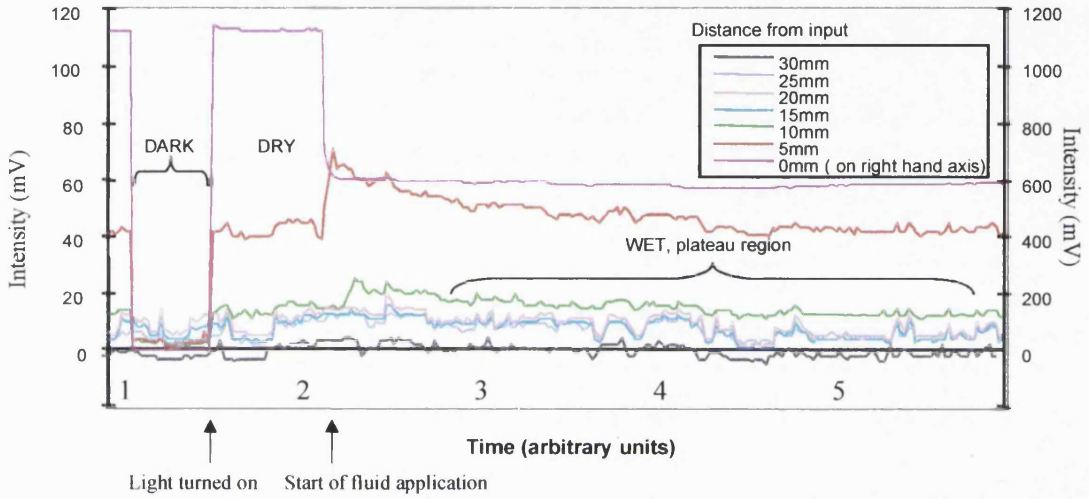

Fig.5.12 Optical crosstalk between optodes, disposable pad at a range of distances

Averages of the four sensors at each distance were calculated, from the relevant plateaux regions (see Fig.5.12) in the case of the wet pad, and from the period just before wetting for the dry case. The Fig.5.13 shows the average intensity received at a number of distances from the transmitting fibre. The inset plot shows the distant optodes in more detail so that the error, representing the standard deviation of the light intensities of each group of four fibres, can be seen.

Best-fit curves have been fitted to these two cases, wet and dry. It was found that for both cases a power law curve given by the least squares rule gave the best fit (i.e. κ^2 was closest to 1). In order to calculate these curves the fibre adjacent to the input was given a nominal separation of 1mm. This is justified since the diameter of the fibres is 1mm, which constitutes the minimum separation between their centres. It should be noted that this adjacent fibre has the most influence on the resulting curve.

The fitted equation for the dry pad was:

$$y = 784.3*x^{-1.89} \qquad \textit{- 5.7}$$

Where y is the average light intensity (mV) and x is the distance from the light source (mm)

The goodness of fit value was $\kappa^2 = 0.975$.

The equation for the wet case was:

$$y = 559.8*x^{-1.79} \qquad \textit{- 5.8}$$

The goodness of fit value was κ^2 =0.999.

In both cases the curve obeys an inverse square law to a good approximation.

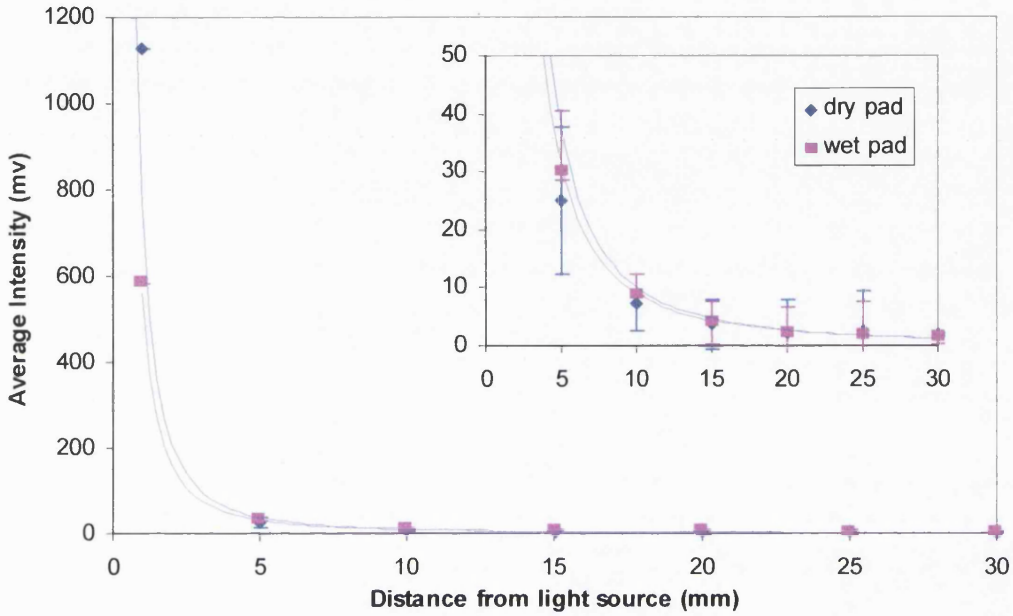

Fig.5.13 Average optical cross talk, insert – close up of distant optodes to reveal error bars

In order to establish what the minimum spacing between optodes could be for crosstalk from surrounding optodes to not obscure the signal, data from this experiment was used to create a simple model of light intensity for multiple optode pairs in a one-dimensional line and a two-dimensional square array.

A model was necessary for this because in experimental work the effects of crosstalk and fluid front profile could be confused. The saturation profile perpendicular to a horizontally moving fluid front (the simplest flow achievable) could not be accurately determined and, for example, could be a dry/wet step function or a gradual increase in saturation, depending on material characteristics.

The model consisted of two inverse square law ($1/x^2$) equations (5.9 and 5.10), where x is the distance from the light source (mm). These were scaled to match the experimentally recorded dry and wet light intensities, respectively of the sensor adjacent to the light source. The fit of these equations to the measured values of crosstalk can be seen in Fig.5.14.

$$I_d = 900*x^{-2} \qquad \textit{- 5.9}$$

$$I_w = 600*x^{-2} \qquad \textit{- 5.10}$$

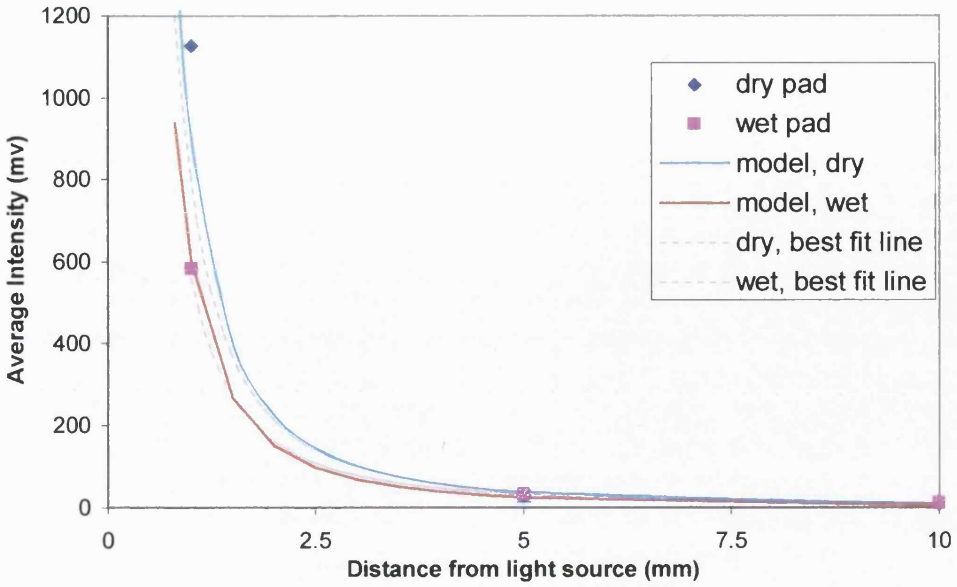

Fig.5.14 Fit of model to measured crosstalk data

An imaginary array of optodes was formed, each optode incorporating a transmitting fibre that would contribute to the light intensity of the central optode's receiving fibre. This contribution was calculated according to equation 5.9 if the transmitting fibre was in an area of 'dry pad' or according to equation 5.10 for a 'wet' area. Results are shown in Fig.5.15 where the 13 optodes have been linearly spaced 5mm apart. A fluid front, moving from left to right, has reached 5mm beyond the central optode. For each optode a bar is plotted using a logarithmic scale, showing the amount of light its input fibre contributes to the signal detected by the output fibre of the central optode and the wet or dry status of pad at that point. The contributions from all the optodes in the array are summed to calculate the total light intensity at the central receiving fibre for various positions of the fluid front. The results are shown in Fig.5.16, along with those from a linear array of optodes spaced 10mm apart.

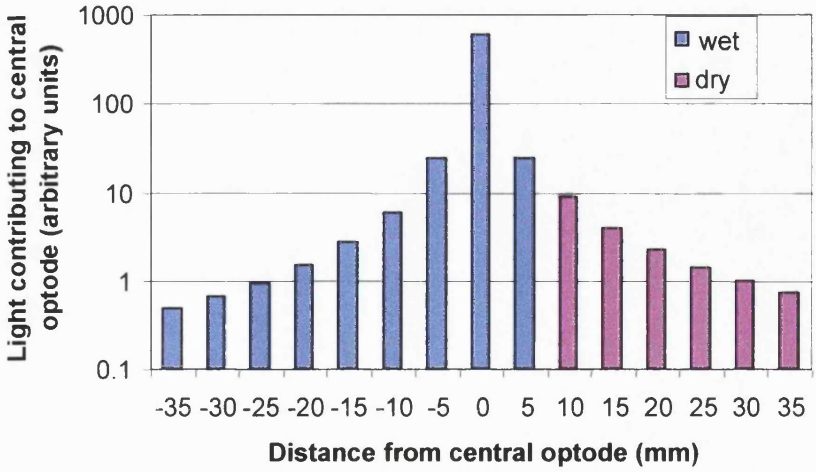

Fig.5.15 Calculated contributions of light to the central optode due to crosstalk from distant optodes

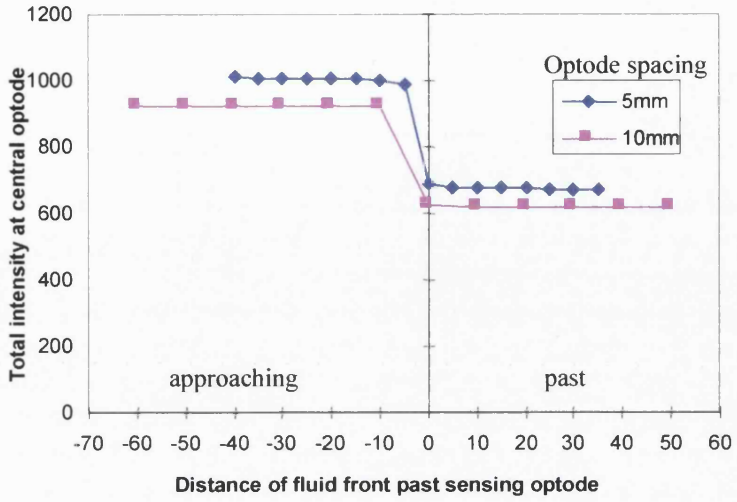

Fig.5.16 Calculated intensity trace for a linear optode array and a planar fluid front moving perpendicular to the optode array

Fig.5.17 shows the effect off applying the above model to a square grid of optodes with inter-optode distances of 5mm and 10mm.

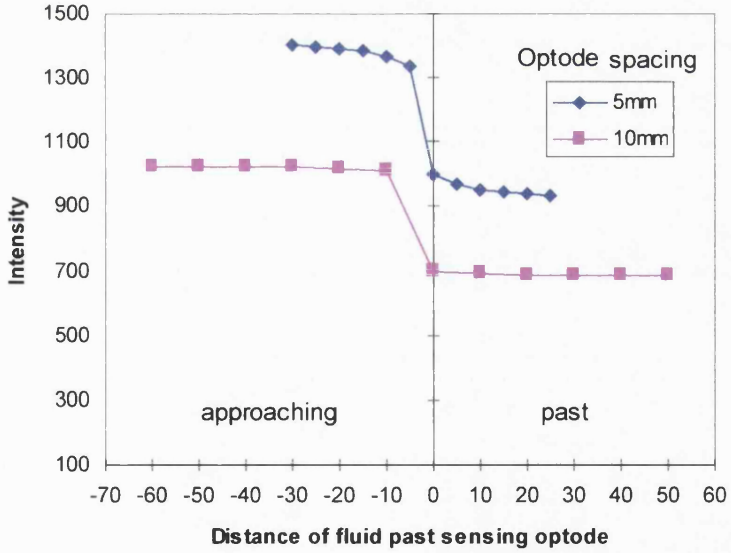

Fig.5.17 Calculated intensity trace for a square array of optodes and a planar fluid front moving perpendicular to the principle axis of the optode array

This model predicts that the actual and percentage intensity changes as the fluid front passes the central optode are slightly less in the case of the 2D array compared with the 1D array, for a given optode spacing (see Table.5.1). This is particularly true of the 5mm spacing and indicates that although this resolution is achievable, crosstalk would be beginning to become significant for the 2D array at this

spacing. Since crosstalk is still immaterial for 5mm spacing in the 1D array it can be assumed that a finer spatial resolution would be possible when using a single line of optodes. Optodes were used experimentally in a 2D array with 10mm spacing without any evidence of crosstalk degrading the data, as predicted. Smaller spacings have not been used because there are tradeoffs between the number of sensors, area covered and spatial resolution, which made it inappropriate to use resolutions less than 10mm.

	5mm optode spacing	10mm optode spacing
1D linear array	300 (30%)	300 (33%)
2D array	335 (25%)	309 (31%)

Table.5.1 Calculated change in light intensity reflected from an absorbent material on becoming wet

The above group of experiments and the resultant model assess the effect of crosstalk between adjacent optodes. It is also important to know how moving the fibres in an optode pair small distances apart affects their performance as this would affect the precision with which they would need to be held.

The effect of optode separation at very small distances was observed by using a translation stage to slowly separate the fibres of an optode pair while they abutted a dry sample of pad. This was repeated with the sample wet. Fig.5.18 shows the intensity of backscattered light as a function of the separation between the transmitting and receiving fibres of the optode. Upon applying best-fit curves to this data, according to the least squares law, it was found that there were two distinct regions for each curve. Comparing Fig.5.18 with Fig.5.13 it can be seen that, after an initial region of 2-3 mm, these results agreed with the previous experiment which used greater optode separations; that is, in this far region the data obeyed an inverse square law with a good degree of accuracy. Distances of less than 3mm were characterised by an exponential decrease in light intensity. This is the near region. The equations of best-fit for these two regions, for both wet and dry pads, are displayed on Fig.5.18.

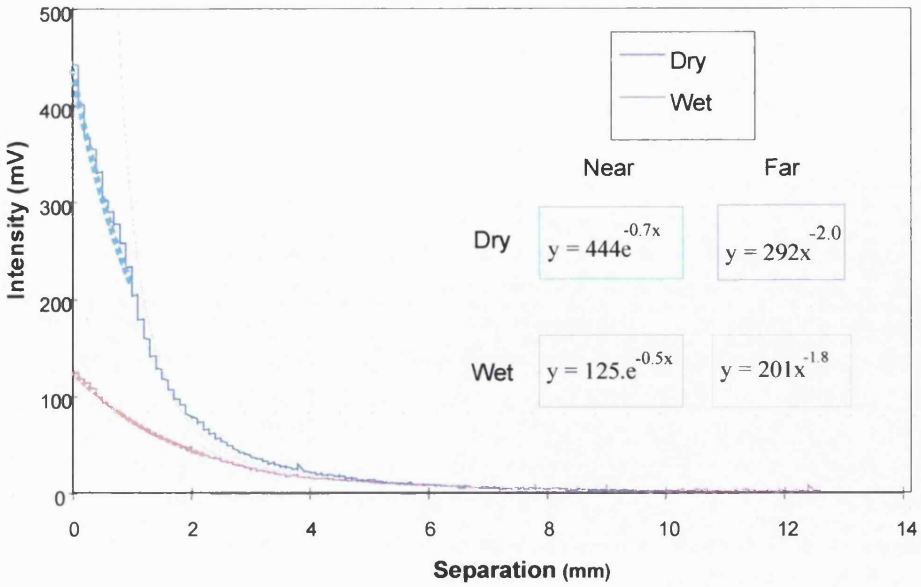

Fig.5.18 Effect of input/output fibre separation on reflected light intensity

These results show that the fibres need to be held as close together as possible - touching, if possible - for the most efficient use of light. In view of this input and output fibre pairs were strapped tightly together.

5.2.7 Separation distance between optode pair and pad sample.

Light emerging from an optical fibre is not collimated but divergent. Thus the distance from a surface to the light source will affect the amount of light projected onto a small area of that surface, following an inverse square law. An optical fibre used to collect light exhibits this phenomenon in reverse. The distance of the fibres from a surface defines the area of the surface from which it gathers light. This gathering of light also depends on the angles at which light is emitted from the surface. The objective of this experiment was to establish the net result of these effects. It is important to know how these effects combine in this situation to determine the accuracy with which the optode/pad distance needs to be maintained during subsequent experimental work.

An optode was held as shown in Fig.5.19, a height 'h' above a scattering tile. The height was varied using a micrometer translation stage. The intensity of the backscattered light was plotted as a function of height as shown in Fig.5.20. A standard scattering tile was used for this as it had a uniformly scattering surface with a scattering efficiency of better than 85%, unlike absorbent products which are non-uniform and which the light penetrates, causing scattering to occur at multiple depths. Using the scattering tile meant that the height 'h' (see Fig.5.19) could be accurately determined and that all effects due to inhomogeneities in the pad could be avoided. The experiment was repeated using a dry sample of disposable pad, to give an indication of the effective depth to which the light penetrated.

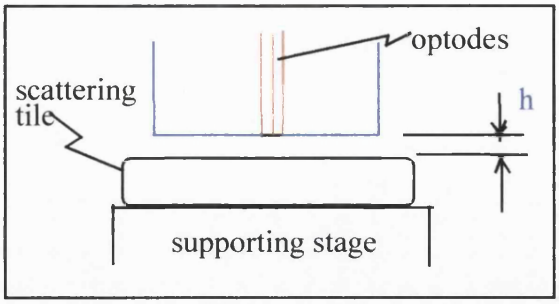

Fig.5.19 Configuration for testing effect of optode/pad separation distance

Fig.5.20 shows that there was an optimum height at about 2.5mm, at which the most light is collected. This point is at approximately the same height for the two materials. The discontinuities in the pad sample trace are due to accidental movement of the sample due to its low mass. Since the positions of the jolts are clear and the peak height is not obscured, it was considered unnecessary to repeat the experiment.

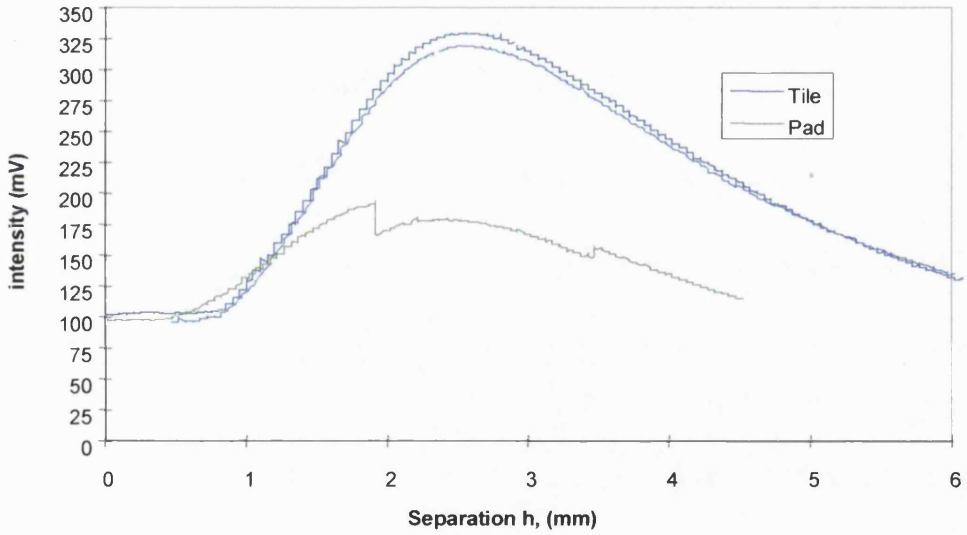

Fig.5.20 Effect on reflected light intensity of separation distance between sample and optode

An initial region was seen (height ≤1mm) where the light intensity did not vary with distance. It was unclear from this experiment whether this was a real effect or an ambiguity in the definition of zero. Elasticity in the system may have allowed the supporting stage to continue to be raised for a short distance after the optodes and sample touched.

If the separation between the optode and pad sample varied during an experiment due to settling of the sample under the weight of the applied fluid, an error may have been introduced into the results. This, however, is unlikely to be a problem if the sample is held flush against the optodes. Although the internal structure of the pad could change (collapse or swell), varying the mean distance from which the light backscattered, this effect was almost certainly much less than the change in intensity caused by fluid presence.

5.2.8 *Effect of variations in composition across a pad*

Absorbent materials, particularly those used in disposable pads are not made from a single homogeneous substance. Even for the simplest case of a reusable material made from a single fibre type, the distribution of the fibres would not be even, probably containing clumps known as Z-pegs, where the material had been needled together during manufacture. This inhomogeneity of incontinence products is much more marked for disposable pads where, apart from random fluctuations in density due to the way the products are manufactured, the pads are deliberately varied in thickness across the pad and incorporate layers of different materials.

Inhomogeneity of both reusable and disposable pads could be seen by eye when a sample was illuminated from behind with diffuse light. The objective of this experiment was to establish the extent to which this inhomogeneity caused variations in intensities detected by the measuring sensors.

A dry one-layer reusable felt strip was placed in various random positions on an array of optodes. The procedure was repeated with the strip saturated. In each case the pad sample was moved to a new position approximately every ten seconds.

The effect of this movement, on five representative optode pairs is shown in Fig.5.21, for the dry felt. Each different coloured trace represents the output from one optode pair for 13 different positions of the felt sample. The act of moving creating a spike in the data. This data was normalised so that percentage changes, in intensity, from that detected at the initial position were seen.

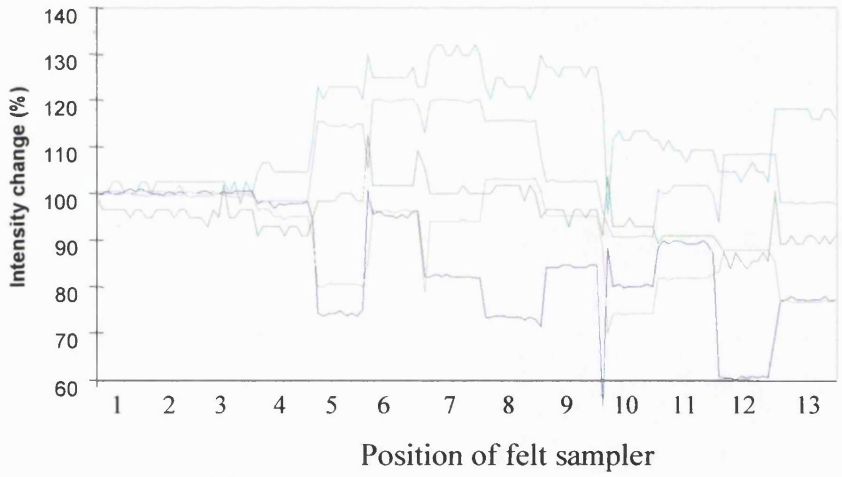

Fig.5.21 Effect of moving dry felt on reflected light intensity measured by five optodes

Although the range seen above covers +/-40 percent, the individual variation of most traces was +/-15 percent about their mean value. The initial intensity value to which each optode is normalised is not necessarily the overall mean for that optode but may represent one extreme of the range. This intensity variation is compared with +/-3 percent when a scattering tile is used instead of a felt sample.

Similar results and percentage changes were seen in the case of a wet felt sample as shown in Fig.5.22.

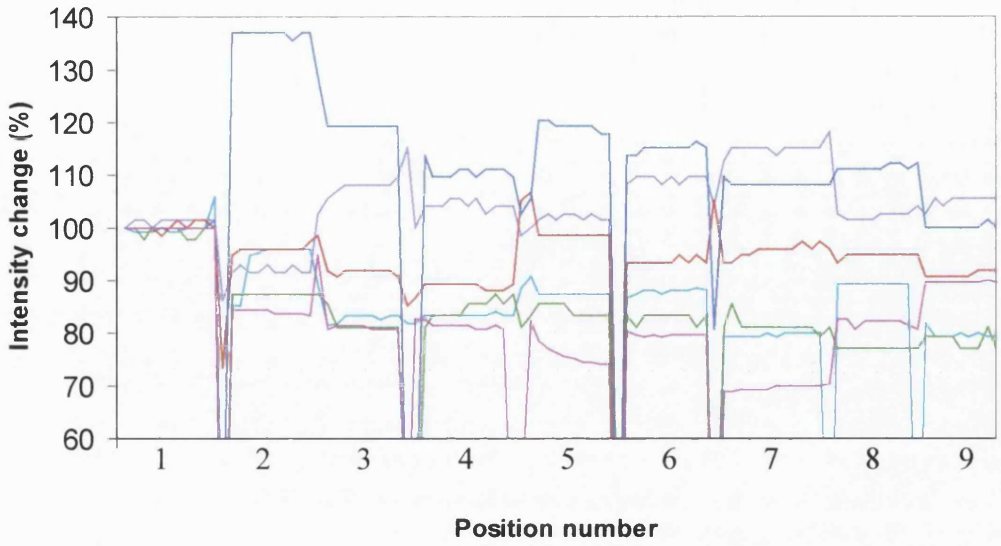

Fig.5.22 Effect of moving wet felt on reflected light intensity measured by six optodes

These results indicate that a significant proportion of the variation in intensity response of the different optode pairs is due to variations within the absorbent product. This experiment, however, only looks at the static case, wet or dry. It is likely that a high dry intensity corresponds to a high wet intensity of light but this question could not be addressed in these experiments due to the impracticality of accurately reproducing the same pad position for wet and dry measurements. Since it has been proved that the light intensity received by an optode – fixed relative to the pad sample - is reduced when the pad is wetted, these results do not invalidate the use of this optical technique for the study of pads. However, in the light of these results all measurements should be made relative to the initial light intensity at that point in order to minimise this effect of variation in pad composition.

5.2.9 Variations in measured optode intensities

The previous experiment looked at the effect of variation within the pad sample on the backscattered light intensity. Although this effect was found to be substantial, it was important to minimise possible intensity variation resulting from variation within measuring equipment.

In order to investigate this effect a diode laser beam was expanded using two lenses as shown in Fig.5.23. This generated a rectangular beam of light with a Gaussian profile of intensities, which just covered the twenty-four optodes, the outer optodes receiving a lower light intensity than the inner ones. The beam could not be further expanded without reducing the intensity of light received by each fibre to an unacceptably low level.

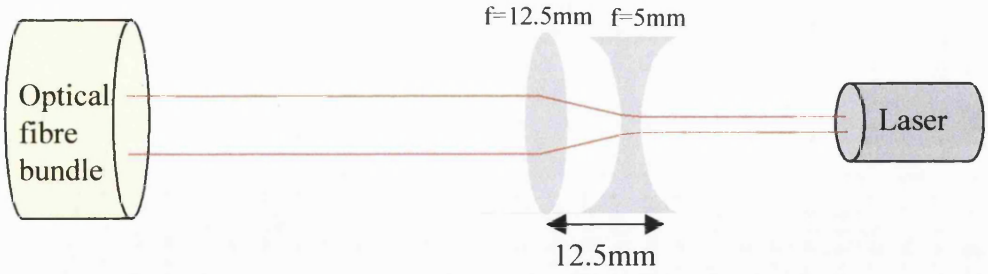

Fig.5.23 First lens system for expanding laser beam to service multiple optodes

The system was slightly simplified by replacing these two lens with a single convex lens of f=25mm (Fig.5.24).

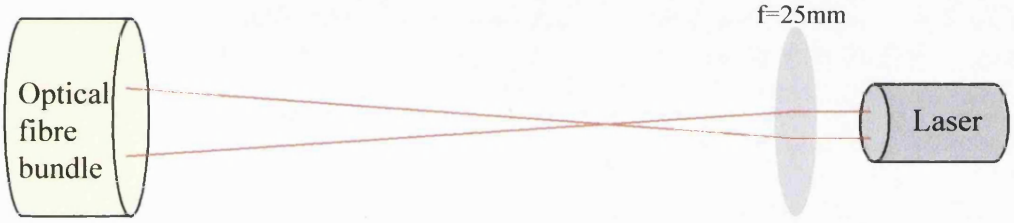

Fig.5.24 Second lens system for expanding laser beam to service multiple optodes

Also up to this stage the ends of the fibres were prepared by cutting with a sharp knife. This method could result in slight roughness of the unpolished ends and would cause an unknown proportion of the light to be reflected back from the end of the fibre. To minimise this effect the ends of all fibres used in later experiments were polished with 12μm lapping paper.

No significant reduction in light intensity variation was found upon use of polishing, although, all further optical fibres were prepared by this method as it minimised the risk of variation subsequently becoming apparent.

5.2.10 Post processing of the data

The previous two sections, 5.2.7 and 5.2.8 sought to identify and reduce the variation in the intensity of the light from a dry or uniformly wet pad. It was found that some variation was unavoidable due to the inhomogeneity of the product in question. For this reason post processing methods of data normalisation were investigated.

Various strategies were tried. Their appropriateness depended on their ease of use in addition to the normalising effect achieved. Combinations of normalising to the dry intensities, final values, minimum values and a combination of wet and dry values (using experiments where the final state at all points was known to be saturation) were considered.

Since the response of any given optode varies between experiments according to the composition of the sample, it was concluded that the normalisation technique chosen could not rely on

data from previous experiments. This precluded the use of wet intensity values as a basis for normalisation because not all areas of a pad would be at the same status of complete saturation. Use of wet intensity values were also inadvisable because the intensity/time profile of an optode frequently reached a minimum when the fluid arrived, before exhibiting a slight rise. This effect may be due to redistribution of the fluid. For these reasons, the technique of choice was dry normalisation:

Normalised intensity = measured intensity/initial dry intensity *100 ***-5.11***

The effect of using this technique for a number of optodes is shown in Fig.5.25 and Fig.5.26. Twenty-two optodes were placed in a horizontal line 10mm apart and covered with a strip of reusable felt. Water was allowed to wick into this strip from the end of the fabric nearest optode 1, until the fluid front had travelled to beyond optode 22. The original, unprocessed intensity traces are shown in Fig.5.25, and very little information can be gained from it. Fig.5.26 shows the data normalised according to equation 5.11. These traces reveal that normalising the data by this method gives a reduction in intensity of between 40% and 60% upon wetting for most optodes, regardless of their initial value. The normalisation also reveals the order in which the optodes were wetted, sequentially from 1 to 22. This information is obscured in the original data because of the wide variation in the backscatted light intensity from the dry pad.

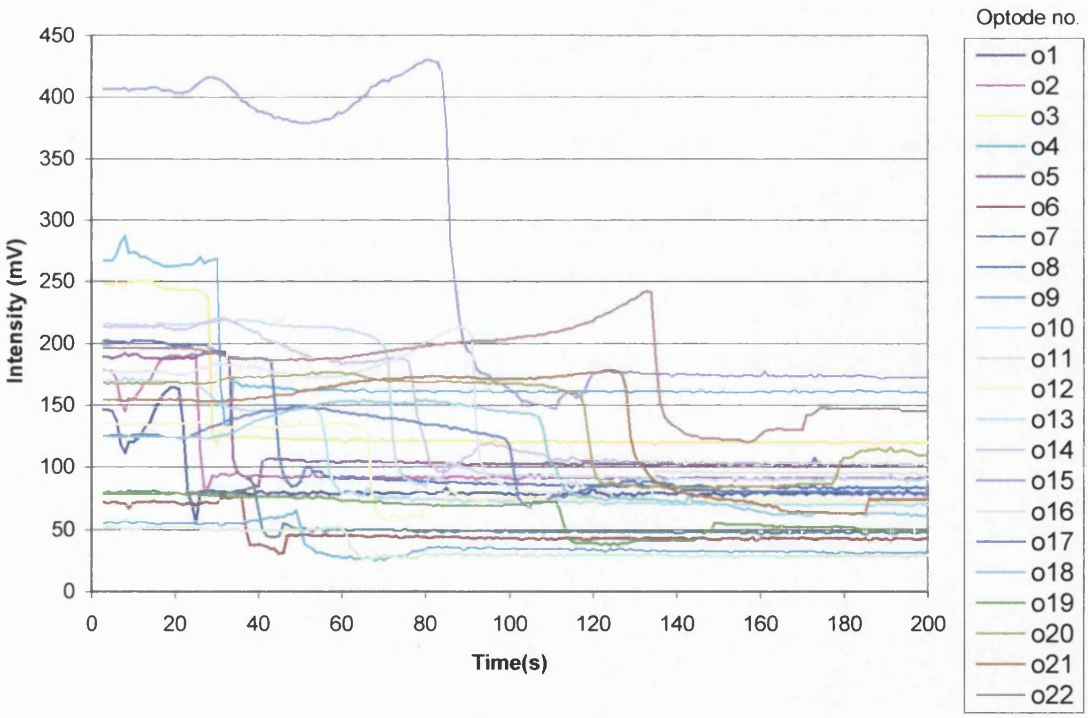

Fig.5.25 Example of un-normalised light intensities traces

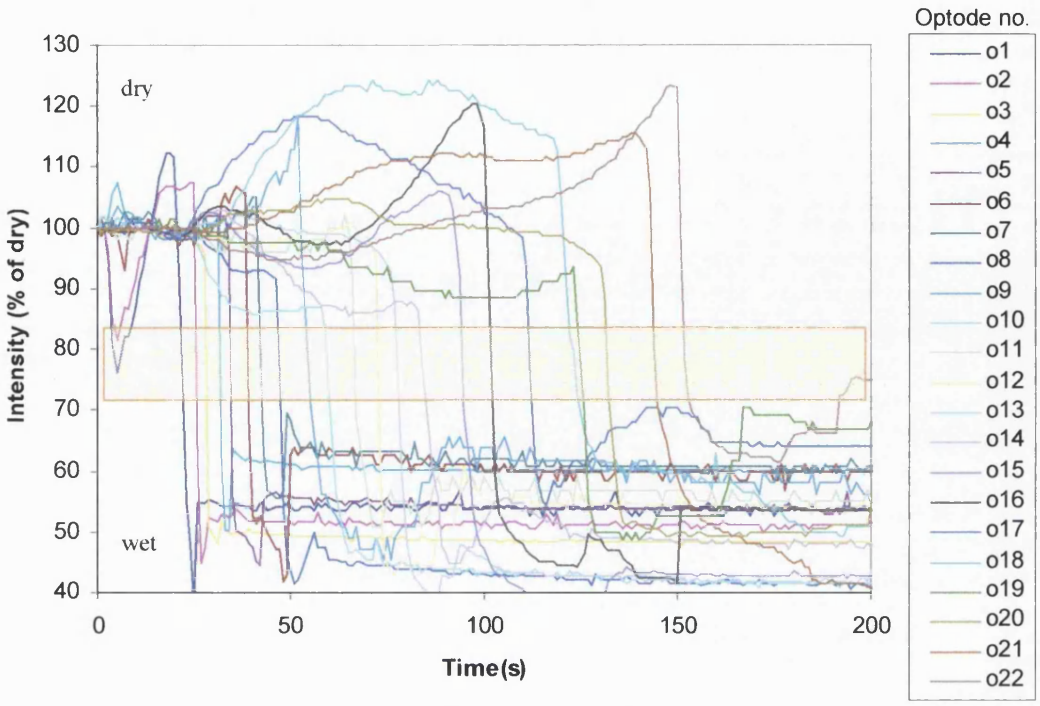

Fig.5.26 Effect of normalising light intensity traces to initial dry value, showing sequential wetting of optodes

5.3 Conclusions to preliminary experiments

Preliminary experiments indicated that backscattered light could be used to measure whether an incontinence pads was wet and that some information on the degree of wetness was achievable.

A spatial resolution of 5mm was practical with this technique and red light was of a suitable wavelength, giving low cross-talk between optodes and exhibiting a measurable change in reflected light intensity from dry and wet absorbent products. Red light was chosen in preference to other wavelengths that also showed a measurable change because bright light sources were readily available in this wavelength region.

Sources of inconsistency between the different optode pairs arose because of the inhomogeneous nature of the pad materials being imaged; this could not be prevented. There was also variation between the efficiencies of the optodes due to the presence of many interfaces between components where small defects in polishing or alignment were magnified. The effect of this could be partially removed by normalising the data after capture. Variations in the separation between the optodes and the pad should be kept constant throughout each experiment to avoid introducing artefacts into the data.

5.4 Refining the system

5.4.1 The light source

All the initial experiments utilised the brightest light source that was readily available, which was a red 3mW laser diode. Although this source was adequate, and sufficient to support 24 optode pairs when expanded with a lens system, it was not ideal for a number of reasons. In view of this, other light sources were identified and investigated. An ultra bright red LED was identified which could also support 24 optode pairs and had the following advantages:

- The size of the LED was less than a quarter of the size of the laser diode.
- The cost of the chosen LED was about 1/20 of the cost of a laser diode.
- All coherent light sources (i.e. lasers) have to meet additional safety precautions that do not apply to other light sources. Also the safety of a laser, as perceived by prospective subjects, could be less than that of an equivalent LED.
- No lenses are required to focus the light from an LED whereas at least one was required to expand the laser beam to an appropriate size. This simplified the system alignment. However, one extra component was required. The addition of a simple perspex rod smoothed the initial gaussian profile of the light so that all the transmitting optical fibres received uniform light intensity, without adding significantly to the complexity of the system.

The Perspex rod smoothed the profile due to the random reflections of light within the Perspex rod. With a rod of sufficient length, the output end of the rod will be uniformly bright regardless of the light intensity profile at the input end (Fig.5.27).

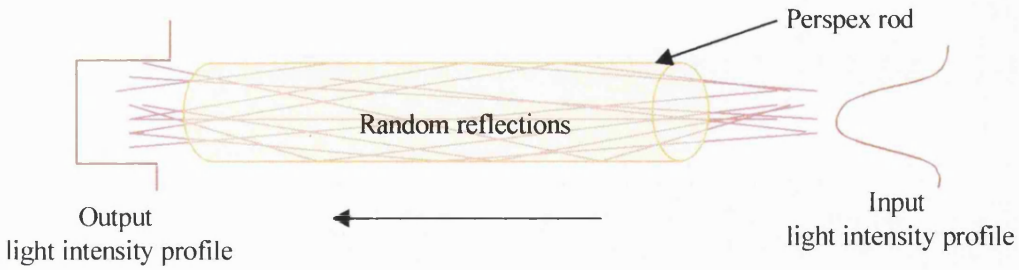

Fig.5.27 Light intensity profile smoothing by a Perspex rod

The laser light leaving an optical fibre becomes uncollimated within the length of the fibre and the angular distribution of the exiting light is predominantly dependent on the characteristics of the optical fibre, not the distribution at the light source. For these reasons the previous conclusions, with regard to the interaction between light and absorbent materials, remain valid for the LED light sources. This would not be true if they had not produced light of approximately the same wavelength as the diode laser.

5.4.2 *The optical fibres*

Throughout the initial experiments, plastic optical fibres, of 1mm diameter, were used (as described in Appendix 4). These single fibres offered a sensible trade-off between robustness, flexibility and the amount of light transmitted.

When considering whether to continue with these fibres in further testing, it was decided that plastic fibres were the most suitable because of their flexibility and low cost. However, experiments showed that a 0.5mm diameter fibre could transmit and receive sufficient light for this application. This was probably due to the consequent reduction in separation between the centres of the transmitting and receiving fibres of an optode pair, in combination with the advantages of an improved detection system (described in section 5.4.4). The decrease in size and stiffness were also major advantages over the 1 mm fibre when considering the long term aim of clinical studies. The use of these fibres should have an insignificant effect on crosstalk as this is a function of the transport of light in the pad and not dependent on the light source. If anything, crosstalk should be reduced slightly due to the reduced amount of light available.

The disadvantage of using plastic fibres was that they did not transmit infrared wavelengths. This precluded the use of high power LEDs designed for telecommunications. However, this factor was out-weighed by the superior flexibility and robustness of these fibres in comparison to glass fibres, which do transmit infrared light.

5.4.3 *The number of optode pairs*

Although 24 optode pairs was a suitable number with which to understand basic principles it was too few to provide coverage of a whole pad. The number of optodes needed was a trade-off between adequate resolution and the related complexity of the imaging system. 500 optode pairs were chosen as a suitable compromise. This number would cover the main region of interest in pads (that is all but the extreme edges of products, which rarely get wet anyway) at a resolution of 10mm spacing between optode pairs or all but the very extremes of the largest pads at 20mm spacing. Not all optodes need be used at any one time and mixed spacing would be possible, including a line of sensors at 5mm spacing for more detailed information along the axis of the pad. This number of optodes provided sufficient flexibility without being excessive.

5.4.4 *The detection system.*

Individual photodiodes, coupled directly to the output fibres were used to detect the light during the preliminary experiments. The outputs of these photodiodes were fed to a computer, via an analogue to digital converter. Apart from uncertainty about the precise alignment of the photodiode/optical fibre connections, which could have been standardised with significant effort, this provided an effective, cheap and compact detection system for small numbers of optodes. To upgrade such a system to monitor 500 fibres would have created bulky apparatus and required a more advanced A/D board with appropriate software.

An alternative option was to image all the optical fibres simultaneously using a CCD or CMOS device. These sensors are relatively cheap and consist of an array of light sensitive areas (or pixels) which are read out periodically in a systematic fashion as a series of analogue voltages corresponding to the light intensity received at a pixel over a period of time. The readout from such a device can be fed into a frame grabber. This is a device that converts the analogue signal into quantized integer valued intensities known as grey scale levels. The system has the same net result as an A/D converter whilst preserving positional information, provided the position of a fibre on the image is known, the light intensity transmitted through that fibre can be measured. Of the two approaches (photodiodes with A/D board or camera with frame grabber) the camera approach was adopted as it offered advantages in reduced size, cost, and in the complexity of the hardware. A commercially available device, known as an '*im*puter' was used (VLSI Vision Ltd). This device possessed an onboard frame grabber, memory and 8032 microcontroller, enabling images to be processed within the device. This facility meant that there was no need to upload each image to a computer (a time consuming process). Instead the image could be processed and only the optode values that were calculated from that image uploaded, via a RS232 connection. The memory facility allowed the possibility of running the system independently of external connections (mains power supply and computer link) using a battery pack and uploading the data later. This would be an advantage during clinical trials that would not be possible with conventional digital imaging systems which often use a remote camera connected to a PC which contains the frame grabber.

The other major feature of the *im*puter was its small size, which is similar to that of a hand held camera. This also would be an advantage in clinical trials.

One potential disadvantage with the *im*puter was that it is limited to 255 grey scale values whereas a photodiode has much finer intensity resolution. However, the signal variation due to other factors meant that 255 grey scale values was more than adequate.

5.4.5 Anticipated system specification

In the light of these results an optical imaging with the following specification should be possible:

- Up to 500 sensors
- Spatial resolution variable between 5mm by 5mm for small areas or 20mm by 20mm for a whole large pad
- Temporal resolution of 0.5s
- Degree of wetness resolution 'dry' plus approximately five levels of 'wet', each of 10% change in measured light intensity.
- Experiment duration up to eight hours for clinical studies
- Portable for clinical studies

6: The Optical Imaging System

6.1 Overview of the system

The results from section 5.4 were used in the design of a complete imaging system for absorbent incontinence products. This consisted of a control box with computer link and interchangeable optode/pad holders.

6.1.1 Hardware

A schematic diagram of the optical imaging system is shown in Fig.6.1 and a photograph of the control box is shown in Fig.6.2 with the lid removed to reveal the various components. Light from each of 10 red LEDs was passed through a Perspex rod, to smooth the light profile, and into a bundle of 50 optical fibres, - each 0.5mm in diameter - encased in a metal ferrule. Each light input fibre was paired with a fibre from the corresponding output bundle and plugged into one of an array of holes in one of the optode holders, such as the neoprene rubber holder shown in Fig.6.4. The output bundles, like the input bundles, were comprised of groups of 50 fibres encased in a metal ferrule, in this case rectangular.

All of the output bundles were viewed by a CMOS imaging sensor within the *im*puter, through a short focus lens. This enabled the image of the fibre bundles to fill the whole field of view of the *im*puter with the image of each fibre covering an area corresponding to nine pixels. Small fluctuations in measured light intensity were present due to interference noise within the sensor, an anomaly of the fabrication process. The resulting image was then manipulated by the attached data processing unit to compress the amount of data uploaded to a computer, as described in section 6.1.2. This uploading could be carried out simultaneously or the data could be stored in the *im*puter and uploaded later. On board storage of data would be essential if the device was used with an ambulatory subject whose movement would be restricted by a computer link.

The complete system is compact enough to be attached to a belt and could be powered from a battery pack to enable monitoring of a pad worn by an ambulatory subject. This would enable factors such as the effect of walking on pad performance to be observed. When used in the laboratory the device could be powered from a standard 12V transformer.

Technical drawings of this system are shown in Appendix 2.

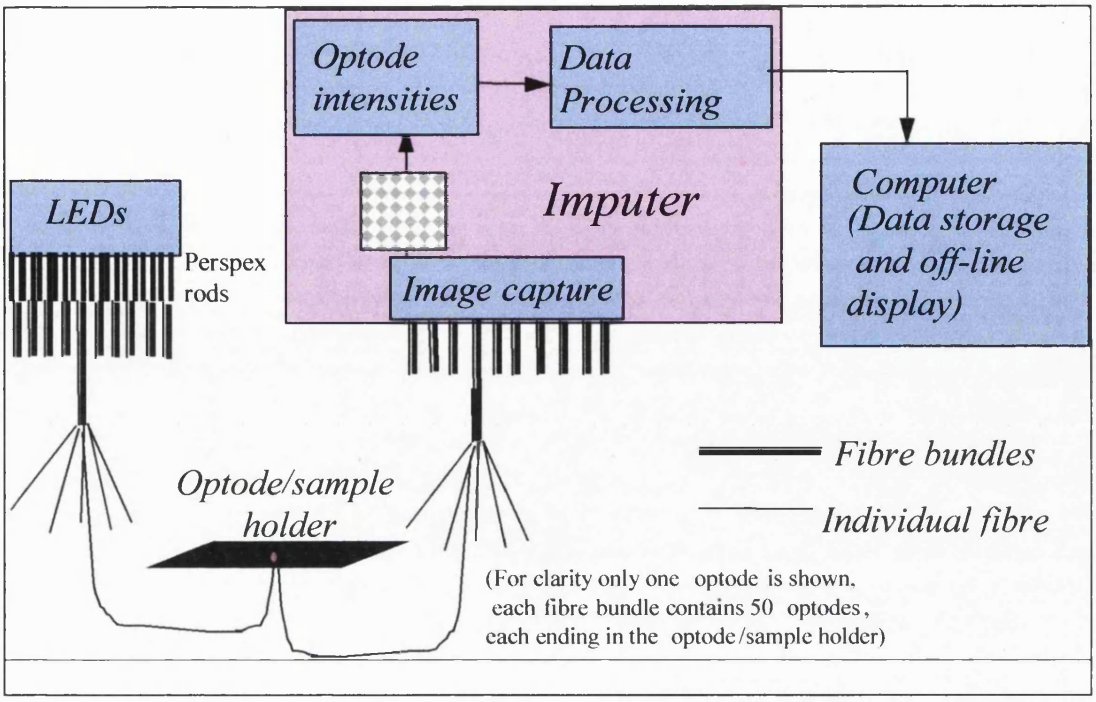

Fig.6.1 Schematic of optical imaging device

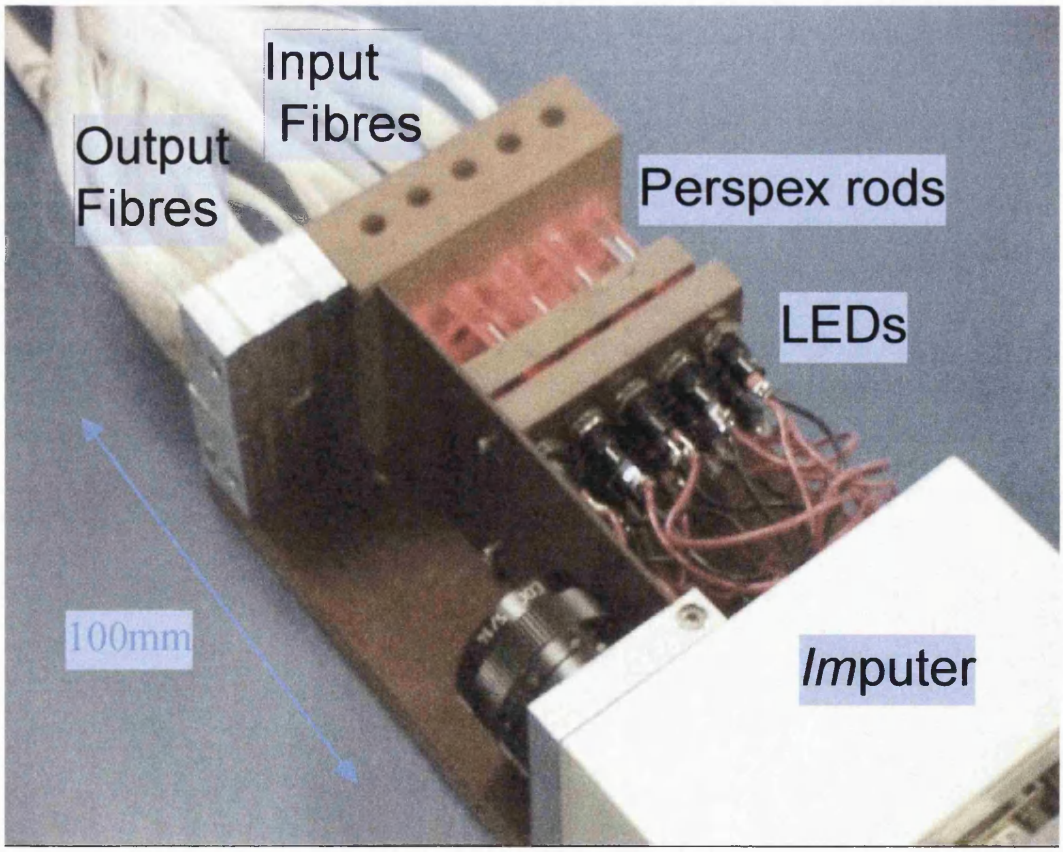

Fig.6.2 Photograph of optical imaging device, lid removed

6.1.2 *Software*

The *im*puter was used to control image capture and process the images as shown in Fig.6.3. The light intensity coming from each fibre was calculated using a look-up table to find the position of that fibre and averaging the grey scale values of the nine pixels corresponding to its position. The time of each image, t, was logged along with a flag, "999", to distinguish this from intensity values. The value of 'noise' was defined in software and could be varied depending on the level of data compression required. Light intensity changes of less than this number of grey scale values were ignored. A value of four was normally used as this removed most of the interference noise without degrading the fluid saturation data. Extracting only the relevant data from each image, in this way, yielded a variable compression rate that depended on the rate of change of the image. If half the optodes showed a change in light intensity in the same image a compression ratio of 65:1 would be achieved. This increased to nearly 3000:1 for a static fluid pattern.

If the data was stored internally during the experiment it did not need to be uploaded to a computer immediately but this had to be done before power was removed from the *im*puter or further data was collected.

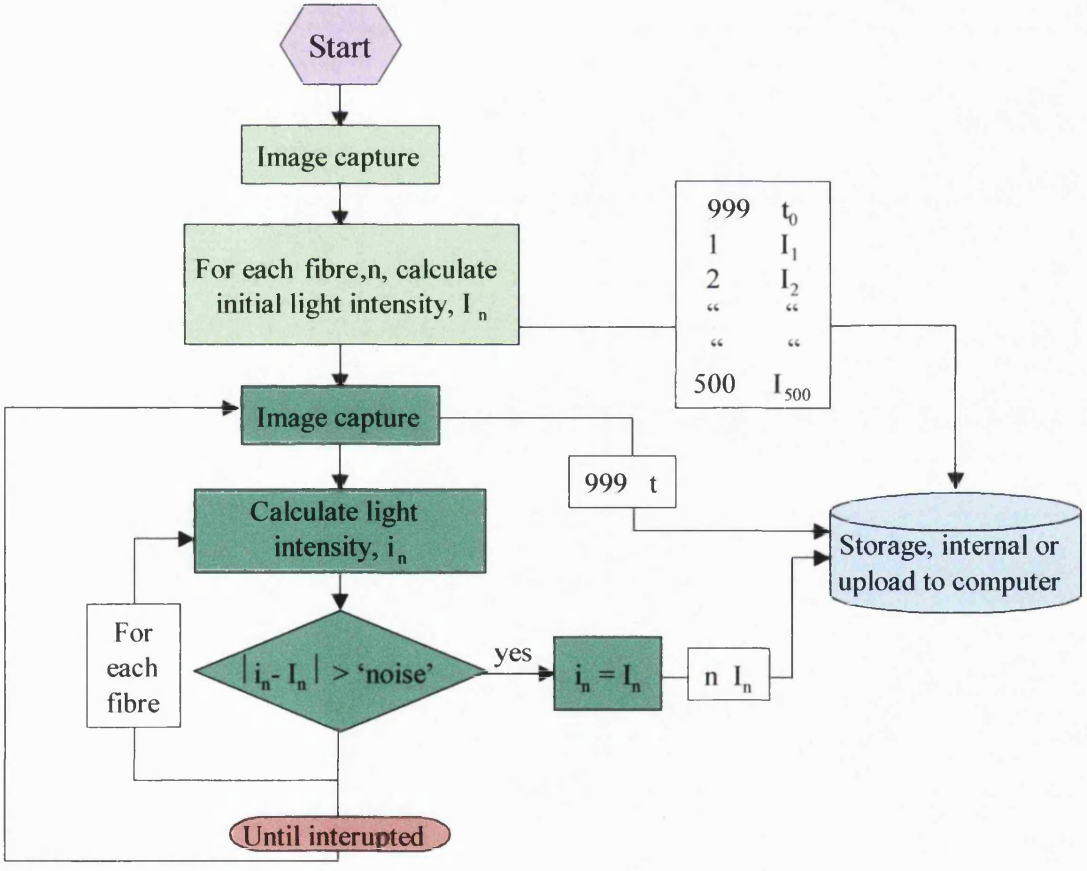

Fig.6.3 Flow chart of *im*puter operations

Design of this program had to take account of the small amount of directly readable memory available. This was handled by directly addressing the memory blocks; that is, specifying a variable by

address not by name, keeping the number of variables to a minimum and shuffling data arrays in and out of other memory banks as they were needed. This ensures that the most efficient use was made of the available memory. The program also needed to be optimised for speed to enable real-time imaging of fluid spread. A speed of one image cycle per second was considered the slowest useful rate for the materials being studied.

The speed that can be achieved was dependent on the number of optodes in use and the number of optodes that exhibited a change in light intensity, per cycle. With 500 optodes the system can run at more then two cycles per second for all but the most extreme of change rates. However, in practice, two cycles per second was chosen for simplicity.

Appendix 3 lists the code for this internal *im*puter program and that used on an external computer to communicate with the *im*puter.

6.1.3 Optode/pad holder for laboratory use

Having established that optical fibres could be used to study fluid flow in pads, and characterised their performance, a means of holding optical fibre pairs in a set position relative to a pad sample, and each other, was required. This would enable whole pads to be studied in a reproducible manner. This system had to facilitate the easy replacement of the pad between experiments, and to be capable of being formed into a number of geometries (e.g. flat, sloped or curved) to imitate the shape a pad would take up clinically. Since this optode holder was for laboratory use, the constraints of holder thickness and other issues, which would arise if the system were to be used in a clinical setting, did not occur.

The initial system used was a 6mm thick neoprene rubber sheet into which an array of holes was drilled. The input and output optodes were taped in pairs, polished and push-fitted into the holes, so as to be flush with the surface of the neoprene. The rubber was chosen so as to be thick enough to hold the optodes perpendicular to its surface. Fig.6.4 is a diagram of this holder.

Advantages of this system included the optical properties of Neoprene: it was black and so reduced interference between optodes. In addition, Neoprene is waterproof. The elastic properties of rubber meant that optodes did not need to be glued in place, instead being held by friction. This enabled the array pattern to be changed easily. The flexibility of rubber meant that the optodes could be held in numerous curved geometries, although, at the thickness chosen the rubber could only curve in one direction at a time, providing cylindrical, but not spherical, shapes. This thickness of rubber also provided sufficient stiffness for a 1m x 0.5m sheet to lie approximately flat when supported at the edges, the rubber dipping by about 10mm in the centre. This was reduced to about 1mm with additional supports.

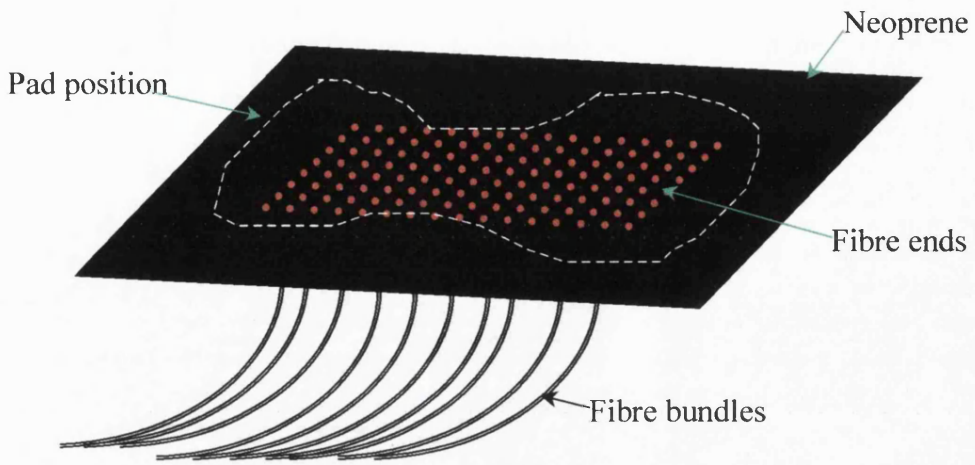

Fig.6.4 Diagram of neoprene optode holder

6.1.4 Problems Encountered

When this design was first implemented in conjunction with the neoprene optode holder a number of problems were identified which were addressed as discussed below.

Performance of light sources

The light sources that were being used were from two separate production batches. There was a visible difference in the emitted light intensity between these batches despite their being nominally the same product. The LEDs originally tested were brighter than later purchases of the same product. Subsequently these LEDs were upgraded to those of a newer model. There is no visible output variation between the newer model LEDs. Also the intensity of light measured by the optodes, above the background level, is 12 greyscale levels greater than for the original LED's. This was a signal improvement of approximately 30%.

Suitability of optode holder

The neoprene optode holding system is useful for basic laboratory work but cannot be used for clinical trials and was found to be inappropriate for use with complex pad curvatures within the laboratory setting. There were two reasons for this. Firstly, the stiffness of the neoprene was greater than anticipated and it would not curve simultaneously in two directions. Secondly, the elastication present in many products caused pads to pull away from the optode holder. In view of these limitations a curved optode holder was designed for laboratory use. This is described in section 6.2. A number of methods for laying the fibres parallel to the pad, and turning the light through 90° at the tip, were investigated for clinical use. This work is reported in section 6.3.

Intensity increases

During most experiments a number of sensors recorded an increase in intensity, implying that the pad had become drier – a fact that is not physically realistic. In some cases this intensity increase had the appearance of random noise but in other cases, a region of brighter intensity surrounded the wet area

or a band of brighter intensity crossed the region. In both these cases this was probably due to an air gap between the pad and sensors diminishing in thickness during the experiment. It has been shown in section 5.2.6 that the intensity of light backscattered from a pad was highly dependent on the size of any air gap. Thus if there was a gap between the pad and the sensing optode the reflected intensity would be low. However, if this gap was reduced, for example by pressure from above, the intensity of the backscattered light would increase. This would explain a 'super-dry' band, possibly corresponding with a packing fold of the pad and the circular super-dry area, which may not be permanent. This would be the case if the pressure was due to fluid that was not directly above the optode, enabling the intensity increase to be reversed when fluid actually arrived at that point and caused the normal decrease in light intensity.

In order to determine whether this effect was due to a varying air gap, a pair of experiments were conducted in which a 45g weight, of area 75 x 45mm, was placed on the pad during the experiment. In the first case the pad was stretched over the neoprene, removing wrinkles but, as can be seen in Fig.6.5, this increased the probability of there being an air gap between the pad and the optode holder. In the second case the pad was smoothed and taped in position without stretching, allowing it to conform to the slight curvature of the neoprene. In neither case was the pad made wet.

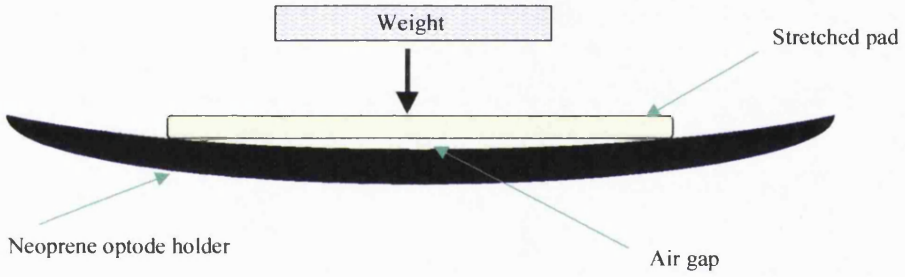

Fig.6.5 Vertical cross-section of pad sample stretched over neoprene optode holder, showing air gap.

Fig.6.6a shows an image of the stretched pad under normal conditions and with the weight applied. Each pixel in the image represents one optode and is coloured according to the percentage change in light intensity from the start of the experiment. If water had been applied to the pad, pink would correspond to a dry pad and blue to a wet pad. The pad was observed to move/collapse under the weight and created a circular region of increased light intensity, at a time corresponding to the placing of the rectangular weight. This suggested that an air gap had been present under the whole central portion of the pad. Fig.6.6b shows the normal image and one with the weight in place for the non-stretched pad. No movement was felt when the weight was added but a slight decrease in light intensity is seen in the central region accompanied by an increase in random noise, due to crushing of the pad.

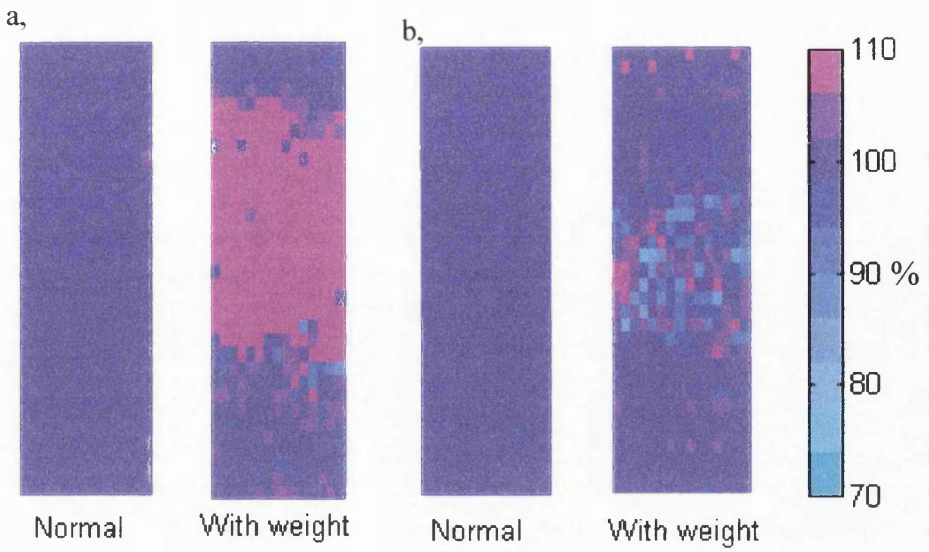

Fig.6.6 Effect of air gap between pad and optode holder on image noise when a weight was applied to the pad. a, airgap present and b, no airgap present

Having been identified, this effect is unlikely to detrimentally affect the performance of the apparatus, as long as care is taken during the set up of each experiment to ensure that there is a good fit between the pad and the optode holder, removing all air gaps.

Variation between optode sensitivities

The performance variations between the optodes was found to be considerable, even after the LED's had been replaced (see above). Fig.6.7 shows a frequency histogram of the initial light intensities, the standard deviation of this is greater than 20% of the mean value. This variation had two main sources:

- A background gradient in the image (see Fig.6.8. This is an image of a uniform piece of black paper and revealed a horizontal intensity gradient in the image on which all other information was superimposed.)
- Efficiency differences along the fibre path. Tiny variations in the assembling of the optodes resulted in variations in the percentage of light lost at junctions in the optical path, in addition to those junctions involving the pad sample.

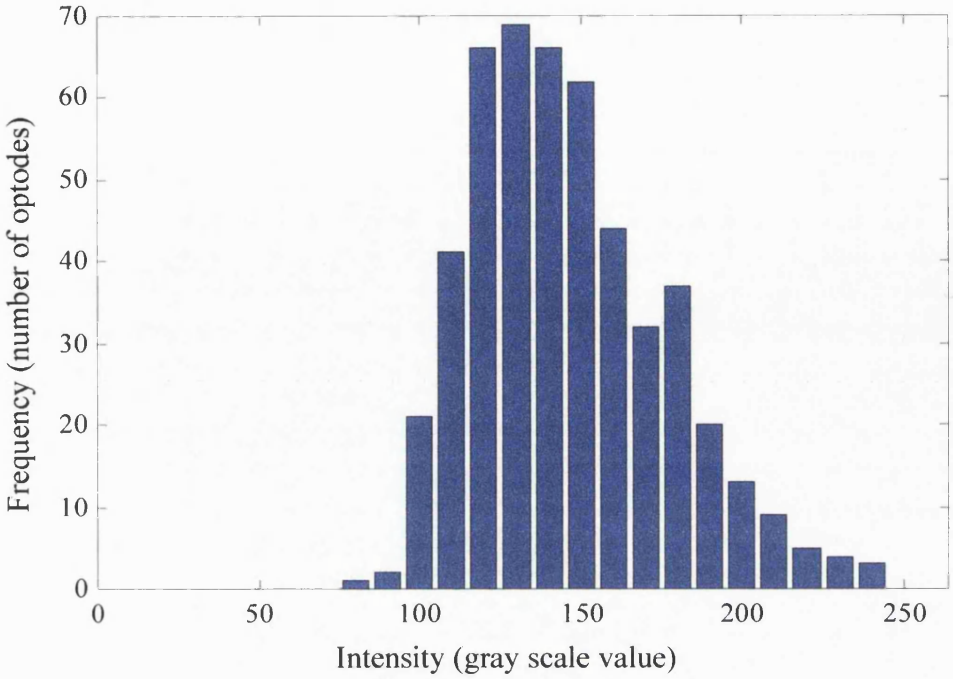

Fig.6.7 Frequency histogram of initial optode intensities

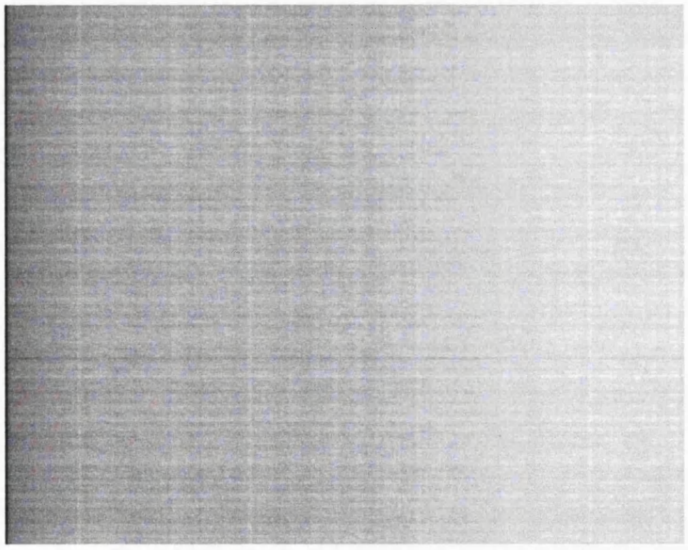

Fig.6.8 Background image from *im*puter

The background gradient (Fig.6.8) was a function of the CMOS device but it could be corrected in software. However, the offset of the gradient was shifted depending on how long the device had been switched on. This was probably a temperature effect and was minimised by allowing the equipment to

warm up for at least ten minutes before conducting any experiments. Thus, the background value at any point was the sum of:

- The average background at that point, as stored in a look-up table
- The deviation, from average, of a spare output optode constantly monitoring the background intensity

This background correction was effectively the offset of the sensor with the efficiency of the sensor analogous to the gain of the system. There were so many interfaces along the path of each fibre that it was impractical for them all to perform identically, particularly at the fibre/pad interfaces, which varied from experiment to experiment. For this reason greyscale values (i.e. light intensities) were expressed as a percentage of their value at the start of the experiment. This normally corresponded to the light intensity from a dry pad.

This normalisation can be summarised as:

$$\text{Normalised intensity reading} = \frac{(\text{intensity reading} - \text{background}) \times 100}{(\text{Initial intensity reading} - \text{background})} \qquad \textit{- 6.1}$$

Any optodes that, for a particular experiment, had very low light levels - that is, which did not have a dry value significantly greater than their background level - were marked as dry throughout. This avoided the problem of minor light intensity fluctuations (due to system noise) being exaggerated and interpreted as wetting of the pad.

This normalisation results in a much clearer image of the fluid than that achieved when the background gradient was not taken into account. This is illustrated in Fig.6.9 a & b. Fig.6.9a shows an image of a wet pad normalised using equation 5.11. Pink areas represent dry/original values and the shades of blue indicate a decrease in the detected light intensity. This corresponds to the wetness of the pad: the brighter the blue, the wetter the pad. Fig.6.9b shows an image of the same data, this time normalised according to equation 6.1. Three optodes in the middle of the wet area were marked dry, due to having low light intensities on this occasion, these were too low to detect fluid when normalised by either method.

It can be seen that normalising the data produces a less noisy image, allowing greater detail to be seen, particularly near the sides of the pad (the right and left margins in Fig.6.9), where the product is thinner.

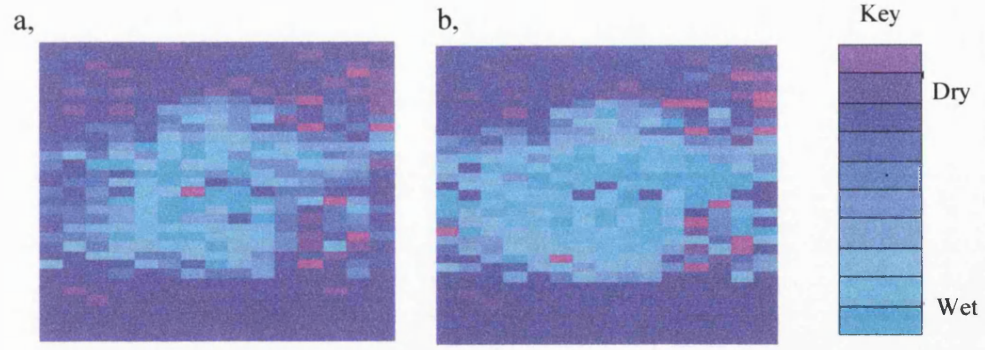

Fig.6.9 Effect on image noise of a, using original normalised method and b, correcting for the background gradient

6.2 Curved Optode Holder

One of the conclusions resulting from the use of the optical imaging system was that there were limitations to the neoprene optode holder used. The neoprene sheet used in this basic laboratory system (see Fig.6.4) enabled pads to be examined while flat or curved about any one axis. This was not clinically realistic and required the shaping elastics to be removed from the pad to enable it to lie flat against the optodes instead of curling up at the edges. A more clinically realistic laboratory optode holder was required.

This optode holder needed to have a simple mathematical shape, to facilitate manufacture and description, while mimicking the essential geometry of the human body. Various workers have built mannequins which reproduce the geometry of a person from waist to thigh and these are often used in leakage performance tests (see section 2.3). However, this approach was not used here, primarily because people vary enormously in size and shape, undermining the realism of using a single representative mannequin. In addition, mannequins are very sensitive to the way products are put on. In view of this it was decided that a simply geometry which reproduced the basic shape and enabled products to be reproducibly fitted to the holder would be best. A ~200mm diameter hemisphere, extended by a cylinder, was chosen, as a mathematically simple shape about which bodyworn pads would fit snugly.

The holder was cast from black resin using a plaster outer mould and a card inner mould. The holder had to be cast in two stages to counteract the resin shrinkage that occurs within an object of this size, which could cause it to crack. Three tubes were fitted, terminating flush with the outer surface. These provided a choice of urethra positions through which fluid could be applied to a pad. The first was positioned at the centre of the hemispherical end of the holder, and the other two angled at 23° & 45°to the axis of the hemisphere, and in line with the central line of optodes (Fig.6.10). The two angled tubes cover the typical range of urethra positions whilst the central position simplifies the geometry of the system, even though it is clinically unrealistic. The optodes were inserted from the inside, through holes drilled in the cast, and glued in place so as to terminate flush with the outer surface. All fibres were held perpendicular to the surface of the holder. The optodes were arranged in a 15 by 33 optode array, a

rectangular grid of 12.5mm by 12.5mm on the cylindrical portion of the hemisphere and with the optodes 12.5mm apart along lines spaced 7.2° apart on the hemisphere, as shown in Fig.6.11. This arrangement translated to an approximately square celled array when "unwrapped" from the surface and laid flat. This is akin to taking a pad off and laying it out flat with its elastics stretched. The complete holder can be seen in Fig.6.12a and in Fig.6.12b with a pad attached.

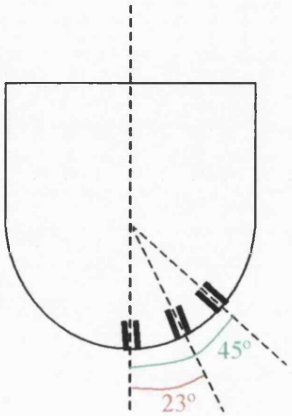

Fig.6.10 Cross-section of curved optode holder through central line of optodes showing urethra positions

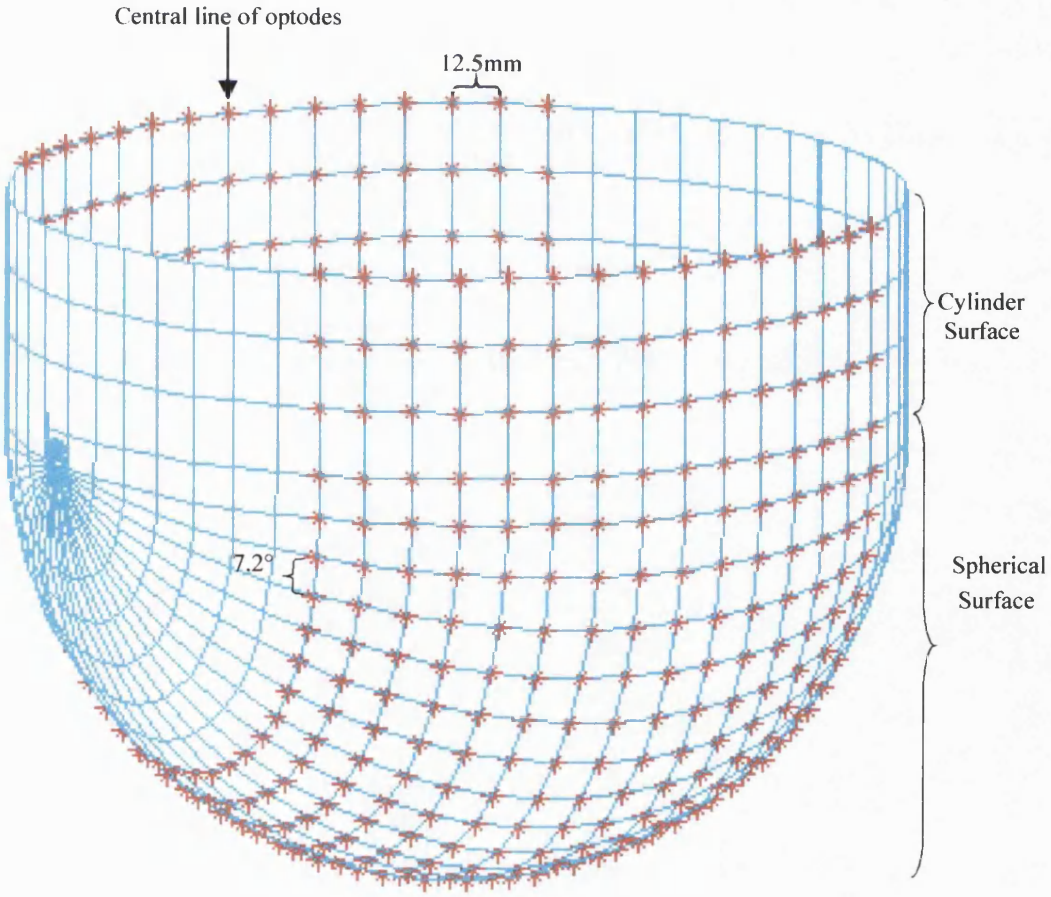

Fig.6.11 Position of sensors in curved optode holder

Unlike the basic optode holder, the curved holder was designed to look at the inside surface of a product; that is, the coverstock. This change was made because of the impracticality of holding pads against the inside surface of a hollow hemisphere when they are designed, often with elastics, to fit, slightly stretched, over a solid object. It was considered that this change would be unlikely to affect the fluid pattern detected because the technique did not actually look at the surface of the product but detected light from a three dimensional volume of scattering material.

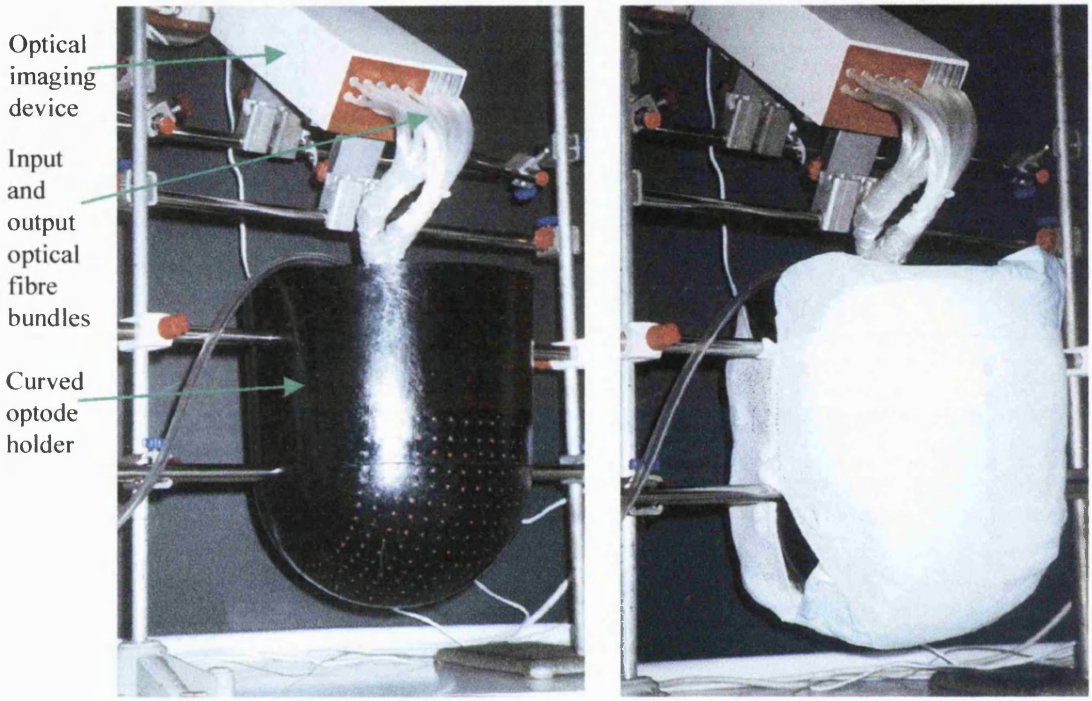

Fig.6.12 The optical imaging device with curved optode holder a, without pad, b, with pad in place

6.3 Modifications of optode ends for use in clinical experiments.

The neoprene and curved optode holders had their optodes positioned perpendicular to the pad surface. These holders were designed for laboratory use where this is not an issue but such a configuration is unsuitable for use in a clinical setting. In order for sensors to be used for monitoring a pad while it is being worn by a person they must be as unobtrusive and comfortable as possible. More specifically, the optical fibres leading to the sensors can not protrude, hedgehog fashion, perpendicular to the pad. In addition to this being an obstruction to the comfort of a sitting or supine subject, the weight of the subject may bend the fibres significantly, causing serious signal loss or even breakage of the fibre. Despite this, light has to travel into and out of the pad – ideally perpendicular to the surface. Thus the major obstacle to creating an optode holder for clinical use was finding a means whereby the optical fibres could be held against the pad surface whilst still emitting and receiving light perpendicular to the surface.

This section describes the development of an optode array that could be used to instrument a pad when worn by a patient.

6.3.1 The problem

A mechanism was needed which enabled the light entering/exiting the fibres to be deflected through 90°, enabling the fibres to lie flat against the pad, curving with its contours. This mechanism should ideally:

- Deflect all the light reaching it through 90°, without directing light from the input fibre straight back down the output fibre.
- Be of small size, not adding bulk to the pad.
- Be robust enough for repeated use
- Withstand washing or sterilising
- Be able to be manufactured reproducibly
- Be of reasonable cost

6.3.2 Solutions considered

Several different solutions to this problem were explored. Details of these are given below.

Diffusing medium (Fig.6.13) – Light travelling through a diffusing medium will, within a short distance, loose all directionality due to multiple scattering and exit randomly from all the surfaces of the material. Most translucent white materials will be, to some degree, a diffusing medium; for example, nylon and any glue which does not dry clear.

To test this approach a large blob of epoxy resin was allowed to set on the end of a sample optode. When this had set there was no detectable difference in light intensity at the output whether the optode tip with diffusing medium was viewing a dark background or a pad sample. This indicated that a low percentage of light followed the desired path, with a significant amount of light reaching the receiving fibre without interacting with the pad. Adding a reflecting surface, which prevented light leaving the diffusing medium from the rear, increased the probability of light leaving from the correct surface. However this did not result in significant improvement and so this mechanism was rejected.

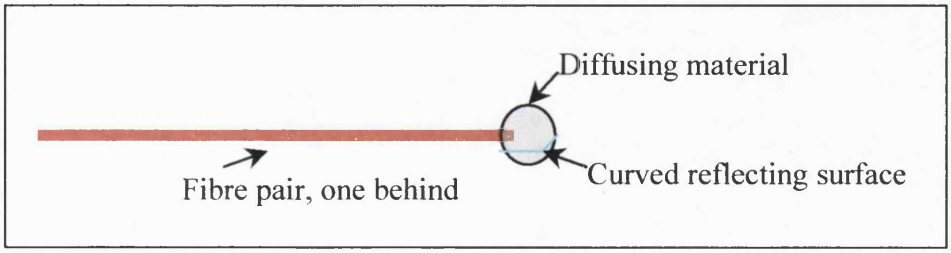

Fig.6.13 Optode with diffusing medium tip

Bending the tip of the fibre (Fig.6.14) – Optical fibres are designed to channel light around bends. This is achieved by a high refractive index difference between their core and cladding materials. However, all optical fibres have a minimum bend radius. If a fibre experiences a bent tighter than this it may allow light leakage through the cladding or it may break.

The recommended minimum bend radius for the type of fibre used is 9mm. This would require a device longer and deeper than 9mm to hold the fibre in the correct position, increasing the thickness of a typical pad by about 50%. Also, it is likely that the stiffness of the pad would be much increased. These factors would combine to disrupt the comfort of a subject as well as distorting the pad away from the normal position of wear. For these reasons this approach was considered inappropriate.

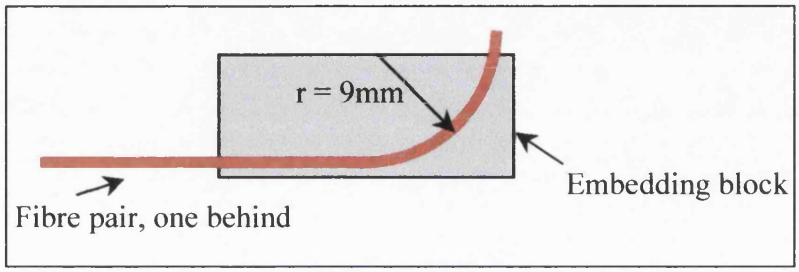

Fig.6.14 Bent optode held in rigid block

In-built prism (silvered) (Fig.6.15) – The ends of optical fibres are usually cut perpendicular to the axis of the fibre. This minimises transmission losses due to total internal reflection. If, however, this surface was polished at 45° most of the light would be internally reflected through 90° and exit from the top of the fibre even if the cladding had not been removed. This effect would be enhanced by placing a mirrored surface on the polished end.

Although this approach is theoretically sound the practical problems associated with cutting and polishing pairs of fibres accurately at 45° are prohibitively difficult, given the small size of the fibres and the number required (about 100 pairs). Holding the fibres at the correct orientation to the pad would also be challenging. In addition, preliminary enquires indicated that the action of depositing a mirrored surface on the end would be expensive with no guarantee of success. It was therefore considered uneconomical to try this approach practically

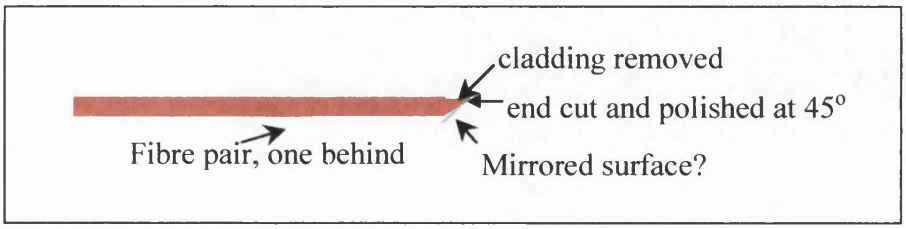

Fig.6.15 Optode with in-built prism (silvered)

Mirror at end of plain cut fibre (Fig.6.16) – Light can be turned through 90° by placing a mirror angled at 45° in the path of the beam.

Although small mirrors could be manufactured from polished metal a number of difficulties were encountered when a small number of prototypes were hand made from metal rods of brass, steel and aluminium. Maintaining the correct angle between the prism and the fibre is critical, but it was found that the fibre/prism join is a natural bend point and so the prism and fibre had to be held in a small, stiff casing. For the joint to be waterproof - which is necessary to ensure hygiene and for preservation of the mirror surface - it must be completely encased within a transparent medium or incorporate a transparent window in an otherwise opaque material. Clear heat-shrink tubing was tried but introduction of this casing reduced the light to unacceptably low levels such that there was less than a 10% difference between the intensity from a dry pad sample and a dark background. The change between a dry and wet pad sample would be less still.

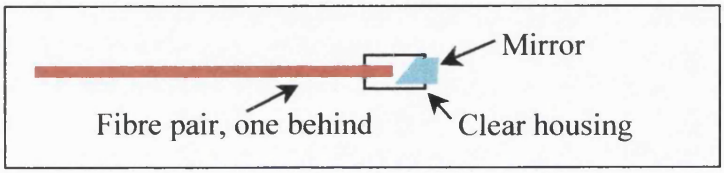

Fig.6.16 Plain cut optode with mirror at tip

Prism cast on end of plain cut fibre pairs (Fig.6.17) – To cast a prism of optically clear material on to the end of a pair of fibres is similar in principle to cutting the end of the fibre at a 45° angle. However, a cast prism would have a number of advantages. The first of these was that the resin would hold the fibre pair together as well as creating the prism. The second is that once a mould had been made all the prisms would be of identical angle and would not need any polishing.

It is practical to cast high quality resin prisms on the end of fibre pairs, (see 6.3.3). However, although prisms will redirect the light effectively when surrounded by air this is not the case if they are surrounded by water or when grease/debris (e.g. finger-marks) accumulates on their surface. This made this design unsuitable for use.

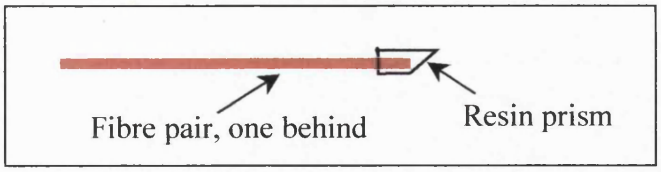

Fig.6.17 Optode with prism cast on tip

6.3.3 Prototyping of chosen solution

As a result of the above considerations and experiments a solution was adopted which was based on the cast prism, although it also incorporated elements from several of the other design approaches. The final design consisted of a prism, with an aluminium foil mirror, cast on to the pair of fibres. This was then encased in another layer of the casting material to protect the mirrored surface and to provide robustness (Fig.6.18).

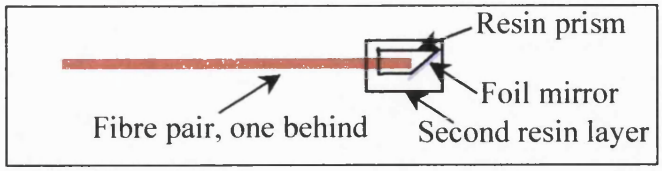

Fig.6.18 Final design, optode with mirrored prism cast on tip

The first prototypes were made using a cast wax mould. A former was cut from a plastic rod to the external shape of the desired prism and used to form the wax mould. The former was replaced with a pair of optical fibres and clear casting resin added (pre-accelerated polyester resin in styrene, Alec Tiranti Ltd). On attempting to remove the wax it was found to have contaminated the cast prism.

The second approach was to cast the prisms against glass microscope slides using an epoxy resin or clear casting resin. The glass was chosen as an optically smooth surface and arranged as in Fig.6.19.

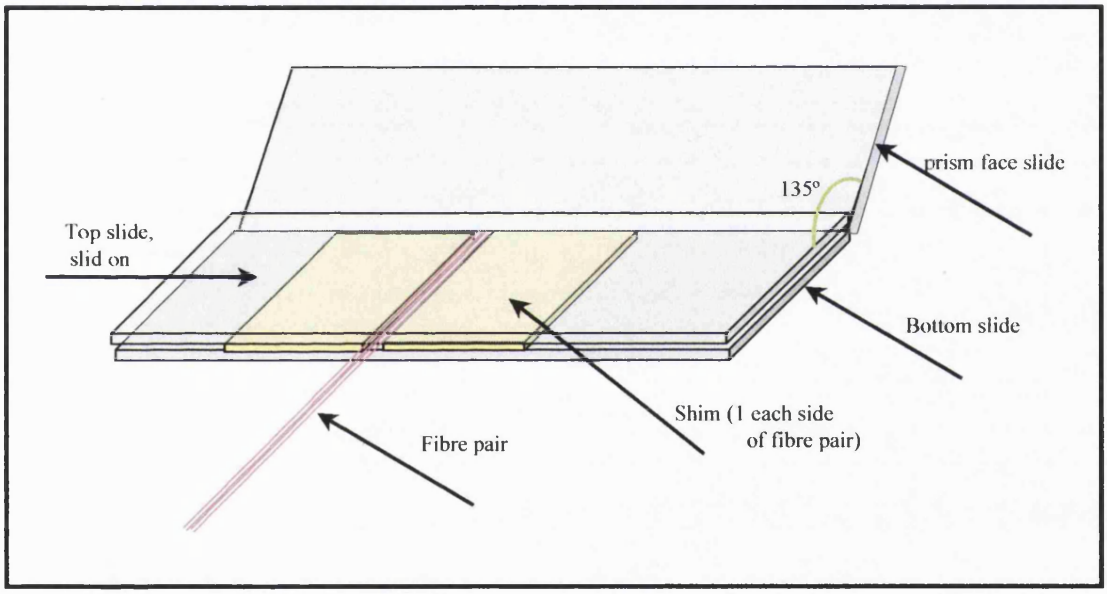

Fig.6.19 Prototype mould for casting prism on the end of an optode

Two microscope slides were held with a 135° angle between them. This formed the bottom and prism surfaces of the mould. A further microscope slide was used to form the top surface of the mould. Small pieces of 0.6mm shim were used to maintain an appropriate separation between the top and bottom slides and form the sides of the mould. A pair of optical fibres was placed between the two pieces of shim and a blob of resign applied to their ends to form the prism. The top slide was then slid into place removing excess resin.

It was found that although both the resins stuck to the optical fibres, due to the relative size of the contact areas involved, they stuck preferentially to the glass slides. This was true even when the slides had been thinly coated with a lubricant. The solution to this was to cover the microscope slides in aluminium foil. Using foil had two advantages. Firstly, although the resins still adhered slightly to the

foil the thinness of this meant that it could be peeled off without damaging the prism. Secondly, the possibility of using the foil as a mirror on the prism surface arose. As mentioned above, a mirror is superior to a plain prism, as its performance as a reflector is not affected by the refractive index of the material touching its back surface. Also any light striking the mirror at less than the critical angle would be reflected – this would be transmitted through a simple prism.

Following further experimentation, clear casting resin, despite having the disadvantage of requiring 12 hours to set, was found to be superior to epoxy resin both optically and mechanically. The epoxy prisms were soft and tended to bend and tear away from the optical fibres even when an additional layer of resin was added to protect the mirror and increase robustness. The casting resin optodes also needed a second layer, but with this added they were rigid and robust. One other disadvantage, which has since been resolved, is that the foil mirror stuck to the casting resin only very weakly and thus the foil mirror almost always became displaced before the second resin layer could be added. A very thin layer of the epoxy resin reattached the foil without significantly altering the optical properties.

The optodes were tested by covering with a sample of dry pad and recording the light intensity from each fibre. The pad was then wetted with sufficient water to be completely saturated. The intensity of the reflected light was again recorded. Although the success rate of casting the prisms was low at this stage, the best optodes were found to have an 11-17% change in light intensity upon wetting. Although this was significantly less than the 30% or more change exhibited by the laboratory optodes under similar conditions, this was considered sufficient for establishing the wetness of the pad.

6.3.4 Large scale model

As an aid to understanding the effects of angle and separation between fibre and foil, a large-scale model of the prism was made. This was necessary for the prism design to be optimised. The angles and distances under question would have been too small to control at the scale of the normal fibres.

A pair of 4mm optical fibres, made of identical material to those used in optode production, were assembled into the imaging device. A variable angle prism was made from water and microscope slides and was mounted on a pair of translation stages (Fig.6.20), the mirrored surface of the prism being made from a foil covered slide. The slide angle and x and y separations (as marked in Fig.6.20) could be altered independently so that the effect of light reflected from the pad sample could be measured.

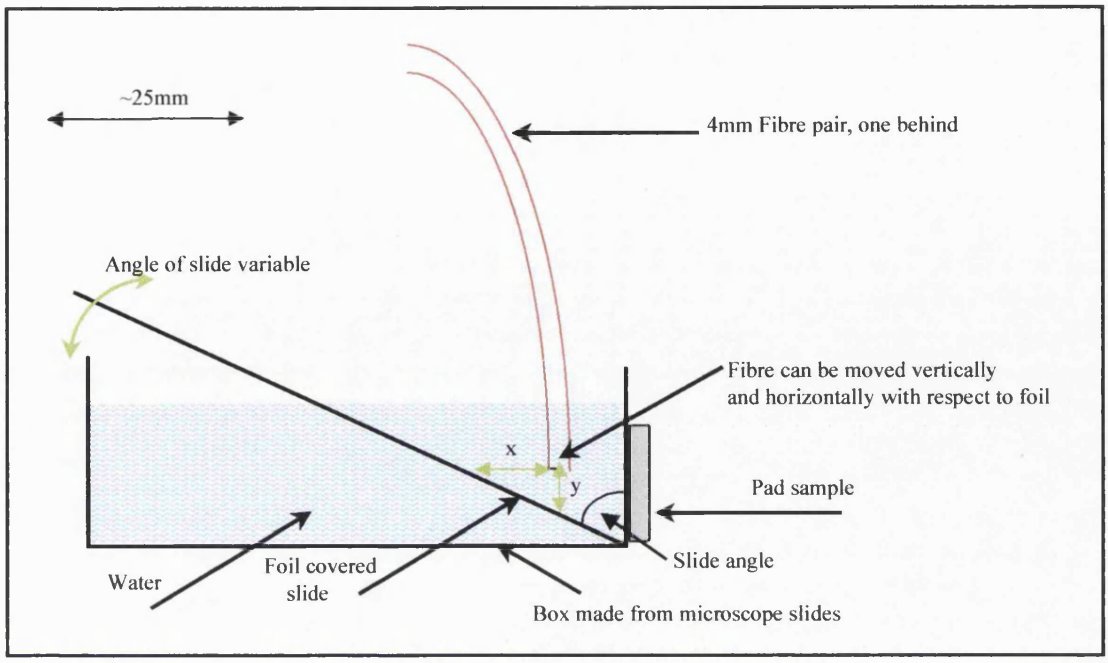

Fig.6.20 Large scale optode with variable prism at end

The angle of the mirror was increased in 5° steps from 25° to 65° and the reflected light intensity was recorded. This was repeated in reverse with steps of -5° for the extremes and -1° for the central region (40-55°). Reflected light intensity is plotted against mirror angle in Fig.6.21. Optical theory predicts that, since angle of incidence = angle of reflection, the peak in light intensity should occur at 45°. The measured peak appears to be at 48°, with the light intensity remaining about constant from 45-50° (Fig.6.21). However, since this is only a small deviation from the theoretical value, less than the size of the constant region, it is more likely that this effect was due to alignment errors in the slide pivot than a true effect.

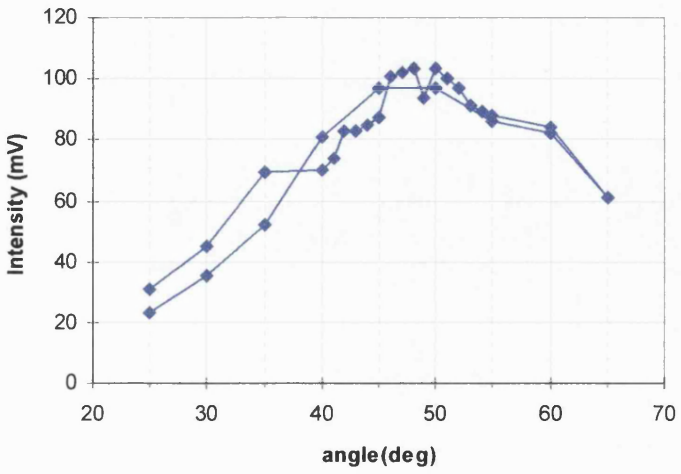

Fig.6.21 Effect of mirror angle on reflected light intensity

The effect of horizontal separation was measured by varying x while keeping y constant and the mirror angle at 45° (see Fig.6.20). The zero point of x was difficult to judge as the optical fibres would flex, altering y rather than providing resistance to further movement at x = 0. Fig.6.22 shows the effect of increasing and decreasing the value of x over a range of about 3mm, the same intensity scale is used as for Fig.6.21 and Fig.6.23 to aid comparison. The position of the x=0 point is not accurate for the reason given above. However, it can be seen that variation in x had only a small effect on the reflected light intensity compared with angle variations.

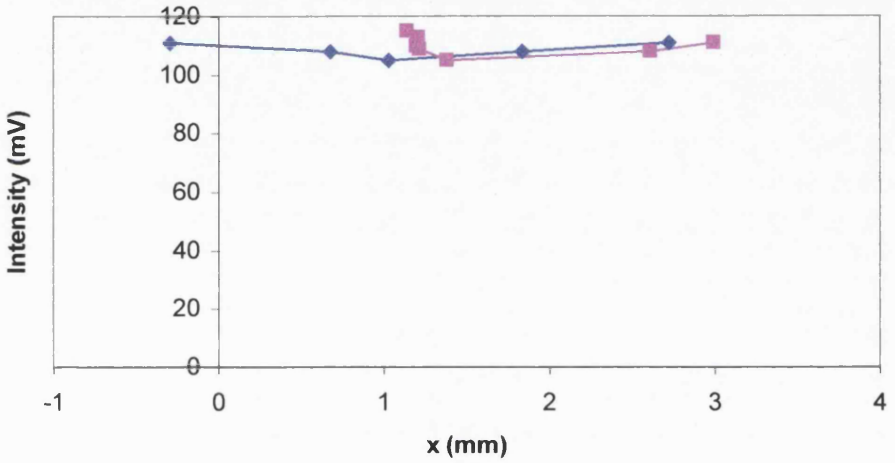

Fig.6.22 Effect on reflected light intensity of varying the horizontal separation between the optode and mirror (the same intensity scale is used as for Fig.6.21 and Fig.6.23)

The vertical separation, y, was increased from 0mm to 3mm with the mirror angled at 45°. The value of x was initially 0, this was not adjusted during the experiment but as it was defined relative to the angled slide, it was allowed to increase as y was adjusted. Therefore, the values of x and y were equal throughout the experiment. The experiment was repeated with decreasing values of y.

Fig.6.23 shows the reflected light intensity as a function of y. This shows an increase in intensity when the fibre pair was moved vertically away from the foil. There are two phases of this effect. The steeper, close phase may be an artefact of the experiment, arising from the fibres bending as they touched the mirror. The second phase was far more significant as it had implications for the design of the cast prisms. This effect was explained by looking at ray diagrams, Fig.6.24. This shows nine representative rays of light emerging from an optical fibre and striking a mirrored surface angled at 45°. The plastic fibres used in these experiments have a divergence angle of 60° thus rays normal (blue), +30° (orange) and –30° (green) to the fibre end are shown for the centre and edges of the fibre. Fig.6.24a shows the fibre touching the mirrored surface. It can be seen that two of the rays (about 20% of the light) are reflected back down the fibre or, worse, into the adjacent output fibre. Raising the fibres above the foil (Fig.6.24b) enables all these rays to be utilised, and has a further advantage in reducing the possibility of the fibres damaging the foil as they are inserted into the mould.

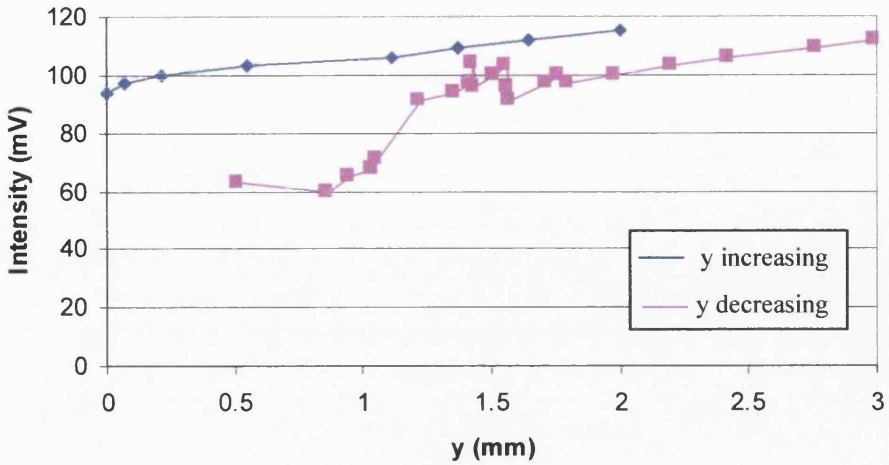

Fig.6.23 Effect on reflected light intensity of varying vertical separation between the optode and mirror

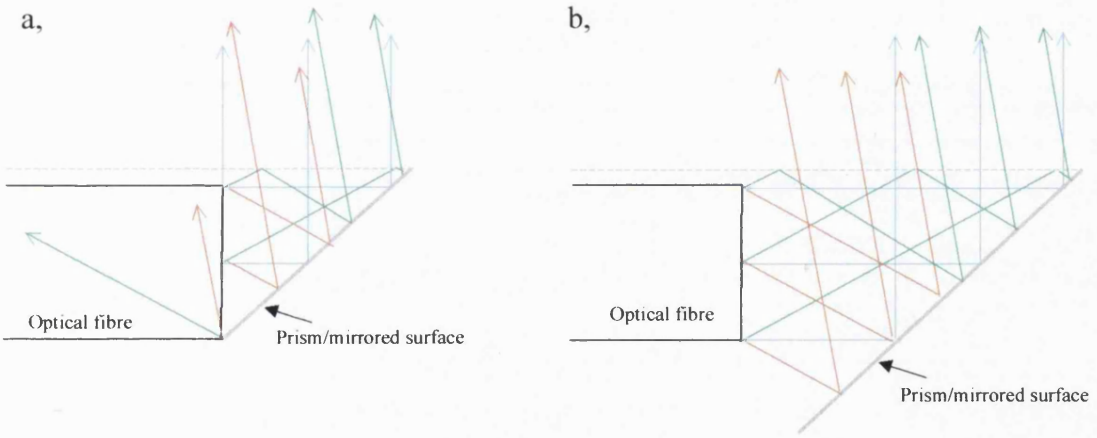

Fig.6.24 Ray diagrams to show effect of optode/mirror separation. a, Optode touching prism b. Optode removed from prism

Overall results from the large scale model confirmed that the prism should have an angle of 45° but indicated that the fibres should be removed from the mirrored surface of the prism, by an amount approximately equal to the diameter of the fibre, to prevent light being reflected back down the fibre without leaving the prism. In view of this the prism making mould was modified to raise the fibres above the base level of the foil by inserting a layer of 0.6mm shim material. No change was made to the prism angle.

6.3.5 *The final mould*

The prototyping mould could only form one optode at a time. It was therefore necessary to design a mould that could be used to produce several optodes simultaneously. A diagram of the finished mould, for five optodes, is shown in Fig.6.25. This mould was very similar to the prototype mould, using two glass slides held at a 135°angle. These were held in a metal block and covered with aluminium foil

before use. As before, removable pieces of shim were used to form the sides of the mould although now six pieces were used, enabling five optodes to be cast in the same mould. A second layer of shim pieces was placed under the fibres to create the mirror/fibre gap recommended in section 6.3.4. The upper shim pieces had their front edge chamfered at 45° to provide a good fit to the angled glass slide and were notched either side of the optode tip. This allowed resin to flow all round the fibres forming a larger and more robust prism. A clamp was provided so that all the fibres and pieces of shim could be held accurately in place while the resin was applied. The upper glass slide was attached to a weight so that an even pressure could be applied while the resin set.

A drop of water was applied to the slides before applying the aluminium foil. The surface tension of the water encouraged close contact between the two surfaces keeping the foil smooth.

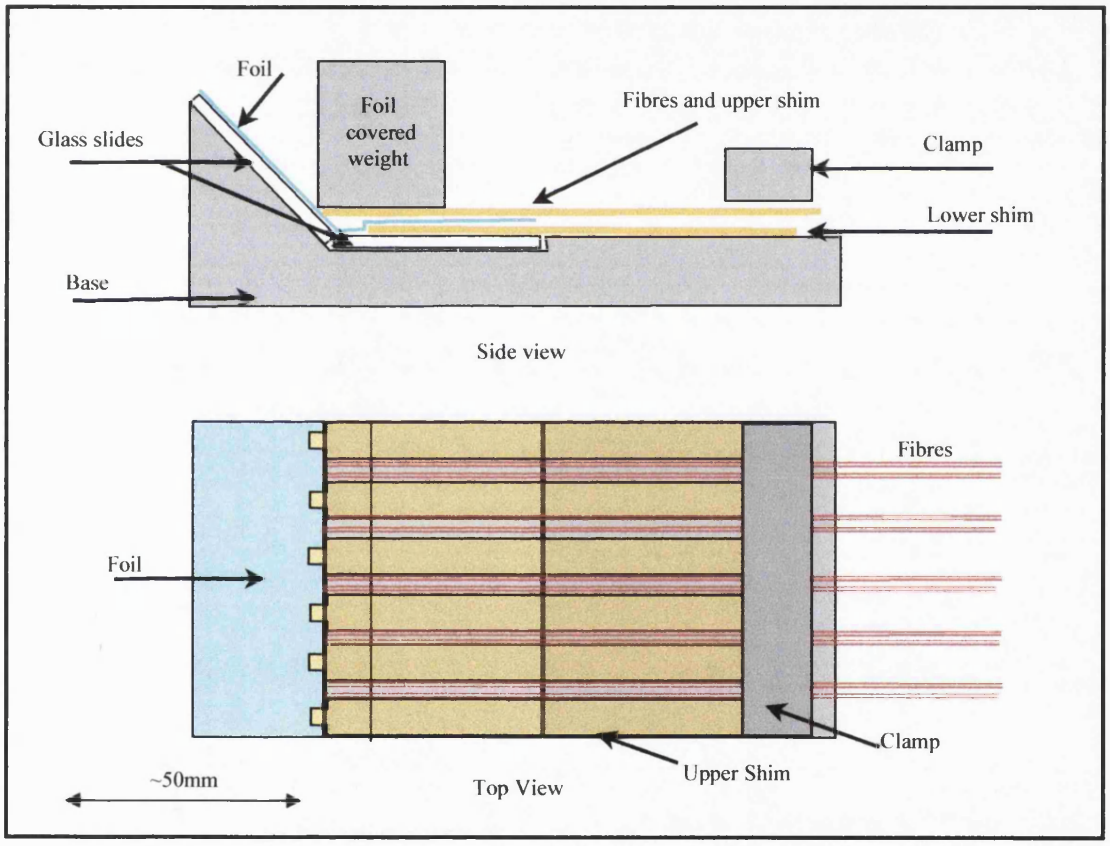

Fig.6.25 Final mould, 1st stage, for casting mirrored prisms onto optodes

A second stage mould, for encasing the mirrored prism in another layer of resin, is shown in Fig.6.26. This mould was comprised of a four-layer sandwich with foil covered slides forming the top and bottom surfaces, separated by pieces of shim. A number of moulds were made, each taking two optodes at a time.

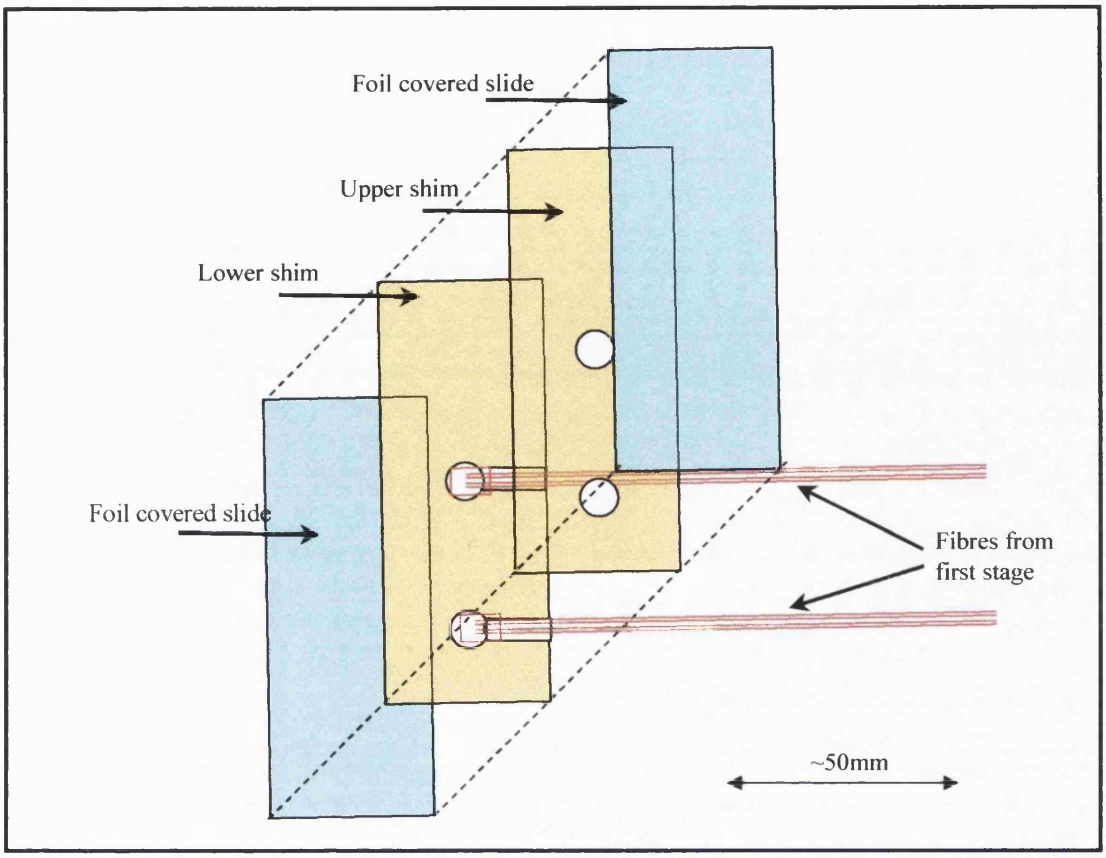

Fig.6.26 Final mould, 2nd stage, for strengthening and protecting optodes with mirrored prisms

6.3.6 Optical ribbon cables

For ease of use, the optodes had to be grouped together in a manner that maintained a fixed spacing between fibres in the group and minimised the set-up time for each experiment while not affecting the comfort of a subject by stiffening the pad. The method chosen was to assemble the fibres into the optical equivalent of a ribbon cable with each cable containing one line of optodes, staggered so that the sensing ends were 2cm apart. To achieve this 16 optodes were woven together using fine nylon fishing line as shown in Fig.6.27. Following assembly the cables were coated in clear silicone rubber to protect the fibres from wear as well as providing a smooth waterproof surface. This was essential to enable cleaning of the cables to clinically acceptable standards. Silicone rubber was chosen as it is waterproof, flexible, non-toxic and does not stick irreversibly to adhesive tapes. This last criterion was necessary as the cables needed to be attached to the backs of pads with tape, but also be removed after the experiment without damaging to the cables. Another factor that was taken into account was that the visual appearance of the final cables should not be off-putting to subjects in a clinical experiment. Self-amalgamating tape (PE) was tried as an alternative to silicone rubber but did not meet the criterion of reversible attachment with adhesive tape - a sticky residue was left behind when the adhesive tapes were removed.

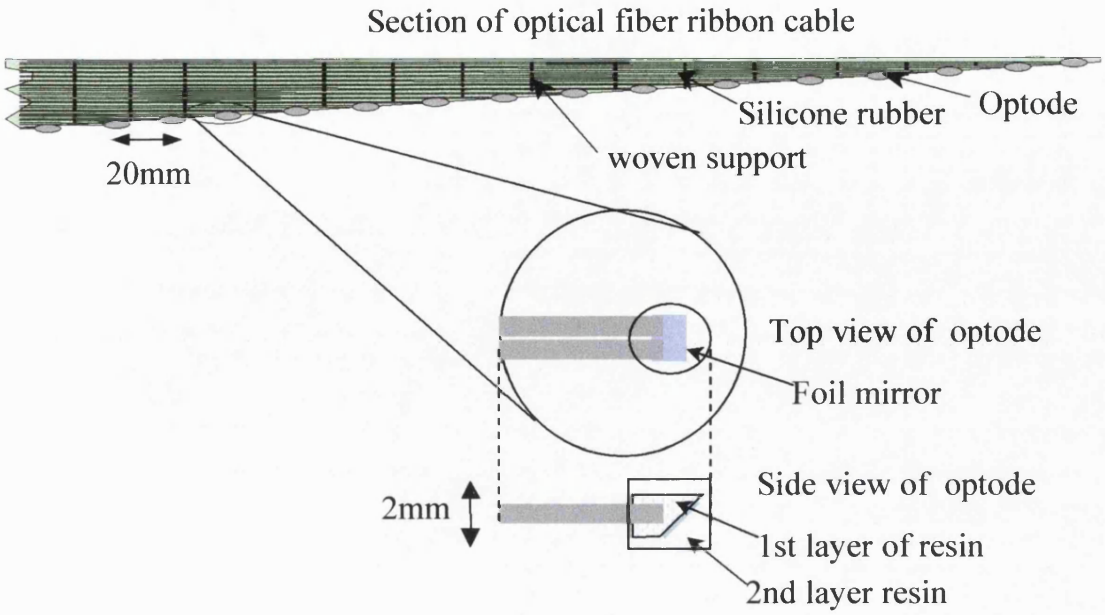

Fig.6.27 Diagram of a section of optical fibre ribbon cable with expanded diagram of one optode

Fig.6.28 shows a photograph of a completed optical ribbon cable, with 15cm ruler for comparison. The inset shows a single prism optode before being incorporated into a ribbon cable. Two bright points can be seen corresponding to the light emerging from the ends of the two optical fibres. The transparent nature of the components from which these cables were made detail difficult to see in these images.

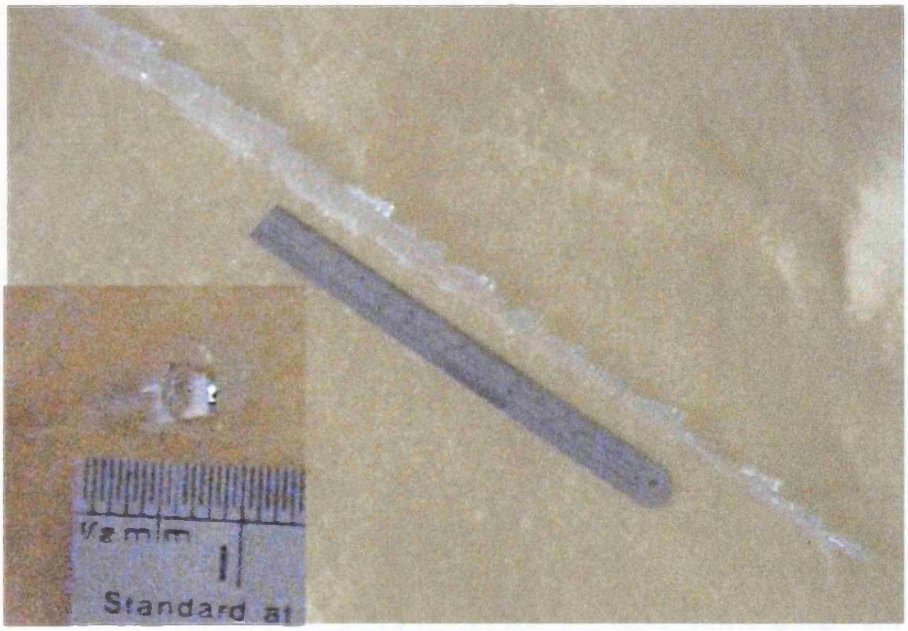

Fig.6.28 Photograph of an optical ribbon cable, insert – one optode

The spacing of 20mm was chosen for the optodes for a combination of reasons. A spacing of 20mm was used with the resistive device (section 4.1.3) to capture the overall shape of fluid distributions. Also, at this spacing about one hundred optodes are required to cover the central, most interesting area of a pad, a number which does not create excessive bulk and can be laid down at a depth of only one fibre (0.5mm +silicone) at any point. A closer spacing of optodes would require the complexity and bulk of multiple fibre layers.

6.3.7 Testing of optical ribbon cables

The optical ribbon cables were tested in the laboratory under controlled conditions in order to assess their performance. A pad sample was laid on top of an optical ribbon cable and then fluid was applied from before the first optode. This wicked along, reaching each optode in turn (see Fig.6.29). Fig.6.30, which is a plot of time against optode position, shows the progress of fluid as imaged by an optical ribbon cable within the laboratory. Dry pad areas are shaded pink with the colouring becoming progressively bluer as the wetness of the pad, as measured by percentage change in light intensity (original dry intensity = 100%) - increases.

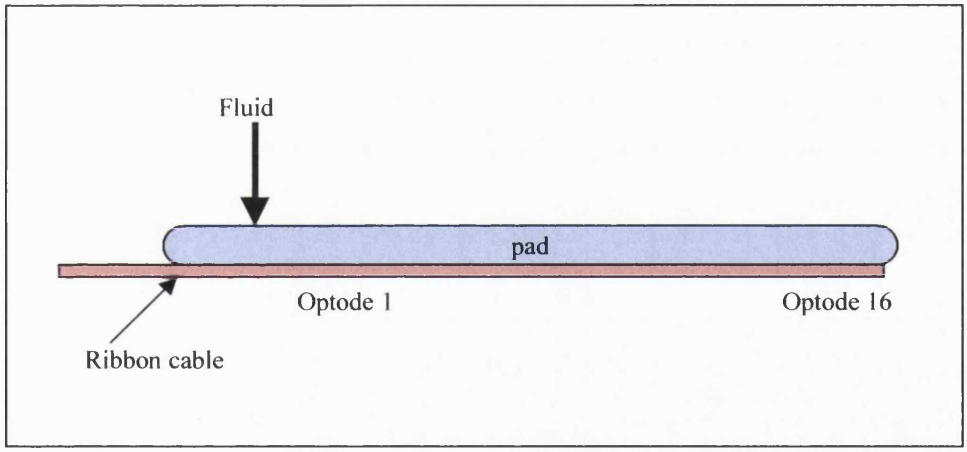

Fig.6.29 Cross-section of set up for optical ribbon cable experiments

Although the performance of the optodes varied, the shape of the fluid front could be clearly followed as fluid progressed from left to right. If all optodes had performed ideally this would have looked like part of an approximately parabolic curve with the lowest point at optode three. Inside this parabola, which would locate the fluid front as a function of time, the shades of blue may have varied over time and space as fluid redistributed within the wet area. Although all the individual optodes were tested before being incorporated into the ribbon cable, and all showed an intensity difference of at least 10% between dry and wet pad samples, the performance of a number of the optodes was reduced in the final cable. Optodes three did not register the wet front at all and optode ten only showed a slight decrease in intensity. A visual inspection did not reveal any physical damage or silicone deposit on the prism surface, but this may have occurred.

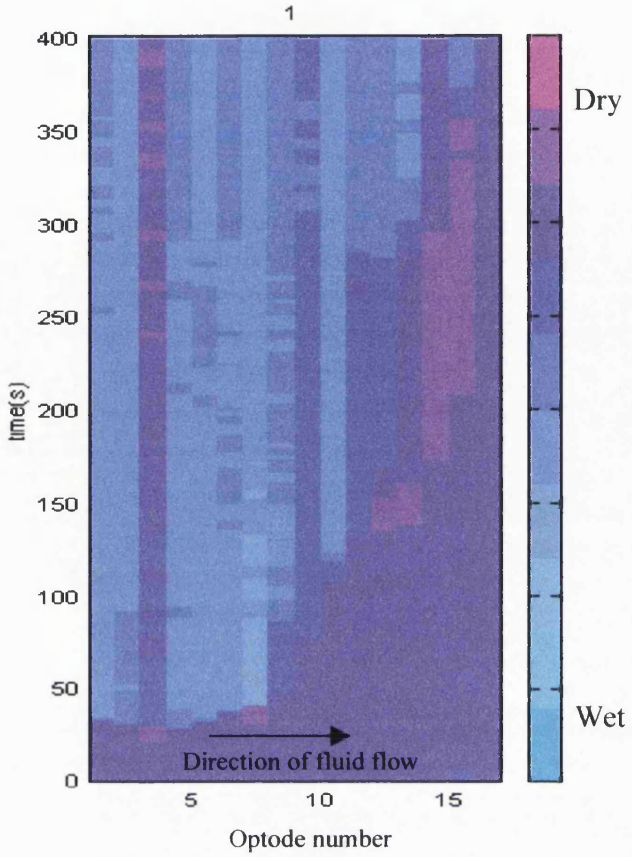

Fig.6.30 Image from optical ribbon cable

Unlike sensors for use in the laboratory, those used clinically have to cope with uncontrolled pressures. Literature indicates that the pressure exerted by a supine subject varies across the contact area and according to the surface on which the subject is lying. Allan et al (1993) and Swain et al (1994) have measured pressures in the range 2.5 - 10kpa with the highest pressure under the buttocks and sacrum. However, they did not study the pressure in the crutch area - where most fluid is absorbed. The pressure exerted by a sitting patient could be higher, depending on the surface they are sitting on. Transitory pressures generated as the subject shifts position could be much higher, but due to their short-lived nature would not be a real problem as any spikes they produced in the light intensity measurements would be of correspondingly short duration and, therefore distinguishable from the rest of the data. However, the pressure changes experienced by body worn pads are likely to be different from those pressures exerted on a mattress or bed pad. Thus, a crutch pressure of less than 2.5kpa is likely to be more realistic and 1.5kpa was chosen but no clinical data is available to confirm this.

Using the experimental set up shown in Fig.6.29, a weight, which exerted a pressure of 1.5kPa over an area 330mm by 250mm,was applied to a pad under various conditions:

- Weight placed on dry pad after start of experiment (= dry pad, pressure added)

- Weight placed on dry pad before start of experiment then removed during experiment (= dry pad, pressure removed)
- Pad wetted during experiment then weight added (= wet pad , pressure added)
- Weight placed on dry pad before start of experiment, pad wetted then weight removed during experiment (= wet pad, pressure removed)

. For each experiment the average percentage change in light intensity for the sixteen optodes in the cable, due to the pressure change, was calculated. The light intensity changes observed due to various pressure changes are shown in Table.6.1.

	Pressure added	Pressure removed
Dry pad	+1% (1.5)	-6.6%(7.2)
Wet pad	+1.3%(3.6)	+0.4%(3.9)

Table.6.1 Effect of pressure on light intensity recorded by optical ribbon cable, percentage change (standard deviation)

In these experiments adding pressure caused less than a 2% increase in light intensity but removal of pressure from a dry pad produced a change in intensity comparable with wetting. The standard deviation of the latter was also much higher than for pressure changes in wet pads and the addition of pressure to a dry pad. It was interesting to note that the addition of pressure did not have an equal and opposite effect to the removal of pressure, under either wet or dry conditions. This may be accounted for by realising that the baseline intensities were different in each case.

The change in light intensity on pad wetting was consistently less than an equivalent laboratory optode, due to light losses within the prism. This is illustrated in Table.6.2 and Fig.6.31. For five repeat experiments the average percentage change in light intensity, due to pad wetting, was calculated for a ribbon cable from the 16 optodes it contained. Three ribbon cables were tested. The average percentage change in intensity was less than the 30% commonly seen with the laboratory optodes and less than the minimum requirement of a 10 % change, although some individual optodes within a ribbon cable would have achieved this. There was wide variation between the performance of optodes within a cable, the average intensity change having a standard deviation of the same order as the average. However, the optodes, and hence the whole ribbon cable performed quite consistently. A comparison of the five experimentally repeats gives a lower standard deviation.

	CABLE1	CABLE2	CABLE3
Repeat 1	-6.6%(4.0)	-2.1%(6.6)	-4.7%(4.8)
Repeat 2	-8.5%(3.6)	-4.0%(5.0)	-7.4%(4.7)
Repeat 3	-5.85(6.4)	+3.2%(3.5)	1.9%(7.6)
Repeat 4	-7.3%(4.8)	+2.5%(6.3)	-4.1%(5.1)
Repeat 5	-6.0%(5.1)	-2.8%(7.2)	-2.6%(6.8)
Mean	-6.84%(0.98)	-0.64%(2.92)	-3.88%(3.06)

Table.6.2 Average percentage change in reflected light intensity on wetting of pad, as measured by optical ribbon cable (standard deviation)

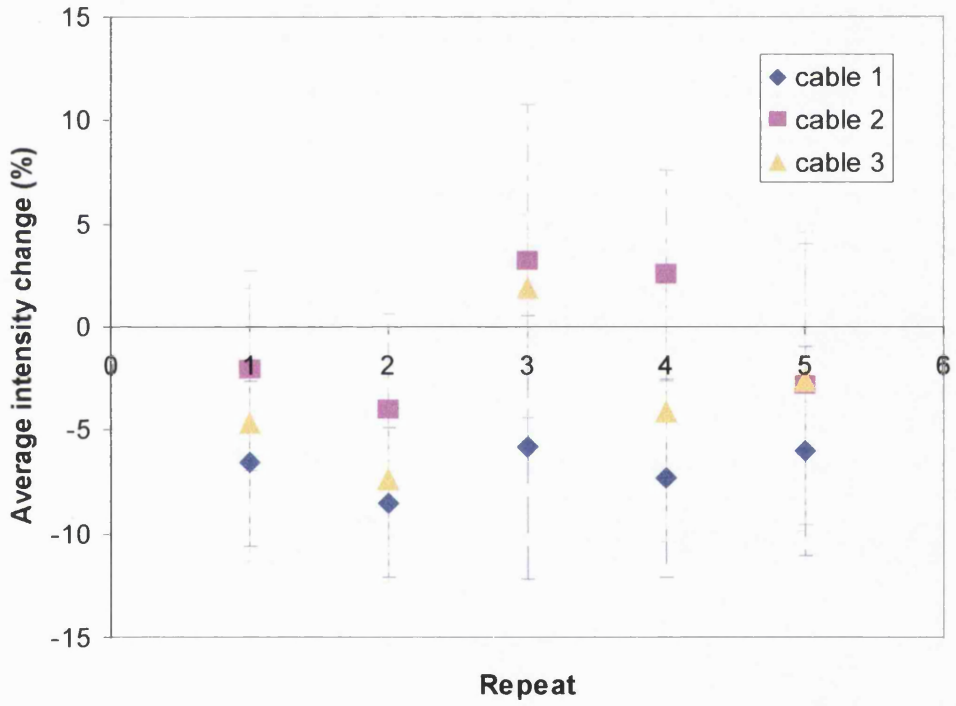

Fig.6.31 Average intensity change upon wetting of three 16-optode ribbon cables for five repeat experiments

The reason for the poor performance of cable 2 is most likely due to a faulty input ferrule, the fibres having worked loose within a temporary glue. The reason for the performance difference between cables 1 and 3 is not known but it should be noted that background correction has not been performed on this data as it was collected before the need for this correction was discovered (see section 6.13). The correction cannot be applied retrospectively because the background light intensity for these experiments can not be measured. This would be likely to make an improvement to the results but does not prevent comparison with laboratory optodes under similar processing.

These results are inconclusive. They indicate that significant changes in the light intensity can be observed under a static pressure but pressure changes of 1.5kPa can cause similar changes in intensity. However, since static pressures do not adversely affect the ability of the cables to detect fluid and the pressure changes which a pad would experience clinically are dependent on the mobility of the subject and are not known, laboratory testing cannot be used to accurately predict the clinical performance of these optical ribbon cables.

6.3.8 Clinical trials

As stated the above results are inconclusive and are measured under unrealistic conditions. Thus, three optical ribbon-cables of 16 optodes each were used, in conjunction with resistive sensors, in a clinical trial. All the sensors were taped down securely to maintain a constant contact with the pad backing. The resistive sensors were used in their normal configuration (see Fig.4.5), to provide data on the fluid distribution against which to compare the optical results. The optical ribbon cables were positioned to run along the length of the pad between the central lines of resistive sensors (see Fig.6.32). The pad was a Molyform extra (see table 8.2) and was worn by an elderly lady resident on a continuing care geriatric ward who was in a semi-recumbent position. Ethics committee approval and a relative's consent had been obtained. Data was collected for 1.5 hours, during which the pad received a total of 65g of urine, probably arising from four insults (starting at approximately 100s, 300, 600s & 2100s). The same computer was used to control both sets of sensors. The overall set up was as shown in Fig.4.3, the only significant difference being the addition of the optical imaging device which was strapped to the chair arm or bed rail because of the short length of the optical ribbon cables.

The results from the resistive sensors are shown in Fig.6.32. Also marked on this image is the positions of the optical ribbon cables. This shows that at least optodes 9-14 of each ribbon cable should have registered wet at some time during the experiment.

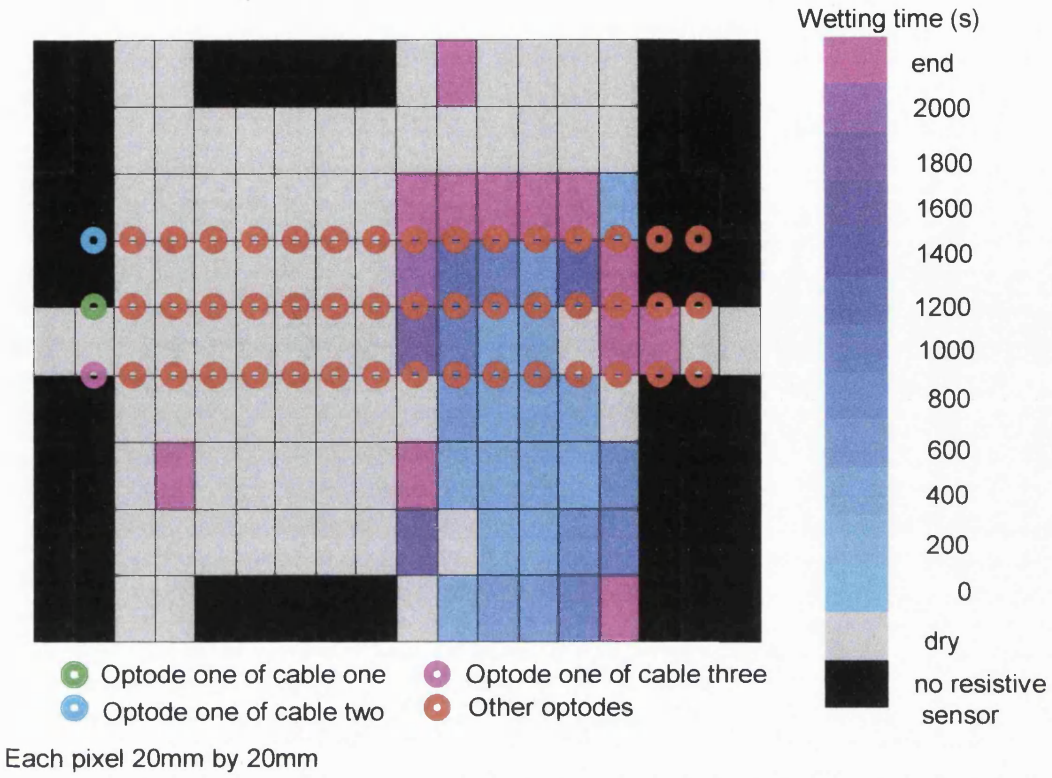

Fig.6.32 Resistive sensor image of clinical data with positions of optodes overlaid

The results from the optical cables are plotted in Fig.6.33 where percentage change in light intensity (from the initial value) is displayed on a time versus optode position image for each cable.

Dry regions of the pad are coloured pink and wet regions are represented by various shades of blue, the brighter the blue the wetter the pad. Superimposed on the data from cable one is the cumulative number of resistive sensors registering wet as a function of time. This indicates some correlation between intensity changes of the central five optodes and the arrival of further fluid insults, as indicated by a rapid increase in the number of resistive sensor registering wet.

Cables 2 and 3 do not appear to register the presence of fluid in the pad. As most of the sensors that show a decrease in light intensity do so from the start of the experiment this is probably an effect of pressure changes within the pad.

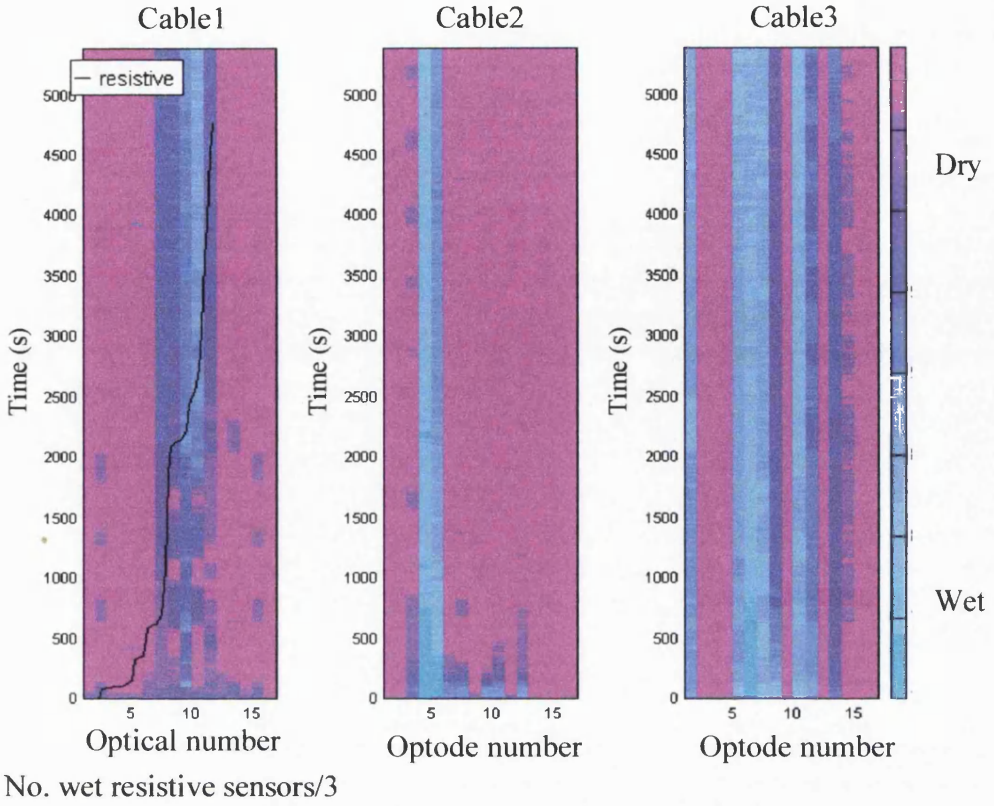

Fig.6.33 Clinical performance of three optical ribbon-cables as a factor of time, with the number of wet resistive sensors (divided by three to synchronise scales) overlaid on image of cable one.

This figure clearly shows the difference in performance between the three, nominally identical, optical ribbon-cables. Cable one repeatedly performed best and cable two continued to be affected by a loose fibres connection. Other clinical trials of this equipment were carried out but did not yield any additional information.

In conclusion, the optical sensors have potential for use in the clinical environment. They are safe, thin flexible and have at least two advantages over the resistive sensors. Firstly these sensors are easier to apply to a pad and, secondly, information on re-wetting of sensors due to repeated insults is possible.

The first advantage is because the optical sensors, unlike the resistive sensors, do not need to be inserted beneath the pad backing and also because the sensors are already held in uniformly spaced strips.

The second improvement is due to the continuous nature, in time and intensity (wetness) measurement, of the optical imaging device. The output of the resistive sensors is only binary and so they can neither record a second wetting or differentiate a fully saturated area of pad from a partly saturated one.

However, the performance of the current ribbon cables proved too poor for reliable data to be gathered. If the efficiency of the prisms could be improved by increasing the accuracy and consistency achieved in all the stages of ribbon cable production then such cables could provide reliable data. Such improvements would possibly be assisted by increasing the input light brightness. Although theoretically the production technique could be improved, great care was taken at all stages of production of those

ribbon cables described here and practical means of improving their production, without incurring great expense have not been identified.

7: Data display and commissioning of the Optical Imaging System

7.1 Development of data display routines

The data collected by the optical imaging device can be displayed in many different formats, depending on the information required. In view of this a wide range of display routines have been developed for converting the raw experimental data into informative graphs. The advantages and limitations of the main formats chosen and developed are described below.

7.1.1 Animation or dynamic image sequence

This method of display can include all the data in a time-lapse animation. In each time frame the data are displayed as a colour map with each pixel representing one sensor. The intensity change, and hence the wetness of the sample, is shown as a colour variation, ranging from pink (= dry) through purple to bright blue (= wet). The animation can be played back at any reasonable frame rate to allow an overall impression of the fluid spread to be gained. The dynamic nature of this method allows subtle, time-dependent, events to be observed (e.g. rapid spreading of the fluid at the start) taking advantage of the sensitivity of the eye to movement. Two limitations of this technique are that the information gained is qualitative and that it cannot be presented in hard copy.

7.1.2 Sequence of snapshots

This is a modification of the above technique that allows for hard copy production. A series of individual frames, spaced at regular time intervals, are extracted from an animation and plotted as shown in Fig 7.1 in which each frame is titled by its time of capture (seconds) after start of experiment. This data set is for 250ml of body temperature fluid, applied with a peak flow-rate of 20ml/s using flow-rate/time profile f_250_20 (section 4.3.2), applied to a Molyform Extra pad (see table 8.2) using the central urethra of the curved optode holder. Fluid application started at 20s and continued until 37s.

Although sequential frames can be compared, subtle changes in the size of the wet area are hard to detect.

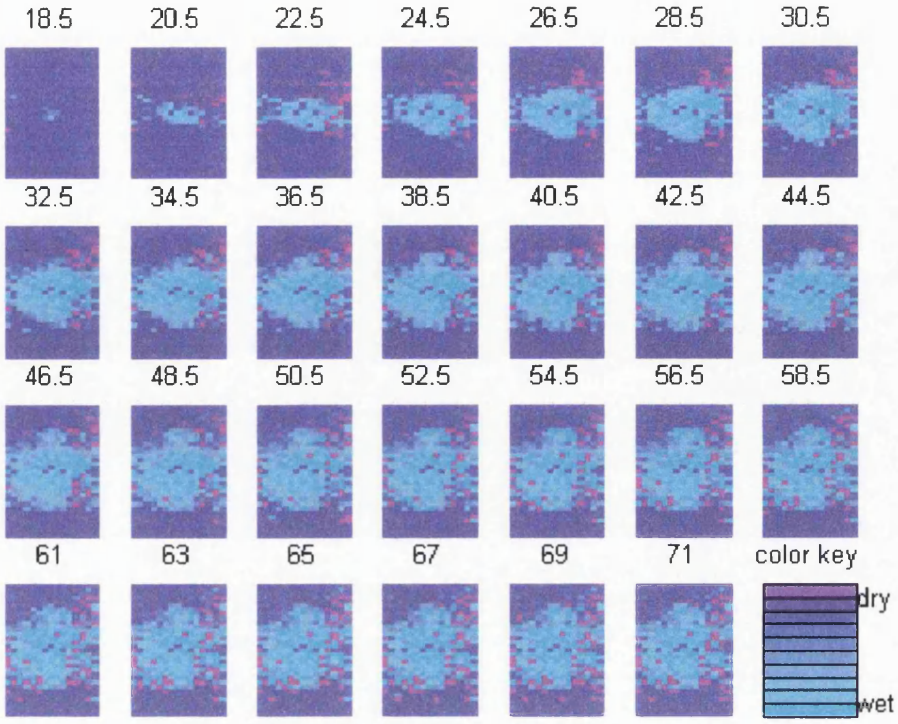

Fig 7.1 Snapshot sequence of sample optical data at times (s) given above each image

7.1.3 Curved plots

Either of these first two display techniques (7.1.1, 7.1.2) can be modified so that the curved geometry of the pad, as held on the curved optode holder, is revealed. Fig 7.2 shows a snapshot sequence with the pad held on the curved optode holder in a supine posture (each frame is labelled with it's time of capture), and a single image each from equivalent experiments performed in sitting and side postures. For each orientation 250ml of body temperature fluid, applied with a peak flow-rate of 20ml/s using flow-rate/time profile f_250_20 (section 4.3.2), applied to a Molyform Extra pad (see table 8.2) using the central urethra of the curved optode holder. Although this method obscures some of the data in each image it is useful in visualising the response of the fluid to gravity.

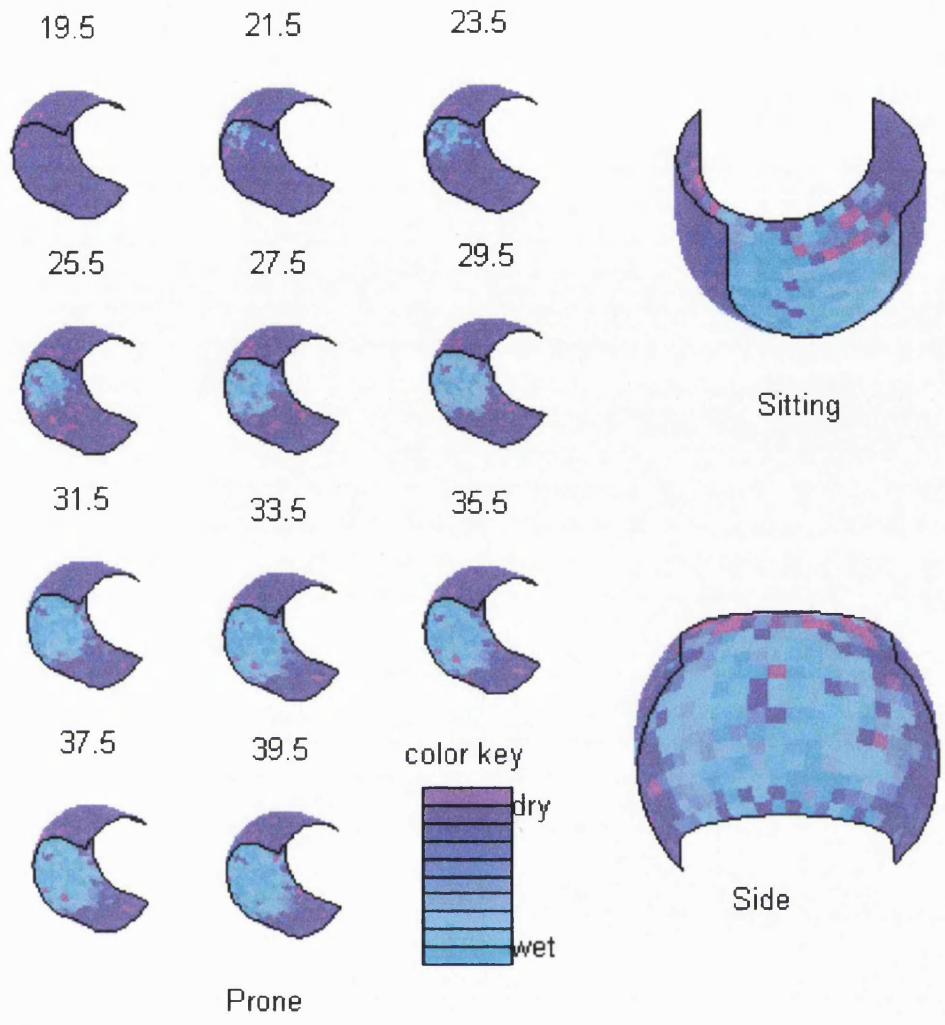

Fig 7.2 Curved plots of sample optical data in three postures

7.1.4 Contour plot

These plots combine time and spatial information in one image, at the expense of reduced detail. Contours are found by converting the data at each time into a binary image using a set threshold value. Looking at sample data sets, 82% of the light intensity original value was found to be an appropriate level for this threshold. It is a trade off between including areas where the pad is damp whilst preventing random fluctuations in the light intensity from being included. A contour is then drawn between these two regions (dry and wet). Fig 7.3 is an example of such a plot, using the same data as Fig 7.1, and shows how this technique can highlight changes in the shape of the wet area over time. This enables a lot of information to be displayed in one figure. However, this is at the expense of all degree of wetness information. Another weakness of this method is that any pixels that temporarily give a false wet reading, such as the one at [13,25] in Fig 7.3, are highlighted.

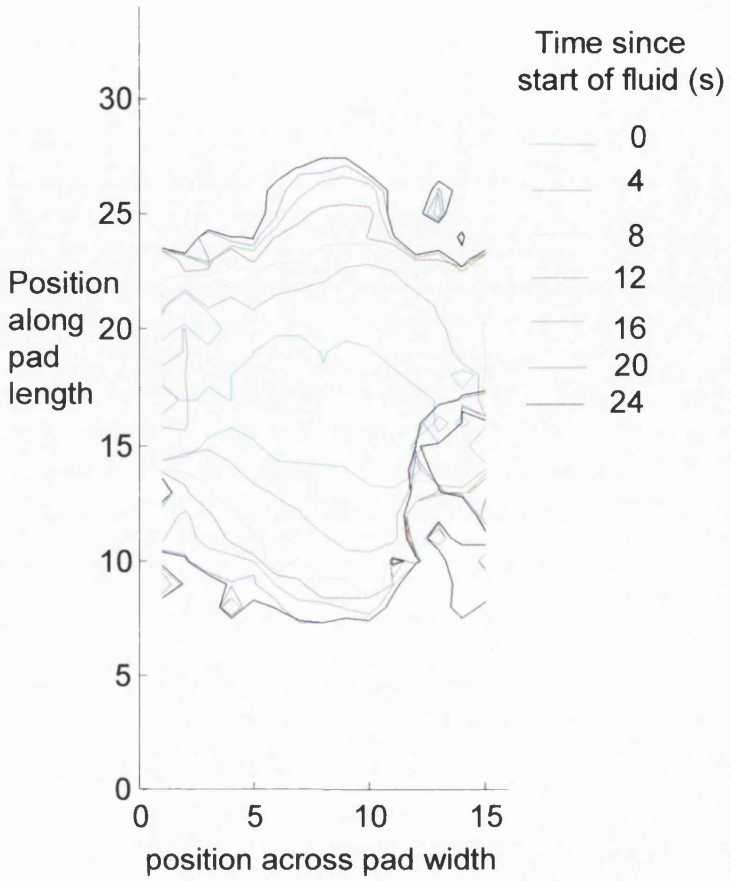

Fig 7.3 Contour plot sample optical data

7.1.5 Time/intensity line plot

These plots allow all the information from one line of sensors to be plotted on a single graph of sensor position versus time. This combines temporal and spatial information in a single image, but only for a single dimension. Fig 7.4 is an example of this type of plot using the same data as in Fig 7.1, and clearly shows the time at which each point on the pad started to get wet. Again the bluer the image, the wetter the pad. On this occasion one of the optodes failed to register wet and other optodes show signs of variable wetness, showing a transition period between dry and fully wet, indicated by bands of different blues. In this case the central column of optodes, along the lengthwise sensor line of the pad, is shown although any column or row of optodes could be plotted.

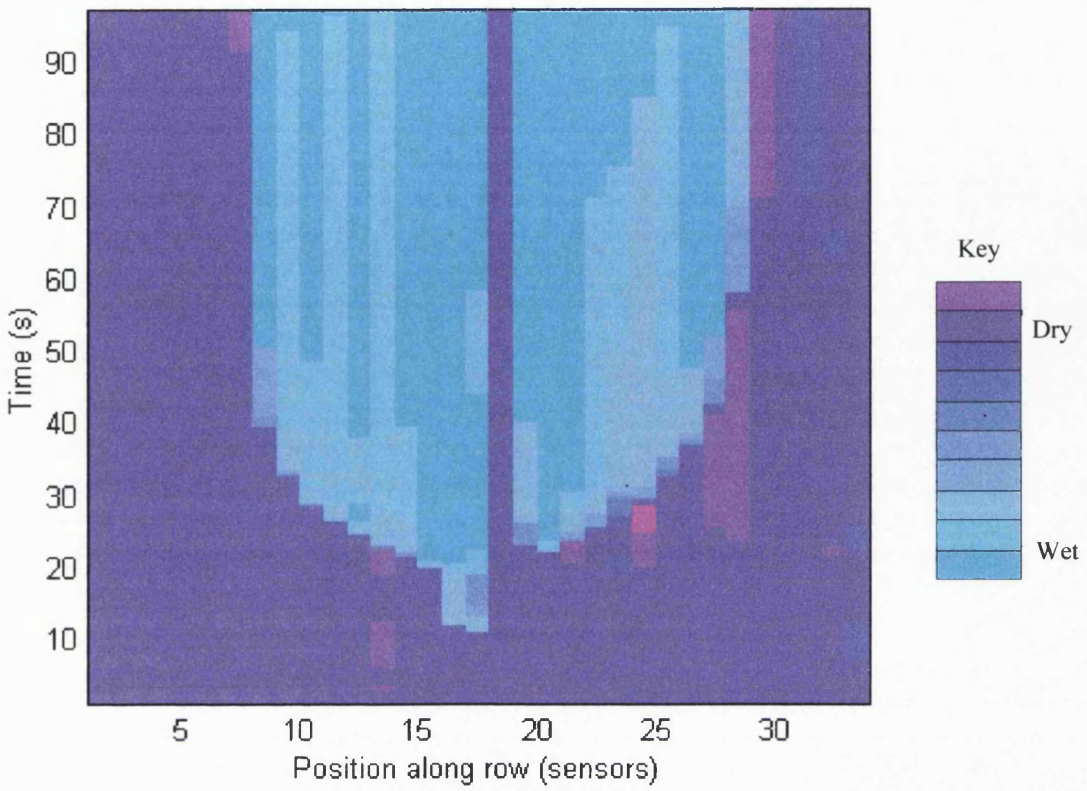

Fig 7.4 Line plot of a single line of optodes from a sample data set

7.1.6 Time/area, Time/intensity, Volume/area & Volume/intensity graphs

Every graph in this group of plots collapses the data to a single characterising value at each time. This means that the results of several experiments can be compared on a single graph.

Two measures that can be used as a characterising factor are the size of the wet area and the average intensity of the light reflected from the wet area. Wet area was simply a count of pixels that had a light intensity below a pre-set threshold. A light intensity of less than 82% of the original value was found an appropriate level for this threshold (see section 7.1.4). The average intensity of the wet area is a simple average of the intensity of those pixels included in the wet area, except that intensities below 0% are counted as 0% (the background level) as such values are not physically realistic. Drift in the background image intensity is continually monitored and corrected for by one representative point in the background (see section 6.1.3). Local variations in this drift may, however, cause the true background at a small number of points to be become lower than the calculated one and low light intensity readings to be incorrectly assigned a negative intensity.

These values can be plotted against time, or scaled so that they are plotted against the volume of fluid present, as calculated from the flow-rate time profile used in the experiment. Fig 7.5 a and b respectively show the size of the wet area and the average intensity of the wet area as a function of time for the data set used in Fig7.1. Fig 7.6 a and b show wet area and average intensity as a function of

volume for the same data set. In this experiment the total volume of fluid was 250ml. In this second pair of plots all the changes which occurred after fluid application ceased are plotted against the total volume.

The average intensity plot (Fig 7.5b) shows a period of instability before fluid was applied. This is due to a small number of pixels that spuriously register wet, often only momentarily. This causes the exaggerated fluctuations in average light intensity during this period. These spurious pixels can also be seen at the start of area/time plots as well but their effect is less dramatic.

Graphs such as these reveal changes in the bulk properties of the wet area, showing things such as the amount of fluid spread that occurs after fluid application has ceased. Those plots that are a function of volume help to differentiate the effects of fluid volume and rate of application. The average intensity plots give information about the changing saturation of the pad. For example, decreasing average intensity indicates that the wet area is probably receiving fluid at a faster rate than the size of the area is increasing, whereas an increase in intensity indicates that fluid is being wicked from the wettest parts of the product faster than it arrives.

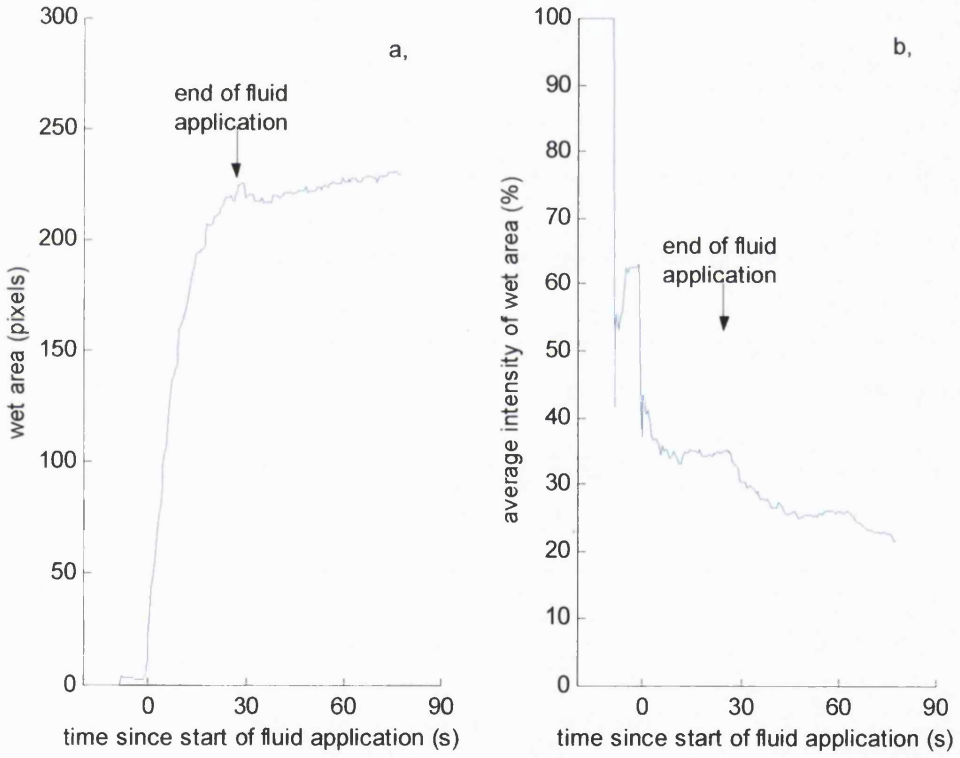

Fig 7.5 a. Size of wet area as a function of time for a sample data set b. Average intensity of light reflected from wet area as a function of time for a sample data set

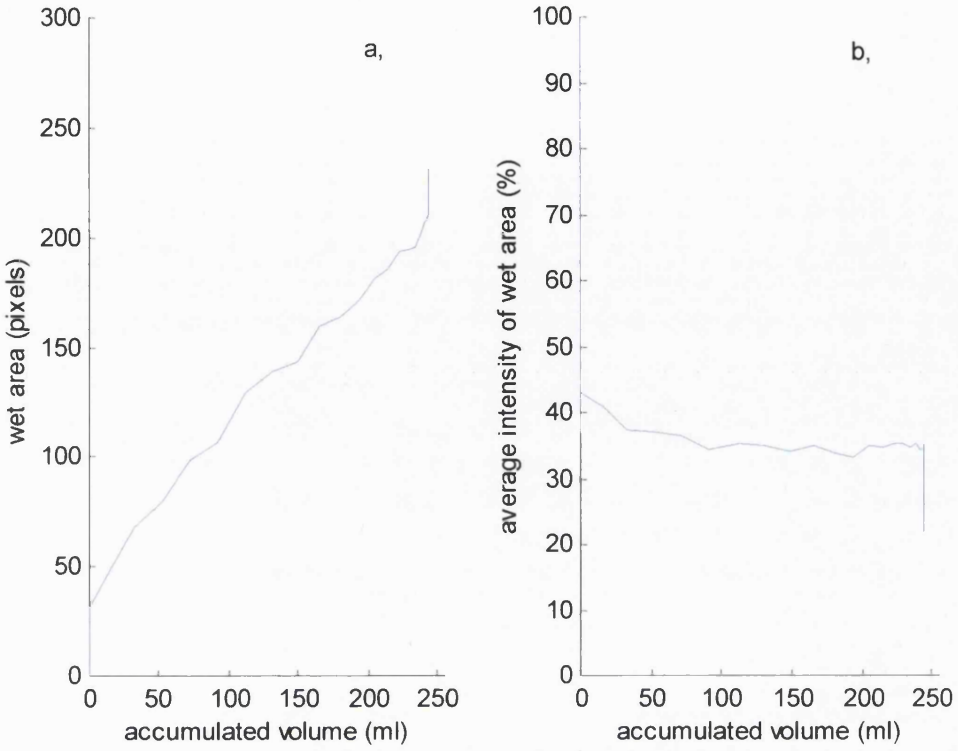

Fig 7.6 a, Size of wet area as a function of accumulated fluid volume b, Average intensity of light reflected from wet area as a function of accumulated fluid volume, for a sample data set

7.1.7 Point value plots

Point value plots are the method of processing that most condenses the data: a single value is returned per experiment. Although they allow very little information about a single experiment to be displayed, they do allow the results of many experiments to be compared.

These point values could be area or intensity values (see 7.1.6) at a specific time or accumulated fluid volume. These points can be plotted against the varying factor in a series of experiments, e.g. pad size, orientation, etc. The experiments plotted on such a graph could show the effect of using different orientations of the pad, different products or any other variable factor.

7.1.8 Combination plots

When comparing data from two different techniques combination plots can be used, allowing the data sets to be overlaid. For example, snapshots of optical imaging data can have contour plots (single contour, at time of snapshot) of resistive imaging data overlaid. Examples of these plots are shown in 7.3 where they are more fully described.

7.1.9 Summary

A wide variety of plotting techniques have been described for displaying optical data sets. Some of the techniques are helpful for looking in detail at one experiment, others for making simple comparisons between the data from many different experiments. For example, if a number of sizes of a product range are to be compared a single value plot of wet area versus dry pad weight may by illuminating. However, where repeated insults of fluid are used, temporal information is important and a time/intensity plot can separate out the growth in size of the wet area that is due to each insult.

A summarising table (Table.7.1) has been constructed to highlight the advantages and limitations of each display method to facilitate a comparison of the techniques.

Display technique	Advantages	Limitations	Example
Animation	Reveals dynamic picture / shape of wet area	Hard copy cannot be produced	
Snapshots	Reveal overall picture/shape of wet area at discrete times	Coarse time scale	Fig 7.1
Curved plots	Provide posture context to image	Hard copy cannot be produced unless course time-scale. Some data obscured	Fig 7.2
Contour plots	Show changes in wet area over time	Wet or dry, no degree of wetness	Fig 7.3
Time/intensity of line	Time, light intensity & fluid position shown simultaneously	Single spatial dimension	Fig 7.4
Time/area	Easy to compare experiments	No spatial information	Fig 7.5a
Time/Intensity	Easy to compare experiments	No spatial information	Fig 7.5b
Volume/area	Easy to compare experiments	No spatial information	Fig 7.6a
Volume/intensity	Easy to compare experiments	No spatial information	Fig 7.6b
Point value plots	Easy to compare data from many experiments	Single value per experiment	
Combination plot	Comparison between two techniques	As for constituent plots	Fig 7.18

Table.7.1 Summarising of performance of optical data display methods

7.2 Commissioning of the Optical Imaging Device and the Mechanical Bladder

It is clear that the spread of fluid in a pad under test will depend not only on the intrinsic properties of the pad but also on such factors as the volume, flow rate and temperature of the fluid, as well as how the pad is applied to the holder. Before the effect of all these factors could be studied, the accuracy with which the test parameters could be controlled had to be established. It was desirable that some factors - notably fluid temperature and the procedure for attaching a pad to the curved optode holder - should be kept consistent. The accuracy needed to maintain this was also investigated. For these reasons every aspect of the experimental procedure was assessed in order to define the current tolerance of each step and any modifications necessary to bring this to an acceptable level were made as detailed below.

7.2.1 Test Fluid

Temperature of fluid

The test fluid was used at 37°C to model body temperature. This was important as many properties of liquids and materials are temperature-dependent. For example, one study seeking to relate product performance to design (Cottenden et al. 1987), found that increasing the ambient temperature from 24°C to 39°C, at a relative humidity of 93-95%, reduced by more than 30% the absorption time for fluid to wick from the bottom to the top of a standard sample of fluff pulp (measured according to the method described in SCAN-C 33:80, 1990). The same study found that the viscosity of both urine and water fall from 1.15cP at room temperature to 0.80cP at body temperature, a drop of nearly 25%. The absorption time of a fluid is likely to be strongly affected by its viscosity.

The temperature at which the mechanical bladder delivered fluid was accurate to within +/- 2°C of 37°C, according to the stated accuracy of the thermostat used. This was checked by placing a mercury thermometer at the fluid outlet (of the curved optode holder, to which the mechanical bladder was attached) and monitoring the temperature as a series of fluid insults were applied. The peak temperature of the fluid varied by no more than +/- 2°C. The temperature variation within the insults was also monitored in the same way, although the thermometer had to be pre-warmed because the response time for large temperature changes, for the mercury thermometer, was a few seconds. There was no evidence of a significant variation in temperature across the duration of a flow-rate/time profile, provided cool fluid was flushed from the urethra just before the pad was put on. Thermal lagging would help prevent such cooling in the connecting tube during repeated insult experiments.

In order to assess the importance of temperature or the rate and final distribution of the fluid spread in products the temperature setting was changed to perform experiments at 31°C and 43°C, as well as 37°C, for a series of experiments. Two disposable products from different product ranges and different sizes (Tena plus and Molyform super, see Table 8.1 for details) were tested with two different flow-rate/time profiles of fluid for each temperature. Each experiment was repeated three times. The flow profiles used were 250ml with a peak flow-rate of 20ml/s and 100ml with a peak flow-rate of 10ml/s

(profiles f_250_20 and f_100_10 respectively, in section 4.3.2). The optical imaging device with the curved optode holder was used, in the standing position, for this test.

No meaningful variation due to temperature was seen for any of the four product/flow- profile combinations. Fig 7.7 is typical of the results and shows the wet-area as a function of time for product 'me' with the 250ml flow profiles. The traces shown all overlap with a spread of about +/- 10% and cannot be grouped into repeats of the same temperature. This indicates that the random variation between pads is greater than temperature effects within this temperature range and, therefore, that a temperature accuracy of +/- 2°C is adequate for these studies.

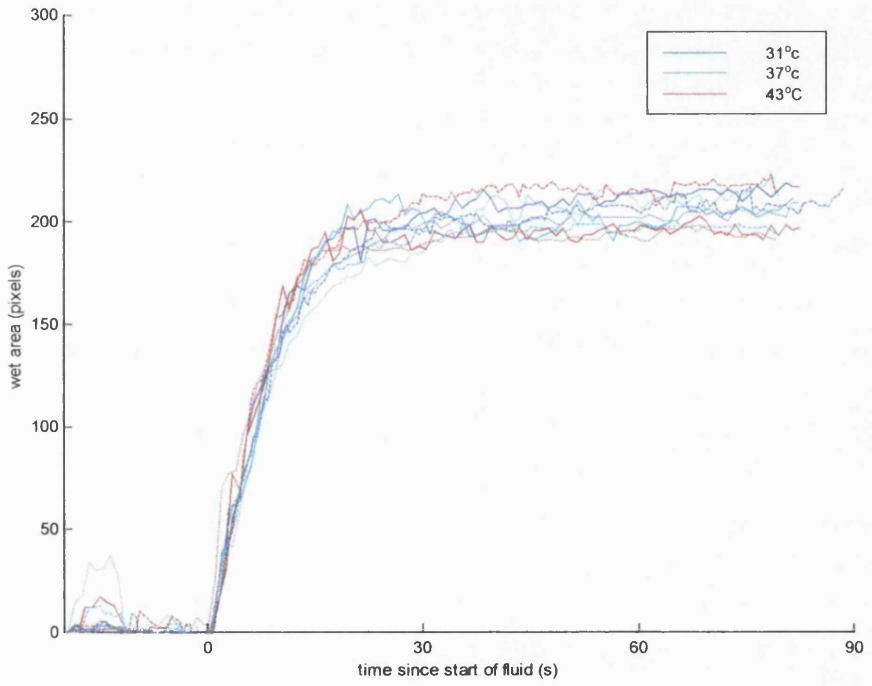

Fig 7.7 Effect of temperature on fluid spread within absorbent product 'me', repeat experiments shown as different line styles

Weight of fluid

The volume/weight of test fluid applied to a pad should be solely dependent on the variable pulse rate applied to the stepper motor, which is determined by the flow-rate/time profile in use. In practice it was found that a number of potential sources of error were present, which fell in to two main groups.

The first of these related to steps being missed by the motor due to excessive friction between the piston seal and the chamber wall. This occurred particularly at the very low flow-rates present at the tail end of flow-rate/time profiles, where the motor was likely to stall. The piston friction may have been dependent on its height within the cylinder, whose cross-section was not a true circle and also varied

slightly along its length. This was counteracted by starting all experiments at the same piston position. Friction was also reduced by the application of silicone grease to the piston seal (see section 4.3.3). It is also conceivable that very tight application of the pad to the holder may have restricted fluid, flow but no evidence (i.e. reduced final pad weights) for this was observed.

The second group of errors relates to fluid dribbling from the outlet tube due to factors such as meniscus inversion, gasses expanding and, seal leakage.

Meniscus inversion occurs when the proximity of absorbent material to the fluid outlet cause the fluid meniscus to reverse allowing the pad to continually draw fluid out of the tube. This increases the weight of fluid in the pad beyond that programmed. Conversely, if this occurred when wiping the optode array between experiments, the fluid weight of the next experiment would be correspondingly reduced. However, this meniscus inversion effect was not seen except where wet pads were left in place for much longer than the normal duration of an experiment and when testing the effect of applying pads with excessive pressure. In these cases, as well as an increase in final pad weight, air was heard and seen to bubble into the mechanical bladder, replacing the fluid that had been drawn out.

Gas bubbles forming on the heating element increase the pressure inside the cylinder and could displace fluid in the outlet tube. However, as the temperature was thermostatically controlled, heating was not continuous, occurring mainly when the mechanical bladder was refilled. This otherwise significant problem was avoided by switching the heater off for the duration of each experiment once the fluid had reached 37°.

Seal leakage occurs when the silicone grease around the piston seal becomes discontinuous. This did not happen often but had to be checked frequently. Leakage was observed by bubbling at the seal, excessive fluid weight in the pad and/or dripping after the pad was removed. Experiments where this occurred were discarded and fresh grease applied to the seal.

The output from a series of flow-rate/time profiles was measured using an electronic balance with computer link. This generated the accumulated fluid weight as a function of time. By differentiating these data a comparison could be made between the achieved flow-rate/time profiles and the flow-rate/time profile calculation used to control the mechanical bladder output. Fig 7.8 shows the calculated and measured flow-rate as a function of time for two different profiles. A close correlation is seen between each pair of lines indicating that the flow-rate time profiles are reproduced by the mechanical bladder to an accuracy of better than +/-2% of the total fluid weight.

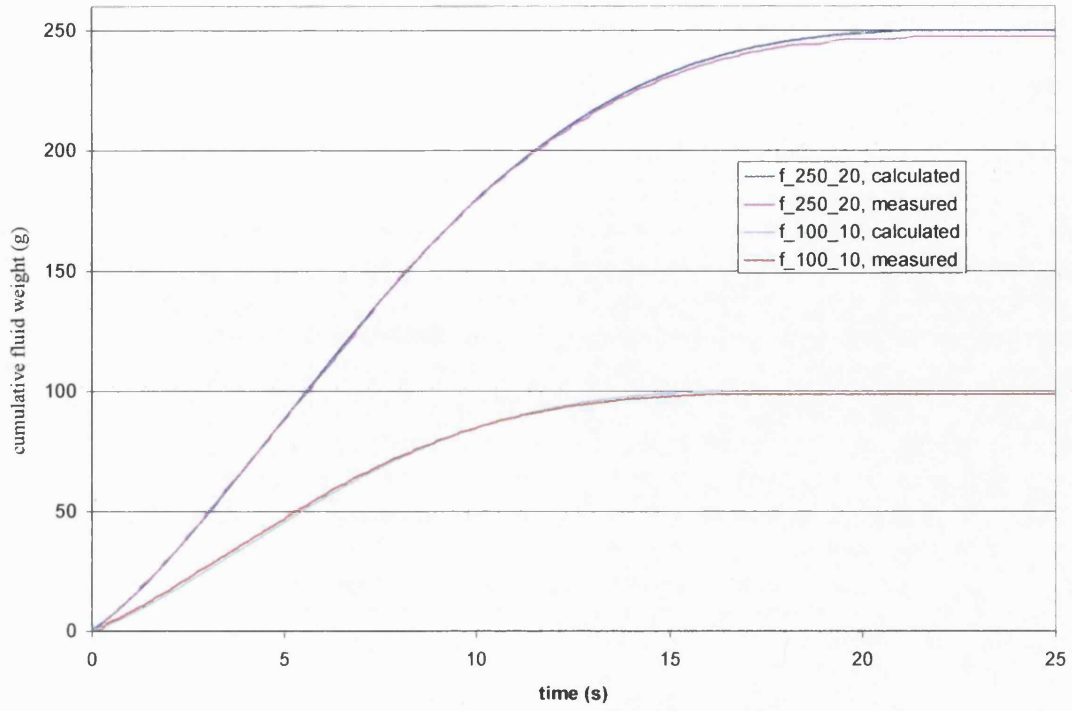

Fig 7.8 Accuracy of flow-rate/time profile reproduction

The accuracy of the total fluid weights is maintained within 2% of the target weight when the system is used with a pad in place. This was illustrated by a representative sample of pads, a random selection of those described in Table 8.3, that had been used in another experiment. Eleven pads did not leak when an insult of 250ml with a peak flow-rate of 20ml/s was applied (flow-rate/time profile f_250_20 in section 4.3.2). These were compared with eleven pads that had received 100ml at a peak flow-rate of 10mls without leaking (f_100_10). The fluid weight for each pad was calculated from the wet weight minus the dry weight. The range of weights recorded is summarised in Table.7.2.

Required	250ml	100ml
Min	247.0ml	98.0ml
Mean	249.3ml	98.8ml
Max	252.1ml	100.2ml
Standard deviation	1.74ml	0.61ml

Table.7.2 Average fluid weights delivered by the mechanical bladder

Composition of fluid

The fluid used in all experiments was 0.9% weight/volume saline. This is specified in a wide range of international, national and industry standards (e.g. European Disposables and Nonwowens

Association (EDANA) in their IISO proposal (1998)) as a good approximation for urine in terms of its physical and chemical properties. The salt was important because of its interaction with super absorbers: the sodium and chloride ions form strong ionic bonds with the superabsorber, blocking the superabsorber from binding to several times as many water molecules.

The solution used was made up from tap water and sodium chloride with a concentration accuracy of better than 1%. Although de-ionised water and analytical grade NaCl could have been used this would have been unlikely to have had an observable effect on the results.

7.2.2 Pad application to curved optode holder

With any optode holder it is important that the pad is applied in a reproducible manner. The way pads were applied to the curved optode holder is described in this section and a reproducible method of application identified.

Effect of pressure

The pressure with which the pad was applied to the optode holder could affect the results in two ways. Firstly, the optical properties of the pad could be altered as shown with the optical ribbon cables in section 6.3.7. Secondly, the fluid holding properties of the pad would be partly dependent on its freedom to swell and hence on the pressure with which it was held against the optode holder. The experiments in this section sought to identify the magnitude of these effects within the range of pressures used to apply the pads to the optode holder.

Pads from two piece products (i.e. pads designed to be held in place with stretch pants) were attached to the curved optode holder with a piece of micropore tape at back and front and with net pants applied over the top, as shown in Fig.6.12. A series of experiments looked at the effect of varying the pressure applied to the pad by the tape. In one experiment these were applied so that the pad (a Moliform super, see table 8.2) was stretched very tightly about the curved optode holder and in the other loosely. A total 250ml of fluid was applied to each pad with a peak flow rate of 20ml/s (profile f_250_20, in section 4.3.2), through the central urethra of the curved optode holder, in the standing posture.

Fig 7.9 shows the results from these experiments. When the pad was applied very tightly meniscus inversion was caused in the "urethra", the only instance of this happening. Pad swelling may have been obstructed resulting in a larger wet area but this effect was minimal and the image was very similar to the one with normal pressure. When the tapes were applied loosely (right-hand image of Fig 7.9), excessive speckle appeared on the image (bright pink) where the pad gives the illusion of having become dryer than at the start of the experiment. This is due to a less consistent/lower average optical contact with the pad. However, although this speckle hindered visual interpretation of the results it did not significantly affect the quality of the statistical information that could be gathered. This can be seen from the wet area/time trace (Fig 7.10) where the trace for the loosely applied pad does not have more noise than the normal pressure and tightly applied pads. What is affected is the size of the wet area, which is smaller than normal with the fluid accumulating in the crutch area, as can be seen from Fig 7.10

which shows wet area/time traces for the three experiments. This shows that 'Hand tight' appears to be an appropriate pressure, as shown in the central image of Fig 7.9.

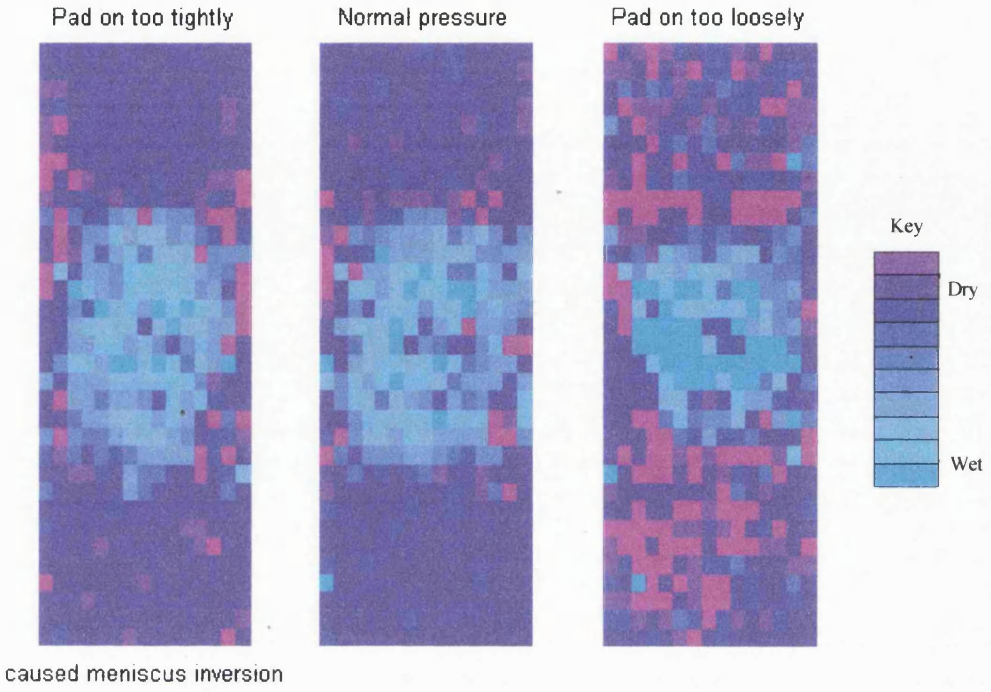

Fig 7.9 Effect of pressure on fluid spread within absorbent materials

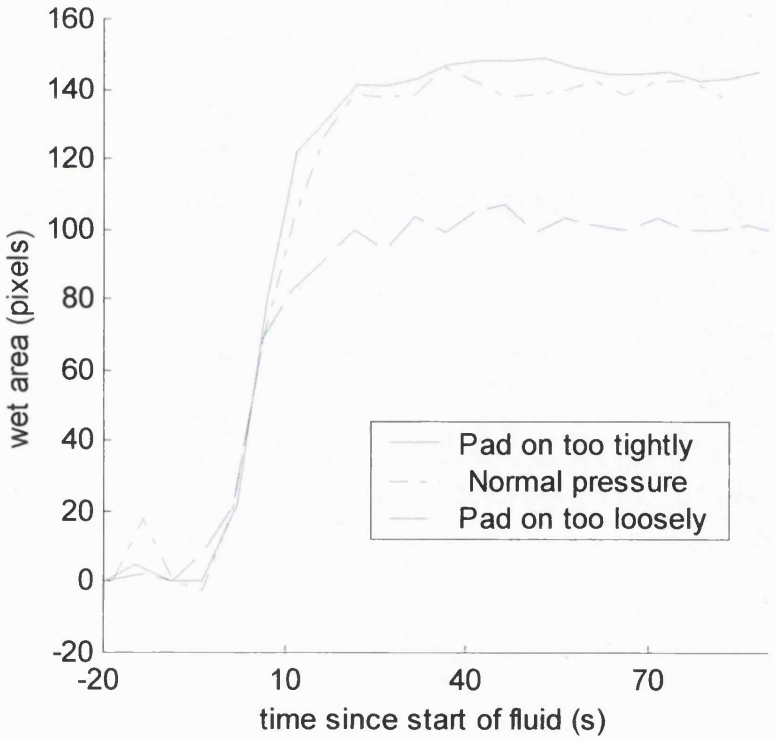

Fig 7.10 Effect of pressure on the wet area size as a function of time for absorbent materials

The impact of the pressure with which the pad was attached to the holder on the fluid spread and image quality was investigated using multiple pairs of stretch net pants similar to those that are used clinically to hold pads in place. These should apply an even pressure over the pad surface. A series of experiments was conducted to assess the effect of using more than one pair of pants, thus varying the all-round pressure applied to the pad. The experiment was also performed with no net pants. The pads were attached to the curved optode holder with the front and back tapes under normal pressure and 0-4 pairs of stretch pants (Security Stretch Briefs, see Fig.1.3) fitted. A total fluid volume of 250ml, peak flow-rate 20ml/s (profile f_250_20 in section 4.3.2) was applied.

Fig 7.11 shows that background speckle (bright pink) was reduced when one pair of pants was used instead of tapes alone. However, there was no further reduction in speckle when more than one pair of pants was used, as is shown by the lack of meaningful difference between the second and fifth images of Fig 7.11. This is also illustrated in Fig 7.12 and Fig 7.13, which show area/time and intensity time traces for these experiments. Although the areas differ slightly is size, the main difference that can be seen in Fig 7.12 is that the trace for 0 pairs of stretch pants is far noisier than those for 1-4 pairs. With Fig 7.13 the intensity trace for 0 pairs of pants shows a lower intensity than the others, indicating that the pad had been pulled away from the sensors by the weight of fluid in this case only. This indicates that the pads should be used as clinically designed: that is, pads of a two-piece system should be used with one pair of net pants to maintain all-round pressure to the pad.

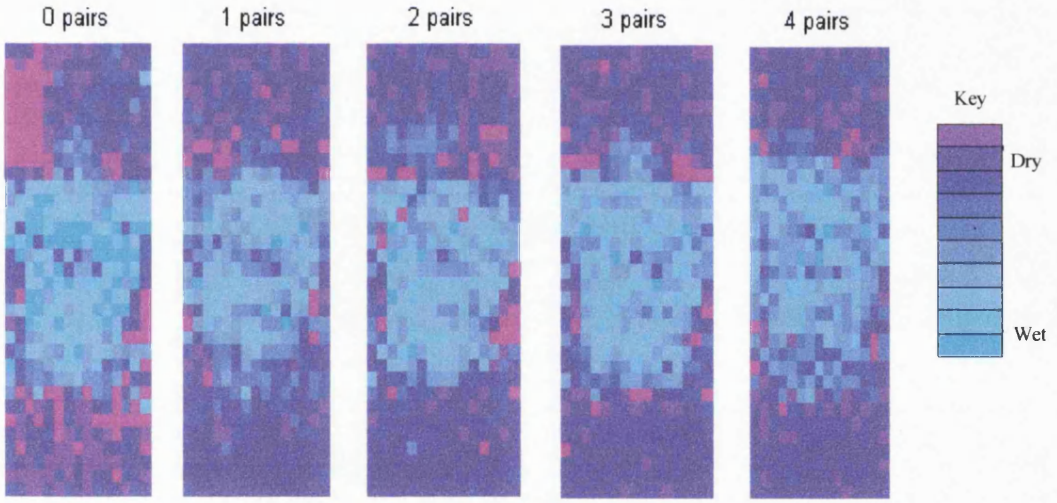

Fig 7.11 Effect on fluid spread of increasing all-round pressure applied to pad

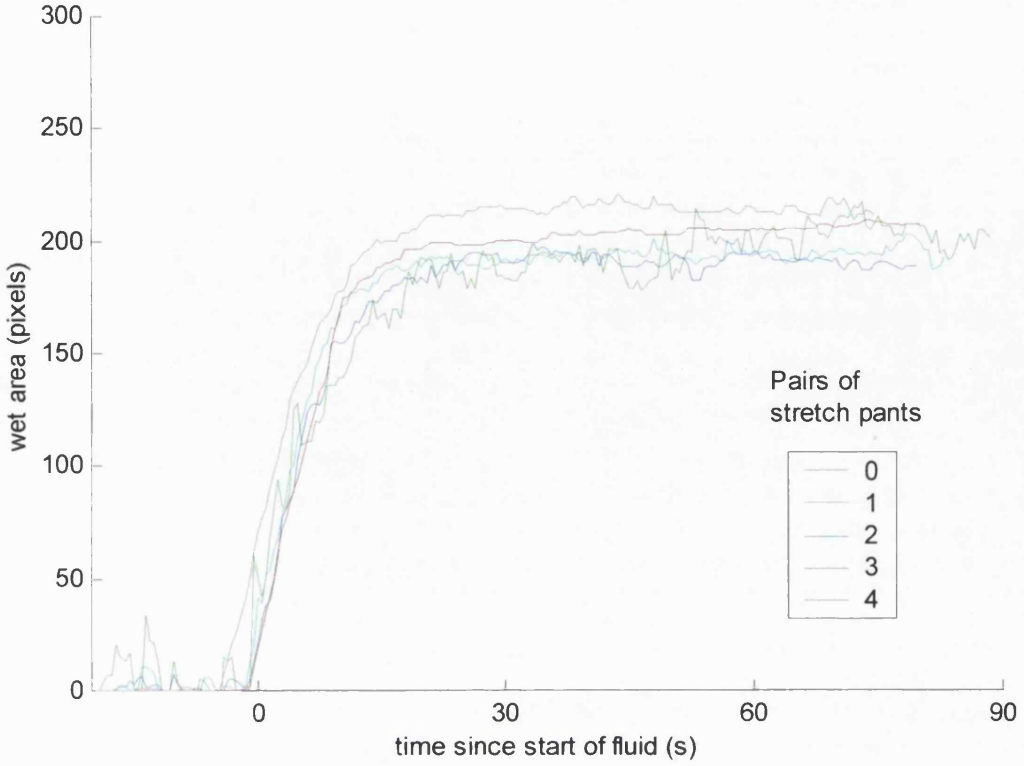

Fig 7.12 The wet area size as a function of time showing effect of varying the number of net pants applied to the pad.

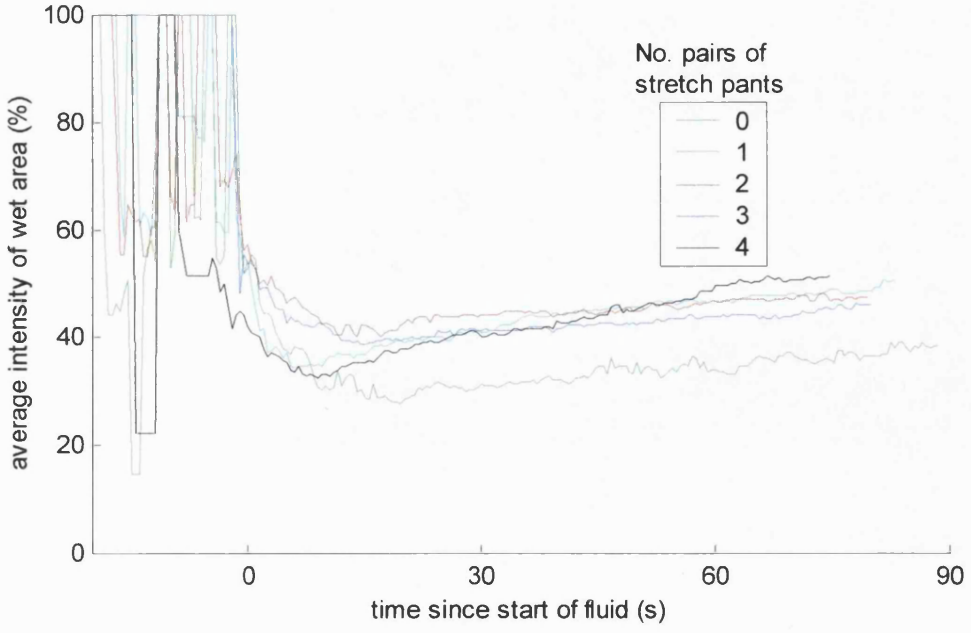

Fig 7.13 Average intensity of wet area as a function of time showing effect of varying the number of net pants applied to the pad

Positioning of pads

All people and all product ranges differ in size and shape. However, in order to compare results from different experiments and, in particular, different products the fluid must be applied to the equivalent position for all pads during laboratory tests. This would normally be a point on the central long axis of the product in the crutch region. Measuring the position of this point is not trivial because the position of the crutch region, relative to the length of the pad, varies from product to product. For this reason a working definition for the 'centre of a pad' was defined as follows (see Fig 7.14):

- On one long edge of the product the line parallel to the long axis of the pad was identified where the crutch shaping indentation was 150mm long.
- A point was marked 40mm along this from the end of the line nearest the back of the product.
- The procedure was repeated on the other long edge of the pad.
- The centre of a line joining these two points marked the 'centre of pad'.

This point was normally placed at the centre of the hemispherical part of the curved optode holder but the pad could be systematically moved to study effects of wrongly positioned pads. To enable the pads to be positioned reproducibly, the two principle axes of the pad were always marked, according to the above definition, and aligned with markers on the curved optode holder.

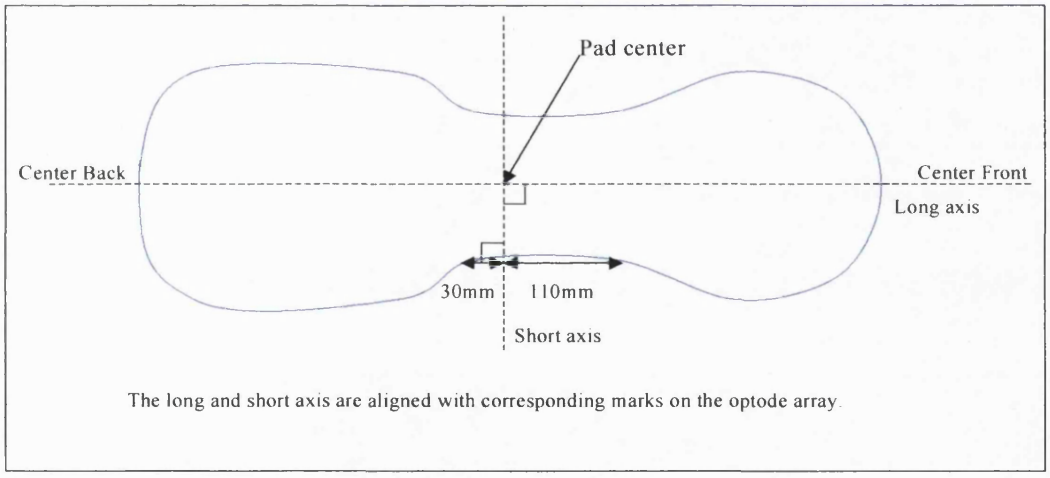

Fig 7.14 Method for determining the centre of a pad

The rationale for this definition was based on the observed fluid entry point of early clinical imaging trials, which indicated that fluid normally arrived at approximately this point. The definition has the advantage of being reproducibly applicable to any shaped pad since it is independent of the proportions of the front and back lobes of the pad.

7.2.3 *Timing of fluid applications*

In order to understand sequences of images it is important to know the relative timing of fluid insults; that is, there needed to be a common zero time for the mechanical bladder and optical imaging device.

The optical imaging device and the mechanical bladder were controlled from the same computer and were synchronised by this so that the first fluid application always started 20s after data collection had started. A delay time of 20s was chosen to allow time for the base line dry state to be monitored for a period. This time delay could be reduced to a few seconds but sufficient time needed to be allowed for the initial dry state to be recorded.

7.2.4 *Length of wet area measurement*

Comparing the length of the wet area according to visual inspection with that recorded by the monitoring equipment provided a useful indication of the performance of the equipment.

Manual measurement of this length involved a subjective judgement of what was wet, with no comparison to the original dry state. It involved stretching a pad out flat on a light box, and measuring the wet length (parallel to the pad length) with a ruler applied to the back of the pad. This was in contrast to the optical system, which compared each point with its dry state, viewing from the front. The back of the pad was used with ruler measurements in order to highlight any discrepancy due to insufficient depth penetration by the optical imaging device. The optical measurement with the curved optode holder had a resolution of 12.5mm whereas 5mm accuracy was achieved by eye. This latter was limited by the indistinct wet/dry boundary of the fluid distribution and the uniformity with which the pad could be held flat. The eye's judgement of what was wet was subjective whereas the optical method used a pre-set definition, counting the number of rows on the image where more than one optode had an intensity less than 82% of the original value. The definition does not attempt to define a wet region as this would be unnecessarily computationally expensive. However, more than two optodes in a row had to measure wet for the row to be counted. This was to prevent isolated, spurious wet points, being included in the length measurement. Both methods were indirect measures of water content and subject to inaccuracy due to varying pad compositions.

The wet lengths were measured by these two methods for the different size pads within four product ranges, Attends Ultracare, Tena Comfort, Comforta Dryform and Molyform. Details of these products can be found in table 8.2. Each product was tested with two flow-rate/time profiles, f_250_20 which had a total fluid volume of 250ml with a peak flow-rate of 20ml/s and f_100_10 with 100ml total fluid volume and a peak flow-rate of 10ml/s, (section 4.3.2). Three repeats were performed for each flow rate and the length measurements averaged. Fig 7.15 shows these length measurements for each product. All the products within a range are grouped together, increasing in size from left to right. The variation between products is considered in section 8.1.2.

Most of the pads showed reasonable agreement between ruler and optical measurements although the optical measurement tended to give the longer reading in each pair. Pads from the attends

product range ('ae', as' and 'ap') showed the most discrepancy between measures, this was probably because the base layer of absorbent material in these products was of very uneven thickness obscuring the true fluid front from the visual observer. Overall, these data indicate that the optical measurement gives an accurate reflection of the true length of the wet area. It is probable that the optical imaging system did not just look at the surface of the pad but performed some averaging over the depth of the product, enabling measurements from the top and bottom surfaces of the product to agree closely.

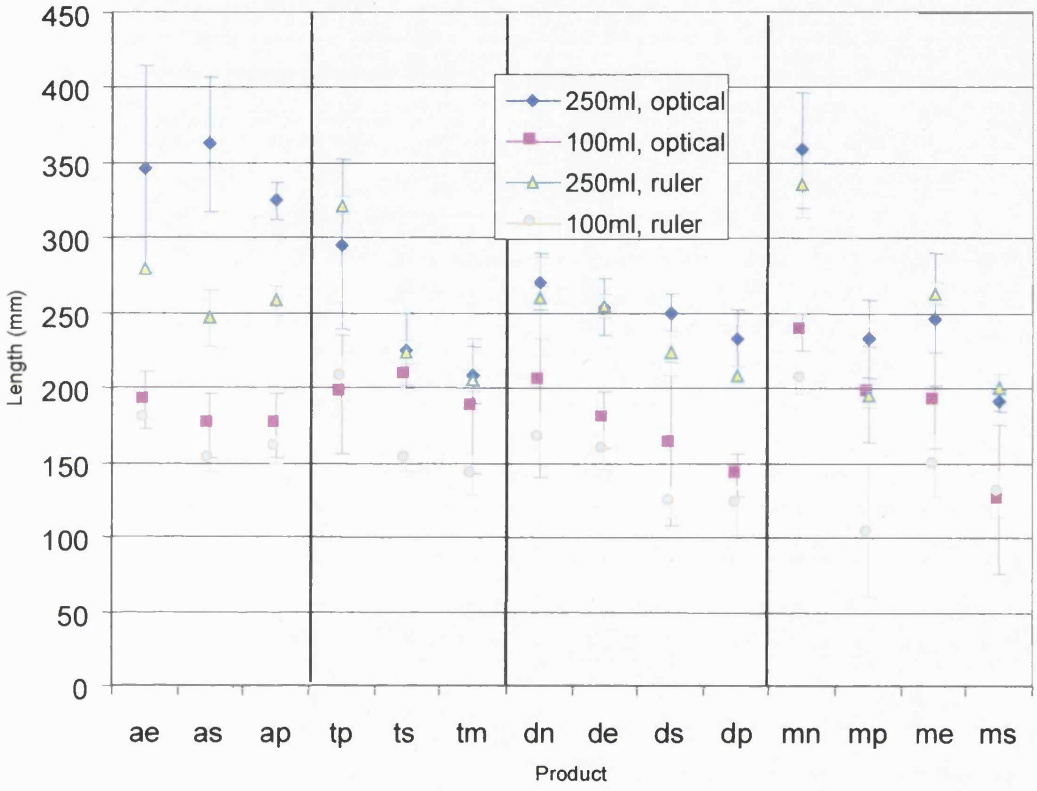

Fig 7.15 Measurement of wet-length for four product ranges, product codes as in table 8.2

Since optical imaging does not provide information about how the fluid distribution varies between the layers of a pad it was found informative to dissect a number of the pads after fluid had been applied. In most cases dissection showed a variation of less than 15% between the wet lengths of the various layers. However, on dissection it was found that this could be more than 50% for 'Tena Plus' ('tp'). For example, the wet length measured from the top (coverstock) of one pad was 150mm, and from the bottom of the same pad, 230mm, after 100ml of fluid had been applied. It is unlikely, but feasible that the wet length increased after the pad was removed from the curved optode holder and laid flat. The optical measurement for the wet length of this pad was 175mm, which is closer to the wet area at the top off the pad than the bottom. This indicates that the optical technique did not interrogate the full depth of the pad.

7.2.5 Penetration depth of measurements

As mentioned earlier, each optode monitors a 3-dimensional volume of pad. The depth to which light detects fluid was investigated using multiple layers of fluff–pulp (as used for the base layer of Hartman all-in-one pads). A diagram of the set up is shown in Fig 7.16. Three layers of fluff pulp, separated by plastic, were imaged using a planar array of optodes. Each layer of fluff-pulp was 3-4 mm thick. The plastic was used to prevent fluid movement between layer of fluff pulp. After assembling the experiment, 50ml of warm saline was applied, via a tube, to each layer in turn at the times indicated in Fig 7.17, which is an intensity time plot of the results.

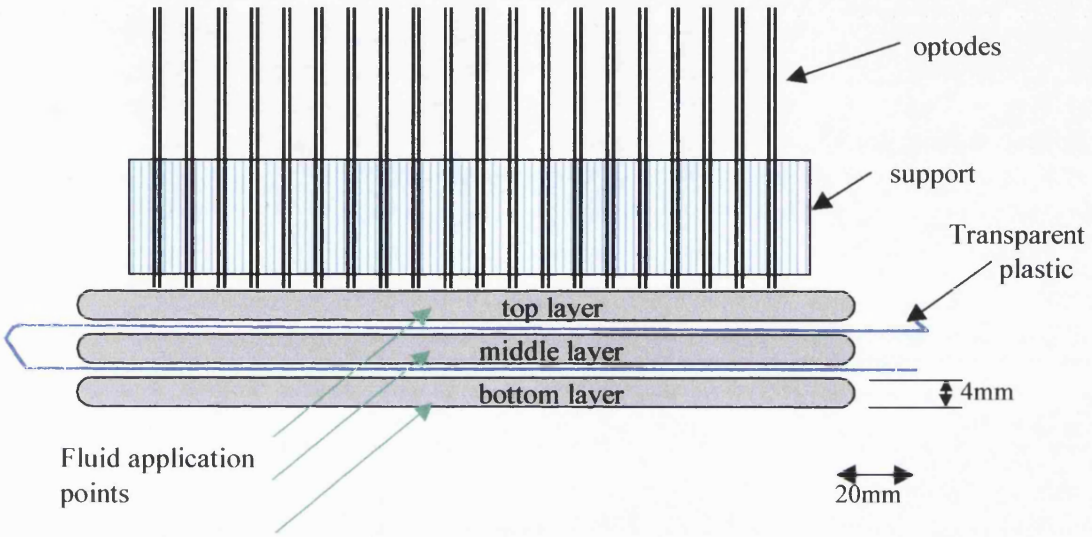

Fig 7.16 Experimental set up for measuring the depth at which fluid can be detected

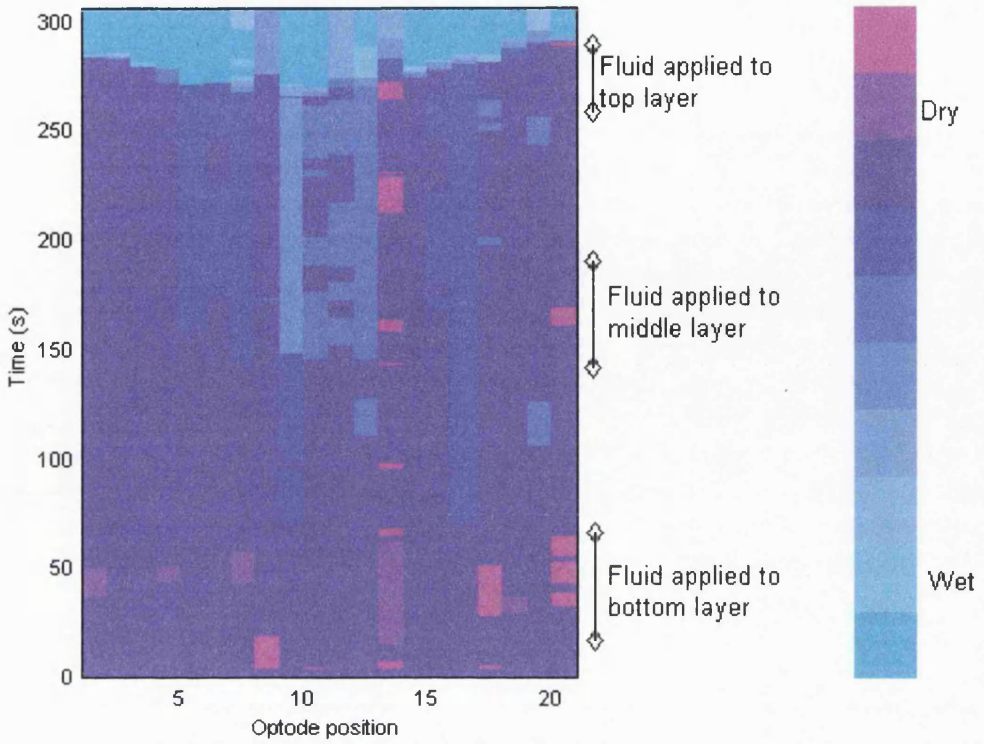

Fig 7.17 Intensity variation over time image showing the depth to which fluid can be detected

Fig 7.17 shows that two sensors registered wet at the end of fluid application to the bottom layer of fluff-pulp (~60s) but this is not enough evidence for a fluid insult to be identified. However, during the period of fluid application to the middle layer of fluff-pulp (~140-200s) seven additional sensors registered wet, forming a curve associated with fluid spreading from a central point (approximately optode 11 or 12). This same shape is seen again, accompanied by a greater intensity change and more sensors registering wet, during the period when fluid was applied to the top layer of fluff-pulp (~270-290s). This means that the fluid can just be detected through 3-4mm of dry fluff pulp but not through 7mm of dry fluff pulp. This means that information from the first two layers of most products can be gained, unless these layers are extra thick, in which case information is obtained from the first layer only.

7.3 Agreement between different techniques for studying incontinence pads

If data from different techniques are to be compared the relationship between the techniques must be known. For example if a wet length of '*x*' is measured using one technique it should be known that this will always correspond to a wet length of '*y*' if it had been measured using a different technique. This section seeks to compare pairs of techniques by using them simultaneously on the same sample.

7.3.1 Agreement between Resistive and Optical imaging techniques

Both the resistive and optical techniques produced images of pad samples. The resistive sensors had been used in clinical studies but the optical system could provide more detailed information in the

laboratory setting. In order to assess the confidence with which data from these two techniques could be compared a small number of experiments were performed, in the laboratory. Resistive sensors were placed in the back of a pad, which was simultaneously imaged using the optical imaging device, using the curved optode holder in the standing position.

Fig 7.18 and Fig 7.19 show the overlaid results from these two techniques for two products of different sizes form different ranges (Tena plus and Molyform normal, see Table 8.2). In both cases fluid was applied to the pad through the central urethra. Fig 7.18 shows product Molyform normal to which 189g of fluid was applied using the second part of flow profile f_250_30. Fig 7.19 shows product Tena super to which 250ml was applied using flow profile f_250_20. On this occasion the pad leaked by 29g.

Contour plots of the resistive data are placed on an image sequence of the optical data. The contour plots consist of a white line marking the area covered by resistive sensors and black lines enclosing those sensors that had registered wet. The final frame of each figure shows the final resistive data where wet sensors are marked black and dry sensors are marked blue. In both of these sets of results a small number of resistive sensors can be identified that triggered before fluid was applied while in the first, three sensors failed to trigger despite being completely contained within the wet area. These faults were most likely due to the soft wire sensor tips becoming bent whilst the equipment was assembled, either short circuiting them or preventing one of the wires from coming into contact with the fluid.

For both products a good correspondence can be seen between the two techniques. This allows comparison of optical and resistive data sets from separate experiments.

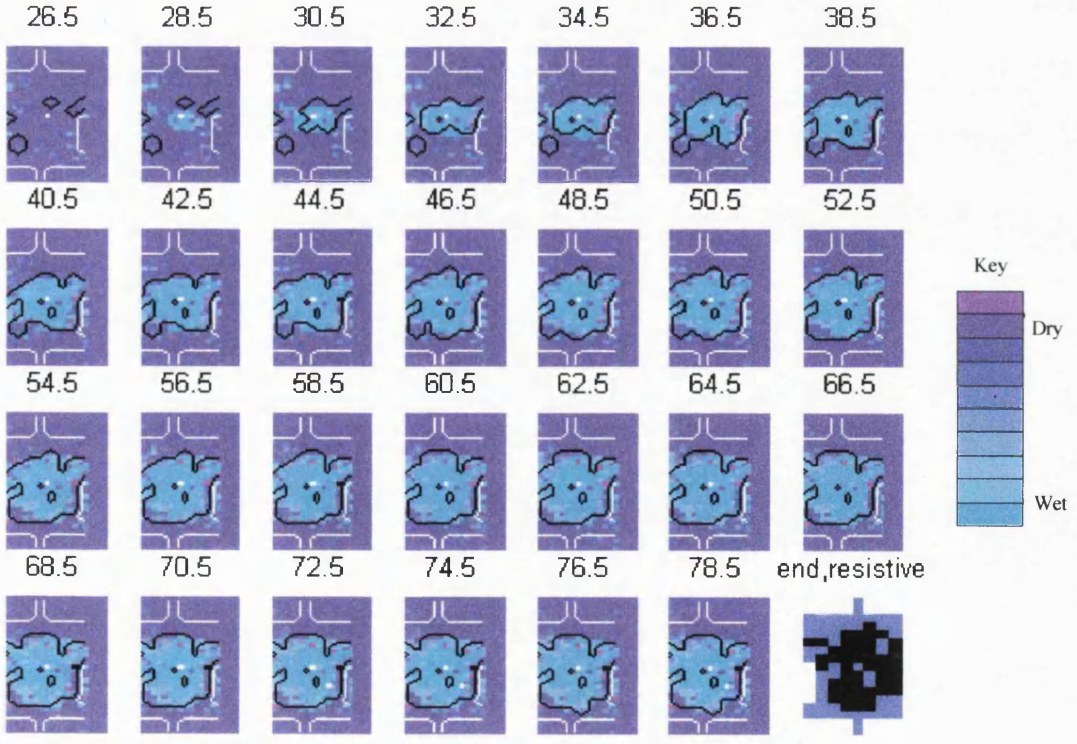

Fig 7.18 Overlay of optical and resistive images – small pad, Molyform normal

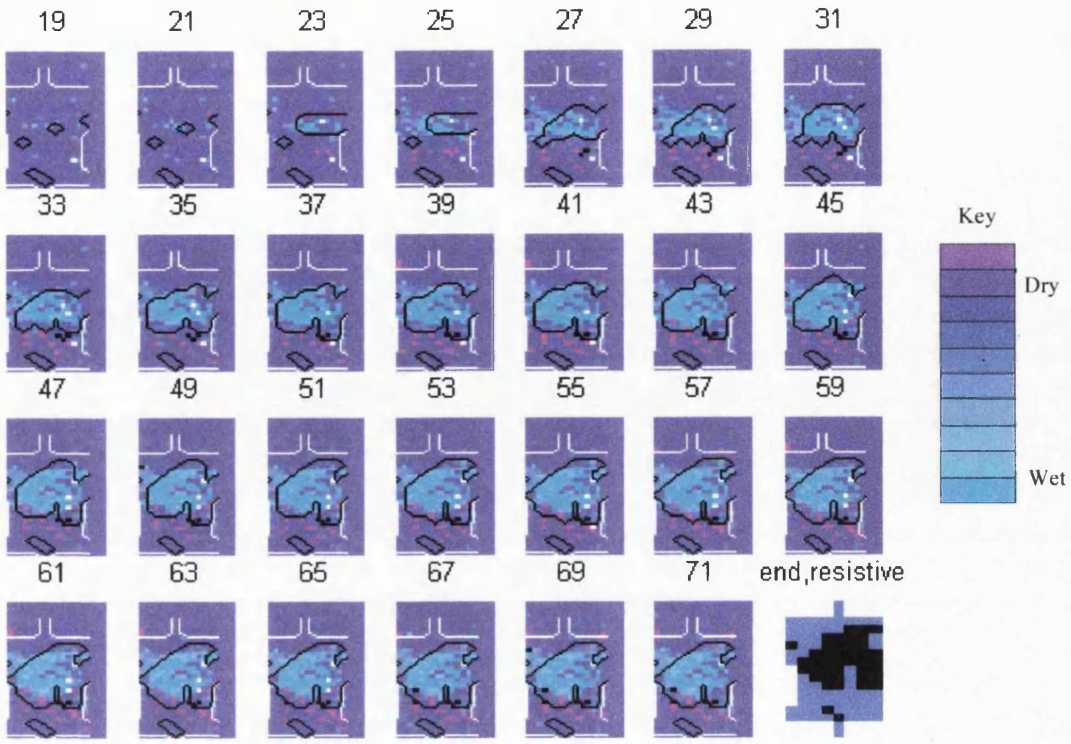

Fig 7.19 Overlay of optical and resistive images – large pad, Tena super

7.3.2 Agreement between Laboratory and Clinical images

This section is not a comparison of techniques so much as a comparison of situations. For laboratory results to be valuable they should correspond to clinical reality; that is, the same fluid distribution should result under equivalent experimental conditions regardless of whether the data are clinical or gathered in a laboratory experiment. This would enable the clinical performance of products to be predicted without the need for clinical data.

As stated previously, the resistive sensors were used to obtain data sets in the clinical setting. Each set of clinical data contained the times at which resistive sensors measured wet, the total increase in pad weight, the posture of the subject and the name of the absorbent product used. A large proportion of the data sets were unsuitable for replication at this stage either because there was evidence that the fluid had arrived in multiple insults or that virtually no fluid had been excreted into the pad. For those data sets which were suitable the same product, posture and total fluid volume as the chosen clinical data set were used in a laboratory experiment with the optical imaging system, with the curved optode holder attached.

Fig 7.20 shows the results of one such experiment. In the clinical experiment the subject had worn a Molyform extra pad ('me', see section 5.2) whilst sitting in a chair. The pad weight had increased by 150g during the experiment. This weight increase appeared to originate from one main insult of approximately 13s duration. Flow-rate/time profile f_150_20 (see section 4.3.2) was used to replicate

this in the laboratory. This profile delivered 150ml of fluid over a 12.7s time period. A Molyform extra pad was used with the curved optode holder, held in its normal upright position. The clinical data were plotted as a series of contour maps over an image sequence from the optical imaging device. The final image shows the final status of the resistive sensors.

This experiment indicated that while the final form of clinical data could be replicated in the laboratory when the product worn by the subject did not become deeply creased, the two image sequences progressed at different rates. This was because the details of the flow-rate/time profile applied in the clinical setting was unknown, and so the flow-rate/time profile chosen to replicate this could only match the clinical insult in total volume and approximate duration. This flow-rate/time profile matching would be even more inaccurate if the clinical data contained evidence of multiple insults. In cases where the geometry of the pad was more complex - for example, if the pad becomes deeply creased - it would become extremely difficult to replicate even the final form of the fluid distribution and the optical imaging technique would be of little use.

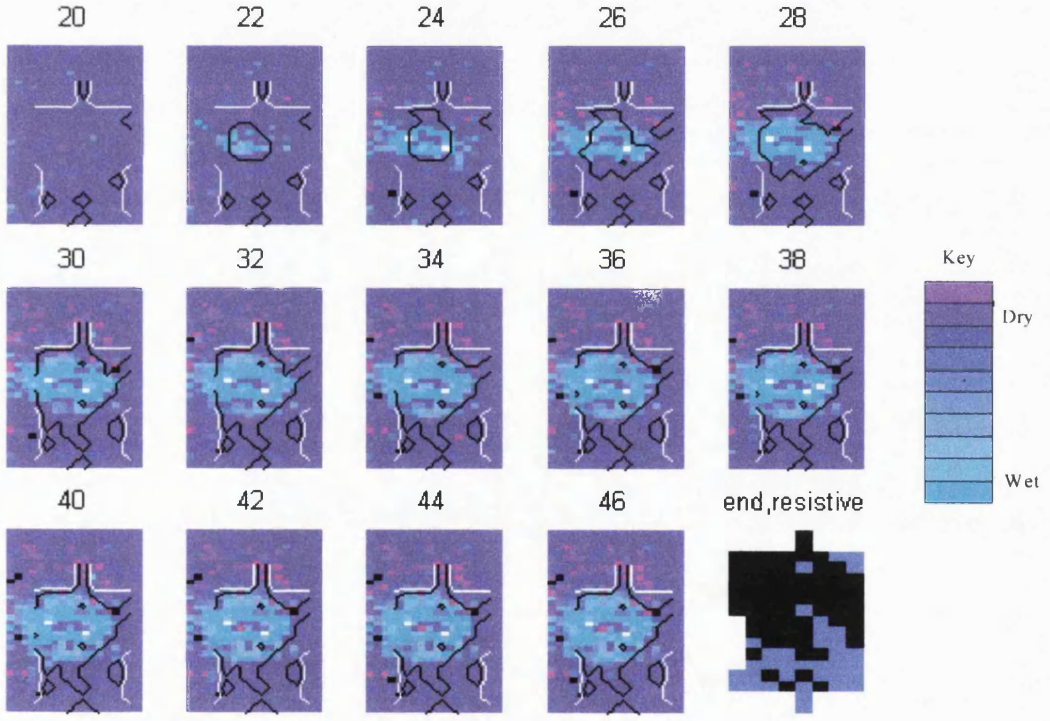

Fig 7.20 Overlay of clinical and laboratory images

7.3.3 Optical and X-ray

The optical technique does not directly measure the fluid content of a sample, since intensity depends partly on the depth at which the fluid is present (section 7.2.5). However, there was evidence to suggest that light intensity could be used as an indication of wetness, as shown in section 5.2.3. To obtain more quantitative information about this, an experiment was performed using optical sensors and X-ray

imaging simultaneously. A 10cm wide strip cut from the rear lobe of a pad of product 'me' (see Fig.8.7) was set up as in Fig 7.21. Whilst continually monitoring the pad with a planar array of optical sensors and applying 40ml of water at 13ml/min using a standard syringe pump, X-ray images were captured (using the amorphous silicon detector and mammography source, see section 4.2.3) as frequently as possible.

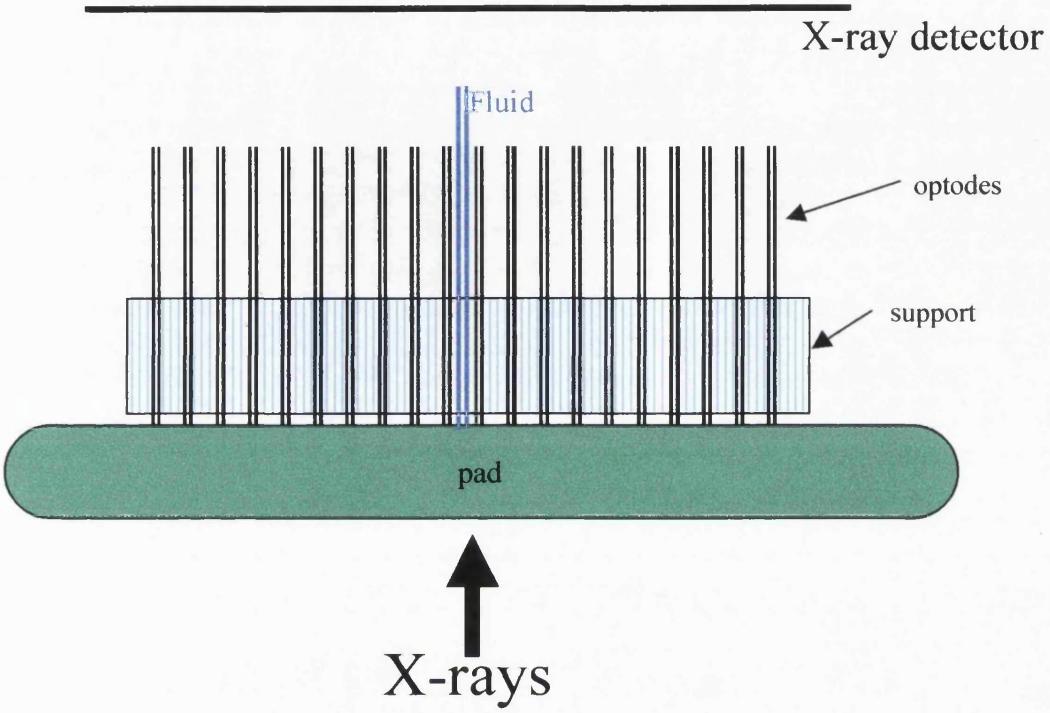

Fig 7.21 Experimental arrangement for simultaneous collection of optical and X-ray images of a pad sample

Fig 7.22 shows an intensity time plot of the optical data with the times at which the X-ray images were taken marked. Fig 7.23 shows the X-ray images, normalised to the dry pad. Ideally these images should only show the position and depth of the fluid because they have been normalised by subtracting a base image of the equipment before fluid was applied. However, slight movement of the optode holder must have occurred as some of the optodes can be seen. On each image three line profiles are drawn, through the positions of optodes 9, 10 and 11 respectively. Fig 7.24 shows the intensity of the X-rays detected along each of these lines, scaled to read as millimetres of fluid. The top plot shows the line through optode 9, at each of the image times and the middle plot line, through optode 10 and the bottom plot that through optode 11.

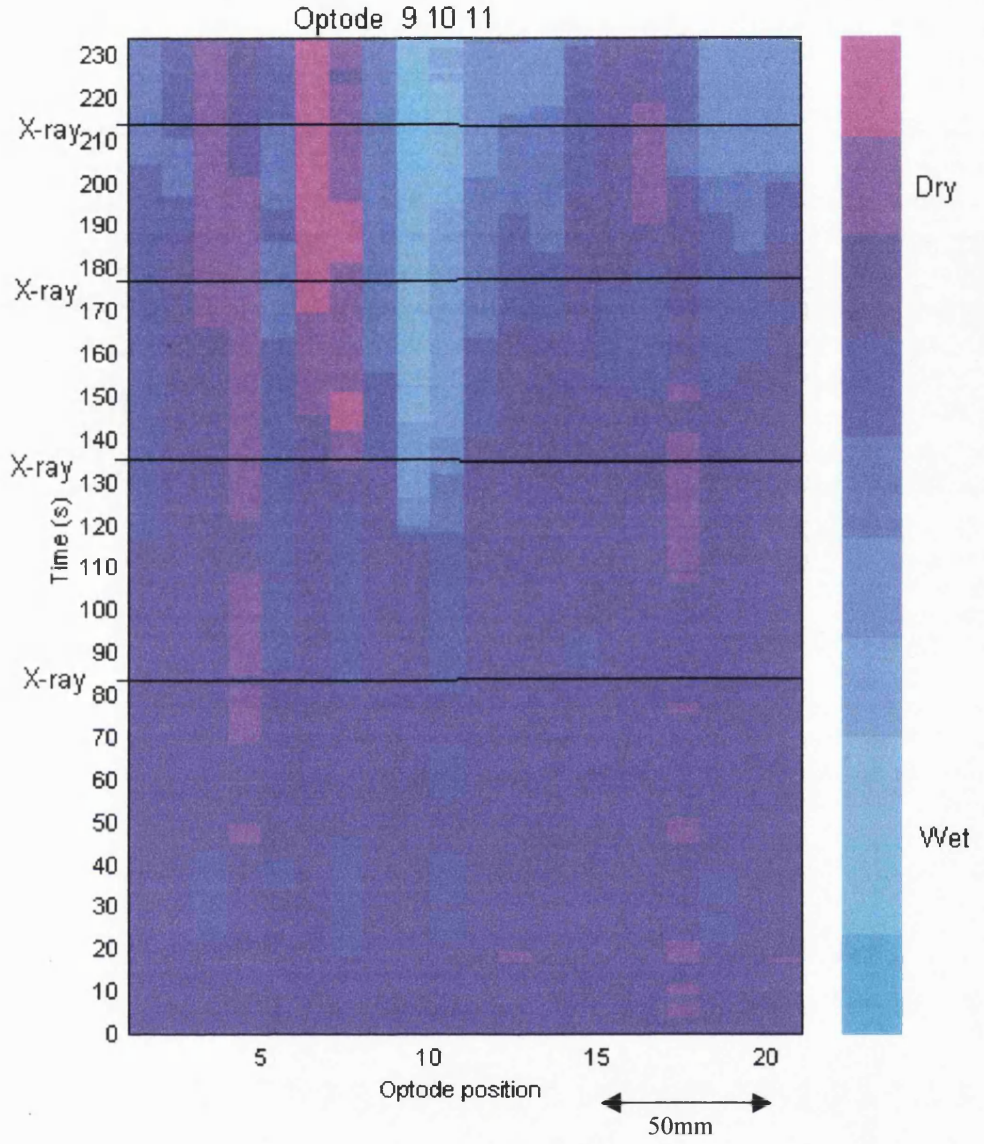

Fig 7.22 Time intensity plot of optical data showing times at which X-ray images were captured

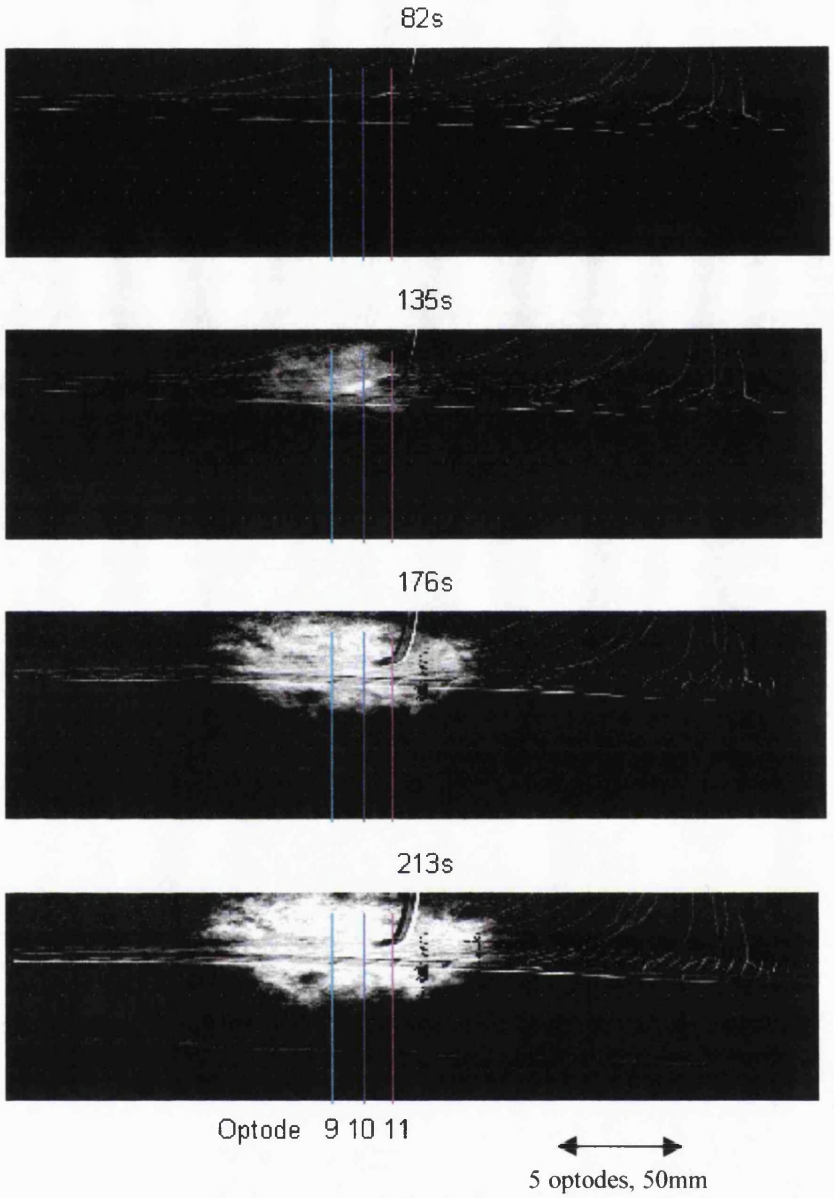

Fig 7.23 X-ray images of a pad sample collected simultaneously with optical data, positions of line profiles through three optode positions are marked

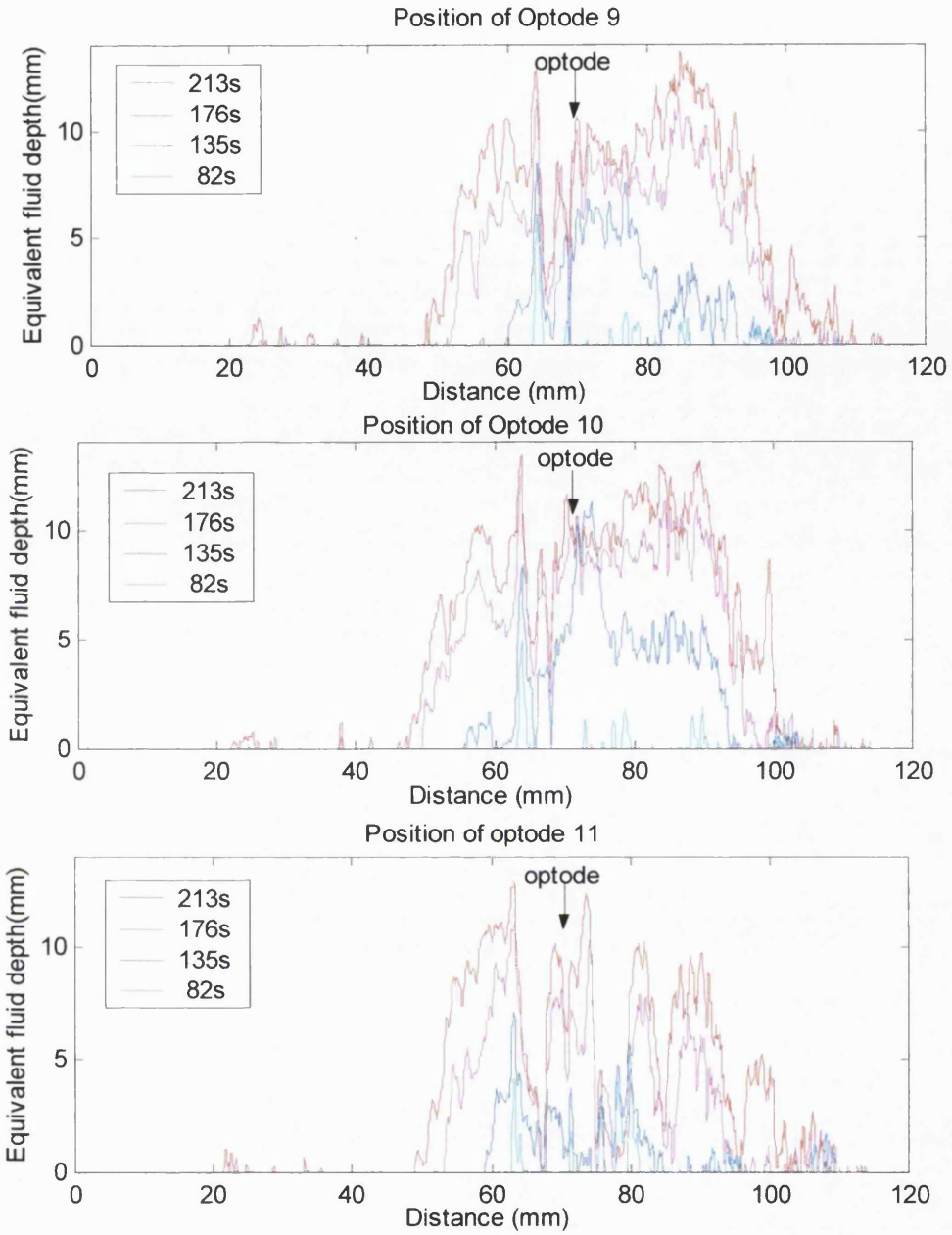

Fig 7.24 Line profiles through X-ray images shown in Fig 7.23 with positions of optodes marked

Fig 7.22 shows that optode 9 was dry at the time of the first X-ray, becoming wet before the second X-ray was taken, followed by a gradual increase in wetness throughout the remainder of the experiment. This same pattern can be seen in the first plot of Fig 7.24 where almost no fluid is detected, at the sight of the optode, in the first X-ray image (85s). At least 5mm of fluid was detected at the second X-ray (135s) and a further increase in fluid depth was seen for the subsequent two X-rays (176s ad 213s). Similar agreement between the data sets can be seen for the other two optodes shown.

These plots show that decreasing optical intensity does correspond to increasing pad wetness, as shown by the increases in equivalent fluid depth recorded with X-ray imaging. However, with X-ray images spaced this far apart, in time, there was not enough information to create a mathematical

description of saturation/intensity relationship. Even if this were possible with this data it would be misleading in cases where the fluid was distant from the sensors, as in section 7.2.5. This demonstrates that wetness information can be obtained using the optical imaging technique but the geometry of the experiment should always be taken into account when interpreting the data.

8: Pad studies

8.1 Factors affecting pad function

Many factors will combine to determine the overall ability of a pad to receive and retain a user's urine, without leaking. Some of these factors will be product dependant; for example, dependant on such factors as the absorption speed, wicking and fluid retention properties of the pad as well as its size and how well it was put on. Other factors are related to the patient; the volume, flow-rate and frequency of their accidents, their body shape (how well the pad fits), size, posture and mobility, for example, could influence the performance of the pad. However, these factors will not contribute equally to pad performance. For example, temperature is very unlikely to affect pad performance since peoples' urine shows hardly any variation in temperature. This section describes a series of laboratory experiments to determine the effects of a number of factors that are likely to be clinically relevant and can be varied in a controlled manner within the laboratory setting.

8.1.1 Flow-rate & Volume of fluid applied

Flow-rate and volume are studied simultaneously because there is clinical evidence (James and Niblett, 1988) that they are linked: large volumes are usually excreted at higher flow-rates than small volumes.

A series of flow-rate/time profiles was chosen with peak flow-rates and total volumes designed to cover most clinically realistic values as shown in Table.8.1. For details on the design of the flow-rate/time profile shape see section 4.3.2. The 100ml and 250ml total volumes represent modal and heavy events, as presented by pad weighing studies (Fader et al. 1998). These flow rate/time profiles were applied to a series of pads using the mechanical bladder and the central urethra. These pads were fitted to the curved optode holder in the standing position, using net pants, and imaged with the optical imaging device. Two products were used in these experiments, both disposable absorbent pads with superabsorber for use with stretch pants. The product labelled 'tp' was the smallest size pad from one product range and 'ms' was the largest absorbency size from a different product range. Details of these products are given in Table.8.2.

	5ml/s peak	10ml/s peak	15ml/s peak	20ml/s peak	25ml/s peak
50 ml total	V			V	
100ml total	F,V	F	F	F,V	F
150ml total	V			V	
200ml total	V			V	
250ml total	F,V	F	F	F,V	F

F = used to study flow-rate effects V = used to study volume effects

Table.8.1 Flow-rate/time profiles used

Fig 8.1 show the size of the wet area as a function of time and of the accumulated fluid volume for total fluid volumes of 250ml, applied at different peak flow-rates. These graphs are for product 'tp'. The end of fluid application for each peak flow-rate has been marked on the area/time plot. Fig 8.2 shows the equivalent pair of graphs for product 'ms'. It can be seen that for product 'tp' the lower the peak flow-rate, the larger the wet area as a function of volume. However, this distinction only occurred for the duration of the flow and was not as obvious for product 'ms'. One distinction that can be seen between these two products is that, particularly for slow flow-rates, for 'ms' the rate of increase of the wet area slows down quite suddenly some time before the end of the fluid application, but for 'tp' the area increases smoothly until fluid application ceases. The overall size of the final wet area was smaller for product 'ms', at ~130 pixels, because this was a thicker pad than 'tp' which had a final wet area size of ~180 pixels.

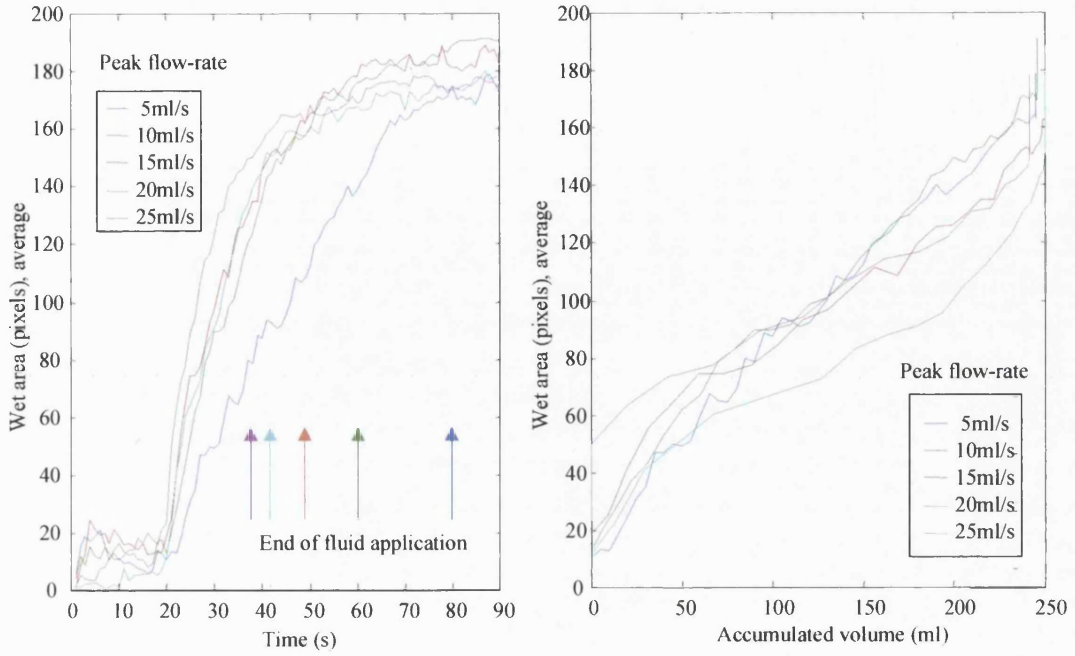

Fig 8.1 Effect of peak flow-rate on wet area, as a function of a, time and b, accumulated volume, product 'tp'.

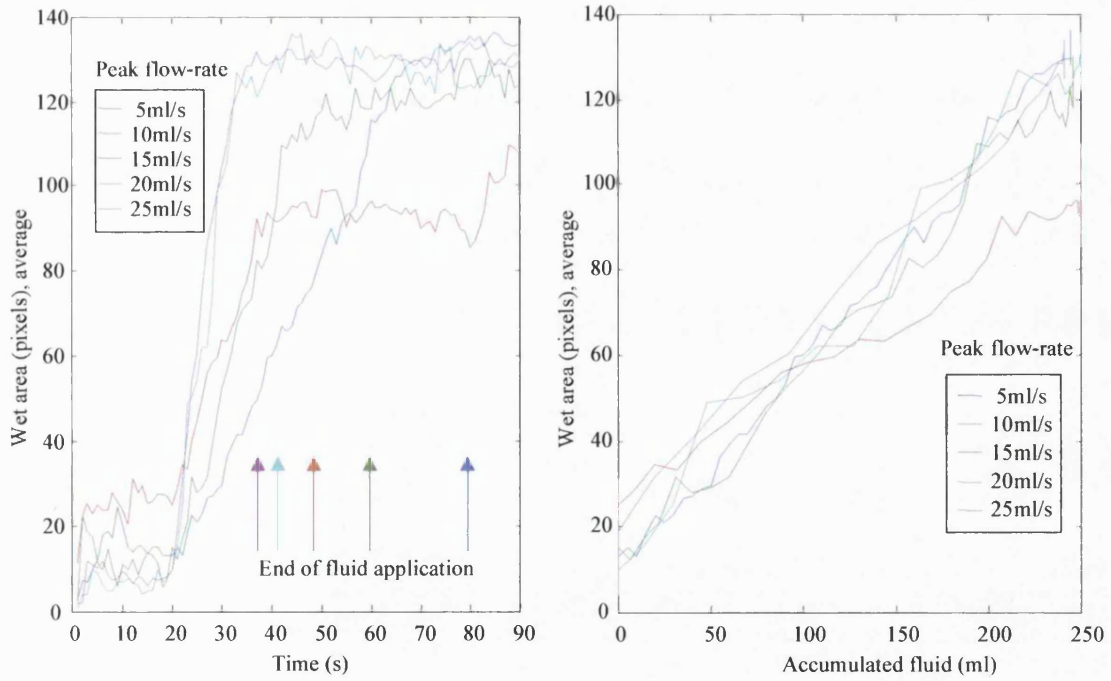

Fig 8.2 Effect of peak flow-rate on wet area, as a function of a, time and b, accumulated volume, product 'ms'

Fig 8.3 shows the size of the wet area 90s after fluid application stopped, as a function of flow rate. This time was chosen as the wet area, for all the total fluid volumes, had stopped increasing by then. Both products and both total volumes are shown on this graph.

Although the larger product (ms) has a smaller wet area than the smaller product (tp) and the smaller volume (100ml) wets a smaller area than the larger one (250ml), the size of the wet area shows no obvious trend with respect to fluid application rate under any of these conditions. Any effects due to differences in flow-rate being was of the same order of magnitude as scatter between repeat experiments at the same flow-rate.

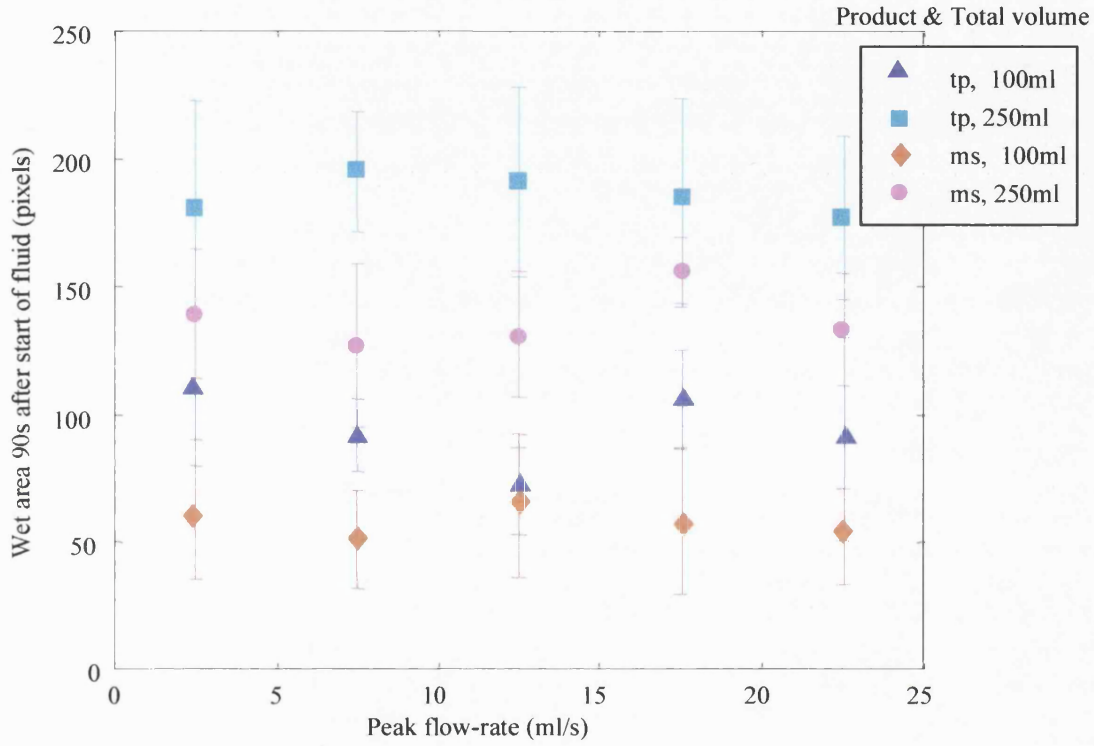

Fig 8.3 Effect of peak flow rate on final wet area for two products and two fluid volumes.

Two types of fluid movement are likely to be present within pads. The first of these is forced wicking where fluid moves within the pad because of the arrival of more fluid. Unforced wicking occurs when the pad properties encourage fluid to redistribute and spread out within the structure. If fluid arrives very fast the superabsorber will not have time to bond with the water, effectively reducing the absorption capacity in that region, which would cause forced wicking to spread the fluid further. Conversely, if the fluid arrives very slowly there is more time for the fluid to spread further through unforced wicking before fluid application stops.

The effect of varying the total fluid volume applied is shown in Fig 8.4 where the size of the wet area, 90s after fluid application finished, is plotted as a function of fluid volume for the two products and two peak flow rates. As expected the size of the wet area increased with increasing fluid volume. Larger wet areas, for a given final volume, were measured at the higher flow-rate than the slower one, for the larger product (ms), but this effect is very slight and is not observed for the smaller product (tp).

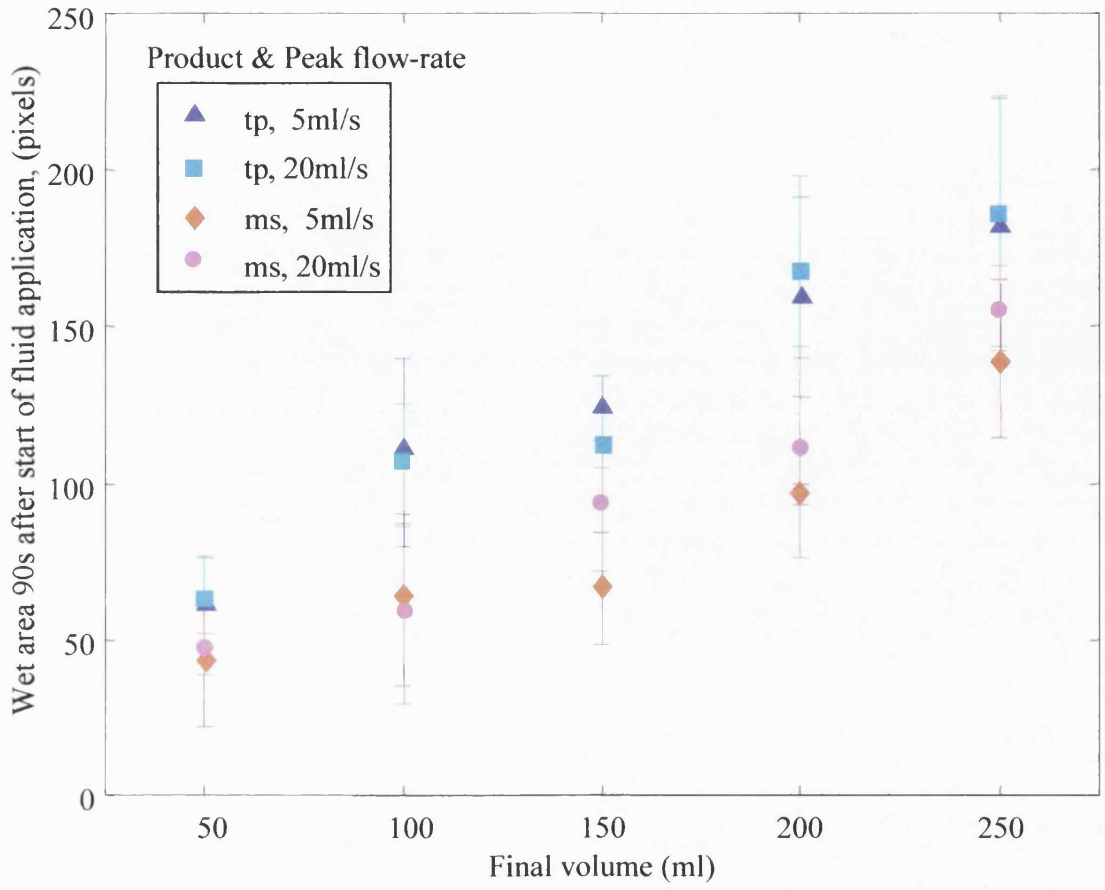

Fig 8.4 Effect of total fluid volume on two products ('tp' and 'ms'), at two peak flow-rates (5ml/s and 20ml/s)

Although both peak flow-rate and total fluid volume applied affected the size of the wet area, this occurred in a predictable manner. Because of this, and the fact that in clinical reality high peak flow-rates tend to be associated with large volumes, and low peak flow-rates with small volumes, two flow profiles were chosen for use in most other experiments. These were:

f_100_10 – 100ml total volume with a peak flow-rate of 10ml/s, and

f_250_20 – 250ml total volume with a peak flow-rate of 20ml/s.

The shape of these two flow profiles can be seen in Fig.4.21.

8.1.2 Product range & absorbency level

Before studying a lot of products it was important to estimate the range of results likely to be obtained from different products and sizes. This would aid the design of future experiments, and help to indicate which experiments were most likely to be informative.

Four product ranges of two-piece, disposable body worn pads for heavy incontinence, with three or four absorbency sizes in each range were arbitrarily chosen from products surplus to a clinical trial (Fader et.al 1998). These are described in Table.8.2 and Fig 8.5. A simplified version of the manufacturers description is used to show the composition of the pads, which had up to three layers

within the absorbent core. These are numbered so that the layer nearest to the patient is Layer 1. All the pads also had Polyethylene backing. These products were tested using the two flow-rate/time profiles f_100_10 and f_250_20 (see section 4.3.2). The absorbent pads were fitted to the curved optode holder in the standing position, with tape and stretch net pants and imaged using the optical imaging device. The fluid was applied through the central urethra. Three repeats at each flow-rate were performed with each product to test the repeatability of the results.

a	Range name: Attends Ultra care (1996)			Manufacturer: Procter & Gamble LTD		
Code	Size/absorbency	Manufactures code	Length (mm)	Max width (mm)	Min width(mm)	Weight (g)
ae	Extra	51058	540	250	135	53.6
as	Super	51392	585	285	135	73.8
ap	Super Plus	51364	585	285	135	80.7

Coverstock: Hydrophylic Polypropylene	Layer1: Curly fibres of cellulose	Layer 2: Cellulose fibres & SAP, Thicker in crotch	Layer 3: Cellulose fibres	Other: Hydrophilic standing cuffs

t	Range name: Tena Comfort (1996)			Manufacturer: SCA Molnycke		
Code	Size/absorbency	Manufactures code	Length (mm)	Max width (mm)	Min width(mm)	Weight (g)
tp	Plus	752850	565	270	140	67
ts	Super	758053	610	300	140	112
tm	Maxi	759055	610	300	140	125

Coverstock: Spunbonded polypropylene	Layer 1: Chemical – thermo mechanical pulp & SAP, concentrated in crotch area	Layer 2: Chemical pulp & SAP concentrated in crotch. Thicker in crotch	Other: Elasticated 'all round barrier'

d	Range name: Comforta Dry-form (1996)			Manufacturer: Comforta Healthcare LTD		
Code	Size/absorbency	Manufactures code	Length (mm)	Max width (mm)	Min width(mm)	Weight (g)
dn	Normal	1710	540	270	130	63
de	Extra	1711	540	270	130	80
ds	Super	1720	590	270	130	115
dp	Super Plus	1721	590	270	130	140

Coverstock: Polypropylene (hydrophilic)	Layer 1: Tissue	Layer 2: Untreated fluff pulp & SAP mixed homogeneously. Thicker in crotch	Layer 3: Tissue	Other: Elasticated leg area

m	Range name: Moliform (1998)			Manufacturer: Paul Hartmann		
Code	Size/absorbency	Manufactures code	Length (mm)	Max width (mm)	Min width(mm)	Weight (g)
mn	Normal	168 028/3	560	270	140	64
mp	Plus	168 228/1	560	270	140	84
me	Extra	168 328/1	560	290	140	100
ms	Super	168 914/1	560	290	140	152

Coverstock: Polypropylene non-woven	Layer 1: Non-chlorine bleached cellulose fluff	Layer 2: Non-chlorine bleached cellulose fluff & SAP, concentrated in crotch	Other: leg area Elasticated, extra plastic layer

Table.8.2 Products used in section 8.1.2, SAP = Superabsorber powder, absorbent layer 1 nearest to coverstock, all pads also had a polyethylene backing

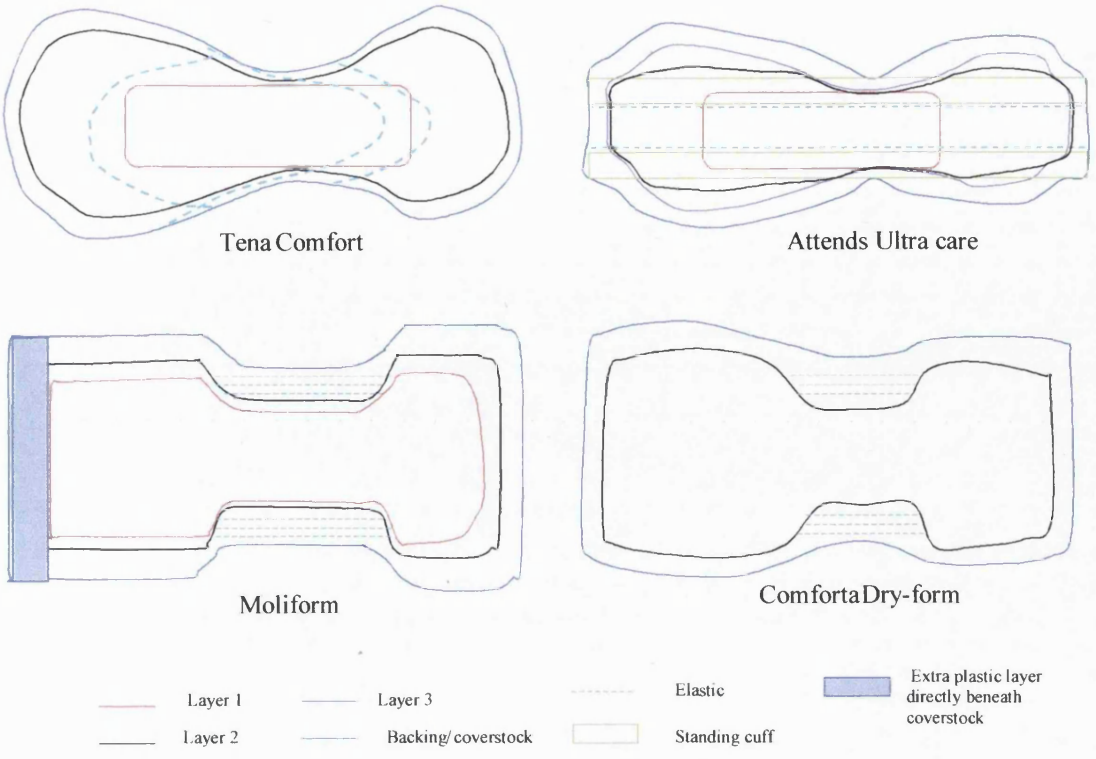

Fig 8.5 Diagrams of products used in section 8.1.2, absorbent layer 1 nearest to coverstock

Fig 8.6a shows the size of the wet area, as a function of time, for one of the products (ap). The three repeats at each flow-rate/time profile are plotted individually. Fig 8.6b shows the average intensity of the light reflected from the wet area for the same data. As expected the two flow profiles can be clearly distinguished in the wet area plot and have a spread of +/- 10-15 % between the repeats that was probably due to slight variations between individual pads due to how the constituent fibres clump together and the precise thickness of the pad. The spread between repeats was of this range for most of the product sizes and ranges used as can be seen in Fig 8.7, which shows area/time plots for all the products tested. Where a greater variation is seen this is probably because, with this small number of repeats, a rogue pad would greatly increase this spread, as probably happened with products 'as' and 'ms'. Fig 8.8 shows intensity/time plots for these same products. The average intensity data are less consistent between repeats than the area measurement due to being more sensitive to factors such as the precise orientation of fluff-pulp fibres within the product. The difference between the flow profiles was less marked although the larger fluid volume generally exhibited the lower average intensity due to greater saturation of the wet area. The slow increase in the average intensity of the wet area, after wetting had finished, may indicate the fluid was spreading out and the distribution becoming more even.

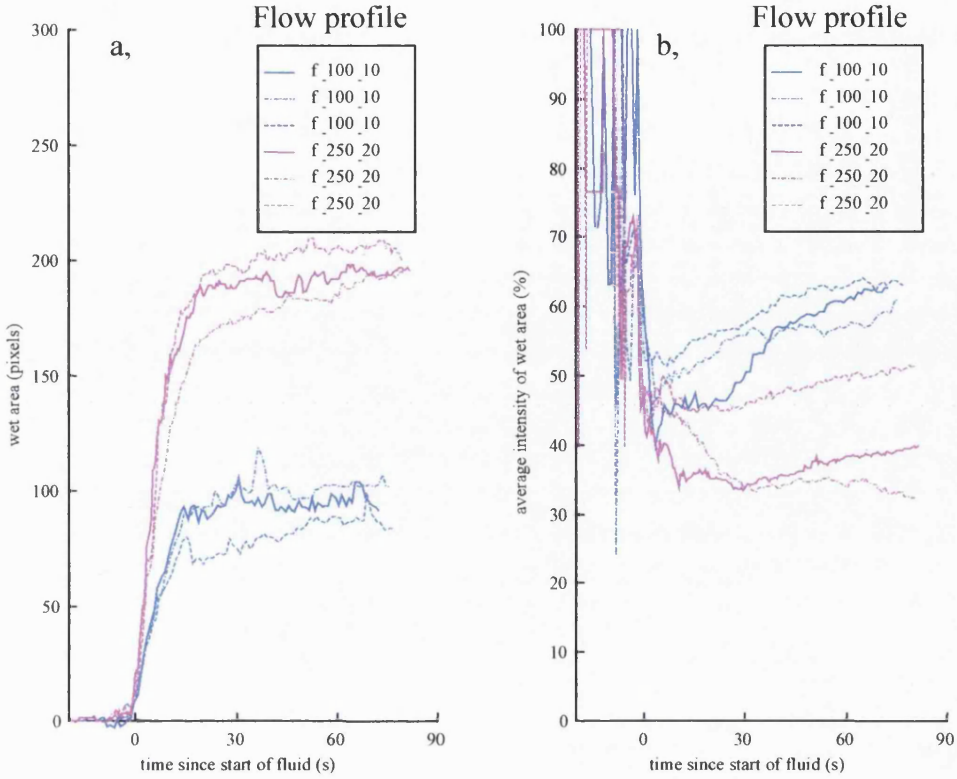

Fig 8.6 Typical wet area/time (a) and intensity/time (b) plots for one product

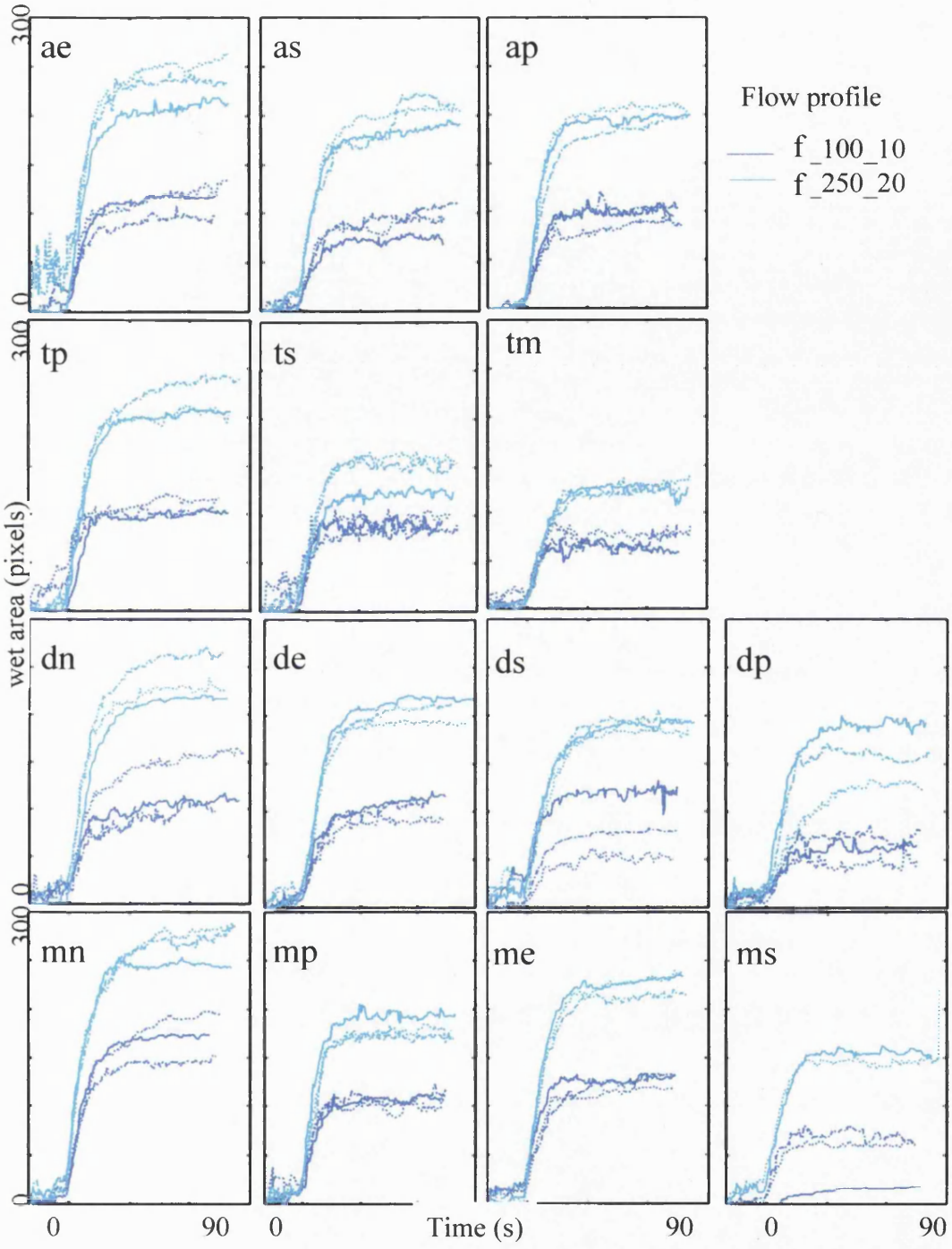

Fig 8.7 Wet area/time plots for all the different product ranges and sizes

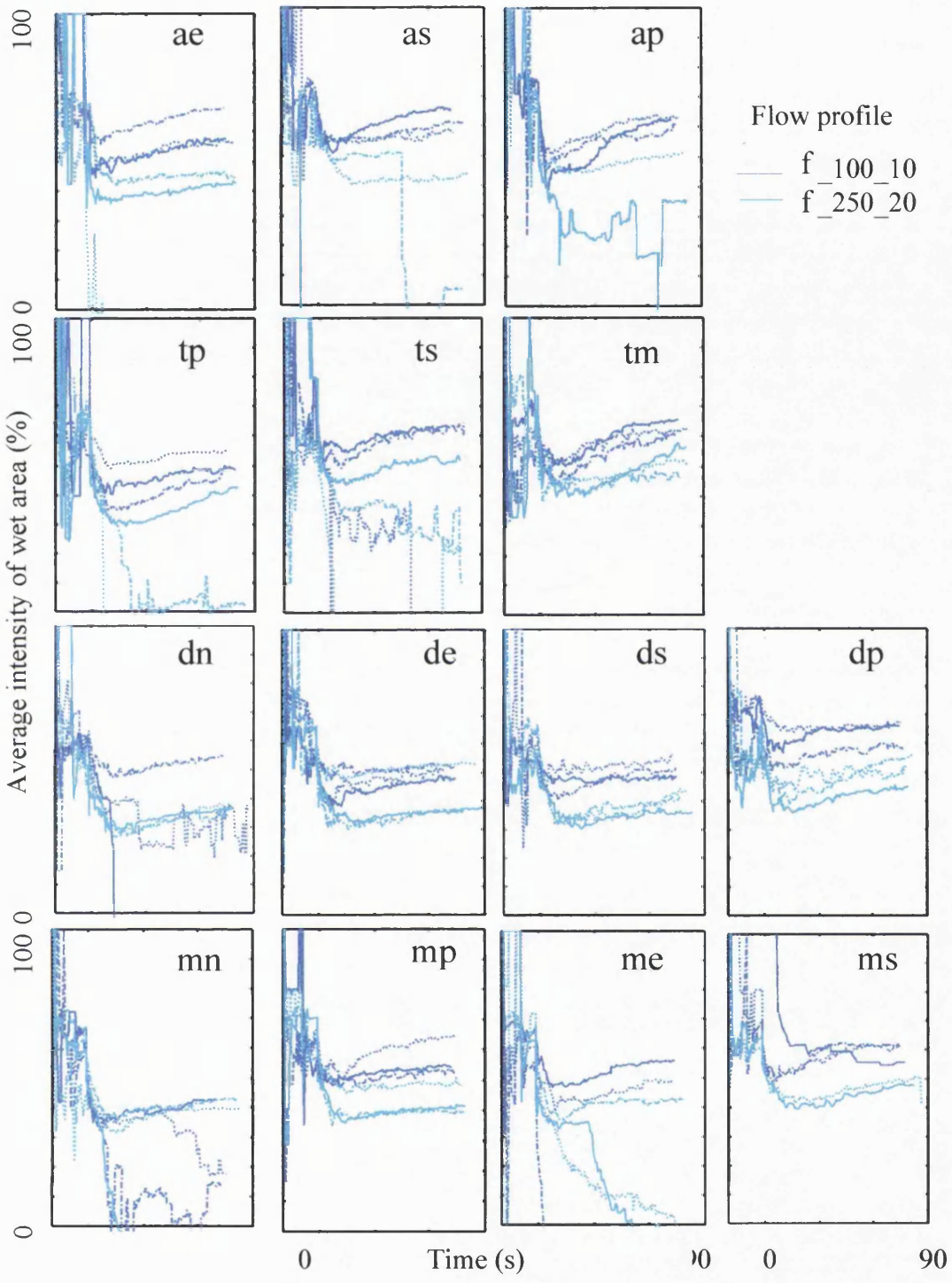

Fig 8.8 Intensity/time plots for all the different product ranges and sizes

The four product ranges are compared in Fig 8.9 in which the average final wet area for each absorbency level, for each product range, is plotted as a function of the dry pad weight, for the two flow profiles. Error bars of plus/minus one standard deviation are included. The average absorption capacity of each product (as measured according to the ISO standard, International Standards organisation, 1996) was used as an indication of product 'size' for the purpose of this figure because every manufacturer's definition of product size is different. Characteristic difference can be seen between both product sizes

and product ranges, with the same trends being seen with both the flow profiles. For example, pad range 't' had the smallest wet areas of all the products for f_250_20 and range 'm' had a smaller wet area in the second size than the third.

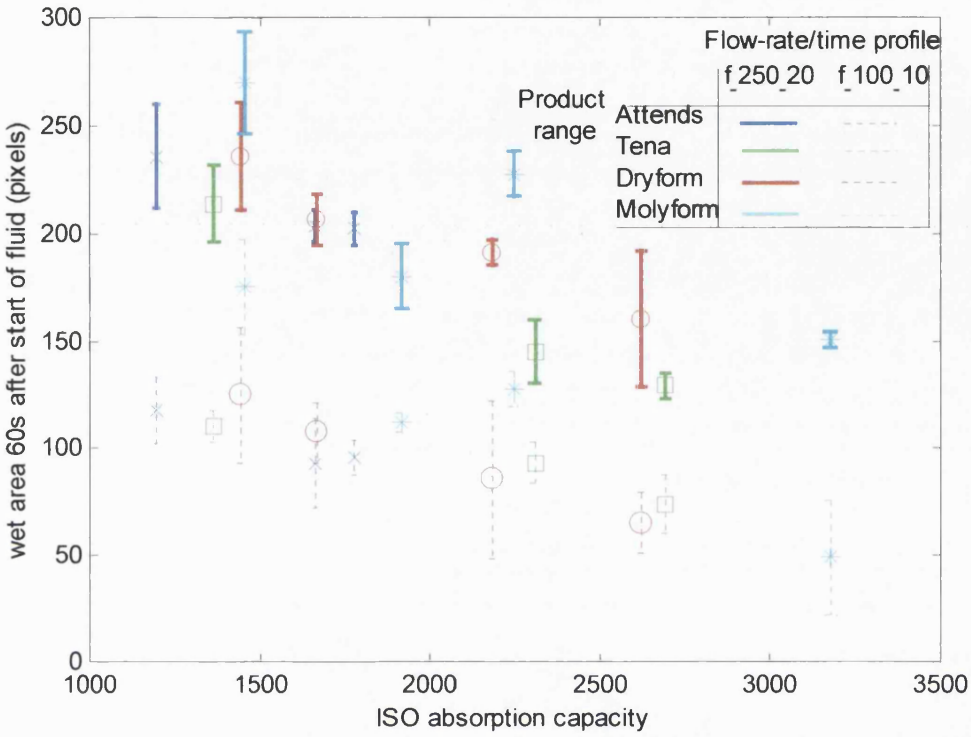

Fig 8.9 Final wet areas for four product ranges.

Studying all the sizes within a number of product ranges yields two types of information, information about the relative performance of the products within one range and information about the differences between the ranges.

The relative performance of products within one range:

In this case the basic composition of all the products is the same; for example, all the pads contain the same fluffpulp and have the same coverstock material. However, they will vary in the size and quantity of these components that they contain. In three of the four ranges studied these variations yielded an approximately linear relationship between the final wet area for 250ml of fluid and the absorption capacity, as shown in Fig 8.9. In the fourth case ('m'), however, the second size pad showed considerable deviation from the trend. Clinical data (Table.8.3) for this product range also revealed that this product had a lower leakage performance than would have been predicted from the performance of the other sizes and its own absorption capacity, being lower than the previous pad size. This information suggested that product designers from that company should look at the relative composition of their products to ascertain the reason for this. If the anomaly had been to the other side of the trend line this would have probably indicated that this product had a superior composition, information that could have been used to improve other products within the range.

Product	Percentage of pads not leaking at all for:		Percentage of pads not leaking a lot for:		ISO absorption capacity (g)
	100g	250g	100g	250g	
Normal	70	58	91	80	1456
Plus	83	55	92	81	1916
Extra	44	42	78	75	2249
Super	93	92	96	96	3176

Table.8.3 Clinical leakage performance of Molyform pads as measured by Fader et al (1998)

Differences in performance between different product ranges:

Comparing ranges rather than individual products has the advantage of removing the difficulties of comparing products of slightly different sizes. In Fig 8.9 it can be seen that the trend line for each product has a distinct gradient and intercept. However, as these four products exhibited very similar leakage performances in the clinical trial (Fader et.al.1998) it is unsurprising that no firm conclusions can be drawn in this case. This plot is only one of many that could be produced; other possibilities included wet area, wet length or increase in wet area after cessation of fluid flow (for a range of flow profiles) which could be plotted against dry pad weight, pad thickness or absorption capacity, in any combination. Similar trends would be observed in any of these plots although they each might highlight a different aspect of product performance.

8.1.3 Repeated insult

It is common for pads to have to cope with several separate applications, insults, of fluid when in clinical use. Fluff-pulp tends to collapse when it becomes wet whereas superabsorbers swell, blocking pores in the structure. This latter is known as 'gel blocking'. Due to these structural changes occurring within a pad following the first insult, fluid is likely to be distributed differently on later insults than the same amount of extra fluid applied at the time of the original insult would have been. To test the performance of pads under conditions of repeated fluid insults, three flow regimes were designed as detailed below and shown in Fig 8.10.

Regime 1. Three insults of f_100_10, starting 5 minutes apart.

Regime 2. Three insults of f_100_10, consecutively without a break.

Regime 3. One insult of f_300_10.

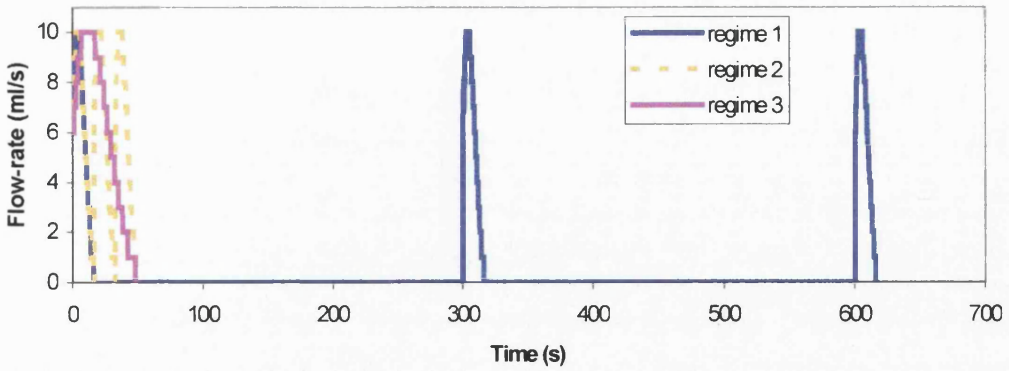

Fig 8.10 Flow regimes 1, 2 and 3

The last flow regime has the same peak flow-rate and total fluid volume as the previous two but a slightly higher mean flow-rate. Whilst the first two regimes allow the effect of insult separation to be studied, the third regime was included so that the effect of continuous flow could be compared with the intermittent fluid application used in regime 2. A separation time of five minutes between insults was chosen for regime 1 as the area/time and intensity/time traces for most experiments reach a plateau by this time. Although not clinically realistic, a longer time was not used in order to avoid excessive amounts of data being collected.

Two products were chosen from the previously used range of two-piece disposable products (see Table.8.2). These were 'tp'- a small product - and 'ms'- a large product from a different range. For each product/flow regime combination, three pads were imaged using the optical imaging device with the curved optode holder in the standing position. Fluid was applied through the central urethra.

Fig 8.11a shows area/time traces for each of these experiments. All repeats of a product/flow regime combination are shown in the same colour. The start times of the second and third insults are shown for regime 1. Fig 8.11b shows the average intensity of the wet area as a function of time for the same data.

Fig 8.12 shows the average size of the wet area after each application of 100ml insult of fluid (approximate for regime 3, because of the accuracy with which a continuous, fast, flow can be subdivided) as a function of product and flow regime. Error bars are shown of height +/-1 standard deviation, calculated from each set of three repeats.

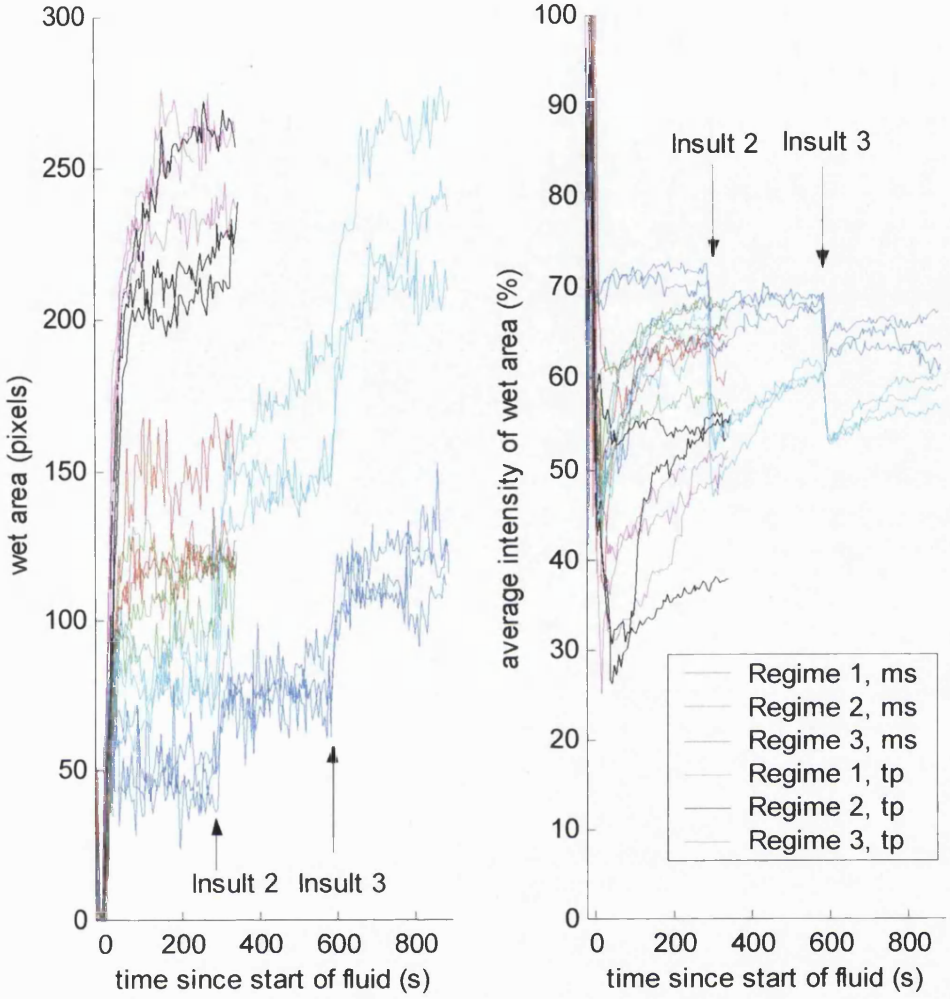

Fig 8.11 Wet area/time and intensity/time plots for two products ('ms' and 'tp') and three flow regimes

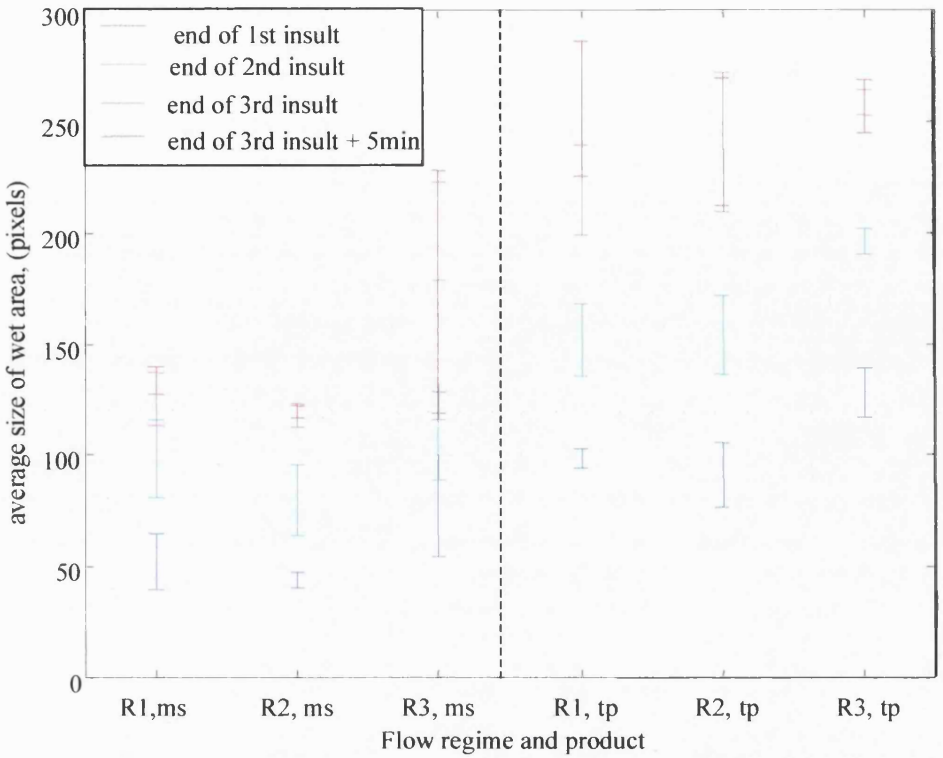

Fig 8.12 Average wet area for each product ('ms' and 'tp') and flow regime (R1, R2, R3)

For both products each insult of flow regime 1 can be easily distinguished in Fig 8.11, affecting both the size and intensity of the wet area, increasing the former and decreasing - at least initially, -the latter. The individual insults of regime 2 cannot be easily distinguished and there is little difference between these traces and those for regime 3. However, for all the regimes a larger wet area and lower light intensity are seen with the thinner of the two pads –'tp'.

With these two products there was little difference between the final wet areas produced by the different flow regimes, as shown in Fig 8.12. Also, from this plot it can be seen that only for regime 1 did the wet area continue to increase significantly after the end of fluid application. Having a gap between the insults slightly increased the size of the wet area, as can be seen by comparing the results for regimes 1 and 2. Whilst the faster average flow-rate of regime 3 resulted in the largest wet areas. Although these effects are small for these products, it is likely that experiments of this nature would be informative in products where gel blocking occurs. This is where the superabsorbant powder within the product swells after the first insult and impedes the absorption of further fluid at that location.

Whilst the above plots (Fig 8.11a and Fig 8.11b) clearly show the changing size and intensity of the wet area they do not show how this changes in shape. Fig 8.13 shows this in two different ways. Fig 8.13a is a series of three images, showing the wet area after each insult of flow regime 1 for product 'tp'. Fig 8.13b shows the intensity of a single column of optodes as a function of time, for the same experiment. Unfortunately a number of optodes failed to function in this experiment, including one, close to the fluid entry point.

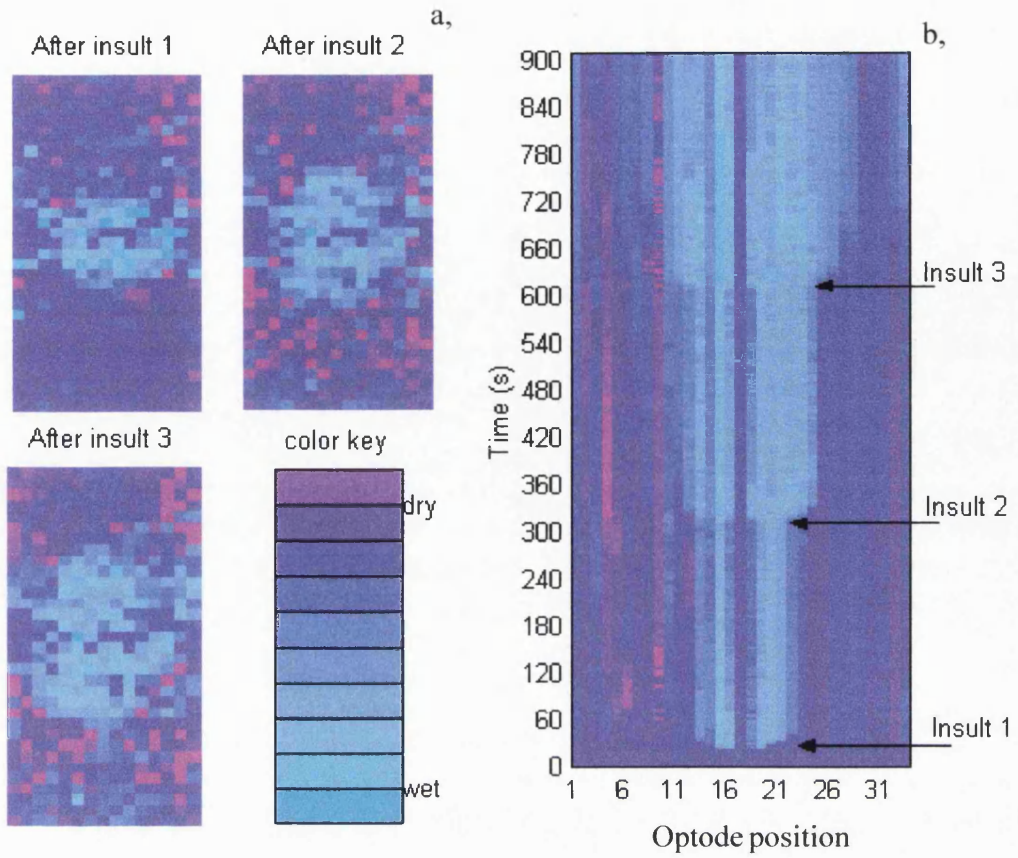

Fig 8.13 a, Image of pad 'tp' at end of each of the three insults of flow regime 1 b, Central Column

In Fig 8.13b each insult is marked by an immediate decrease in intensity (brighter blue colour) of some of the wet optodes and a slightly slower increase in the number of optodes measuring wet. Although this pad did not leak, the third image of Fig 8.13a shows the wet area extending to the right hand edge of the image, which was also the edge of the pad. This may indicate that the pad was on the point of leaking at this point.

8.1.4 Orientation

Pads do not only need to function in a sitting/standing position. This, in fact, is probably the least demanding geometry a product has to face as gravity draws the fluid into the cup-shaped crotch of a pad, away from the sides. Night-time pads, in particular, have to cope with insults when worn by someone lying on their back or side, encouraging fluid to drain towards one edge of the pad. Such postures could be replicated with the optical imaging equipment using the curved optode holder. The frame for this holder allowed it to be tilted forwards or backwards by any angle between -90°(as for a person lying on their back, that is, supine) and 90° (equivalent to a person lying on their front). The holder could also be rotated to represent a person lying on their side.

A series of products were imaged using the optical imaging device and curved optode holder at orientations of –90°, -45°, 0, 45° and 90° front/back rotation and lying on side. Flow profiles f_250_20 and f_100_10 were applied using the mechanical bladder, though the central urethra.

Fig 8.14 show the results for product 'me' and Fig 8.15 for product 'tp', each with flow profile f_100_10. For each orientation of the pad, a curved snapshot image of the pad is shown above a contour plot of the fluid spread. In no case did the pad lead.

The curved snapshot images show the approximate orientation of the product and the final wet area for each experiment. The front right-hand cornet of the pad is marked 'F' in each image.

The contour maps show the outline of the wet area as a function of time for the same data. The front right-hand corner of the pad is at position [0,0] in each image. The fluid can be clearly seen to follow gravity. In each image, using the fluid entry point as a reference, observe that the fluid spreads preferentially in the direction of gravity, resulting in up to a five-pixel (62.5mm) shift in position between supine and upright postures. The even distribution in the 'upright' case is due to the fluid entering the pad at the lowest point anyway. With product 'me' the side posture shows a little more noise than other positions, particularly at the ends of the pad, and the process of drawing the contours has highlighted this.

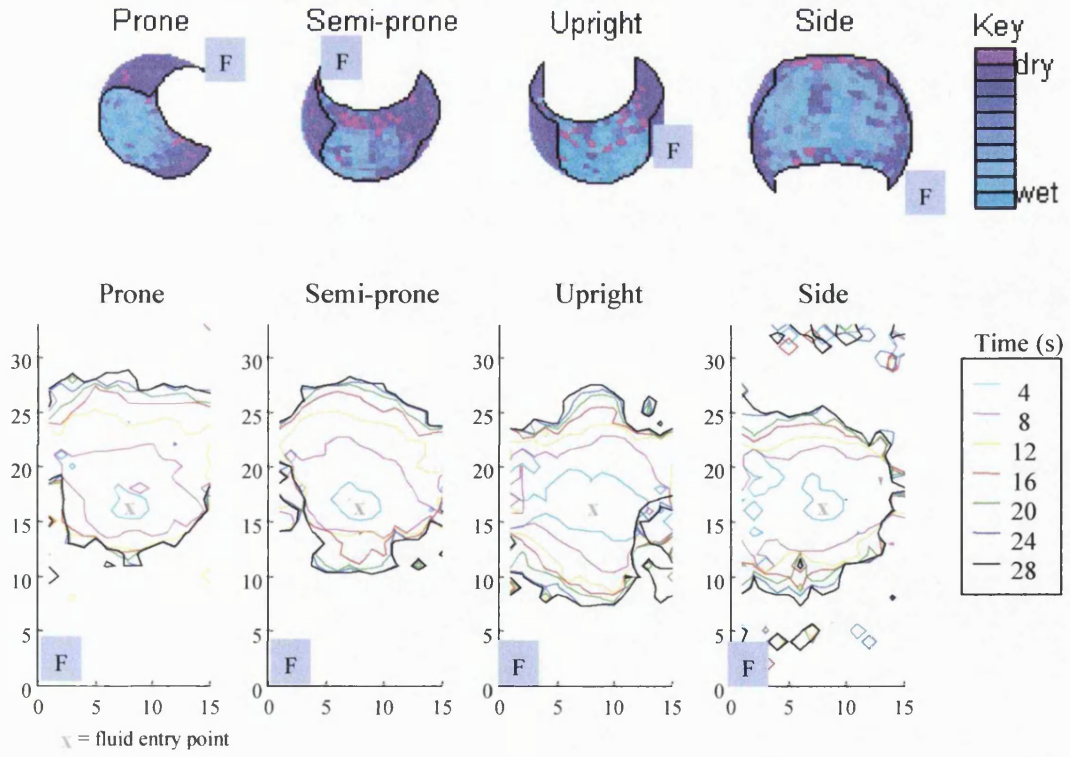

Fig 8.14 Curved snapshots and contour plots of the product 'ms' in different postures.

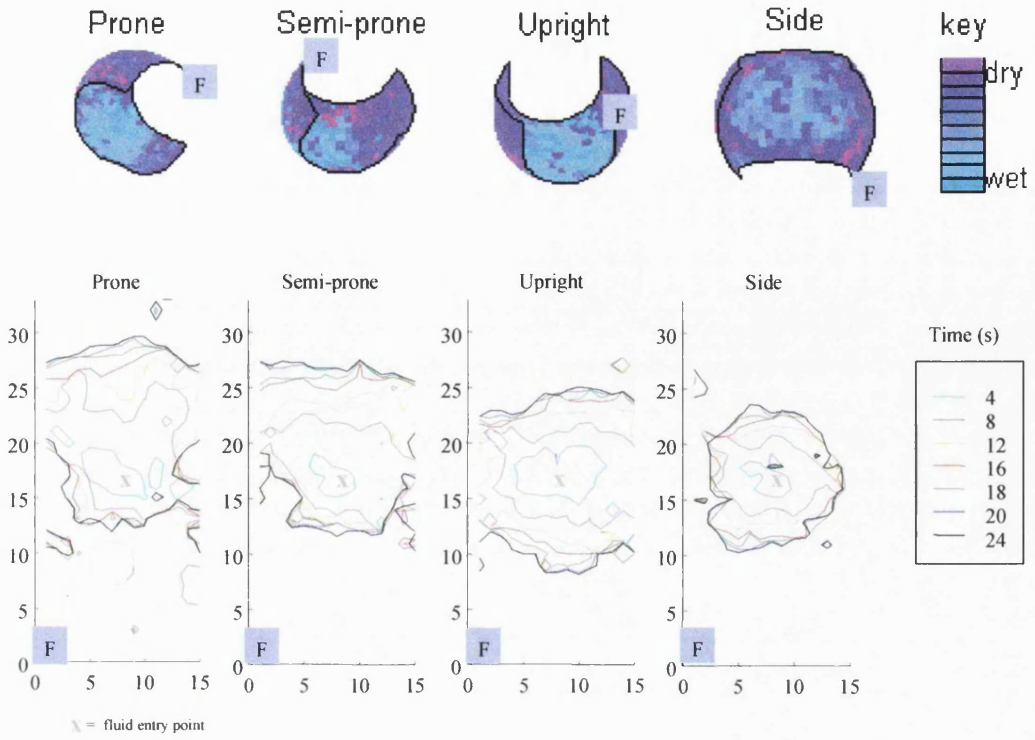

Fig 8.15 Curved snapshots and contour plots of the product 'tp' in different postures.

8.1.5 Entry point

Although, for most experiments, the simplest case of fluid entering the pad at the lowest point of the curved optode holder was used, this is not the clinical reality. For this reason, the curved optode holder is fitted with three urethras.

The mechanical bladder was used to apply fluid to a product through the third of these urethras. This was angled at 45° from the centre of the hemispherical part of the curved optode holder, as described in 6.2. The flow profile f_250_20 was used in conjunction with product 'me' (see Table.8.2) with the optode holder oriented in the normal, standing, posture.

Results from this experiment were compared with data from an otherwise identical experiment that used the first (0°) urethra. These results are displayed in Fig 8.16 as a pair of contour images (front right hand corner at position [0,0]. The final distribution of the fluid (outermost/black contour line) for the angled urethra was only slightly shifted in comparison with the normal urethra. This shift was much less than the difference in original entry point, as shown by the grey cross, and indicated that gravity is a more significant factor than the entry point of the fluid.

This result shows a very similar effect to that of orientation (Fig 8.14), the fluid tending to flow to the lowest part of the pad. However, the fluid was arriving at a different point relative to the pad crutch and this may have had an effect on leakage performance for some products. For example, due to fluid arriving at a wider area of the product, performance could be improved, or conversely, the performance could be reduced because of the absorbent layer being thinner at that point.

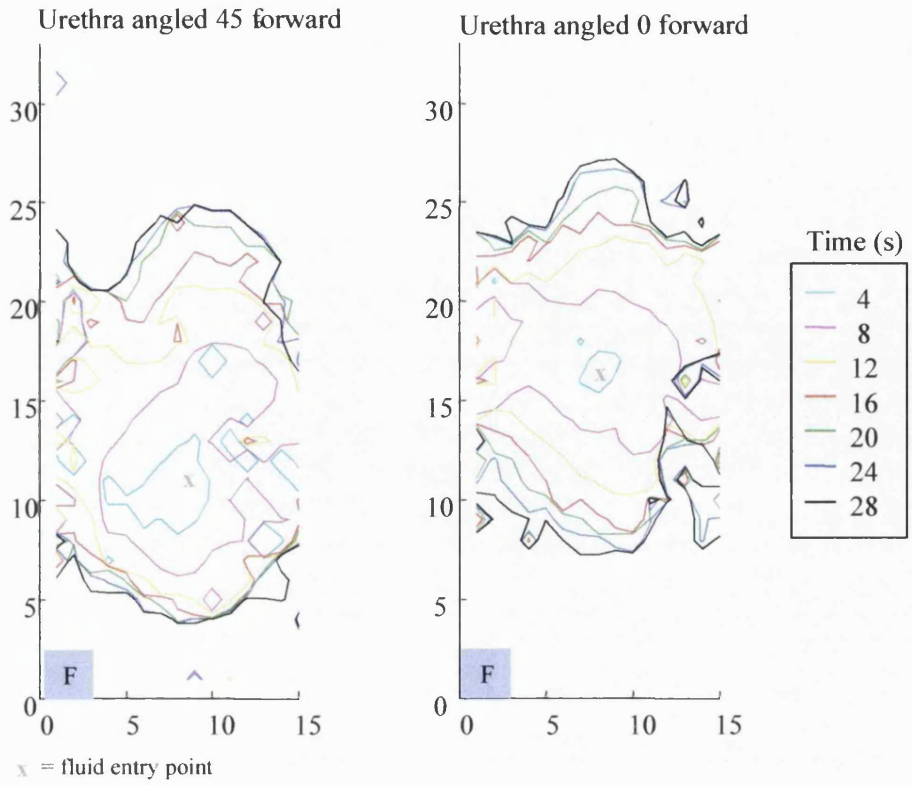

Fig 8.16 Contour plots of product 'me' showing effect of fluid entry point.

8.2 Comparison between products

8.2.1 Disposable 2-piece systems

Currently extensive user trials are the only reliable way to compare the performance of product ranges, and these need large numbers of testers in order to have statistically robust results. This is costly and time consuming. Six product ranges used in one such trial (Fader et al. 1998) were chosen and tested on the optical imaging device. Apart from the possibility of future blind ranking of products, which could aid buying decisions, this sort of test enables the mechanisms that differentiate pad performance to be studied.

Six products were chosen to cover the whole range of leakage performances measured in the study. Two of these had good leakage performance in the clinical study, two performed poorly and two had intermediate performance, when the whole product range was considered. The smallest size pad in the range was used to test five of these products. The second smallest size was used for the other product because this had an absorbency (as measured for the clinical trial) which matched that of the others more closely. Details of these products are found in Table.8.4 and Fig 8.17. A simplified version of the manufacturers description is used to show the composition of the pads.

b	Range name: Senset (1996)			Manufacturer: Care Shop		
Code	Size/absorbency	Manufactures code	Length (mm)	Max width (mm)	Min width(mm)	Weight (g)
ba	Day	Sen650	520	310	150	72
Coverstock: Non-woven	Layer 1: pulp insert		Layer 2: Fluff pulp with SAP concentrated in crotch		Other: Standing cuffs	

e	Range name: Abrena – Abri-san (1996)			Manufacturer: Bambo (A/S)		
Code	Size/absorbency	Manufactures code	Length (mm)	Max width (mm)	Min width(mm)	Weight (g)
ea	Plus	9078	575	250	150	63
Coverstock: Polypropylene (hydrophilic)	Layer 1: EC-fluff (long fibres) non-chlorine bleached		Layer 2: EC-fluff (long fibres) non-chlorine bleached		Other :	

j	Range name: Moliform (1996)			Manufacturer: Paul Hartmann		
Code	Size/absorbency	Manufactures code	Length (mm)	Max width (mm)	Min width(mm)	Weight (g)
ja	Normal	168 028/3	560	270	140	64
Coverstock: Polypropylene non-woven	Layer 1: Non-chlorine bleached cellulose fluff		Layer 2: Non-chlorine bleached cellulose fluff & SAP, concentrated in crotch		Other: leg area Elasticated, extra plastic layer	

a	Range name: Attends Ultra Care (1996)			Manufacturer: Proctor & Gamble Ltd		
Code	Size/absorbency	Manufactures code	Length (mm)	Max width (mm)	Min width(mm)	Weight (g)
aa	Extra	51058	580	250	135	53.6

Coverstock: Hydrophylic Polypropylene	Layer1: Curly fibres of cellulose	Layer 2: Cellulose fibres & SAP, Thicker in crotch	Layer 3:Celulose fibres	Other: Hydrophilic standing cuffs

q	Range name: Humancare (1996)			Manufacturer: Humancare Ltd		
Code	Size/absorbency	Manufactures code	Length (mm)	Max width (mm)	Min width(mm)	Weight (g)
qa	Day	H352	520	270	150	63
Coverstock: Spunbonded polypropylene	Layer 1: Single layer with SAP mixed throughout core. Core thicker in crotch.				Other : Elasticataion at legs	

u	Range name: Tendercare (1996)			Manufacturer: Tanner Brothers		
Code	Size/absorbency	Manufactures code	Length (mm)	Max width (mm)	Min width(mm)	Weight (g)
ub	Day Plus	420575	570	250	130	77
Coverstock:	Layer 1: Unbleached and CTMP fluff pulps & SAP (uniform distribution)		Layer 2: Unbleached fluff pulp & SAP (uniform distribution)		Other: Standing cuffs, elastication at legs	

Table.8.4 Products used in section 8.2.2, SAP = Superabsorbant powder, absorbent layer 1 nearest to the coverstock., all the pads also had a Polyethylene backing

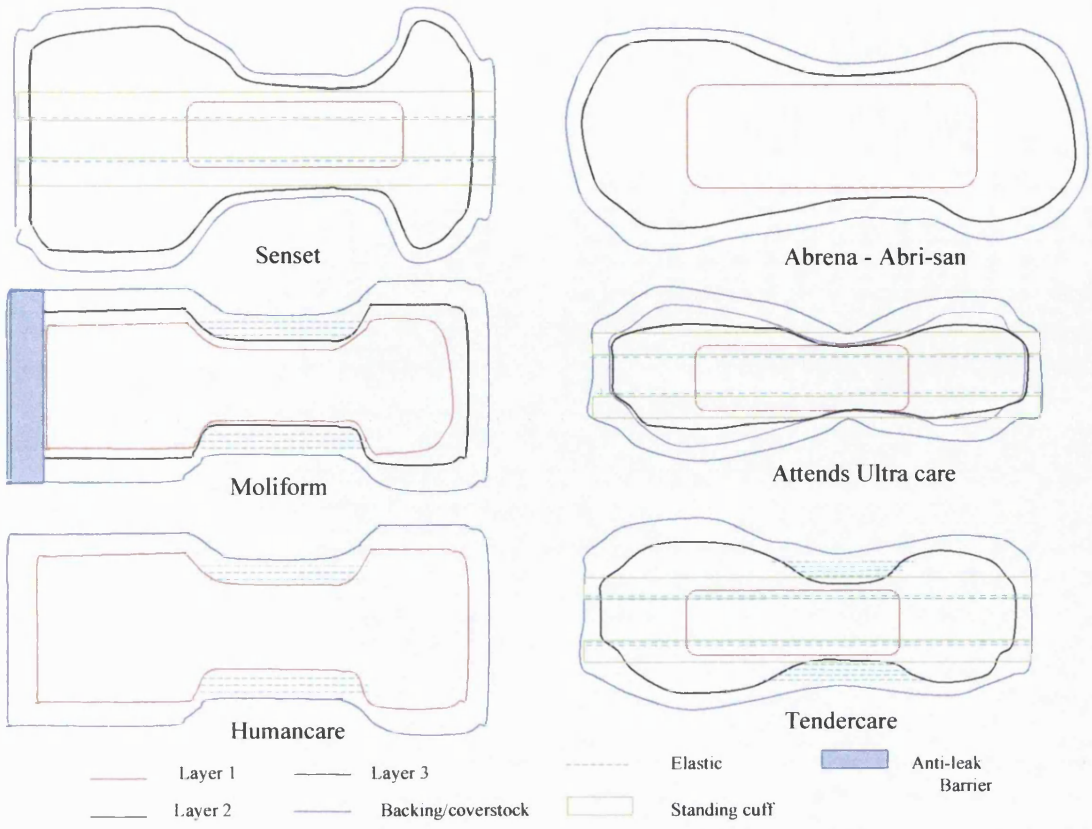

Fig 8.17 Diagrams of products used in section 8.2.2, absorbent layer 1 nearest to coverstock

The products were tested with two flow-rate time profiles, f_250_20 and f_100_10, in standing, supine and side postures, using the curved optode holder with the central urethra and the optical imaging device. Repeated insult tests were also carried out using three insults of flow profile f_100_10 with three minutes between the starts of consecutive insults. All experiments were repeated three times.

Looking for trends in the results proved difficult partly because there are so many ways in which the clinical data could be used for the ranking of pads. This is illustrated in Fig 8.18 where three different clinical measures of performance, obtained from the user trial, are plotted for the six products. These clinical measures are defined as follows:

The percentage of pads not leaking at all at 100g, for that particular pad type.

The percentage of pads not leaking at all at 250g for that particular pad type.

The percentage of carers who considered, after a week's use, that the leakage performance of the product was good or acceptable.

The first two of these clinical measures were calculated from a linear logistic regression modal fitted to the clinical leakage performance data. The third measure, carer's opinion, was the average score given to the leakage performance of the pad when the carer filled in a questionnaire after a week's use of the pad.

As can be seen from Fig 8.18 each of the measures ranks the products in a different order with respect to their performance. However, comparing the product against its measured performance

(percentage of pads not leaking at 100g/250g) is likely to be more reproducible than the subjective opinions of the user, which may be influenced by many other factors such as the length of time the pad had been on and even the mood of the carer that day.

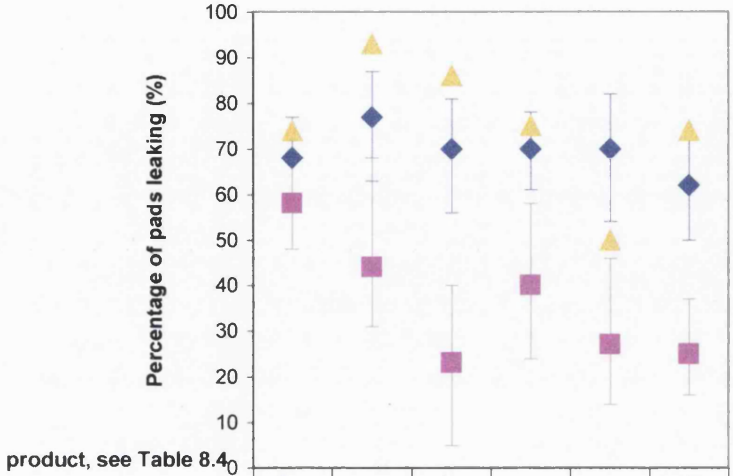

	ba	ea	ja	aa	qa	ub
◆ % pads not leaking at 100g	68	77	70	70	70	62
■ % pads not leaking at 250g	58	44	23	40	27	25
▲ Carer opinion	74	93	86	75	50	74

Fig 8.18 Variation in product ranking as a function of three clinical measurements of performance (error bars, 95% confidence intervals)

Fig 8.19 compares the length and size of the wet area for the six products with the curved optode holder held in the supine position, i.e. lying on its back, while three fluid insults were applied each of flow profile f_100_10. Each product is represented by a bar whose height represents the length (Fig 8.19a) or size (Fig 8.19b) of the wet area. The colours on the bar represent different times, e.g. by 260s the wet area reached the top of the yellow portion of the bar. Fluid application started at 20s, 200s and 380s, continuing for approximately 17s in each insult.

Wide variation between the products can be seen in the rate of growth of the size of the wet area as well as the final length (along the long axis of the pad). For example product 'ja' had a much larger wet area at the end of the first insult than product 'qa' but the difference was much reduced by the end of the third insult. It is also informative to note that neither product 'ea' nor 'aa' showed an increase in wet length upon the application of the third fluid insult. It is likely that these trends are due to differences in the wicking properties of these pads, for example due to the properties of the fibres and the relative thickness of the absorbent layers in the pads.

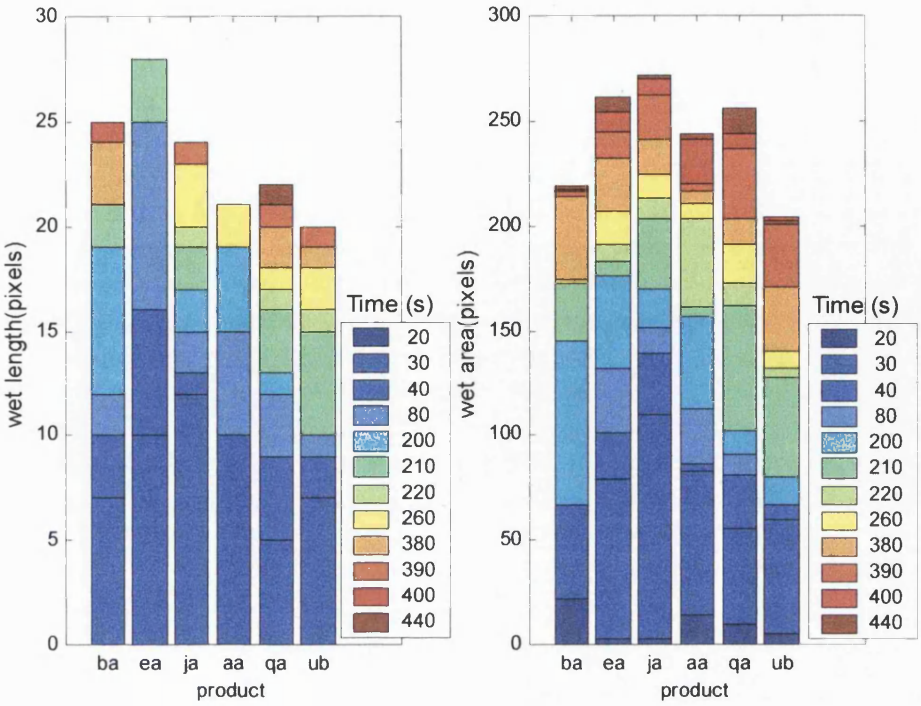

Fig 8.19 Performance of six products worn in the supine posture, which received three fluid insults
a, Length of wet area as a function of time b, Size of wet area as a function of time

Fig 8.20 shows the average length of the wet area at four times for a single insult of 250ml of fluid into each of the six products when worn in the standing position. Each experiment was repeated three times and the results averaged. These lengths have been plotted against the percentage of pads not leaking at all at 250g (p250), as found in the clinical trial. A linear trend line has been added for the final time. This has a gradient of 0.016 pixels/% and a coefficient of correlation of 0.89. However, as the error bars (plus/minus one standard deviation) are as large as the slope of this line, more data is needed before this can be considered a reliable trend.

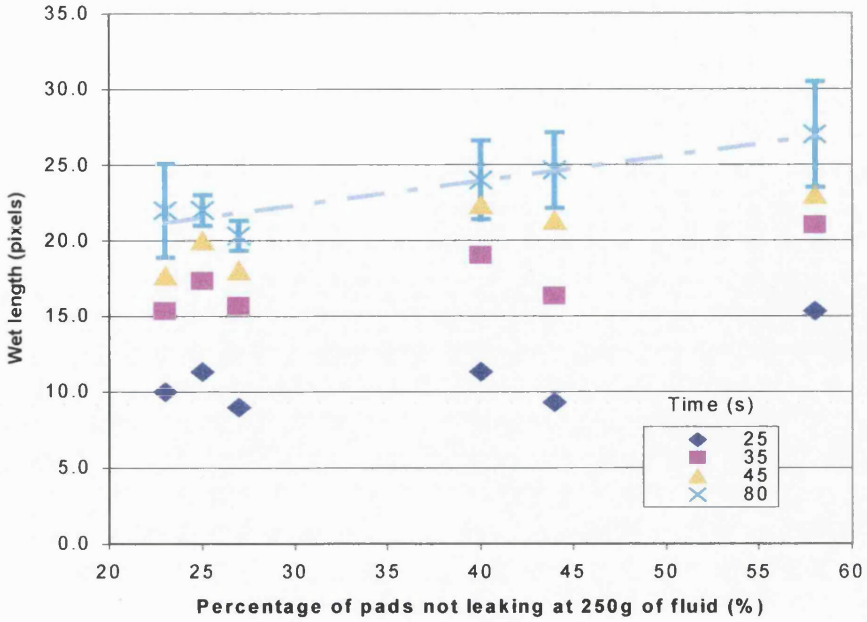

Fig 8.20 Length of wet area of 250ml insult at various times as a function of clinical leakage performance of pad, for standing posture

This particular graph (Fig 8.20) is plotted because, of all the permutations of clinical measure and laboratory measure that were tried, this yielded the most plausible trend line.

Since no better linearly correlating measure was obvious, it is likely that pad performance is determined by a number of factors whose effects combine to contribute to the clinical performance. For example, it can be hypothesised that wet area is a function of resistance to fluid flow, wicking ability and superabsorber content. Although these six products showed a wider spread in clinical performance than those used in section 8.1 it is likely that product size variations affect these results. If all product sizes in each range were studied the effect of size could probably be separated out from other factors affecting the performance of the pads.

8.2.2 Reusable products for light incontinence

The optical imaging system is not restricted to use with disposable products. When used with the curved optode holder any body worn product can be assessed and the original, flat, laboratory holder can be used to assess bed and chair pads.

A reusable product for light incontinence was assessed on the equipment (Kilie Lady, super (100ml) absorbency, hips 122-132cm, ref. 0192724G, from Simcare Ltd.). The product was placed on the curved optode holder and held in place with stretch net pants because the hip-size available was too big to fit the optode holder unassisted (the circumference of this being 74cm at the top). The mechanical bladder was used to apply flow profile f_100_10 to the product.

Fig 8.21a shows the final fluid position as measured by the optical imaging device. It should be noted that the pad leaked by 49g - about half the fluid applied - and so only about 50g of fluid

contributed to this image. For comparison, Fig 8.21b is the final fluid position for a small disposable product (tp, see Table.8.2) that had received one insult of flow profile f_050_20. Taking the small volumes involved into account the images obtained show similar fluid spread. This result demonstrates that the techniques applied to disposable products can also be used for the study of reusable products.

Further work indicated that a small subset of the non-woven materials used as the absorbent component of reusable pants show no visible change in optical performance upon wetting. Although this technique cannot be used to study these materials, the technique is still a valuable tool in the study of most products.

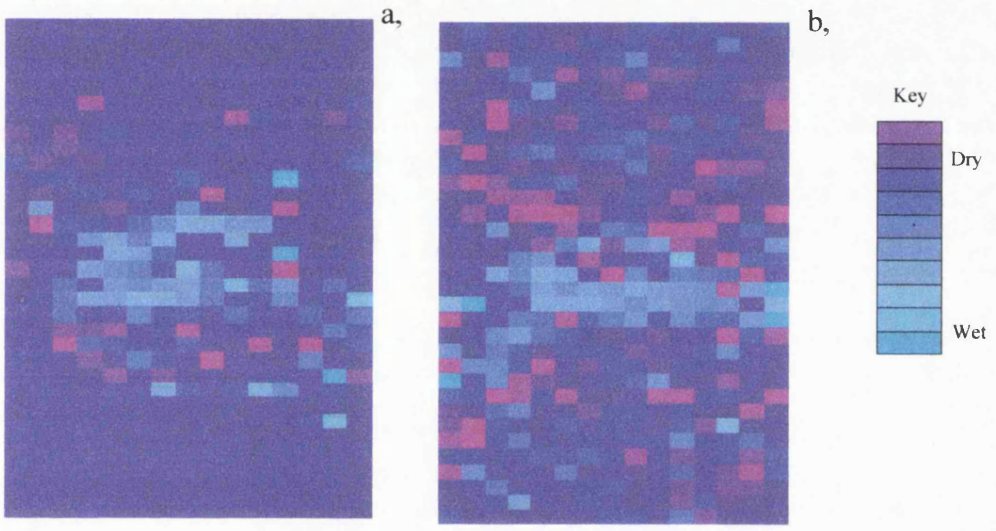

Fig 8.21 Comparison between images of reusable and disposable pads after 100ml insult:

Fig 8.22 a, Small reusable pant b, Small disposable pad

9: Discussion and Conclusion

9.1 Discussion

As stated in chapter 3, the aim of this thesis was 'the development of instruments/techniques capable of plotting the distribution of urine in absorbent materials in real-time, in both the clinical and the laboratory setting'. Although, at the end of this thesis this aim has not been fully met, much progress has been made on many of the aspects and an understanding of the limitations and difficulties present in studying materials of this nature has also been obtained. These areas of progress and identification of difficulties fall broadly into two categories, those relating to the imaging/data collection method and those relating to the usefulness of imaging in the study of incontinence products.

Looking first at the imaging equipment developed during this project, an imaging system has been developed, mainly for laboratory use, which uses optical sensors to detect the fluid distribution within pads. The system can be used in a range of clinically realistic positions and, unlike resistive sensors, does not disrupt the structure of the pad. The equipment is suitable for routine use, providing information on the current fluid distribution every 0.5s, without producing excessive amounts of data. Data processing and display routines have been developed that display the results in a range of clear formats, dependent on which aspect of the information it is most informative to highlight.

Although this equipment is a valuable addition to current product testing equipment, this system has a number of weaknesses, not all unique to this technique.

Like other pad imaging techniques this equipment images one (curved) plane of the pad. This means that fluid distribution information is not obtained for the whole volume of the pad, only for the 3-4mm closest to the sensors. In conjunction with this point, optical sensing does not provide a direct measurement of fluid so although information about the saturation status of a pad can be gained, care is needed when interpreting the results so as not to confuse this with depth information. Also because the measure is dependent on the composition of the product, a small proportion of products cannot be studied with this technique as they exhibit an insufficient change in optical properties upon wetting.

Despite these disadvantages this technique has significant advantages over existing techniques. These advantages include the ability to provide some degree of saturation information, enabling repeated insults to be much more easily identified, both in terms of timing and area of pad affected, whereas only an increase in size could be measured with resistive imaging. The other significant advantage of this technique is that the results have been compared to clinical data and an appropriate correlation found, thus clinically validating the technique.

X-ray imaging has been found to be a complementary laboratory tool, providing much finer spatial resolution, capable of revealing the swelling of superabsorbent granules, but this is at the expense of temporal resolution and realistic pad geometries. The other advantage of X-ray imaging is that the fluid content of the pad, at each point in a 2D plane, can be directly measured.

The tailor-made fluid delivery system is compatible with all the imaging modalities used and provided a reliable method of applying a predetermined flow-rate/time profile of fluid to a pad. This flexibility and reproducibility greatly reduces the sources of statistical noise present within collected data, reducing the number of experimental repeats necessary for significant results to be obtained. This is a major advantage over user trials of products where, because very little information about the fluid insult can be gained, let alone controlled, the statistical noise on the data is very high.

In parallel with the development of laboratory imaging systems, the quantitative measurement of fluid distribution within clinically worn pads was also investigated. It was anticipated that optical imaging could be used clinically and, although this was not actually achieved, an appropriate method was developed. The major obstacle to using the optical system clinically was the need to lay optical fibers parallel to the pad but turn the light through 90° to enter the pad, without significantly increasing the size of the sensors. A method for casting miniature prisms on the ends of the optical sensors was developed which met all the criteria. However, the efficiency of these sensors did not meet expectations, resulting in reduced signal strength. There is no theoretical reason for this, but it requires improvements in the precision with which such sensors are made which could not be obtained within the cost constraints of the project. The other potential problem identified with using optical sensors in a clinical setting is their sensitivity to changes in the local pressure on the pad. Although static pressures have been measured (Allan et al 1993, Swain et al 1994) these do not give an indication of pressure changes occurring whilst a pad is sat on. This cannot be assessed without the sensor efficacy problems being resolved.

The potential for detecting repeated insults within the clinical setting is a major advantage of the optical system over the resistive system, although, unlike the optical sensors, this latter is developed to a usable stage.

The second area requiring discussion is that of the usefulness of imaging data. Product imaging provides richer information than mannequin based leakage tests helping to identify the cause of leakage as well as the location and time of the leak. Imaging also provides information about the pads that don't leak, indicating whether fluid was on the point of leaking at any location or whether there is always surplus capacity in a particular region.

Product imaging complements tests such as absorption capacity and wetback (see section 2.3) by providing information on how the product performs as a complete unit under clinically realistic test conditions as opposed to the single parameter which each of these tests assess using standard conditions that do not, usually, replicate clinical reality.

Four pad ranges and six other pads were imaged with the optical imaging device under a range of conditions. The data from these experiments, in conjunction with data from a clinical trial (Fader et al 1998), were assessed in many different ways. The resulting information indicated that characteristic differences in the dynamic fluid distribution could be identified between the different products but that relating these differences to the clinical performance of the pads was not possible using this data only. One of the main reasons for this is the large size of the confidence limits on the clinical data compared to the clinically measured differences in product performance, for example, for the smallest pad size of each range, the percentage of pads not leaking at 100g of urine varied between 52% and 84%, with one

outlying point, but the 95% confidence limits on each result were typically +/- 11. This compounded the fact that there was no definitive information about how the design of a product relates to it's clinical performance, other than the bigger it is the less it leaks.

Due to these factors, pad imaging cannot currently be used to predict the clinical performance of products. However, the equipment developed in this thesis provides valuable tools for collecting the information that would be necessary to establish such a link. In this context, this work has established that it is preferable to test all product sizes within a product range. This is because each manufacturer has their own definition of pad sizes, the absorbency of pads varying widely between ranges (e.g. the smallest size of one range may have 10% or 20% more absorbency than the smallest size of another range) but pads within a range usually vary in a systematic way allowing a trend line to be generated for each product range, such as those shown in Fig.8.12, which is a graph of wet area as a function of pad size (as measured using an absorbent capacity test). Many other performance measures could be treated in this way and the trend lines of different product ranges compared. However, although ranking products relative to their competitors would be useful, it is in the area of product development that this equipment will be extremely useful.

Very rarely will a new product be designed from scratch, it will be based on a previous design by the company. The changes made will usually be aimed at correcting a weakness that they identified in their product. Laboratory imaging of the original and prototype products enables the overall effect of the changes to be quantified - possibly leading to further design modifications. All this could be achieved with a small number of each type of prototype pad, without the need to develop them to a clinically usable stage.

Another use of the optical imaging technique is in studying the effect of user determined perimeters such as the total volume of fluid applied and the flow-rate/time profile of the fluid insult or insults as well as posture effects. Preliminary experiments have also been performed looking at these effects and identifiable trends observed.

Two main areas for further work are envisaged. The first of these has been mentioned above, that of gathering data from which to deduce the link between laboratory and clinical performance. This should be done by studying all the sizes and product ranges included in a rigorous clinical trial, such as that of Fader et al 1998. However, it should be noted that the statistical noise within the clinical data is likely to present a substantial problem and it is highly probable that clinical performance is dependent on many interrelated factors linked to the size/shape of the pad and the fluid holding/transport properties of it's constituent materials. Information from imaging and traditional pad testing methods should be utilized.

The other main area of use for the imaging techniques is in the area of product development. Valuable information would be obtained by comparing pads in which one component had been varied, e.g. the quantity or distribution of the superabsorbent powder. Using an imaging system has advantages over tests such as absorption capacity and absorption time because the interaction of the various components, which make up the inhomogeneous whole, are included so that the functionality of the complete pad is studied using realistic flow profiles and geometries.

9.2 Conclusions

Optical imaging of pads in the laboratory has been developed to a routinely usable stage and the technique validated against clinical data. This technique should be used in conjunction with the purpose built fluid delivery system so that statistical noise due to unintentional variation with the fluid flow-rate/time profile is virtually eliminated.

Pad imaging has been found to be a valuable addition to existing product testing methods with potential for use when comparing competing products and during product development.

This information can be supplemented by X-ray images, which enable flat sections of pad to be viewed at high resolution.

An existing resistive imaging system was successfully used in the clinical environment providing information against which to validate the optical technique. A clinical version of the optical imaging system was designed which sought to address the limitations of the resistive system in terms of ease of use and by providing information about the degree of wetness of the different areas of pads. The design was theoretically capable of meeting these requirements, however, a fully working prototype was not possible within the constraints of the project.

Preliminary data using the optical imaging device within the laboratory indicates that clear differences can be identified between the dynamic fluid distribution generated in different products. However, it was not possible to relate this to the clinical leakage performance of the pads using the available clinical data.

Preliminary data also shows the effect of posture, the fluid distributes within the pad so as to flow preferentially in the direction of gravity. Total fluid volume and peak flow-rate have also been studied showing that the size of the wet area increases with increased fluid volume but the effect of peak flow-rate is slight, dependant of the composition on the pad.

A1: Appendix 1

A1.1 *im*puter program written to control optical imaging device

```
                                /*      scan3b.c          */


/* Imputer programme for continual monitoring of optodes,
 storing the data in onboard memory.
The data is sent back to a computer via a serial link after the 'halt'
 button is pressed or 's1' is pressed twice : 1st to stop data collection
                                                    2nd (<5s after 1st) to start data upload*/


 /* The amount of data compression can be altered by varing the value of
'noise'.
if 'noise' is high the data is very compressed (at expense of small
fluctuations).*/


   /* to alter number of optodes:
                        alter optode number.
                        update word code mask[].
                        (update byte code norm[].)
                        check 1 reset just after capture image.
                        check define z & zz is max there is room for.*/


     /*time now in 1/10ths of seconds*/



   #include <stdio.h>
   #include <stdimp.h>              /*L25*/
   #include <timer.h>
   #include <icomms.h>
```

```
#define optno /*48*/495
//#define pixno 9
//#define pixh  (100/pixno)
#define noise 4 /*4*/
#define z 8 /*29 47*/
#define zz 2    /*should be a factor of 32768, ie. 2,4,8,16....*/
#define tflag 999
//#define mflag 888
void main(void)
{
word code mask[] = { 53177 , 55501 , 51660 , 54210 , 37323 , 38860 , 45005 , 48077 , 46541 , 54217 ,
49613 , 43974 , 41932 , 40140 , 37064 , 47304 , 56006 , 42438 , 36802 , 53194 ,
43210 , 50118 , 45768 , 47808 , 38853 , 37821 , 51654 , 40647 , 52417 , 43712 ,
48840 , 53189 , 55482 , 48827 , 54205 , 46786 , 49344 , 44992 , 39104 , 50623 ,
40896 , 41664 , 51898 , 50105 , 38329 , 41148 , 47291 , 39354 , 45497 , 43706 ,
42426 , 51355 , 49562 , 54935 , 53401 , 53651 , 45978 , 51871 , 51852 , 47518 ,
43162 , 49310 , 44958 , 41369 , 42142 , 54684 , 46495 , 43679 , 40090 , 41620 ,
36765 , 39582 , 53406 , 44698 , 50591 , 38046 , 37005 , 43150 , 50574 , 38291 ,
37273 , 55442 , 38553 , 36754 , 50324 , 48027 , 48277 , 52116 , 53901 , 46485 ,
44692 , 38285 , 45709 , 39821 , 40084 , 43157 , 47761 , 41358 , 49298 , 44431 ,
47245 , 40863 , 37984 , 45406 , 42085 , 43871 , 49759 , 55133 , 55665 , 55652 ,
51042 , 51550 , 39263 , 41054 , 46685 , 40294 , 48478 , 51562 , 46436 , 45158 ,
43628 , 48486 , 37224 , 52323 , 53343 , 46436 , 47472 , 49764 , 53859 , 42334 ,
38758 , 54632 , 40555 , 53097 , 39020 , 61642 , 22615 , 38257 , 36973 , 50544 ,
48491 , 45675 , 44401 , 43628 , 56177 , 57201 , 41585 , 55150 , 47729 , 53104 ,
53098 , 38257 , 42865 , 55862 , 52275 , 49712 , 52279 , 43058 , 46892 , 47416 ,
49208 , 36395 , 49712 , 37675 , 50497 , 40501 , 37176 , 54069 , 45114 , 43307 ,
46644 , 55085 , 56623 , 53039 , 55345 , 44597 , 48429 , 51245 , 39738 , 49709 ,
45613 , 38715 , 40495 , 40747 , 44335 , 38955 , 38704 , 47166 , 37184 , 42815 ,
```

37168 , 42031 , 41277 , 38710 , 44352 , 50237 , 48445 , 45888 , 43576 , 42294 ,
50743 , 54073 , 52545 , 54592 , 52494 , 45832 , 54804 , 38415 , 53508 , 52225 ,
44043 , 56072 , 50945 , 49664 , 44290 , 46338 , 44550 , 55045 , 51467 , 39424 ,
48394 , 46860 , 55055 , 53257 , 50960 , 56334 , 41221 , 51463 , 53268 , 49928 ,
45586 , 49423 , 36879 , 56338 , 43013 , 54794 , 45325 , 39941 , 49683 , 37632 ,
48404 , 47873 , 47887 , 46866 , 39177 , 37642 , 40457 , 51476 , 42763 , 39955 ,
44046 , 44051 , 41488 , 38675 , 14352 , 11799 , 14869 , 13334 , 16405 , 6424 ,
13323 , 7945 , 8471 , 9995 , 17675 , 5393 , 19990 , 9489 , 20496 , 7698 ,
17942 , 14858 , 11532 , 14596 , 21509 , 24075 , 15888 , 11531 , 22032 , 19217 ,
6669 , 10519 , 11026 , 23300 , 9991 , 12561 , 8708 , 20230 , 21770 , 21782 ,
7173 , 11781 , 24322 , 19467 , 16388 , 16388 , 13060 , 5131 , 23304 , 16396 ,
23573 , 8202 , 5639 , 12359 , 20037 , 17989 , 21310 , 16710 , 21059 , 12354 ,
9543 , 21306 , 13634 , 16187 , 8263 , 19263 , 17983 , 15943 , 17467 , 13639 ,
16447 , 21044 , 10306 , 11330 , 6204 , 6466 , 10295 , 18746 , 10822 , 9026 ,
14908 , 7746 , 13116 , 6727 , 5191 , 22580 , 20026 , 14390 , 5430 , 4150 ,
14912 , 19508 , 4668 , 8764 , 13111 , 16692 , 17973 , 7484 , 11580 , 10045 ,
11831 , 6455 , 10295 , 9015 , 20839 , 10858 , 4457 , 7785 , 13674 , 14435 ,
8805 , 12650 , 6505 , 7268 , 9321 , 15210 , 18024 , 16745 , 19560 , 17507 ,
11619 , 13913 , 21085 , 21090 , 19555 , 13156 , 4451 , 8289 , 19293 , 10340 ,
15973 , 15709 , 17500 , 12632 , 14431 , 10840 , 11100 , 12893 , 9567 , 22620 ,
7007 , 9305 , 8023 , 5988 , 3934 , 5727 , 3671 , 6744 , 5464 , 15703 ,
17239 , 18775 , 20055 , 21592 , 14730 , 23945 , 6280 , 7816 , 12168 , 13967 ,
9608 , 6797 , 8591 , 7834 , 18830 , 4762 , 13208 , 18569 , 17293 , 14730 ,
24462 , 20111 , 22924 , 22684 , 16522 , 15247 , 18072 , 5269 , 7827 , 16278 ,
12175 , 18067 , 17041 , 24725 , 21148 , 23448 , 22164 , 14996 , 19609 , 18588 ,
6298 , 6547 , 17053 , 15516 , 9870 , 10648 , 12940 , 9113 , 9109 , 20630 ,
10891 , 19603 , 10387 , 23186 , 6847 , 9659 , 22712 , 16567 , 24247 , 15287 ,
15811 , 14271 , 10422 , 20918 , 13499 , 11711 , 15290 , 21692 , 12475 , 13252 ,
8128 , 9411 , 19126 , 11972 , 7862 , 9143 , 6583 , 14007 , 19131 , 14533 ,
20671 , 10691 , 19907 , 18627 , 22211 , 8131 , 12991 , 22972 , 6852 , 7355 ,

```
 16831 , 10939 , 8379 , 16827 , 12470 };
   byte j, f, avet[z], /*y,*/ w;
   byte xdata *ave = (byte xdata *)0;
   word xdata *ans = (word xdata *) 0;
   word time, temp, i, l,lw[13], x, y, anst[zz], q;

   TIMER timer;
   imputer_init();

   set_main_xbank( 0 );
         set_uio(5,1);/*not max exposure*/
         set_uio(6,0);/*HLD exposure*/    /*L50*/
         set_uio(7,1);/*set gain*/
         wait(5000);
while (getkey() != 's')
{
}

         set_uio(7,0);/*agc off*/

/*set_main_xbank( 1);
capture_image( GB_STANDARD);
upload_image(1,0,256,256,DT_IMAGEGS);*/

   time = 0;

         y=0;
         x=0;
         w=2;
```

```
for (i = 0; i <optno; i++)
        { ave[i]=0;
        }
for (i=0; i<z; i++)
        { avet[i] = 0;
   }

set_main_xbank( 1);

start_timer( &timer, T_MSECS, 0);
while ( !halt() && !UIO2 )
{
        f=0;
   capture_image( GB_STANDARD);

 /*l = 0;*/ (optno - z);
 for(i=0; i<optno; i++)  /*L75*/
 {  if ((i==0)||(i==(l+z)))
          {      set_main_xbank(0);
                 for (j=0; j<z; j++)
                  {  ave[l+j] = avet[j];
                     avet[j] = ave[i+j];
                  }
                 l = i;
                 set_main_xbank(1);
           }
                 temp = 0;
                 for (j=0; j<3; j++)          /* pixels -> optode */
                 {       temp += XBYTE[mask[i]+j];
                         temp += XBYTE[mask[i]+256+j];
```

```
            temp += XBYTE[mask[i]+512+j];
}
temp = (temp/9/*norm[i]*/);
                                                    /*compression*/
if (((temp - avet[i-l]) > noise)&&((temp-avet[i-l])<(65536-noise)))/* if sig diff*/
{    avet[i-l] = temp;
    if (f==0)
          {
           if (y > (zz-2))
           {set_main_xbank(w);      /*L100*/
           for (j=0; j<y/*10*/; j++)              /*prob?*/
                  { ans[x+j] = anst[j];
                  }
           x += y;
           y=0;
           if (x>(32768-z))
                  {lw[w-1] = x;
                   w += 1;
                   x=0;
                  }
            if (w == 14)
                  {//go to end
                  }
           set_main_xbank(1);
           }
          anst[y] = tflag;/*65535;*/
          y +=1;
          anst[y] =  time;
          y +=1;
       f = 1;
```

```
                    }
                    if (y > (zz-2))
                    {set_main_xbank(w);
                    for (j=0;j<y;j++)
                      {ans[x+j] = anst[j];                    /*L125*/
                      }
                    x += y;
                    y = 0;
                    if (x > (32768-z))
                    {lw[w-1] = x;
                     w += 1;
                     x=0;
                    }
                    if (w == 14)
                    { /* go to end*/
                    }
                    set_main_xbank(1);
                    }
                anst[y] = i;
                y +=1;
                anst[y] = /*q*/avet[i-l];
                y +=1;
              }
              }
/*time*/temp = (time_since_timeout(&timer)/100);
if (temp < (time + 5))                    /*L150*/
      {wait(100*(time + 5 - temp));    // wait till time interval has elapsed
       time += 5;
      }
    else
```

```
    time = temp;
  }
        {  /* save last data batch*/
        set_main_xbank(w);
         for (j=0;j<y;j++)
          {ans[x+j] = anst[j];                    /*L125*/
          }
        x += y;
        y = 0;
        if (x > (32768-z))
        {lw[w-1] = x;
         w += 1;
         x=0;
        }
        if (w == 14)
        { /* go to end*/
        }
        set_main_xbank(1);
    }
        lw[w-1] = x;
if (w == 14)
{}
else
{lw[13] = 0;}
    set_uio(6,1);/*HLD exposure - purly as indicater of data collection finished*/
        wait(5000);
        while ( !halt() && !UIO2 )
        {wait(1000);
        }
        {       set_uio(5,0);
```

```
            for (i=2; i<(w+1); i++)
            { set_main_xbank(i);
                    {l=lw[i-1]/2;
                    }
              for (y=0; y<l/*65536*/; y++)
                    {printf(" %u %u", ans[2*y], ans[(2*y+1)]);
                    wait(1);
                    }
            }
        }
        set_uio(5,1);
        printf(" %u %u %u %u %u %u",tflag,tflag,tflag,tflag, tflag,tflag);
           reset_imputer() ;
}
```

A1.2 Q-basic program written to control Mechanical Bladder and communicate with optical imaging device

```
'                    flowrep.BAS

'running mechanical bladder repeated insult
'new bladder control programme
'                    READINa.BAS


'Program for receiving data from imputer running scan3.

' Press 's2' twice to start upload. (min 5s gap)
'Program end when all data uploaded (if need to interupt- reset imputer
' and follow above procedure with negligible collection time.)
'#1 = sploge viewer communications
'#2= output$ - results
'#3 = input$ - flow profile
'#4 = to mech. blad.
CONST waitt = 2'0      'Time (s) before first event

'Enter flowprofile
u$ = "c:\flows\fl_fill.txt"
a$ = "c:\flows\fl250_25.txt"     '"c:\splodge\f_250_30.txt"
b$ = "c:\flows\fl250_20.txt"  '"c:\splodge\f250_21.txt"    '"c:\f_150_09.txt"
c$ = "c:\flows\fl100_10.txt"  '"c:\splodge\f100_17.txt"    '"c:\f_128_09.txt"
PRINT
PRINT "u="; u$
PRINT "a="; a$
PRINT "f="; b$
```

```
PRINT "s="; c$
PRINT "o = other profile"
PRINT "flow profile = "
INPUT temp$
 IF temp$ = "u" THEN
 infile$ = u$
 GOTO 14
 ELSEIF temp$ = "a" THEN
 infile$ = a$
 ELSEIF temp$ = "f" THEN
 infile$ = b$
 ELSEIF temp$ = "s" THEN
 infile$ = c$
 ELSE
 PRINT "full file name ="
 INPUT infile$
 END IF

'gap between start of insults
INPUT "Gap between starts of insults (s) = ", igap
INPUT "Number of insults = ", numb
numb1 = 1

 INPUT "output file name = ", outfile$
 OPEN outfile$ FOR OUTPUT AS #2
 'OPEN "c:\splodge\temp.txt" FOR OUTPUT AS #2
 OPEN "COM1:9600,N,8,1,CD0,CS0,DS0,OP0,RB8192,RS" FOR RANDOM AS #1

 PRINT "is tap open?"
 'PRINT "hi!"
```

```
PRINT #1, "s"


ON TIMER(waitt) GOSUB 11
TIMER ON
DO: LOOP UNTIL INKEY$ = CHR$(27)          'esc
GOSUB 15
11
time1 = TIMER
14


remainder = 0!
tima = TIMER
PRINT tima,
i = 1
CLOSE #3
OPEN infile$ FOR INPUT AS #3
INPUT #3, x, z, tot
DO UNTIL i > 1000 OR INKEY$ = CHR$(27) 'esc
'DO: LOOP UNTIL (TIMER > tim + .05)
'tim = tim + .05
'PRINT tim
GOSUB flow
i = i + 1
LOOP
15
CLOSE #3
IF numb1 = numb THEN
GOTO 12
ELSE
PRINT time1 + igap * numb1
```

```
q = 1
DO UNTIL (TIMER > time1 + igap * numb1) OR INKEY$ = CHR$(27)'esc
LOOP
numb1 = numb1 + 1
PRINT numb1
OPEN infile$ FOR INPUT AS #3
GOTO 14
END IF

12
PRINT tim, TIMER
IF infile$ = u$ GOTO 1

PRINT "esc to stop or spacebar before starting upload"
tim = TIMER
i = 10
DO:
IF INKEY$ = CHR$(27) THEN 'esc
PRINT "interupted"
GOTO 1
ELSEIF INKEY$ = CHR$(32) THEN
PRINT "ready to start upload"
GOTO 2
ELSEIF TIMER >= tim + i THEN
PRINT i;
i = i + 10
END IF
LOOP
2
 INPUT #1, tim
```

```
PRINT tim; "!",
PRINT "starting upload"
.

3


PRINT "after first"
DO:
GOSUB hand
LOOP UNTIL INKEY$ = CHR$(27) 'Esc
PRINT "stop"



CLOSE #1, #2
1 END


'12 END


flow:
        IF EOF(3) THEN
        PRINT "eof",
        PRINT TIMER,
        GOTO 15
        END IF
        tim2 = tim
        INPUT #3, tim, rate
        tim1 = tim - tim2
        steps = rate * tim1 * 5 'convert ml/s to steps
        steps = steps + remainder
        isteps = INT(steps)
        remainder = steps - isteps
```

```
        IF isteps > 0 THEN
        gap = timl / isteps
        'PRINT rate, isteps, gap, timl, remainder
        FOR j = 1 TO isteps
        FOR k = 1 TO 30
        OUT &H2FC, 1
        NEXT k
        FOR k = 1 TO 30
        OUT &H2FC, 0
        NEXT k
        DO: LOOP UNTIL TIMER > (j * gap + tima + tim2)
        NEXT j
        END IF
    ' PRINT (tim - TIMER + tima),
        DO:
        'PRINT "hi";
        LOOP UNTIL (TIMER > (tim + tima))
RETURN

flowold:
        IF EOF(3) THEN
        PRINT "eof",
        PRINT TIMER,
        GOTO 15
        END IF
        tim2 = tim
        INPUT #3, tim, rate
        timl = tim - tim2
        steps = rate * timl * 5 'convert ml/s to steps
        steps = steps + remainder
```

```
        isteps = INT(steps)
        remainder = steps - isteps
        IF isteps > 0 THEN
        gap = INT(4500 * timl / isteps)  'was 4600
        'PRINT rate, isteps, gap, timl, remainder
        FOR j = 1 TO isteps
        FOR k = 1 TO gap
        OUT &H2FC, 1
        NEXT k
        FOR k = 1 TO gap
        OUT &H2FC, 0
        NEXT k
        NEXT j
        END IF
    ' PRINT (tim - TIMER + tima),
        DO:
        'PRINT "hi";
        LOOP UNTIL (TIMER > (tim + tima))
RETURN



hand:
 INPUT #1, tim, tim2, tim3, tim4
 'PRINT tim
 IF tim4 = 999 THEN
  PRINT "?end",
  IF tim2 = 999 THEN
   PRINT "end";
   GOTO 1
```

```
 ELSE
  PRINT #2, tim; tim2;
  INPUT #1, tim, tim2
  IF tim2 = 999 THEN
   PRINT "end";
   GOTO 1
  ELSE
   PRINT #2, tim3; tim4; tim; tim2;
  END IF
 END IF
ELSE
PRINT #2, tim; tim2; tim3; tim4;
END IF
RETURN
```

A2: Appendix 2

A2.1 Technical drawings for mechanical bladder

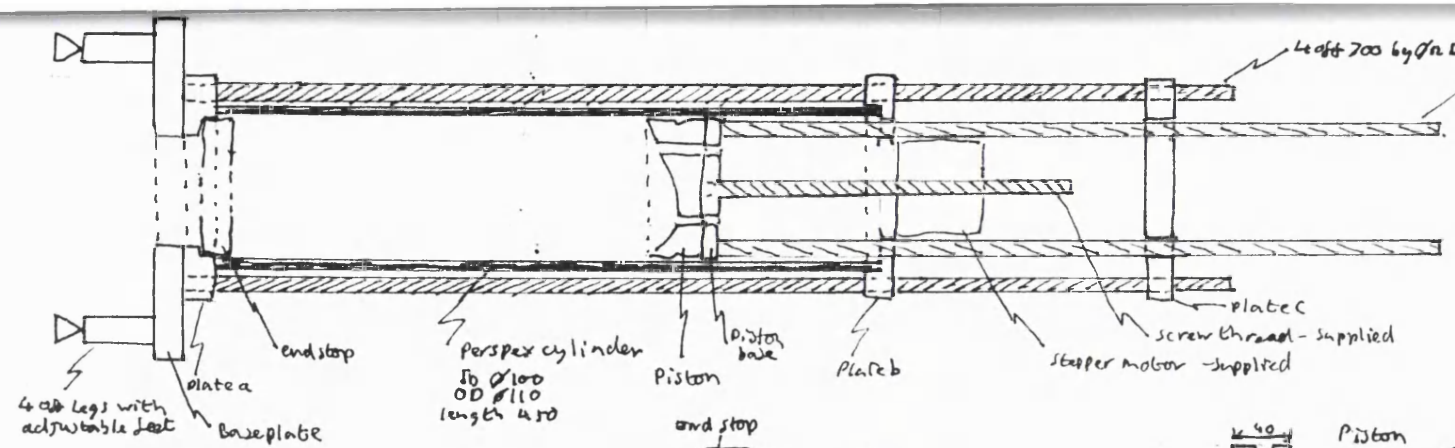

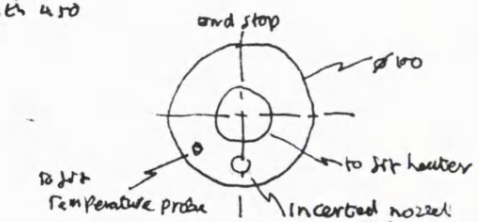

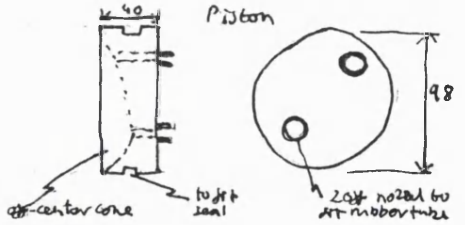

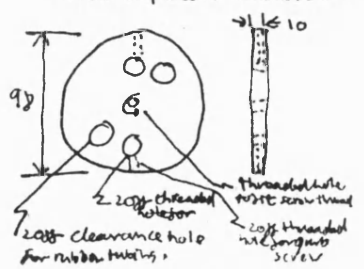

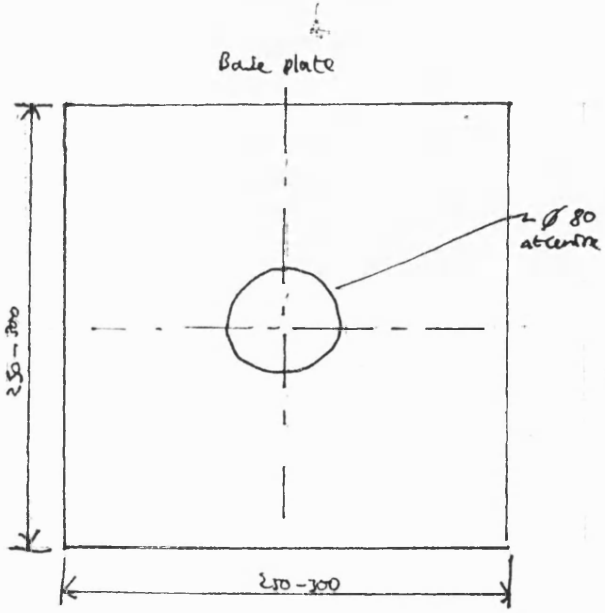

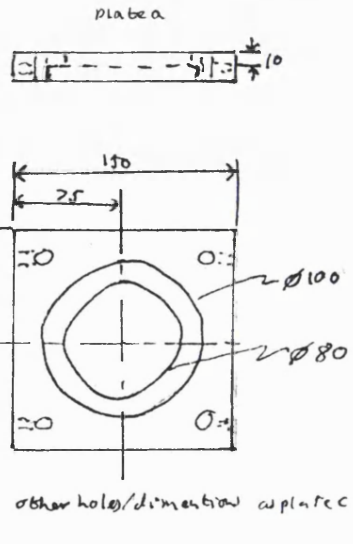

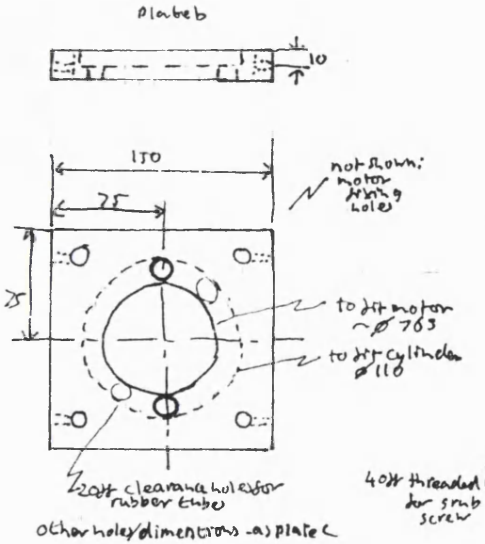

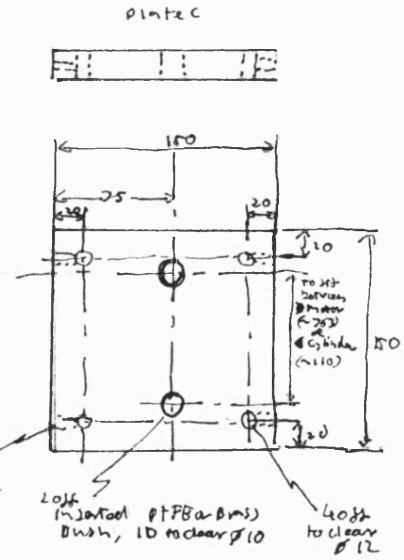

Plates a, b, c - 20mm (or 3/4") thick

A2.2 Technical drawings for optical imaging device control box

R.

BASE PLATE

off TUFNOL

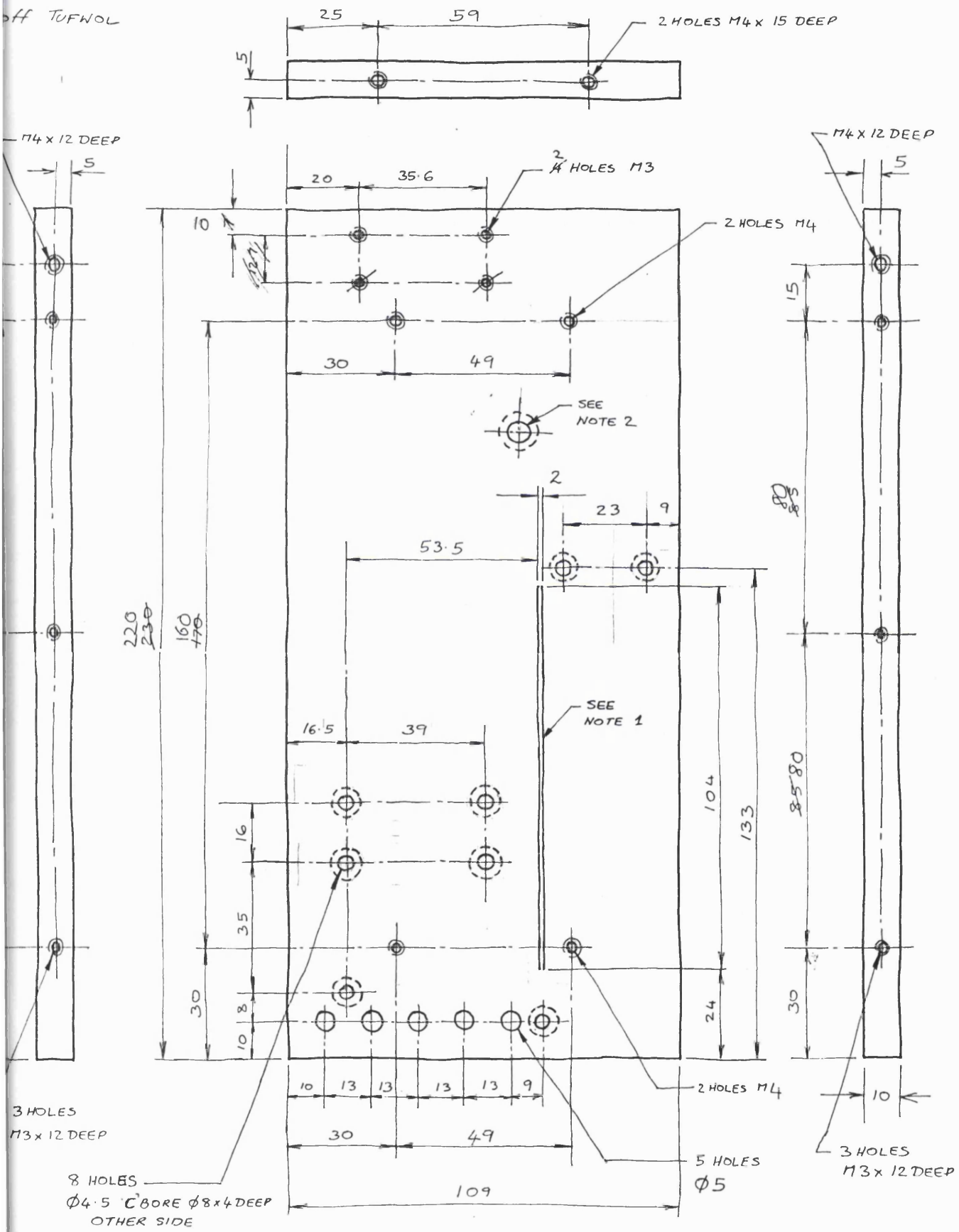

NOTE 1: SLOT 2 WIDE x 2 DEEP FOR DIVIDER. RUN OUT BOTH ENDS ACCEPTABLE

NOTE 2: Ø 1/4" CLEARANCE HOLE C'BORE OTHER SIDE. POSITION SO THAT IT ALIGNS WITH ONE ON THE IMPUTER.

IMPUTER HOLDER

RY.

1 off AL

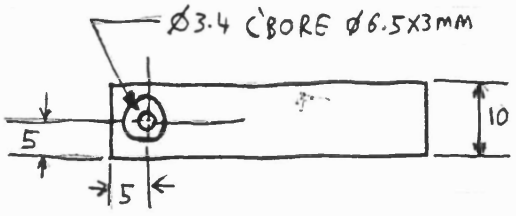

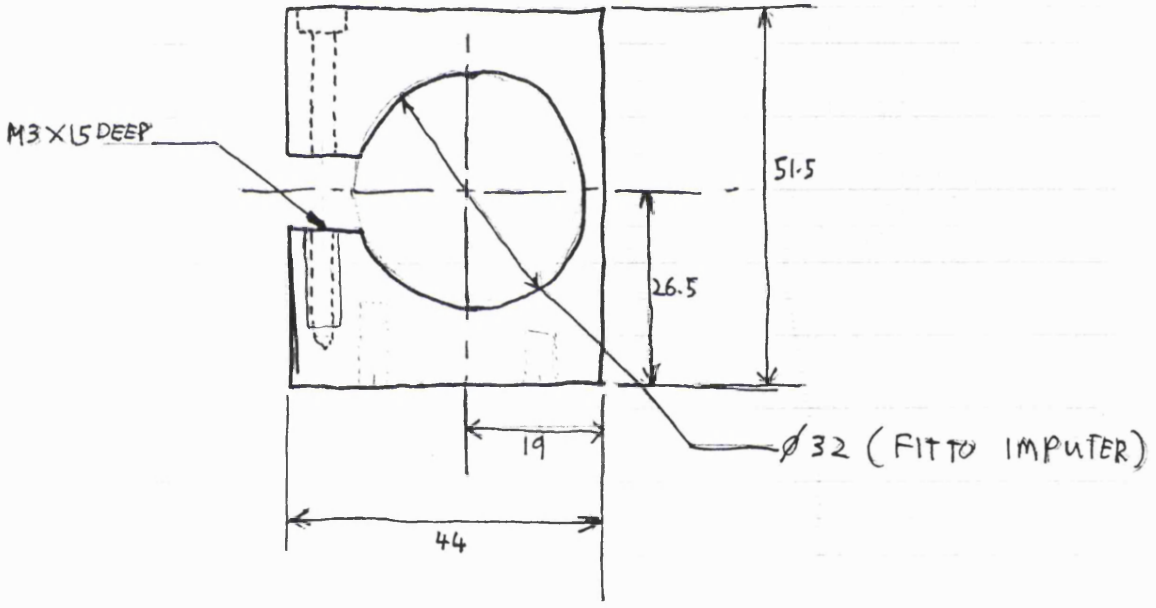

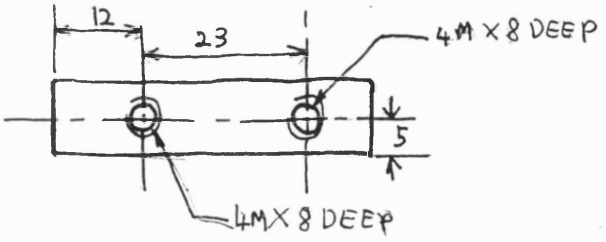

LED FERAL HOLDER

R.Y.

1 Off Tufnol

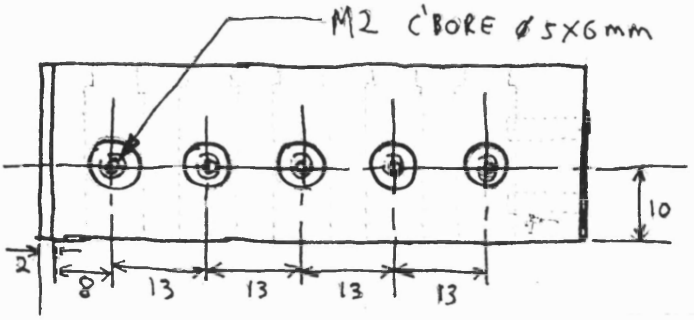

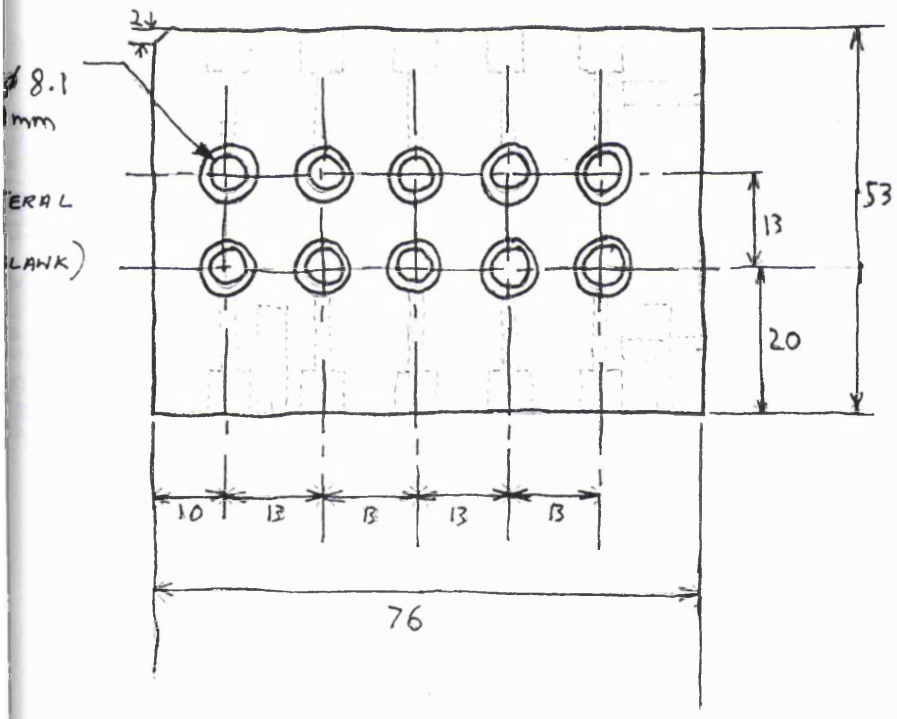

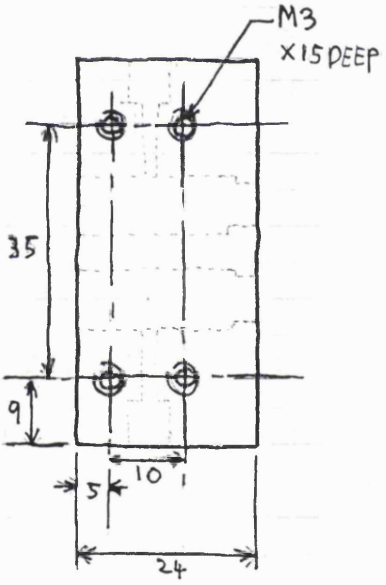

(Can be upto 26 so 1" stock can be used)

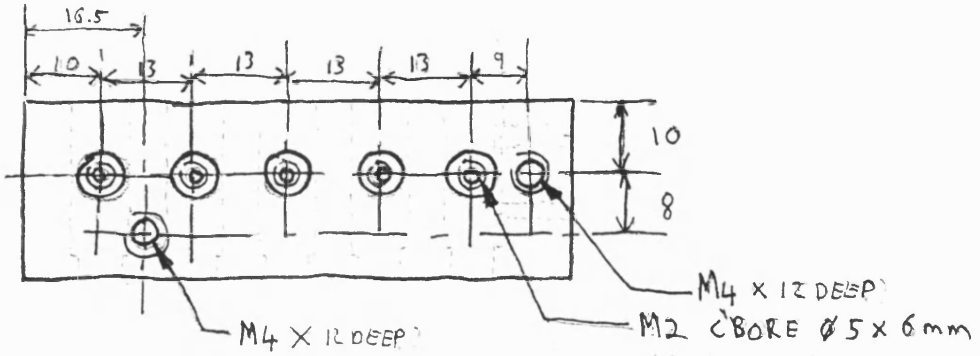

PERSPEX HOLDER

1 off Tufnol

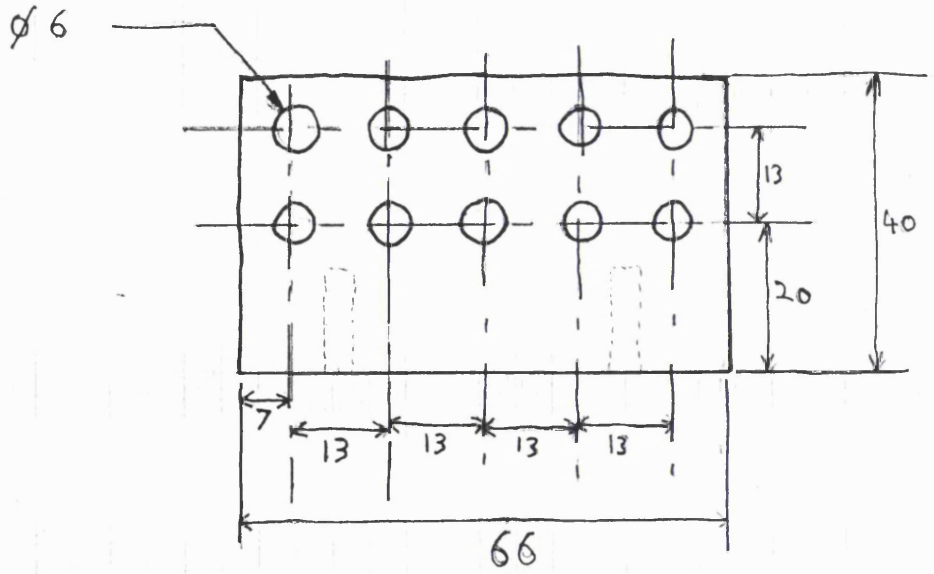

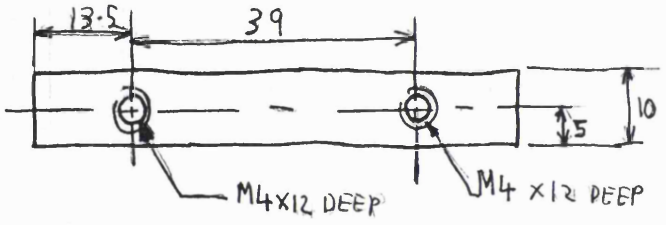

1 off Twinol

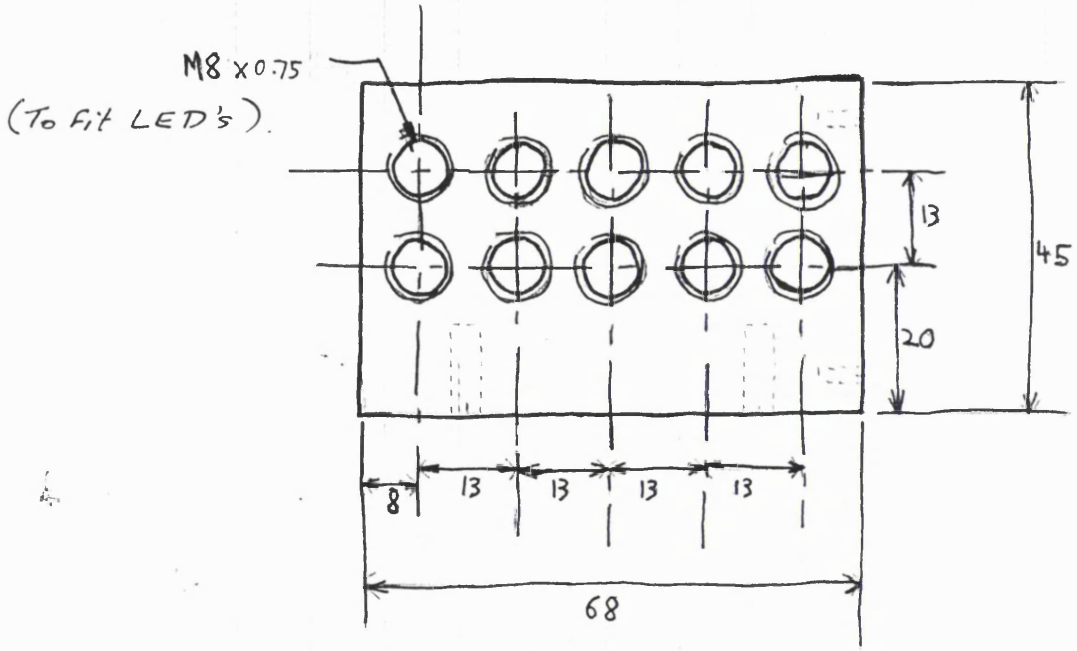

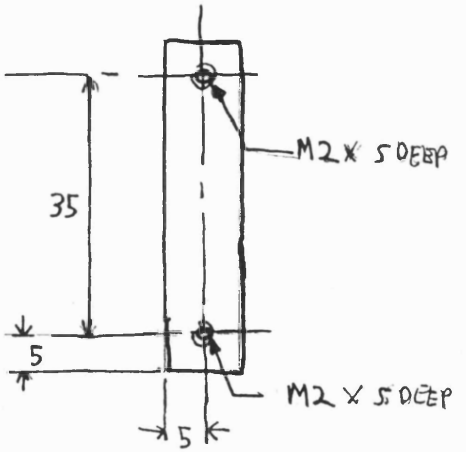

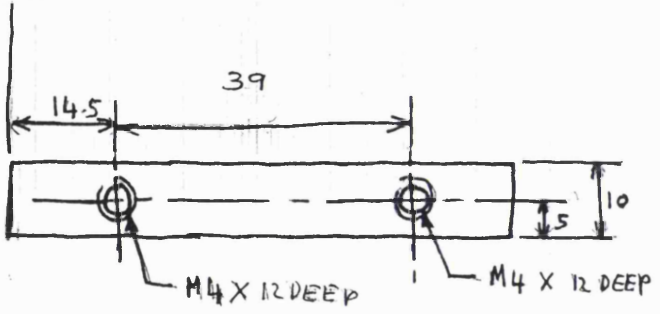

201

FERALS

R.Y

LED FERAL

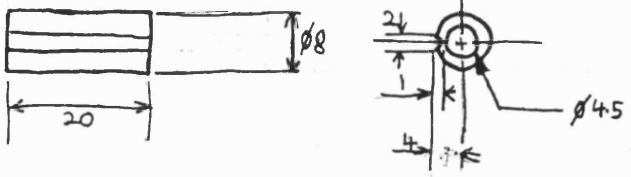

20 off AC

LED BLANK

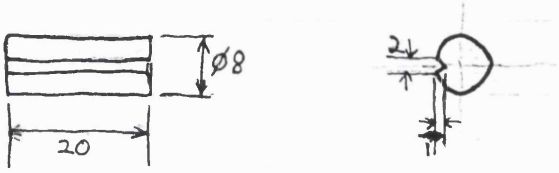

9 off AC

OUT PUT FERAL (2 PARTS)

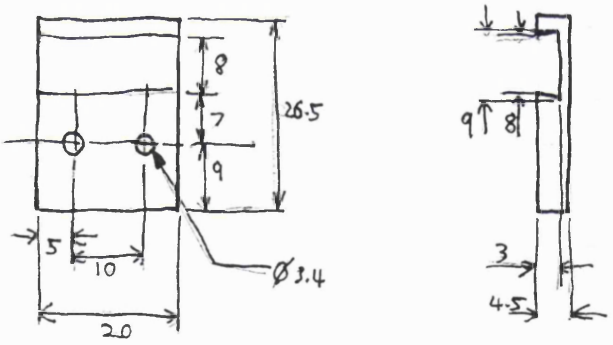

20 off AC

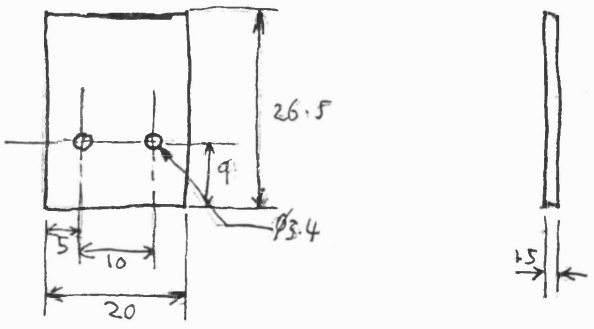

20 off AC

OUT PUT BLANK

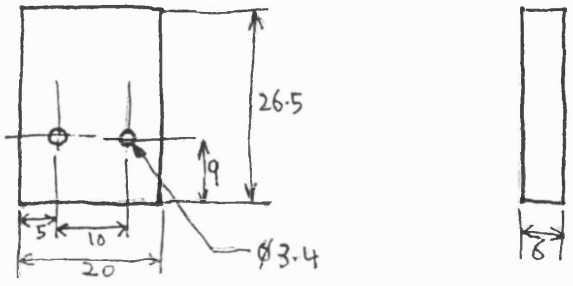

9 off AC

PERSPEX ROD

R.Y

10 off PERSPEX

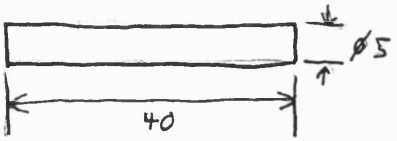

ENDS POLISHED

END BLOCK 1

1 off AL

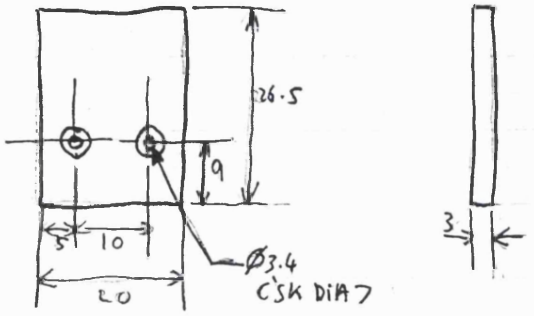

END BLOCK 2

1 OFF AL

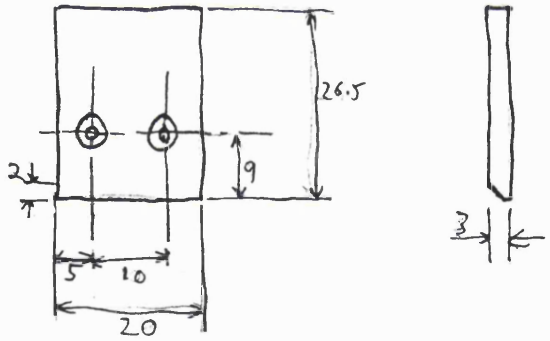

SWITCH BOARD

1 OFF BREAD BOARD - SUPPLIED

4 HOLES ø3.4mm

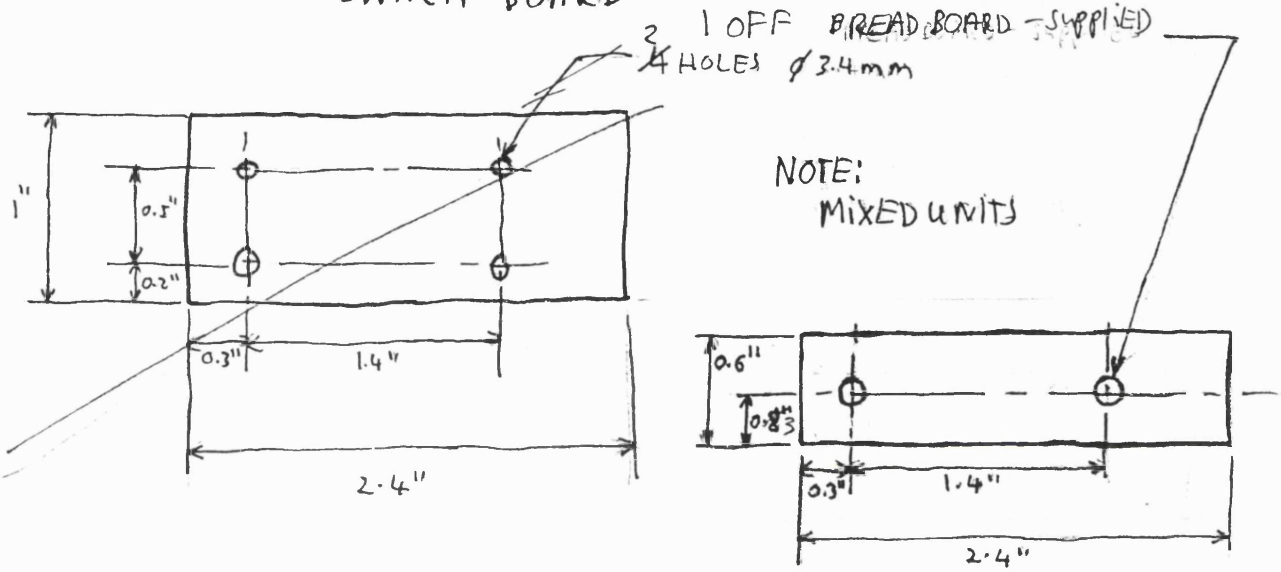

NOTE:
MIXED UNITS

DIVIDER 1 off TUFNOL R.Y

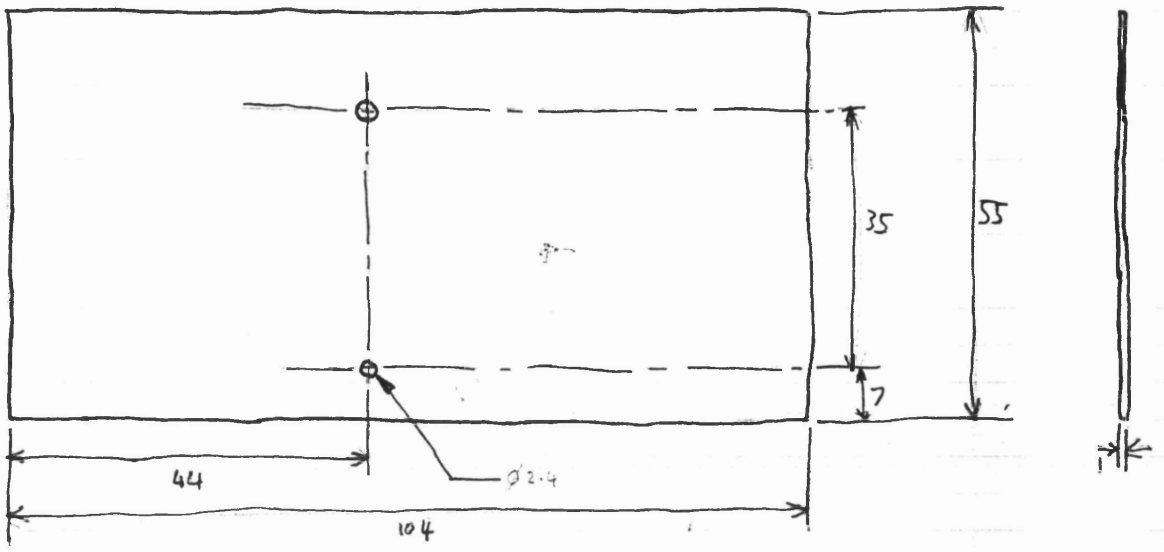

Back 1 OFF AL

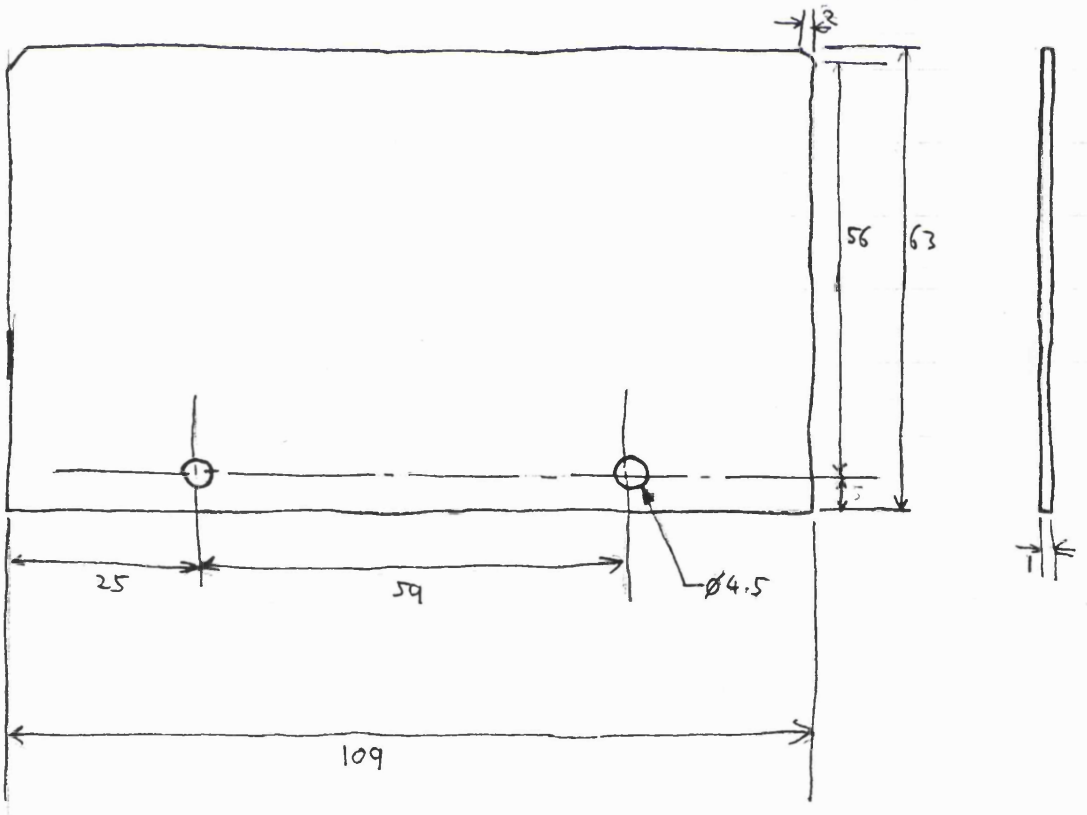

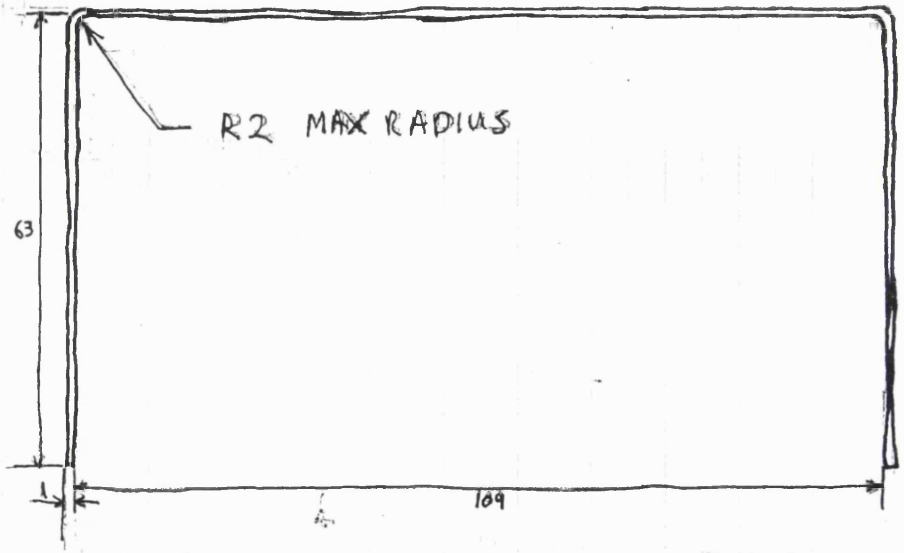
R2 MAX RADIUS
63
1
109

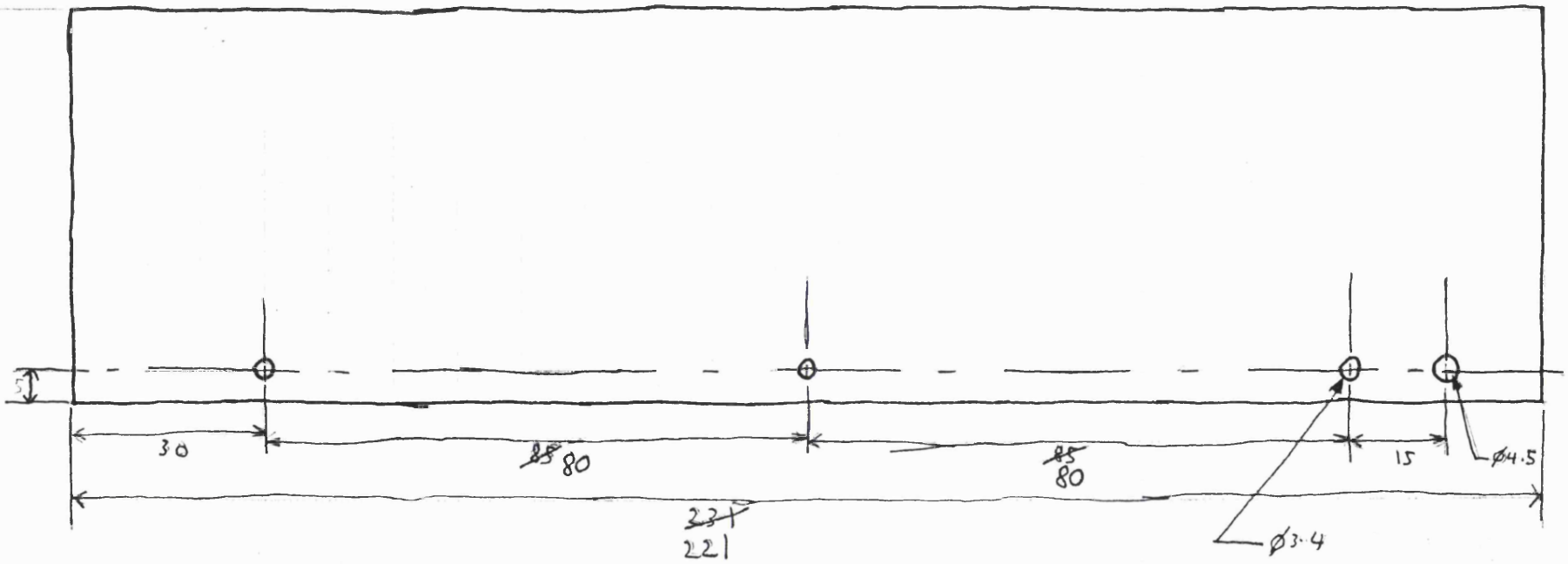
5
30
~~85~~ 80
~~85~~ 80
15
ø4.5
~~231~~ 221
ø3.4

A3: Appendix 3

A3.1 Scattering and absorption of light: background theory

A3.1.1 Material characteristics

The primary substances studied in this thesis are

- Fluffed wood pulp fibres (cellulose). Being natural fibres these vary widely in size depending on the tree species and country from which they originate, as well as the process by which they are extracted. Typically fibres have a diameter of 25-50μm and a mean length of 2-3mm about which there is a wide distribution of lengths. They form hollow ribbons when dry, swelling to a circular cross-section when wetted. Bulk collapse of the fibre assembly occurs on wetting reducing the surrounding void space.
- Superabsorbent particles - size 300-600mm spheres when dry swelling to 1-2mm spheres when wet
- Air
- Water/saline

A3.1.2 Absorption

Theoretically, one option for measuring the content of water within fluff pulp would be to choose a wavelength at which water is a strong absorber. An absorption peak exists at 1.4μm, others are in the UV and far infrared regions. However, the requirement of this work for many sensors (~500) and the desire to create a portable imaging device meant that, size, cost and complexity constraints limited the range of suitable detectors to visible light imaging devices - CCD or CMOS (see section 5.4.4). Visible light falls within a region known as the 'water region' where virtually no absorption of light by water occurs.

Fig.5.9 shows the wavelength response of a CCD detector that has been deliberately cooled so as to detect light in the near infrared. Even with this cooling the detector is unable to detect light at 1.4μm, let-alone UV or far infrared light. For this reason optical pad imaging can not utilise the absorption processes.

A3.1.3 Scattering

Of the substances within a pad, the scattering caused within the fluids (air and water/saline) is minimal compared with that due to the fluff pulp fibres. This is demonstrated visually by looking at samples of each – air and water are virtually transparent but even a thin layer of fluff pulp looks opaque white because of its strongly scattering properties. However, air and water do affect scattering from the fluff pulp fibres as the refractive index of water/saline is a much closer match to that of the fluff pulp fibres than that of air is.

Various theories seeking to model the transport of light through scattering materials have been developed over the years, each theory being most applicable to a different set of physical constraints, details of these can be found in most optical physics text books, e.g, Besancon.

Rayleigh scattering applies to particles that are small compared with the wavelength of the incident light. However, fluff pulp fibres have large diameters relative to light, including far infared wavelengths; $\pi D >> 10\mu m$ where D is the diameter of the fluff pulp fibre; and fibre lengths are several orders of magnitude longer still and so the Rayleigh model don not apply.

Rayleigh-Ganz-Debye (RGD) theory is for large tenuous scatterers but cannot be used in analysing the scatter from pad materials as this theory is only valid for small relative refractive indices. There are large refractive index differences between fluff pulp fibres and air.

Mie theory (1908) gives a mathematical solution for scatter from a sphere of arbitrary radius and refractive index although it is also used, with correction factors, for other shapes. However, although it applies for particles much larger than a wavelength, the less spherical the particle the less accurately predicted is the resulting scatter pattern and fibres are far from spherical. Nevertheless using this theory still reveals the dependence of the scatter on factors such as wavelength and relative refractive index.

Mie theory uses dipoles, quadruples and poles of higher orders to represent the field of radiation due to a particle. This results in a highly complicated expression which is dependent on the complex relative refractive index, the particle radius and the wavelength of the light used.

The solution to this expression is an infinite series of Bessel functions and predicts a radiation pattern of the form shown in Fig A3.1.

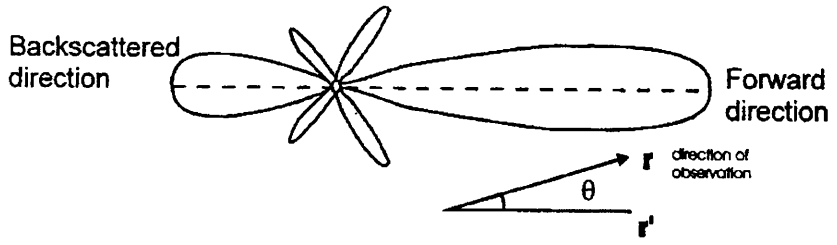

Fig A3.1 Intensity of scattered light as a function of angle as predicted by Mie theory

An expansion of the first few terms can be simplified to the following equation (Bohren and Huffman, 1981) -

$$\frac{I_s}{I_i} = \frac{8\pi N' r^6}{\lambda^4 z^2}\left[\frac{m^2-1}{m^2+2}\right]^2\left(1+\cos^2\theta\right) \qquad \text{-A3.1}$$

where I_i is the incident light intensity

I_s is the resulting scattered light intensity

N' is the complex refractive index of the particle

m is the complex relative refractive index of the particle to its surrounding medium

r is the radius of the particle

λ is the wavelength of the light

and z is the observation distance

From this we can see that I_s is most strongly dependent on the radius of the particle:

$$I_s \propto r^6$$

Scattering is also strongly dependent on wavelength :

$$I_s \propto \lambda^{-4}$$

However, in the case of scatter from a pad λ is constant for the duration of the experiment and, because r is a function of the material under investigation, the range of fibre diameters within the pad cannot be altered in order to change the value of I_s. In fact the mean diameter of cellulose fibres increases slightly upon wetting, the effect of this being small and dependent on the orientation of the fibres.

Since only the relative refractive index, m, changes significantly during an experiment, equation A3.1 can be rewritten to give :-

$$\Delta I_s \propto \left[\frac{m_a^{\,2}-1}{m_a^{\,2}+2}\right]^2 - \left[\frac{m_w^{\,2}-1}{m_w^{\,2}+2}\right]^2 \qquad \text{-A3.2}$$

Where ΔI_s is the change in scattered light intensity when water displaces the air in fluff pulp

m_a is the relative refractive index of fluff pulp fibres in air

and m_w is the relative refractive index of fluff pulp fibres in water

Water-based liquids have a much closer refractive index match to the fibres than air. Therefore as the material absorbs water the value of m decreases, reducing the intensity of the scattered light according to equation A3.2.

Equation A3.2 shows that the percentage change in scattered light intensity upon wetting is independent of λ. However, ΔI_s is required to be large to reduce the effects of signal noise. Equation A3.1 indicates that I_i should be large and λ small to facilitate this. The viewing distance z is the only other factor which can be altered and this should be kept as small as possible.

As mentioned previously, practical constraints limit the choice of detectors to CCD and CMOS devices. Such detectors have a peak response between 700 and 800nm, the response falling off rapidly to either side such that at the detector response is virtually zero below 600nm and above 1,000nm. Although ΔI_s increases rapidly with decreasing λ, the response of the detector decreases more rapidly. It is counterproductive, for example, to halve the wavelength, thus increasing ΔI_s by a factor of eight, if this results in a ten-fold reduction in the sensitivity of the detector. Although not shown in equation A3.2, m_a

and m_w are dependent on λ. However this dependence is only weak between 650nm and 900nm (Fig 5.8).

Detector response and the intensity of the light source is therefore the prime consideration when choosing the interrogating light source and a wavelength of $\approx$ 600nm (red light) was chosen as brighter LEDs are available for red light than for other wavelengths in the appropriate wavelength range.

A4: Appendix 4

A4.1 Background theory of fibre optics and measurement technologies.

An optical fibre is a strand of material that can collect light at one end and carry it to the other. The fibre usually consists of at least two materials that have different refractive indices. The inner or core material (see A1.1.1Fig A4.1Fig A4.1) has a higher refractive index than the surrounding cladding layer. This means that light entering the fibre at a shallow enough angle experiences total internal reflection (see section 5.1) each time it encounters the core/cladding boundary. Thus light is trapped inside the fibre, reflecting from side to side until the further end is reached.

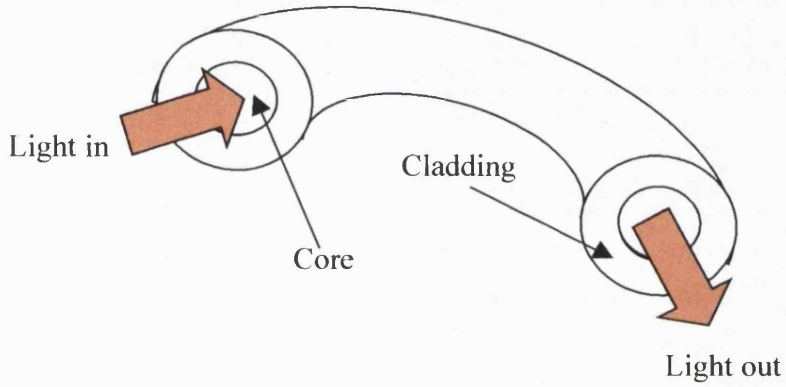

Fig A4.1 Optical fibre

A1.1.2 Numerical aperture and modes of propagation

The amount of light that an optical fibre can collect is dependent on the physical size of the core, the maximum angle at which light can enter the fibre while still meeting the requirements for total internal refraction, and the shape of the refractive index profile across the core diameter. The maximum angle (α) is dependent on the refractive indices of both the core and the cladding as shown in Fig A4.2

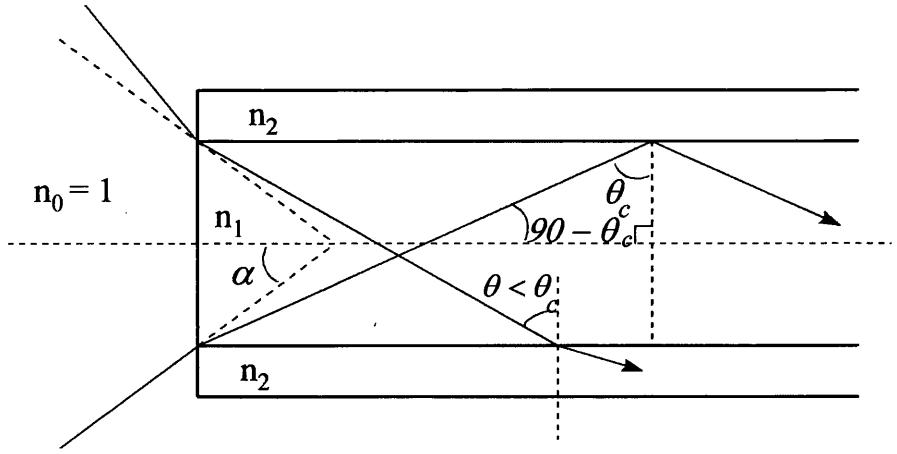

Fig A4.2 Acceptance angle of an optical fibre

Using equation 5.2 we can write

$$n_o \sin \alpha = n_1 \cos \theta_c \qquad \text{-A4.1}$$

Where n_o is the refractive index of air, n_1 is the refractive index of the core and θ_c is the critical angle for the core/cladding boundary. The cladding has a refractive index of n_2.

Since, by definition, the angle of refraction = 90° when the angle of incidence equals the critical angle we can write

$$n_1 \sin \theta_c = n_2 \sin 90$$

Therefore

$$\sin \theta_c = n_2 / n_1 \qquad \text{-A4.2}$$

Substituting A4.2 into A4.1 and simplifying gives

$$n_o \sin \alpha = [n_1^2 - n_2^2]^{1/2}$$

The value ($n_o \sin \alpha$) is independent of variations in n_o and is known as the numerical aperture (NA). This equation can be simplified to give:

$$NA = [n_1^2 - n_2^2]^{1/2} \qquad \text{-A4.3}$$

Defining the numerical aperture like this implies that all light incident at an angle less than or equal to α would be successfully propagated down the optical fibre. However, due to the wave properties of light propagation can only occur if the total phase change after two reflections is equal to $2m\pi$ radians, where m is an integer. Under these conditions constructive interference occurs and a stable field distribution is produced. This is known as a mode. If a fibre is narrow enough only a single mode of light can be propagated but as the diameter of the fibre is increased additional discrete modes can be added. Fig A4.3 shows some typical modal profiles for circular fields.

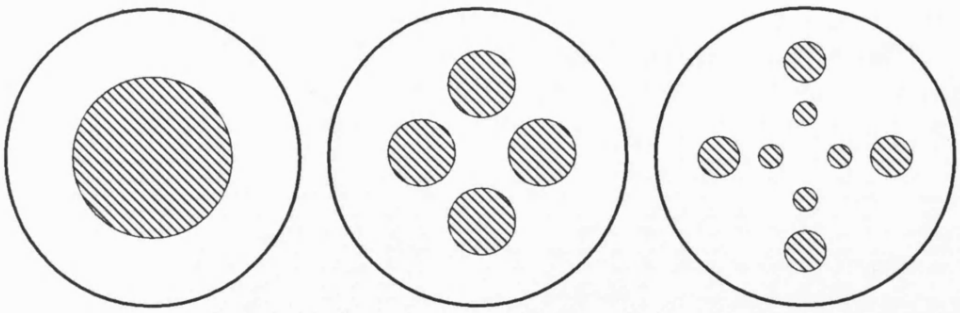

Fig A4.3 Typical modes in an optical fibre

A fibre supporting only a single mode is known as a single or mono mode fibre and typically has a core 10 microns in diameter. A multimode fibre may have a diameter of 100 microns or more.

So far optical fibres with only two refractive index layers have been considered. This is the simplest case and such fibres are known as step index fibres. The other main type of fibre is the graded index fibre. As indicated by the name, the refractive index of the material from which these fibres are made changes gradually from the core outwards. In these fibres a ray of light is refracted further and further from the normal the further it travels from the fibre axis until internal reflection occurs. This is illustrated in Fig A4.4

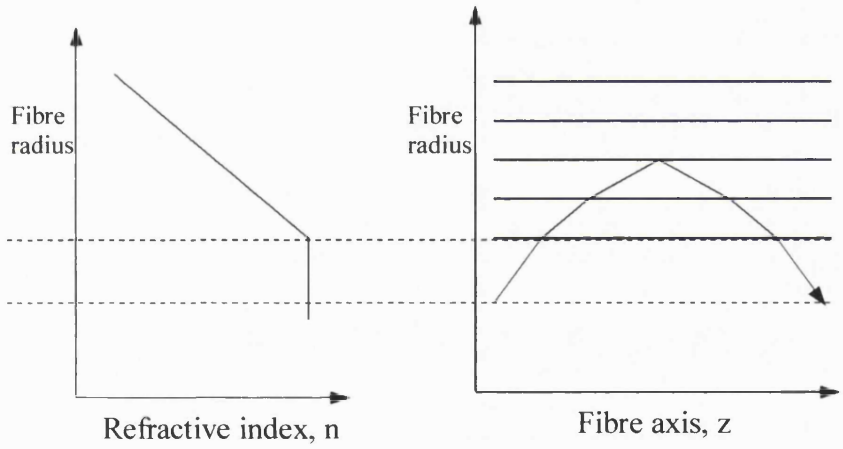

Fig A4.4 Reflection in a graded index fibre

These fibres have a numerical aperture whose equation will have the same form as equation A4.3 but using an effective value for n_2. Single or multiple modes of propagation are also supported.

A1.1.3 Choice of fibre type

Each type of fibre has advantages and disadvantages. The obvious advantage of the multimode fibres is that more light will be transported than a single mode fibre, however this is at the expense of increased dispersion.

A light ray in the lowest mode travels closer to the fibre axis than one in a higher mode. This means that the lower mode has the shorter total path length and hence reaches the end of the optical fibre

before the higher mode ray (see Fig A4.5). Thus a monochromatic pulse of light entering a multimode fibre will have a longer duration when exiting the fibre than when entering it as light travelling in each mode arrives at a slightly different time. A single mode fibre would not lengthen such a pulse as the path length is identical for all rays.

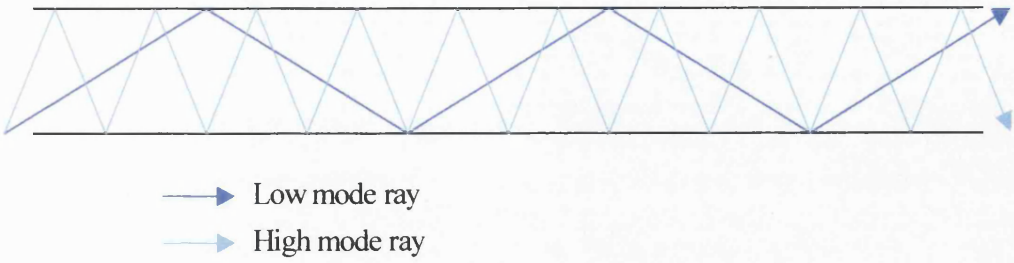

Fig A4.5 Dispersion in a multi-mode fibre

Dispersion due to changes in refractive index as a function of wavelength can also occur for light sources having a wide linewidth.

For applications requiring high digital data rates, laser light sources, mono-mode fibres and fast detectors should be used. If, however, the fibre is required for illumination, for example, a large multimode fibre with a high numerical aperture is required to increase the total intensity of light transported.

Graded index fibres have improved dispersion characteristics when compared to step index fibres when used in large bandwidth applications. This is because the refractive index of a material - which is a measure of the speed of light in that material - is a function of wavelength. The slower wavelengths follow a shorter path than the faster ones, so a graded index fibre can be designed to reduce the effects of wavelength-dependent dispersion.

A1.1.4 Light losses in fibres

Light losses along optical fibres consist of intrinsic and extrinsic components.

Intrinsic components comprise absorption and scattering losses due to impurities in the fibre material acting as absorption and/or scattering centres. These losses are dependent on the composition of the fibre and the wavelength of light used since Rayleigh theory for small scatterers states that scatter intensity is dependent on λ^{-4}.

Extrinsic losses relate to bending of the fibre, which reduces the angle of incidence with the core/cladding boundary along the outside of the bend (Fig A4.6). If this angle is reduced to less than the critical angle the light will escape from the optical fibre at that point.

Extrinsic losses also occur at joints between fibres if these are not properly aligned.

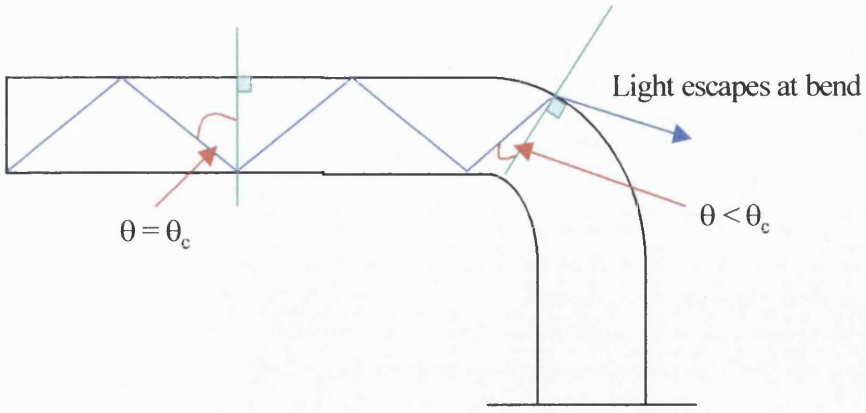

Fig A4.6 Bending losses in an optical fibre

A1.2 Characteristics of optical fibres used:

The requirements of the optical fibres for this project are discussed in section 5.4.2. This concludes that the use of fibres with a small minimum bend radius was critical to this application. The smallest such radii are found in plastic fibres. Since timing in this application was relatively course (0.5s) dispersion was not a relevant issue but as diffuse light sources were being used the fibres were required to have a large acceptance angle in order to collect as much light as possible. Attenuation was not critical as only short lengths of optical fibres were being used. The wavelength and temperature range required did not limit the choice of fibre.

In the light of these considerations, a plastic optical fibre with the following manufacture's specification was used

- Diameter 0.5mm
- Material – core: Polymethyl methacrylate
  - cladding: fluorinated polymer
- Numerical Aperture 0.50
- 400nm to 800nm wavelength
- Acceptance angle 60°
- Temperature range -40°C to +70°C
- Min Bending Radius 9mm
- Attenuation at 650nm (dB/m) max 0.25

A1.3 Measurement Technologies

Fibre optics can be used as part of a wide range of measurement devices. For example fibre sensors can be used to measure temperature, pressure, electrical current, presence of chemical species and strain of materials, as well as the intensity and spectrum of light.

Conceptually the simplest use of optical fibres is as a flexible link separating the test location from the main body of the detector. Such a set up is particularly useful in situations where access is limited or environmental conditions are harsh/corrosive.

This link may be a single fibre or, provided they retain their spatial orientation, bundles of fibre optic cables can be used to transmit images to an array detector, which is particularly useful in monitoring hazardous environments.

In general, multimode fibres can be used in applications where phase and polarisation of the transmitted light is not important. For applications where these factors are necessary, single mode fibres should be used.

Sensors that are sensitive to chemical species are usually constructed from multimode fibres. These generally rely on spectroscopy effects, where a certain chemical species may preferentially absorb, reflect, scatter or luminesce at a particular wavelength. This effect may also be used indirectly, for example in pH probes. Generally, fibre pH sensors will consist of optical fibres with an addition chemical attached to the end of the fibre. The chemical will be chosen so that it changes colour in the presence of material of different pH, in the same way as litmus paper. The material is probed by light of a certain wavelength, which will reflect back down the fibre detector. The change in reflected light can be use to infer the pH of the region surrounding the end of the fibre.

In addition to this, the response to various external factors of light transport in optical fibres has been exploited to create novel sensors. For example, temperature sensors have been formed which determine temperature from the phase shift of a pulse of light backscattered at some location in the fibre. If the timing of returned pulses is taken into account a single optical fibre can be used to measure the temperature along a tunnel or pipeline.

Fibre optic water ingress detectors have also been developed along similar lines (see section 2.5).

These are only a few examples of a rapidly growing field.

References

Allen.V, Ryan.D.W. Murray.A. Repeatability of subject/bed interface pressure measurements. J. Biomed. Eng 1993;15:329-32

ATS Assistance Technique Scientifique, Z.I. des Milles, Actimart, 1140 re Ampère 13851 Aix-en-provence cédex 3, France

Besancon, The encyclopedia of physics, 2nd edition. Van Nostrand Reinhold

CF Bohren and DR Huffman, Absorption and scattering of light by small particles. Dover publications, New York, 1981

Brown, D, Diapers and underpads, part 2; Cost outcomes. Ostomy/wound management, Vol 40, No.9, p34-40 1994

Colman.E.A, The fibreglass electrical soil-moisture instrument. Soil science 67, 1949, p425.

Continence products directory, The Continence Foundation

Contray Consulting labservice, Centre Tertia, Z.I. Douai Dorignies, 710 Rue Jean Perrin F - 59500 Douai France

Cottenden A.M et al, Disposable bedpads for incontinence: predicting their clinical leakage properties using laboratory tests. Med Eng. & Phys 1998 20. P347-359

Cottenden A.M., Ledger D.J. Predicting the leakage performance of bodyworn disposable incontinence pads using laboratory tests. J.Biomed.Eng 1993; 115:212-202

Cottenden A.M, Fader M.J, Barns K.E, Jones T.M, Malone-Lee J.G. The Performance of Incontinence Products in relation to their design. Proceedings Pica Nonwovens Conference Brighton Nov. 1987

Cottenden.A.M. Instrument for the testing of incontinence pads. UCL internal report 1987.

Cottenden A.M. Pads and Products. In: Abrams P, Khoury S, Wein A, editors. Incontinence. Health Publications Ltd, 1999:753-8.

Cottenden A.M, Moore K.N, Fader M.J, Cremer A.W.F, Is there a risk of cross-infection from laundered reusable bedpads? Brit. J. of Nursing, 1999, Vol 8, No 17, p1161-1163

Datasorb, Greenfields Technology Park, Brombrough, Wirral Ch62 3RS, UK

Defever.M, Kesteloot.K, Coucke.K, Steeman.E, Gruwez. Socio-economic evaluation of incontinence in adults.1997. Katholieke Univesiteit Leuven, Belgium

Elwell.C. A practical users guide to near infrared spectroscopy. Hamamatsu Photonics KK ,1995.

Fader.M et.al. Disposable shaped bodywarn pads with pants for heavy incontinence. Medical Devices Agency report IN.1, March 1998.

Fader.M, Barnes.E, Malone-Lee.J, Cottenden.A. Choosing the right garment. Nursing Times April, 15, 1987 78-85

Farr R.F & Allisy-Roberts PJ. Physics for medical imaging . W.B. Sunders, 1997

Gillespie T, The capillary rise of a liquid in a vertical strip of filter paper. J.Colloid Sci. 1959; 14: 123-130

Graham N.B, Hydrogels: Their Future, Part II, Medical Device Technology April 1998 p23-25

Grow.R, Osczevski.R. The interaction of water with fabrics. Textile.Res.J. 68(4) 1998, p280-288.

Hill.S, Rapid Non-destructive Testing of Carbon fiber reinforced plastics, Materials World August 1996, p450.

Hy-Tec Hygiene Technologie GMBH, Bekker Hof 3, D-40885 Ratingen, Postfach 3102 D-40848 Ratingen

Imputer VLSI Vision Ltd Aviation House, 31 Pinkhill, Edinburgh, EH12 7BF

Incontinence: causes, management and provision of services. J Royal College Physicians London, Jul/Aug 1995 14: 272-274

International Continence Society (1998) Standardisation of Terminology of Lower Urinary Tract Function. Scandinavian Journal of Urology and Nephrology, Supplementum 114, 5 -19.

International Standards Organization, Urine absorbing aids: Guidance on evaluation of single use adult incontinence absorbing aids from the perspective of the users and caregivers. ISO/CD 16021:1988(E).

International Standards Organization. Urine absorbing aids – Part1: Whole product testing : ISO11948_1:1996

International Standards Organization. Urine absorbing aids – Part2: Determination of short time liquid release (leakage) performance under conditions of light incontinence and low pressure ; ISO 11948-2 ; 1997.

International Standards Organization. Urine absorbing aids General guidance for tests. ISO/DIS 15621:1997 (E)

International Standards Organization, Urine absorbing aids – Guidance on evaluation of single use adult incontinence absorbing aids from the prospective of users and caregivers ; ISO\TC 173\SC3 N238 - Annex A. 1999.

James E.D, Flack F.C, Caldwell K.P.S, Martin M.R, Continuous measurement of urine loss and frequency in incontinent patients. British J. Urology, 43:233-237, 1971

James.E.D, Niblett.P.G. Provisional study to quantify and compare parameters of urine leakage in stress and instability incontinence. British J. Urology, 62:233-277, 1988

Grow.R, Osczevski.R. The interaction of water with fabrics, Textile.Res.J 68(4): 280-288, 1998

LIXI. Company literature (1996). LIXI.inc 1438 Brook Drive, Downers Grove, Illinois 60515 U.S.A.

Mc Murdo, M, Davey, P.G, Elder. M, Miller. R, Old. D.C, Malek, M, A cost effectiveness study of the management of intractable urinary incontinence by urinary cathertsation of incontinence pads. Journal of Epidemiology and Community Health, 40:2220226, 1992

Michie.W.C et al., Distributed pH and Water Detection using Fiber-Optic sensors and Hydrogels, Journal of Lightwave Technology 13, no7, 1995

Middleditch L T V, A description of the Caidwell stereofluoroscope, AJR 5: 546, 1918

Mutsumasa Jukahashi MD, Yasashi Ozawa Routine Biplane cerebral Angiology with stereoscopic magnification, Bs. Radiology 136:113-117, 1980.

Norton.C. Nursing for continence, 2nd edition. Published by Beaconfield, 1996

Office of Population Censuses & Surveys, National Population Projections, Series pp2 no.18 1991 based.

Proctor and Gamble, Absorbent article with fiber optic waste inspection system, Patent number WO99/23985, 1999

Royal College of Nursing, A briefing paper in the cost of continence Oct.1997, 000 809

Royal College of Physicians of London (journal of) Incontinence: Causes, management and provision of services Vol.29 No. 4 July/August 1995

SCAN-C 33:80, Scandinavian Pulp, Paper and Board testing committee, 1990

Shishoo.R. Test methods for evaluating urinary incontinence aids. Tappi. Journal July 1987 94-100.

Sowell.V.A, Schnelle.J.F, Hu.T. Traughber.B. A cost comparison of five methods of managing urinary incontinence. QRB, December 1987

Swain.I.D, Stacey.P.O, Dunford.C.E, Nicholls.R.E, Clark.E. Static mattress overlays: a comparative evaluation, Medical devices Agency (London) report PS2; October 1994

Takahashi M, Tanakawa Y, Goto K, et al. Serial cerebral angiography in stereoscopic magnification. AJR 126: 1211-1218, Jan. 1976.

Tamura.T, Naajima K, Matsushita T, Fujimoto T, Shimooki S, Nakano T. A warning detector for urinary incontinence for home health care. Biomed-Instrum-Technol. Jul-Aug 1995 29(4):343-9.

Thomas T.M., Plymat K.R., Blannin J, Meede T.W. Prelevence of urinary incontinence BMJ 1980; 281:1243-5

Tobe T, Satio, Toda N, Sato S, Hantori N, Ishimosoto M, Simultaneous stereoentgenography, Gunma J Med Sci 15: 23-31, 1966.

Yerworth.R.J. A Comparison of Instrumentation Techniques for Real-time Fluid Flow Imaging. UCL internal report 1996.

Glossary

Coverstock – the top layer of incontinence pads, in contact with the subject.

Insult – a single application of fluid to a pad

Supine – position of lying on one's back

Semi-supine – position when lying in a reclined position

Superabsorber – A powdered polymer that absorbs many times its own weight of water and is present in many absorbent incontinence products.

Two piece pad – bodyworn incontinence pad for wear with stretch net pants

Wicking – fluid transport within a material along a saturation gradient.

Acknowledgements

The author would like to thank the following companies for sponsoring this project.

Paul Hartmann AG (Germany)

Proctor and Gamble ltd (USA)

SCA Hygiene AB (Sweden)

The author would also like to thank those wards of St Pancras Hospital London who provided valuable assistance during the clinical trials:

Ash House

Towerview

Foxfield

Parkview

Thanks are also given to the supervisors of this project:

Dr A.M. Cottenden

Dr N. Stewart

and to their colleges at UCL and Sira, especially Dr. J. Gilby

This research was undertaken within the Postgraduate Training Partnership established between Sira LTD and University College London, Postgraduate Training Partnerships are a joint initiative of Department of Trade and Industry and the Engineering and Physical Sciences Research Council. They are aimed at providing research training relative to a career in industry, and fostering closer links between the science base, industrial research, and industry.